Universitat de Girona

OXIDATION OF UNACTIVATED C–H BONDS CATALYZED BY MANGANESE COMPLEXES: CONTROL OVER SITE- SELECTIVITY AND ENANTIOSELECTIVITY

Michela Milan

Per citar o enllaçar aquest document:
Para citar o enlazar este documento:
Use this url to cite or link to this publication:

http://hdl.handle.net/10803/664865

http://creativecommons.org/licenses/by/4.0/deed.ca

Aquesta obra està subjecta a una llicència Creative Commons Reconeixement

Esta obra está bajo una licencia Creative Commons Reconocimiento

This work is licensed under a Creative Commons Attribution licence

Doctoral Thesis

Oxidation of Unactivated C–H bonds Catalyzed by Manganese Complexes: Control Over Site-selectivity and Enantioselectivity

Michela Milan

2018

Doctoral programme in Chemistry

Supervised by: Dr. Miquel Costas Salgueiro and Prof. Massimo Bietti

Tutor: Miquel Costas Salgueiro

Presented in partial fulfilment of the requirements for a doctoral degree from the University of Girona

Universitat
de Girona

Dr. Miquel Costas Salgueiro of Universitat de Girona and Prof. Massimo Bietti of Università degli Studi di Roma “Tor Vergata”,

WE DECLARE:

That the thesis “Oxidation of Unactivated C–H Bonds Catalyzed by Manganese complexes: Control over Site-selectivity and Enantioselectivity”, presented by Michela Milan to obtain a doctoral degree, has been completed under our supervision.

For all intents and purposes, we hereby sign this document.

Dr. Miquel Costas Salgueiro Prof. Massimo Bietti

Bietti

Girona, 3rd September 2018

“This is how it always ends. With death. But first there was life. Hidden beneath the blah, blah, blah. It’s all seated beneath the chitter chatter and the noise. Silence and sentiment. Emotion and fear. The haggard, inconstant flashes of beauty. And then the wretched squalor and miserable humanity. All buried under the cover of the embarrassment of being in the world, blah, blah, blah… Beyond there is what lies beyond. I don’t deal with lies beyond. Therefore… let this novel begin. After all… It’s just a trick. Yes, it’s just a trick.”

The Great Beauty, Paolo Sorrentino

Ai miei genitori e a mia sorella Elisabetta

A mio nonno Giuseppe

FULL LIST OF PUBLICATIONS

This thesis is based on a compendium of the following publications:

CHAPTER III

"Tuning Selectivity in Aliphatic C–H Bond Oxidation of *N*-Alkylamides and Phthalimides Catalyzed by Manganese Complexes" Milan, M.; Carboni, G.; Salamone, M.; Costas, M.; Bietti, M. *ACS Catal.*, **2017**, *7*, 5903-5911. (Impact factor: 11.384, Q_1)

CHAPTER IV

"Highly Enantioselective Oxidation of Nonactivated Aliphatic C–H Bonds with Hydrogen Peroxide Catalyzed by Manganese Complexes" Milan, M.; Bietti, M.; Costas, M. *ACS Cent. Sci.*, **2017**, *3*, 196-204. (Impact factor: 11.228, Q_1)

CHAPTER V

"Aliphatic C–H Bond Oxidation with Hydrogen Peroxide Catalyzed by Manganese Complexes: Directing Selectivity through Torsional Effects" Milan, M.; Bietti, M.; Costas, M. *Org. Lett.*, **2018**, *20*, 2720-2723. (Impact factor: 6.492, Q_1)

Publications not included in this thesis:

“Readily Accessible Bulky Iron Catalysts exhibiting Site Selectivity in the Oxidation of Steroidal Substrates” Font, D.; Canta, M.; Milan, M.; Cussó, O.; Ribas, X.; Klein Gebbink, R. J. M.; Costas, M. *Angew. Chem. Int. Ed.*, **2016**, *55*, 5776-5779.

“Non-Heme Iron Catalysts with a Rigid Bis-Isoindoline Backbone and Their Use in Selective Aliphatic C−H Oxidation” Chen, J; Lutz, M.; Milan, M.; Costas, M.; Otte, M.; Klein Gebbink, R. J. M. *Adv. Synth. Catal.*, **2017**, *359*, 2590-2595.

“Electronic and Torsional Effects on Hydrogen Atom Transfer from Aliphatic C-H Bonds: A Kinetic Evaluation via Reaction with the Cumyloxyl Radical” Salamone, M.; Martin, T.; Milan, M.; Costas, M.; Bietti, M. *J. Org. Chem.*, **2017**, *82*, 13542-13549.

“Chemoselective Aliphatic C-H Bond Oxidation Enabled by Polarity Reversal” Dantignana, V.; Milan, M.; Cussó, O.; Company, A.; Bietti, M.; Costas, M. *ACS Cent. Sci.*, **2017**, *3*, 1350-1358.

“Enantioselective Aliphatic C-H Bond Oxidation Catalyzed by Bioinspired Complexes” Milan, M.; Bietti, M.; Costas, M. *Chem. Commun.,* **2018**, *54*, 9559-9570.

“The Quest for Selectivity in Hydrogen Atom Transfer Based Aliphatic C-H Bond Functionalization” Milan, M.; Salamone, M.; Costas, M.; Bietti, M. *Acc. Chem. Res.,* **2018**, DOI: 10.1021/acs.accounts.8b00231.

LIST OF ABBREVIATIONS

ºC	Celsius degrees
δ	Chemical Shift
^{1}H-NMR	Proton nuclear magnetic resonance
^{13}C-NMR	Carbon nuclear magnetic resonance
2-eha	2-Ethylhexanoic acid
5-mha	5-Methylhexanoic acid
AcOEt	Ethyl acetate
AcOH	Acetic acid
Ar	Aryl
BDE	Bond dissociation energy
BF_3	Boron trifluoride
BzIm	Benzylimidazole
Cat	Catalyst
CF_3SO_3, OTf	Trifluoromethanesulfonate anion
CH_2Cl_2	Dichloromethane
CH_3CN	Acetonitrile
Conv	Conversion
Cyt P450	Cytochrome P450
DiBAlH	Diisobutylaluminium hydride
DMF	Dimethyl formamide

dMM	Dimethylmethoxide
e^-	Electron
Ee	Enantiomeric excess
Equiv	Equivalents
Et_2O	Diethyl ether
ESI-MS	Electrospray ionization Mass Spectrometry
EDG	Electron donating group
EWG	Electron withdrawing group
FT-IR	Fourier transform infrared spectroscopy
GC	Gas chromatography
GC-FID	Gas chromatography-flame ionization detector
GC-MS	Gas chromatography-mass spectrometry
h	Hours
HAT	Hydrogen atom transfer
H_2O_2	Hydrogen peroxide
HBF_4	Tetrafluoroboronic acid
*i*Pr	*Iso*-propyl
L	Ligand
K	Kelvin
kcal	Kilocalories
KIE	Kinetic isotope effect
m	Multiplet
M	Metal

mcp	*N,N′*-dimethyl-*N,N′*-bis(2-pyridylmethyl)-cyclohexane-1,2-diamine
Me	Methyl
MeOH	Methanol
min	Minutes
mL	Milliliter
mM	Millimolar
m/z	Mass to charge ratio
MW	Molecular weight
N_2	Molecular nitrogen
NDO	Naphthalene-1,2-dioxygenase
O_2	Molecular oxigen
OAc	Acetate group
OPiv	Pivalate group
Ox	Oxidant
p	*para*
p.	Page
PCC	Pyridinium chlorochromate
P4H	Proline 4-hydroxylase
pdp	*N,N′*-bis(2-pyridylmethyl)-2,2’-bipyrrolidine
Ph	Phenyl
PhIO	Isodosylbenzene
Py	Pyridine

q	Quadruplet
rt	Room temperature
s	Singlet
t	Triplet
T	Temperature
*t*Bu	*Tert*-butyl group
TFDO	Trifluoromethyl dioxirane
TFE	Trifluoroethanol
THF	Tetrahydrofuran
TIPS	*Tris*-(triisopropyl)silyl group
Ts	Tosyl group

LIST OF FIGURES

Figure VI.1. Structures of the iron and manganese complexes studied. [a]*N*-methylbenzoimidazole instead of pyridine. (p. 79)

Figure VI.2. ESI-MS spectrum of $[Fe(pdp)(S10)+O\text{-}H]^{2+}$. The spectrum was obtained by adding a solution of H_2O_2 in CH_3CN (1.0 equiv) to an acetonitrile solution at 0 ºC of S10 (1 equiv), Fe(pdp) (1 mol %) and AcOH (13 equiv). Sample was taken after 10 minutes of peroxide addition, and analyzed by high resolution mass spectroscopy (HRMS). (p. 85)

Figure VI.3. Structures of the iron and manganese complexes studied. [a]Benzimidazole instead of pyridine. (p. 87)

Figure VI.4. Structures of the manganese complexes studied changing the mcp backbone. (p. 87)

Figure VI.5. Structures of the catalysts used. (p. 93)

Figure VI.6. Transition structures for HAT from tertiary equatorial and axial C-H bonds of disubstituted cyclohexanes to a generic HAT reagent $X^{\bullet}$. (p. 94)

LIST OF TABLES

Table VI.1. Oxidation of *N*-pentylpivalamide (S1) with different catalysts. (p. 80)

Table VI.2. Oxidation of *tert*-butylcyclohexane (S1) with different catalysts. (p. 88)

Table VI.3. Oxidation of different cyclohexane derivatives. (p. 89)

LIST OF SCHEMES

Scheme I.1. a) Simplified C-H hydroxylation mechanism via initial hydrogen atom transfer (HAT) from a C-H bond to high valent metal-oxo species. b) Proposed mechanism of dioxirane-mediated oxidations. (p. 8)

Scheme I.2. General scheme of bond dissociation energies of different aliphatic C-H bonds. (p. 9)

Scheme I.3. Electronic effects on C-H bond oxidation reactions. (p. 10)

Scheme I.4. Effect of EWGs on site-selectivity in the oxidation tertiary C-H bonds. (p. 11)

Scheme I.5. Protonation or complexation driven remote C-H bond oxidation of amines. (p. 12)

Scheme I.6. Steric effects on C-H oxidation reactions of simple substrates. (p. 14)

Scheme I.7. Representative examples in which steric and electronic effects are overridden by the presence of a carboxylic acid directing group. (p. 15)

Scheme I.8. Hyperconjugation by cyclopropanes and heteroatoms activates vicinal C-H bonds. (p. 16)

Scheme I.9. Strain release as an important factor in controlling site selectivity in C-H bond oxidation reactions. (p. 17)

Scheme I.10. Late-stage C-H bond oxidation reactions. (p. 19)

Scheme I.11. Representative scheme of the active site of Cyt P450 BM3 and proposed catalytic cycle for alkane hydroxylation. (p. 20)

Scheme I.12. Active Site of Naphthalene 1,2-Dioxygenase (NDO) and Proposed Catalytic Cycle. (p. 21)

Scheme I.13. Proposed mechanism of proline hydroxylation catalyzed by human P4H. (p. 22)

Scheme I.14. Description of the possible mechanism at the origin of enantioselectivity. (p. 23)

Scheme I.15. Representative scheme of desymmetrization reaction with a chiral catalyst. (p. 24)

Scheme I.16. Oxidative desymmetrization using Mn-salen complexes as catalysts. (p. 26)

Scheme I.17. Enantioselective oxidation of spirocyclic oxindoles derivatives by Ru-complex. (p. 27)

Scheme I.18. Oxidations of spyrocyclic tetralone and indanone derivatives catalyzed by manganese complex. (p. 28)

Scheme I.19. Hydroxylation catalyzed by Fe catalyst 64. (p. 29)

Scheme I.20. Asymmetric oxidation using salen manganese catalysts. (p. 30)

Scheme I.21. Catalytic asymmetric hydroxylation of tertiary alkanes. (p. 31)

Scheme I.22. Enantioselective oxidation of indane with Mn(salen) catalyst 69. (p. 32)

Scheme I.23. Ruthenium catalyzed asymmetric alkane oxidation. (p. 33)

Scheme I.24. Asymmetric hydroxylation catalyzed by Mn or Fe porphyrin systems. (p. 34)

Scheme I.25. Benzylic oxidation reactions in the presence of manganese complex. (p. 35)

Scheme I.26. Oxidation of ethylbenzene, 4-methylethylbenzene and propylbenzene in TFE with different manganese catalysts. (p. 36)

Scheme I.27. Effects of substituents X and R on the catalytic enantioselective hydroxylation of 3,4-dihydroquinolones and interaction between the active species deriving from complex and substrate. (p. 37)

Scheme II.1. General scheme of the objectives. (p. 45)

Scheme VI.1. Oxidation of different *N*-pentyl derivatives. (p. 82)

Scheme VI.2. Oxidation of different *N*-2-(5-methylhexyl) derivatives. (p. 83)

Scheme VI.3. Conformational equilibrium for rotation around the N-CH$(CH_3)_2$ bond in *N*-isopropylpivalamide. (p. 83)

Scheme VI.4. Oxidation of different *N*-1-(3-methylbutyl) derivatives**.** (p. 84)

Scheme VI.5. Oxidation reactions with Fe(pdp) complex. (p. 85)

Scheme VI.6. Oxidation of bioactive molecules. (p. 86)

Scheme VI.7. C-H oxidation reactions using different carboxylic acids and *N*-cyclohexylpivalamide (S8). (p. 91)

Scheme VI.8. Impact of the structure of the acyl moiety in site-selective and enantioselective C-H oxidation of *N*-cyclohexyl amides with (*S,S'*)-Mn(^{TIPS}ecp) as catalyst. (p. 92)

Scheme VI.9. Oxidation of *cis* and *trans* 1,2-cyclohexanediamides. (p. 94)

Scheme VI.10. Oxidation reactions of cyclohexane-derived pivaldiamides. (p. 95)

Scheme VI.11. Oxidation Reactions of *cis:trans* mixtures of 4-X substituted *N*-cyclohexyl amides. (p. 96)

Scheme VI.12. Enantioselective oxidation of *trans*-4-X substituted *N*-cyclohexyl amides. (p. 97)

AGRADECIMIENTOS

En estas páginas me gustaría agradecer todas las personas que han contribuido de una manera o de otra, a la realización de esta Tesis Doctoral.

En primer lugar, me gustaría agradecer mi primer director de tesis Miquel Costas, por haberme dado la posibilidad de trabajar en su grupo, por su dedicación, motivación y supervisión continua, por demostrarme cada día la confianza en mí depositada. De la misma manera, quiero dar las gracias a Massimo Bietti, mi segundo director de tesis, por compartir conmigo el conocimiento, la química, las ideas, la manera de trabajar, las luchas estúpidas, las risas y los buenos recuerdos. Un agradecimiento muy grande va para Anna y Xavi por animarme siempre y por los buenos ratos juntos. Mis gracias van a Raquel por su disponibilidad y su fuerza infinita. Gracias a Alicia por sus preciosos consejos.

Sin toda la gente pasada y presente del QBIS esta tesis no sería la misma, así que quiero agradecer todo el grupo por haber compartido conmigo estos cuatro años, siempre me habéis hecho sentir como en casa y querida. Muy especialmente mis agradecimientos van para Sabeña por su gentileza desde mi primer día en el QBIS, a mis compañeros de vitrina Diego y Marco, os agradezco nuestros días de risas y de charlas, gracias por ser mis espaldas en los días difíciles; a Joan por haberme dado siempre su apoyo y por ser un ejemplo de seguir; a Oriol por ayudarme siempre cuando lo necesitaba y para las risas juntos; a Carles y Lorena y nuestras cortinas y barcos hundidos. En el barco conmigo siempre ha estado Cristina, quiero darte las gracias por escucharme, animarme y por todos los momentos compartidos felices y sinceros.

A las personas que he conocido en estos años, quiero agradecer a todas por haber compartido un trocito de vida conmigo.

Già sapete che questo non è proprio il mio forte, spero mi perdonerete se non riuscirò a comunicarvi nel modo giusto quanto sono felice di avervi conosciuto. Giorgio grazie per essere stato la mia guida, per tutti i consigli, gli insegnamenti e per essere un vero amico. Roberta grazie per il tuo sostegno ed i momenti

condivisi insieme. Valeria grazie per avermi caricata sempre con la tua allegria e la tua onestà, grazie per tutte le nostre infinite chiacchierate.

Vorrei ringraziare Olaf per essermi stato vicino in ogni momento, per aver condiviso con me una parte importante della nostra vita e per avermi resa felice ogni giorno.

Questa tesi è dedicata anche ai miei compagni di vita a Roma, anche se lontani in questi anni sono stati sempre presenti, Martina e Jacopo, Chiara e Simone, Silvia e Federico, Riccardo C., Danilo, Pierpaolo, Michele, Riccardo M., Francesca, Flaminia, Livia, Giulia e Alessandra.

Il ringraziamento più grande va sicuramente a tutta la mia famiglia per avermi sempre sostenuta e incoraggiata. Ai miei zii Sandro e Daniela, Susanna e Roberto, a mia cugina Tiziana e suo marito Giuseppe, a mio cugino Andrea, ai miei nonni. Alle mie colonne portanti, i miei genitori Massimo e Maria Antonietta, per la vostra costante e fondamentale presenza. Infine ringrazio l’altra metà del mio cuore Elisabetta, la persona che preferisco al mondo.

ACKNOWLODGEMENTS

This work would not have been possible without the following collaborations:

- Serveis tècnics de Recerca (STR) from Universitat de Girona for technical support, with special remark to Dr. Laura Gómez.
- Dr. Antoni Riera from Institute for Research in Biomedicine of Barcelona for the access to the polarimeter.
- Financial support by:

  CTQ2015-70795-P

  Generalitat de Catalunya/ 2014 SGR 862

GRAPHICAL ABSTRACT

Summary (p. 1)

Chapter I. General Introduction (p. 5)

Chapter II. Objectives (p. 43)

Chapter III. Tuning Selectivity in Aliphatic C–H Bond Oxidation of *N*-Alkylamides and Phthalimides Catalyzed by Manganese Complexes (p. 47)

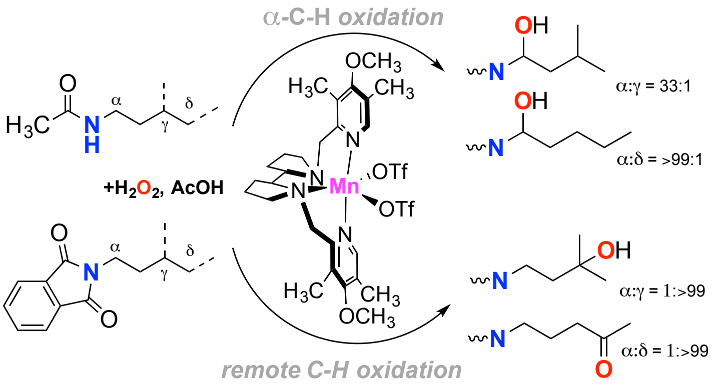
α-C-H oxidation
$+H_2O_2$, AcOH
α
γ
δ
OCH_3
H_3C
CH_3
N
Mn
OTf
OTf
OH
α:γ = 33:1
α:δ = >99:1
α:γ = 1:>99
α:δ = 1:>99
O
remote C-H oxidation

Chapter IV. Highly Enantioselective Oxidation of Nonactivated Aliphatic C–H Bonds with Hydrogen Peroxide Catalyzed by Manganese Complexes (p. 59)

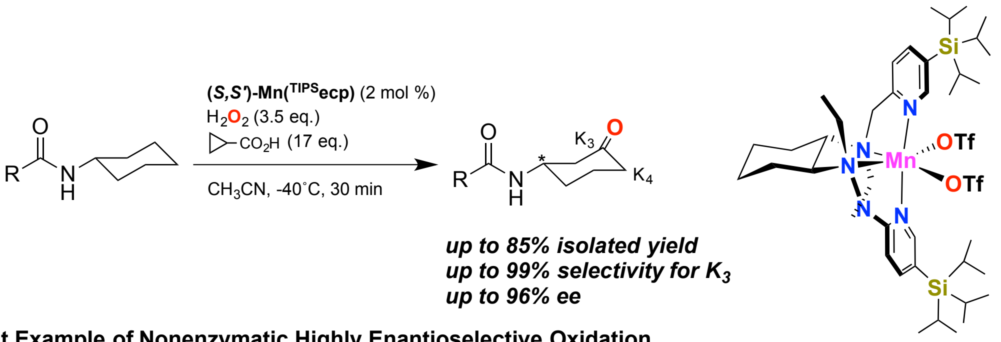
(S,S')-Mn(^{TIPS}ecp) (2 mol %)
H_2O_2 (3.5 eq.)
CO_2H (17 eq.)
CH_3CN, -40˚C, 30 min
R
N
H
O
K_3
K_4
*
up to 85% isolated yield
up to 99% selectivity for K_3
up to 96% ee
Si
Mn
OTf
OTf

First Example of Nonenzymatic Highly Enantioselective Oxidation of a Nonactivated Methylenic Site

(S,S')-[Mn($OTf)_2$(^{TIPS}ecp)]

Chapter V. Aliphatic C–H Bond Oxidation with Hydrogen Peroxide Catalyzed by Manganese Complexes: Directing Selectivity through Torsional Effects (p. 71)

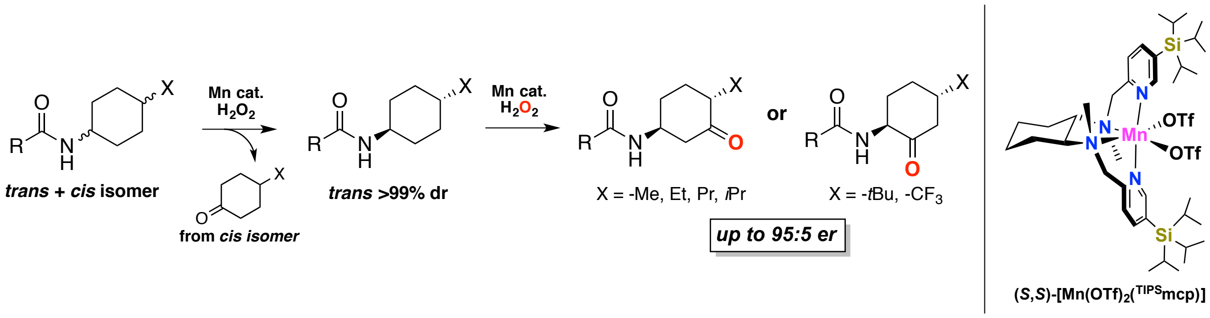
R
O
N
H
X
trans + *cis* isomer
Mn cat.
H_2O_2
O
X
from *cis isomer*
trans >99% dr
Mn cat.
H_2O_2
X = -Me, Et, Pr, *i*Pr
or
X = -*t*Bu, -CF_3
up to 95:5 er
Si
N
OTf
Mn
OTf
N
N
N
Si
(*S*,*S*)-[Mn(OTf)$_2$(^{TIPS}mcp)]

Chapter VI. Results and Discussion (p. 77)

Chapter VII. General Conclusions (p. 101)

Experimental Section (p. S1)

TABLE OF CONTENTS

Summary 1
Resum 2
Resumen 3
Chapter I. General Introduction 5
I.1. Challenges in C-H Bonds Functionalization 7
I.2. Control over Site-Selectivity in C-H Bonds Oxidations 7
  I.2.1. Bond Dissociation Energy 8
  I.2.2. Electronic Effects 9
  I.2.3. Steric Effects 13
  I.2.4. Directing Effects 14
  I.2.5. Stereoelectronic Effects 16
    I.2.5.1 Hyperconjugation Effects 16
    I.2.5.2 Strain Release 17
  I.2.6. Control over Oxidation in Complex Molecules 18
I.3. Enantioselective Aliphatic C-H Bond Oxidations 19
  I.3.1. Introduction 19
  I.3.2. Origin of Stereoselection in C-H Oxidation 23
  I.3.3. Typology of Enantioselective C-H Oxidation Reaction 23
    I.3.3.1 Enantioselective Desymmetrization of Alkanes 23
    I.3.3.2 Enantioselective C-H Bond Hydroxylation 29
I.4. References 38
Chapter II. Objectives 43
Chapter III. Tuning Selectivity in Aliphatic C-H Bond Oxidation of *N*-Alkylamides and Phthalimides Catalyzed by Manganese Complexes 47
Chapter IV. Highly Enantioselective Oxidation of Nonactivated Aliphatic C-H Bonds with Hydrogen Peroxide Catalyzed by Manganese Complexes 59
Chapter V. Aliphatic C-H Bond Oxidation with Hydrogen Peroxide Catalyzed by Manganese Complexes: Directing Selectivity through Torsional Effects 71
Chapter VI. Results and Discussion 77
VI.1. Tuning Selectivity in Aliphatic C-H Bond Oxidation of *N*-Alkylamides and Phthalimides Catalyzed by Manganese Complexes 79
VI.2. Highly Enantioselective Oxidation of Nonactivated Aliphatic C-H Bonds with Hydrogen Peroxide Catalyzed by Manganese Complexes........ 87
VI.3. Aliphatic C-H Bond Oxidation with Hydrogen Peroxide Catalyzed by Manganese Complexes: Directing Selectivity through Torsional Effects 93

VI.4. References 98
Chapter VII. General Conclusions 101
Experimental Section S1
    Experimental Section: Chapter VI.1. .... S5
    Experimental Section: Chapter VI.2. .... S19
    Experimental Section: Chapter VI.3. .... S43

Supplementary Data Information

Pdf file of the Ph. D. Dissertation.
Pdf file of the Digital Annex containing additional NMR, GC and HPLC spectra.
CIF files for crystal structure of **Mn(^{TIPS}mcp)**, **Mn(^{TIPS}ecp)** and **P10** oxidation product of **Chapter VI.2.**

SUMMARY

The oxidation of aliphatic C-H bonds is a very powerful reaction because it allows the functionalization of inert C-H bonds, converting them into a suitable sites for further chemical elaboration. However, it also represents one of the most challenging reactions in modern synthetic organic chemistry because the multitude of aliphatic C-H bonds in a molecule makes site selective oxidation particularly difficult. Moreover, the introduction of chirality represents an unmet but very appealing challenge, because the asymmetric oxidation of hydrocarbons produces chiral compounds of high value in organic synthesis from readily available starting materials. Until now, examples of enantioselective oxidation of nonactivated aliphatic C-H bonds remain exclusive to enzymes. Taking inspiration from the mechanism of action of transition metal dependent oxygenases, such as cytochrome P450, naphthalene 1,2-dioxigenase and proline 4-hydroxylase, this thesis has been devoted to the development of new catalytic systems capable to oxidize nonactivated aliphatic C-H bonds in a site-selective and enantioselective manner. In particularly, chemo- and enantioselective aliphatic C-H oxidation reactions, especially focused in amide containing substrates have been developed. These reactions have been carried out employing bioinspired manganese and iron complexes, bearing N-based tetradentate ligands, hydrogen peroxide as oxidant and carboxylic acids, in short reaction times and under mild conditions. Moreover, well aligns with sustainability criteria, extremely important in today's society; it is based on first row transition metal catalysts (iron and manganese), less toxic than the noble metals traditionally employed in catalysis, in combination with hydrogen peroxide, an oxidant that exhibits a high atom economy and that only generates water as by-product. Chapter III describes the site-selective C-H bond oxidation of *N*-alkylamides and phthalimides. It has been demonstrated that amides can be employed as superior functional groups for modulating site-selectivity in C-H bond oxidation reactions, where by means of electronic, steric and stereoelectronic effects, activation or deactivation of proximal C-H bonds can be finely tuned. In Chapter IV a family of chiral sterically demanding manganese complexes, characterized by the presence of the *tri*isopropylsilyl group (TIPS) on the pyridine rings of the ligand, were synthetized as catalysts. The impact of the steric properties of the catalysts in C-H bond oxidation reactions have been studied using mosubstituted cyclohexanes as substrates. The positive role of carboxylic acids in the activation of hydrogen peroxide and on the reaction stereoselectivity has been also studied. From these studies, manganese complexes bearing TIPS groups on the aminopyridine ligands, in combination with the optimal carboxylic acid, have emerged as particularly efficient and stereoselective C-H oxidizing systems. In Chapter V, torsional effects have been disclosed as powerful site directing tools in the C-H oxidation of disubstituted cyclohexane scaffolds. This element allows the kinetic resolution of *cis*-*trans* mixtures of 4-substituted *N*-cyclohexylamides, leading to quantitative conversion of the *cis*-isomers, allowing the isolation and successive conversion of the *trans*-isomers into densely functionalized oxidation products with excellent site-selectivity and good enantioselectivity.

RESUM

L'oxidació d'enllaços C-H alifàtics és una reacció altament interessant perquè permet funcionalitzar l'enllaç C-H inert, generant molècules d'alt interès sintètic. No obstant, també es tracta d'una de les reaccions que més atenció ha generat en en el camp de la química orgànica sintètica moderna perquè la multitud d'enllaços C-H alifàtics present en una mateixa molècula fa que l'oxidació selectiva d'un enllaç específic sigui particularment difícil. A més, la introducció de quiralitat en aquesta reacció representa, encara a dia d'avui, un repte molt atractiu, ja que l'oxidació asimètrica d'hidrocarburs, compostos altament abundants a la naturalesa, permet l'obtenció de compostos quirals d'alt valor en síntesi orgànica; i de moment, segueix sent una transformació exclusiva dels enzims. Inspirada en el mecanisme d'acció de les oxigenases dependents de metalls de transició, com el citocrom P450, la naftalè 1,2-dioxigenasa i la prolina 4-hidroxilasa, aquesta tesi està enfocada en el desenvolupament de nous sistemes catalítics capaços d'oxidar enllaços C-H alifàtics no activats d'una manera selectiva i enantioselectiva. En particular, s'han desenvolupat reaccions d'oxidació de C-H alifàtiques quimio- i enantioselectives, enfocades en substrats que contenen un grup funcional amida. Aquestes reaccions s'han obtingut utilitzant complexos bioinspirats de manganès i ferro basats en lligands tetradentats de tipus *bis*-amina-*bis*-piridina, peròxid d'hidrogen com a oxidant i àcids carboxílics, en temps de reacció curts i en condicions suaus. A més, aquest sistema compleix els criteris de sostenibilitat, cada vegada més importants en la societat actual; ja que es basa en catalitzadors de metalls de la primera sèrie de transició (ferro i manganès), menys tòxics que els tradicionals metalls nobles (ruteni, rodi, osmi), en combinació amb peròxid d'hidrogen, un oxidant que exhibeix una elevada economia atòmica i que només genera aigua com a residu. El Capítol III descriu les oxidacions selectives de l'enllaç C-H de *N*-alquilamides i ftalimides. S'ha demostrat que les amides es poden emprar com a excel·lents grups funcionals per modular la selectivitat en les reaccions d'oxidació. S'ha demostrat que les propietats electròniques, estèriques i estereoelectròniques de les amides es poden modular, activant o desactivant els enllaços C-H proximals. En el Capítol IV es mostra la síntesi d'una família de complexos de manganès quirals voluminosos, caracteritzats per la presència del grup *tris*-(isopropil)silil (TIPS) a les piridines del lligand. L'impacte de les propietats estèriques dels catalitzadors en les reaccions d'oxidació de l'enllaç C-H s'ha estudiat utilitzant ciclohexans monosubstituïts com a substrats. També s'ha estudiat l'impacte de l'àcid carboxílic en l'activació del peròxid d'hidrogen i en l'estereoselectivitat de les reaccions. A partir d'aquests estudis, els complexos voluminosos de manganès, en combinació amb l'òptim àcid carboxílic, han estat identificats com a sistemes oxidants particularment estereoselectius i eficients. En el Capítol V, s'han estudiat els efectes torsionals a la selectivitat per a l'oxidació de ciclohexans disubstituïts. Aquest efecte permet la resolució cinètica de mescles *cis*-*trans* de *N*-ciclohexilamides 4-substituïdes, permetent la conversió quantitativa dels isòmers *cis* i l'aïllament i la conversió successiva dels isòmers *trans* en productes d'oxidació densament funcionalitzats amb excel·lent selectivitat i bona enantioselectivitat.

RESUMEN

La oxidación de los enlaces C-H alifáticos es una reacción altamente interesante porque permite funcionalizar el enlace C-H inerte, generando moléculas de mayor interés sintético. Sin embargo, también se trata de una de las reacciones que más atención ha generado en el campo de la química orgánica sintética moderna porque la multitud de enlaces C-H alifáticos presente en una misma molécula, hace que la oxidación selectiva de un enlace especifico sea particularmente difícil. Además, la introducción de quiralidad todavía representa un reto muy atractivo, ya que la oxidación asimétrica de hidrocarburos, compuestos altamente abundantes en la naturaleza, permite la obtención de compuestos quirales de alto valor en síntesis orgánica; y de momento, sigue siendo una trasformación exclusiva de los enzimas. Inspirada por el mecanismo de acción de las oxigenasas dependientes de metales de transición, como el citocromo P450, la naftaleno-1,2-dioxigenasa y la prolina 4-hidroxilasa, esta tesis está enfocada en el desarrollo de nuevos sistemas catalíticos capaces de oxidar enlaces C-H alifáticos no activados de una manera selectiva y enantioselectiva. En particular, se han desarrollado reacciones de oxidación de C-H alifáticas quimio- y enantioselectivas, enfocadas en sustratos que contienen un grupo funcional amida. Estas reacciones se han obtenido usando complejos bioinspirados de manganeso y hierro basados en ligandos tetradentados de tipo *bis*-amina-*bis*-piridina, H_2O_2 como oxidante y ácidos carboxílicos, en tiempos de reacción cortos y en condiciones suaves. Este sistema cumple con los criterios de sostenibilidad, cada vez más importantes en la sociedad actual; se basa en catalizadores de metales de la primera serie de transición (Fe y Mn), menos tóxicos que los tradicionales metales nobles (Ru, Rh, Os), en combinación con peróxido de hidrógeno, un oxidante que exhibe una elevada economía atómica y que sólo genera agua como residuo. El Capítulo III describe las oxidaciones selectivas del enlace C-H de *N*-alquilamidas y ftalimidas. Se ha demostrado que las amidas se pueden emplear como excelentes grupos funcionales para modular la selectividad en las reacciones de oxidación. Se ha demostrado que las propiedades electrónicas, estéricas y estereoelectrónicas de las amidas se pueden modular, activando o desactivando los enlaces C-H proximales. En el Capítulo IV se muestra la síntesis de una familia de complejos de manganeso quirales voluminosos, caracterizados por la presencia del grupo *tris*-(isopropilo)sililo (TIPS) en las piridinas del ligando. El impacto de las propiedades estéricas de los catalizadores en las reacciones de oxidación del enlace C-H se ha estudiado utilizando ciclohexanos monosustituidos como sustratos. También se ha estudiado el impacto del ácido carboxílico en la activación del H_2O_2 y en la estereoselectividad de las reacciones. Los complejos voluminosos de manganeso, en combinación con el óptimo ácido carboxílico, han sido identificados como sistemas oxidantes particularmente estereoselectivos y eficientes. En el Capítulo V, se han estudiado los efectos torsionales en la selectividad para la oxidación de ciclohexanos disustituidos. Este efecto permite la resolución cinética de mezclas *cis*-*trans* de *N*-ciclohexilamidas 4-sustituidas, permitiendo la conversión cuantitativa de los isómeros *cis* y el aislamiento y la conversión sucesiva de los isómeros *trans* en productos de oxidación densamente funcionalizados con excelente selectividad y buena enantioselectividad.

Chapter I

General Introduction

I.1. Challenges in C-H Bond Functionalization

The functionalization of nonactivated aliphatic C-H bonds is a very powerful reaction because it converts these inert bonds, ubiquitous in organic molecules, into functional groups suitable for further chemical elaboration. However, it constitutes one of the most challenging reactions in the field of modern synthetic organic chemistry because of the inert nature of the C-H bonds. This general lack of reactivity derives from the fact that C and H atoms are held together by strong, non-polarized and localized bonds. Neither low-energy empty orbitals, nor high-energy filled orbitals that could facilitate a chemical reaction are available. Along with the problems derived from their inert character, the multitude of aliphatic C-H bonds in a molecule makes site selective functionalization particularly arduous. This problematic issue is further accentuated because the high reactivity of the species capable of breaking these bonds is often incompatible with chemo- and site-selective transformations. A powerful class of reactions is represented by C-H bond oxidations, that introduce oxidized functionality directly into aliphatic (sp^3) C-H bonds. The direct incorporation of an oxygenated functionality into a molecule is important from a synthesis economy point of view, and moreover, further transformation of these groups into an array of functional groups can disclose new and more efficient synthetic pathways.

I.2. Control over Site-selectivity in C-H Bond Oxidation

In order to plan selective C-H bond oxidation, the relative reactivity of these bonds has to be deeply understood. Consequently, in the last decade a lot of efforts have been dedicated to this issue. These studies have led to the definition of selectivity factors, based on the operation of electronic, steric, directing and stereoelectronic effects. Collectively, these factors determine the relative reactivity of C-H bonds against electrophilic oxidizing agents. A thorough understanding of these factors permits the reliable prediction of preferential oxidation sites in molecules containing multiple and not equivalent C-H bonds. Among the available strategies for the selective functionalization of aliphatic C-H bonds, reactions promoted by hydrogen atom transfer (HAT) to radical or radical-like species, such as dioxiranes and metal-oxo species have attracted great interest.

Metal-catalyzed oxidation mechanism are well established (Scheme I.1., a).[1-2] As shown in Scheme I.1.a, after the oxidation of the metal to generate a high-valent metal-oxo species, the oxygen atom is transferred from the oxo complex to the substrate through a two-step process: HAT from the substrate, followed by fast rebound of the hydroxyl group to the first-formed carbon radical. Different mechanisms have been proposed for aliphatic C-H bond oxidation promoted by dioxiranes in the works reported by Murray and Curci,[3-8] Minisci[9-10], Bach[11] and Houk.[12] Recently, a detailed computational study on the reaction of dimethyldioxirane (DMDO) with substituted cyclohexanes and *trans*-decalin has been carried out by Houk et al.[13] This study strongly supports a mechanism that proceeds through HAT followed by in cage collapse of the first formed radical couple. This mechanism is also supported by experimental evidences found in these reactions, such as site-selectivity and retention of stereochemistry at the oxidized carbon. In 2016, Houk published another work describing the molecular dynamics of DMDO C-H oxidation of isobutane, providing additional support to this mechanistic hypothesis.[14] (Scheme I.1.b).

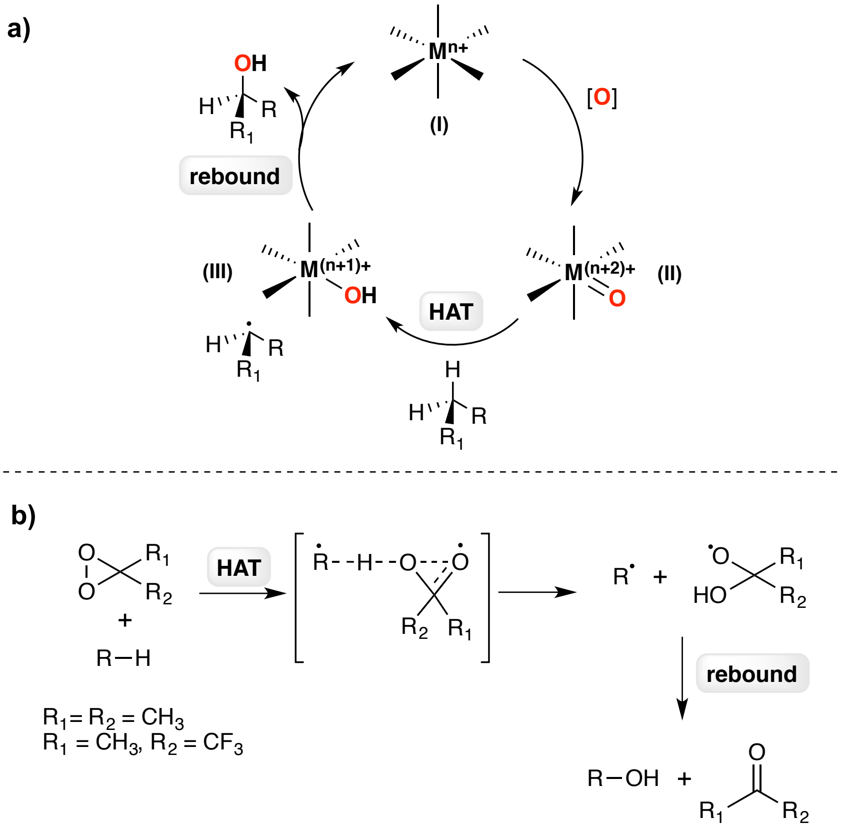

Scheme I.1. a) Simplified C-H hydroxylation mechanism via initial hydrogen atom transfer (HAT) from a C-H bond to high valent metal-oxo species. **b)** Proposed mechanism of dioxirane-mediated oxidations.

I.2.1. Bond Dissociation Energy

C-H bond strengths represent the major factor dictating their relative reactivity. The bond strength is measured by the homolytic bond dissociation energy (BDE), that is the energy necessary to break a generic R-X bond. The pertinent BDEs for different types of C-H bonds are reported in Scheme I.2. Benzylic, allylic and C-H bond that are α- to an heteroatom are relatively weak C-H bonds, characterized by relatively low BDEs (85.4, 87.0 and 92.1 kcal/mol for ethylbenzene, cyclohexene and tetrahydrofuran, respectively).[15] As a consequence, cleavage of these C-H bonds is generally relatively easy . Instead, the oxidation of aliphatic C-H bonds represent a more difficult reaction, due to the higher BDEs, comprised between 96 and 101 kcal/mol (Scheme I.2.).[15] Moreover, when considering aliphatic oxidation reactions, by taking into account that the majority of C-H oxidizing reagents display an electrophilic character, the more electron rich is the C-H bond the more reactive it is toward its oxidation. For instance, the following trend is generally observed in C-H bond oxidation reactions: tertiary > secondary > primary C-H bond (Scheme I.2.).

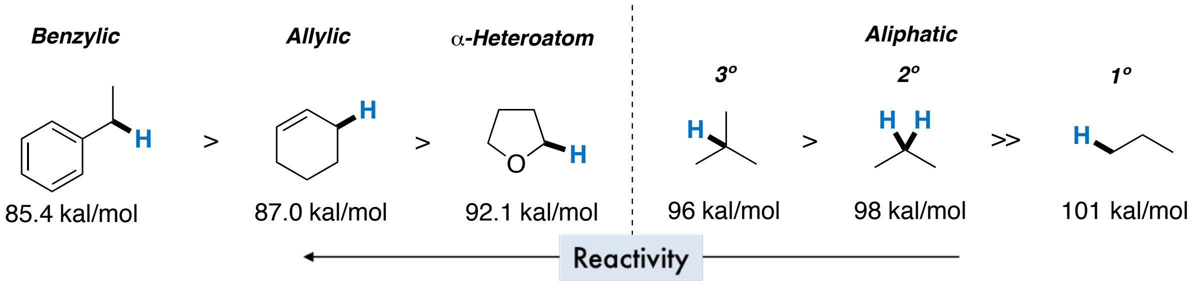

Scheme I.2. General scheme of bond dissociation energies of different aliphatic C-H bonds.

I.2.2. Electronic Effects

Electrophilic oxidizing species can result sensitive to the local chemical environment of the substrate. In a substrate to be oxidized, the electronic character of the C-H bonds can strongly influence the site-selectivity of the reaction. For example, it has been observed that the presence of an electron-withdrawing group (EWG) deactivates proximal sites via inductive effects (Scheme I.3., above), thereby the introduction of different EWG or ERG led to a drastic change in site-selectivity for the C-H bond oxidation reactions. Is also possible that differences in steric environment between two electronically similar tertiary C-H bonds, can operate synergistically with inductive effects to achieve selectivity. Moreover, while tertiary positions are the most electron rich, the secondary methylene groups are more accessible and the selectivity can be influenced by the reagent employed (Scheme I.3., above). For example, the use of small oxidizing reagents such as methyl(trifluoromethyl) dioxirane (TFDO) gave preferential oxidation at the more electron rich and sterically hindered tertiary C-H bonds, while sterically demanding reagents such as an iron-oxo N-based complex (White's catalyst), exhibited a lower selectivity for tertiary sites.

The results obtained in some aliphatic C-H oxidation reactions with different electrophilic reagents are reported in Scheme I.3: $[Fe(II)(pdp)(CH_3CN)_2](SbF_6)_2$, **Fe(pdp)** (Scheme I.3.a),[16-17] methyl(trifluoromethyl) dioxirane (Scheme I.3.b, TFDO)[18] and a *N*-bromoamide derivative (Scheme I.3.c).[19] In substrates bearing EWGs, functionalization occurred preferentially at the most remote secondary or tertiary position, in all the cases with very high site-selectivity.

C-H bond oxidation reactions catalyzed by **Fe(pdp)** in the presence of AcOH and H_2O_2 as oxidant are reported in Scheme I.3.a .[16-17] It has been demonstrated that the use of AcOH has a beneficial effect on epoxidation of alkenes and aliphatic C-H bond oxidation reactions, increasing the catalytic activity of the iron complexes, thus improving product yields and selectivities.[20-21] Moreover, the use of different carboxylic acids can strongly impact the stereoselectivity of Mn or Fe catalyzed epoxidation reactions with related catalysts.[22-24] These acids can bind to the metal center, *cis* to the site where H_2O_2 is activated, and contribute in defining the active site.[25-26] The results obtained with the other substrates shown in Scheme I.3. underline the selective, electrophilic nature of the active oxidant generated with the iron complex and H_2O_2.

The same trend was observed for the oxidation of ester substrates achieved employing the electrophilic TFDO as the oxidant (Scheme I.3.b).[18] The oxidations of linear and cyclic aliphatic esters with TFDO are reported in Scheme I.3.b. It is well established that in the oxidation of aliphatic C-H bonds TFDO displays an electrophilic character,[4, 27-28] accordingly, ester groups, being EWGs impact on the relative reactivity of C-H bond in close proximity of this functional group, and the reactivity of the methylenic groups increases with increasing the distance from the ester function. Oxidation occurs at the most remote position of the aliphatic chain and C_α-H and C_β-H bonds are typically not oxidized. Instead, the presence of a tertiary C-H bond in the ester substrate, gave the oxidation on the tertiary C_β-H as major product, because the electronic deactivation induced by the ester group is overlaid by the weaker nature of tertiary over secondary C-H bonds.

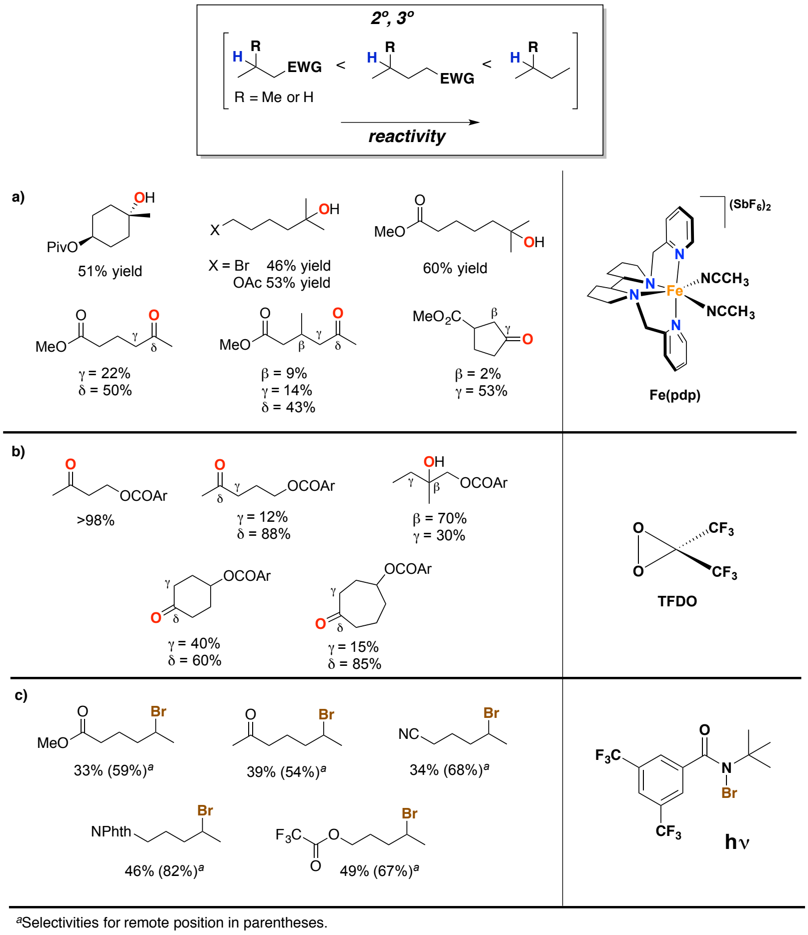

2°, 3°
EWG
R = Me or H
<
reactivity
a)
OH
PivO
51% yield
X
X = Br 46% yield
OAc 53% yield
MeO
60% yield
γ = 22%
δ = 50%
β = 9%
γ = 14%
δ = 43%
MeO2C
β = 2%
γ = 53%
(SbF6)2
N
Fe
NCCH3
Fe(pdp)
b)
OCOAr
>98%
γ = 12%
δ = 88%
β = 70%
γ = 30%
γ = 40%
δ = 60%
γ = 15%
δ = 85%
CF3
TFDO
c)
Br
33% (59%)a
39% (54%)a
NC
34% (68%)a
NPhth
46% (82%)a
F3C
49% (67%)a
hν
aSelectivities for remote position in parentheses.

Scheme I.3. Electronic effects on C-H bond oxidation reactions.

Aliphatic C-H bond functionalization reactions initiated by HAT are also affected by the presence of different EWGs on the substrate. Scheme I.3.c shows that intermolecular aliphatic C-H brominations with *N*-bromoamides and visible light proceed with high site-selectivities.[19] The scheme displays a series of linear monofunctionalized hydrocarbons as substrates. Functional groups include an ester, a ketone, a nitrile and a phthalimide. The selectivity for the δ position depends on the relative electron-withdrawing character of the functional group. Indeed, the presence of the phthalimido group induces the higher selectivity for functionalization at the remote position and no α or β functionalization was observed.

The sensitivity of the electrophilic iron catalyst **Fe(pdp)** to the electronic environment of a tertiary C-H bond is illustrated in Scheme I.4., where the oxidation of a series of dihydrocitronellol derivatives with different EWGs in α or β positions to one of the two tertiary C-H centers is shown. In the substrate where no EWG is present, alcohol products in both tertiary centers are formed in an equimolar amount. In all other cases, hydroxylation occurred preferentially at the remote tertiary position. β-Acetate and halogens gave modest selectivity while α–EWGs gave an excellent selectivity for the remote site, up to >99:1 when an acyl moiety is directly bound to the proximal tertiary site.

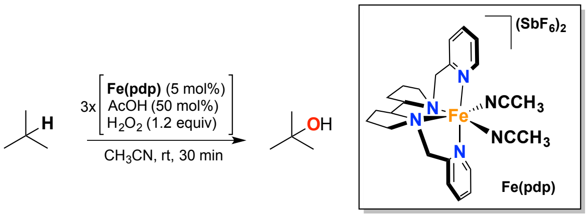

Entry	Substrate	Major Product		Isolated yield % (rsm)^a	Remote: Proximal
1	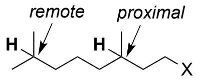	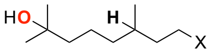	X = H	48 (29)	1:1
2			X = OAc	43 (35)	5:1
3			X = Br	39 (32)	9:1
4			X = F	43 (20)	6:1
5	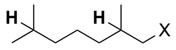	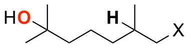	X = OAc	49 (21)	29:1
6			X = Br	48 (17)	20:1
7	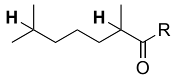	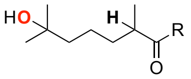	X = CH_3	52 (18)	>99:1
8			X = OCH_3	56 (32)	>99:1

^{a}rsm = % recovered starting material. ^{b}GC analysis

Scheme I.4. Effect of EWGs on site-selectivity in the oxidation tertiary C-H bonds.

Nitrogen-containing molecules such as aliphatic amines (3º, 2º, 1º), pyridines and imides are a very important class of compounds, present in the core structures of different organic materials, natural products and bioactive molecule.[29-30] Existing methods for the C(sp^3)-H functionalization of aliphatic amines involve both functionalization at the more activated C-H bond in α to the nitrogen atom[31-35] or the use of the nitrogen atom as a part of a directing group.[36-38] To achieve remote oxidation reactions on amines, protonation or complexation of the nitrogen atom converts it in a strong electron-withdrawing group, deactivating the proximal C-H bonds. In metal catalyzed reactions, protonation also avoids the common catalyst deactivation by binding of the amine to the metal center. This methodology to achieve remote C-H reactions on primary and secondary amines was pioneered by Asensio and co-workers using dioxiranes as oxidants.[39] Representative results are shown in Scheme I.5.a. Ammonium salts were prepared *in situ* by adding tetrafluoroboronic acid to the solution of the amine. The strong electron withdrawing effect of the ammonium group directs oxidation to the remote tertiary C-H bond, leading to the formation of the aminoalcohol product in high yield.

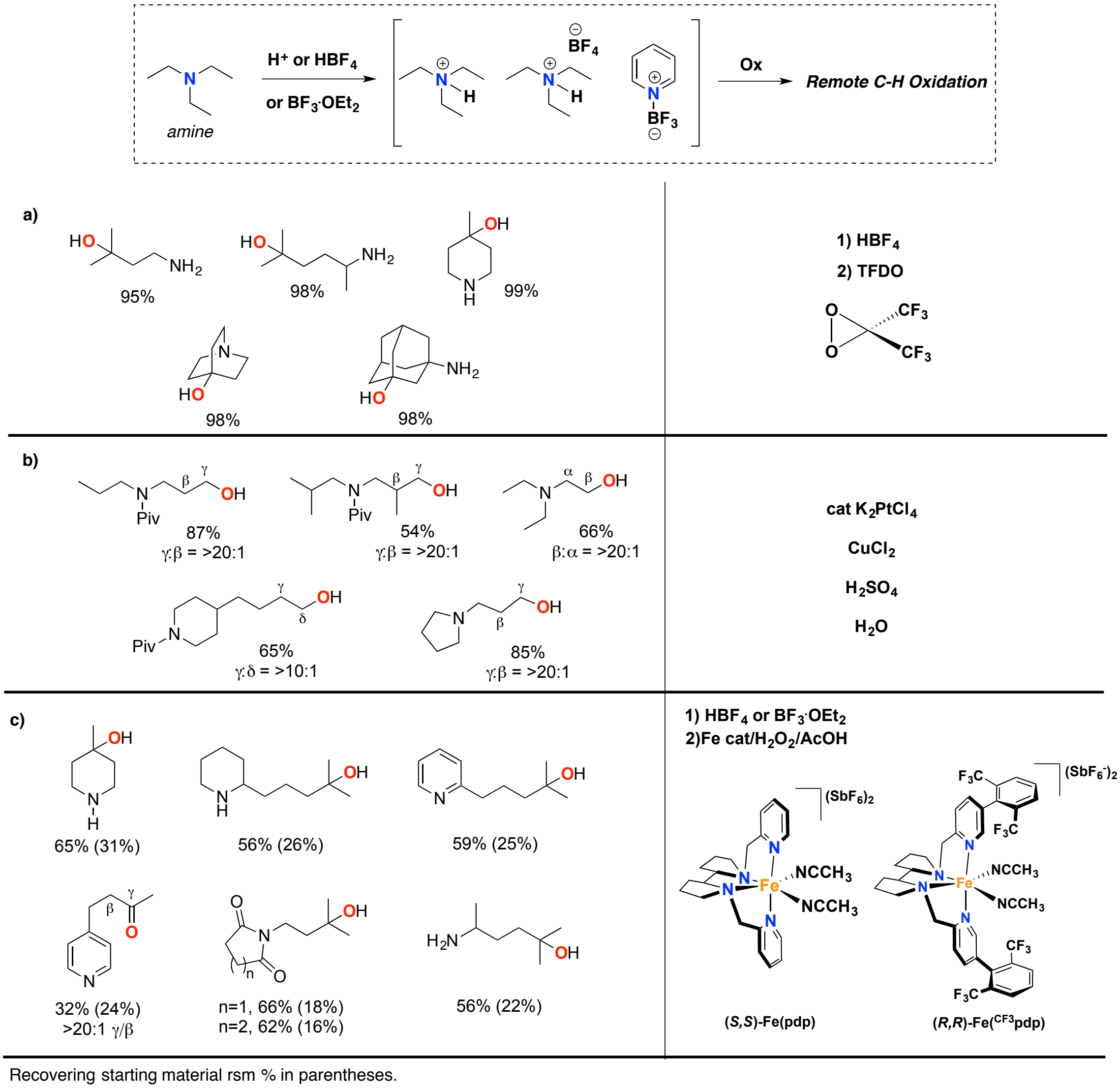
amine
H+ or HBF4
or BF3·OEt2
BF4
H
H
N
BF3
Ox
Remote C-H Oxidation
a)
95%
98%
99%
98%
98%
1) HBF4
2) TFDO
CF3
CF3
b)
Piv
87%
γ:β = >20:1
54%
γ:β = >20:1
66%
β:α = >20:1
65%
γ:δ = >10:1
85%
γ:β = >20:1
cat K2PtCl4
CuCl2
H2SO4
H2O
c)
65% (31%)
56% (26%)
59% (25%)
32% (24%)
>20:1 γ/β
n=1, 66% (18%)
n=2, 62% (16%)
56% (22%)
1) HBF4 or BF3·OEt2
2)Fe cat/H2O2/AcOH
(SbF6)2
(SbF6-)2
NCCH3
(S,S)-Fe(pdp)
(R,R)-Fe(CF3pdp)
Recovering starting material rsm % in parentheses.

Scheme I.5. Protonation or complexation driven remote C-H bond oxidation of amines.

Following the same concept, Sanford and co-workers reported the protonation-driven remote oxidation of primary, secondary and tertiary amines. In Scheme I.5.b representative examples are shown.[40-42] In particular, good to excellent terminal selectivity was observed for the products displayed in all the highlighted examples. The terminal selectivity also reflects the inherent steric preference of the Pt catalyst for activation of 1º over 2º or 3º C-H bonds.[43-46]

Deactivation of the vicinal positions to a nitrogen group, was also obtained by White and co-workers (Scheme I.5.c).[47] The complexation of the nitrogen atom with Lewis or Brønsted acids affords the remote C(sp^3)-H oxidation catalyzed by electrophilic **Fe(pdp)** iron complexes. Reaction with a Lewis acid (BF_3) or irreversible protonation with tetrafluoroboronic acid (HBF_4) transforms the amine group into a very strong EWG, deactivating the α-C-H bonds toward oxidation. Piperidines, pyridines, imides and also primary amines are oxidized at remote tertiary or secondary positions with modest to high isolated yields and excellent site-selectivity.

I.2.3. Steric Effects

Sterically hindered positions are oxidized with lower efficiency as compared to less-hindered counterparts.
In Scheme I.6. two examples are shown where steric effects play a significant role in determining the site-selectivity of the reaction. The iron-catalyzed oxidation of (–)-acetoxy-*p*-menthane shows the importance of steric hindrance in dictating selectivity.[16, 48] The tertiary position of the cyclohexyl ring is oxidized preferentially in comparison with the isopropyl group. This result can be rationalized on the basis of the reduced steric hindrance of the endocyclic tertiary C-H bond as compared to the exocyclic one, since both tertiary C-H bonds are similar in terms of electronic environments. The use of the bulkier **Fe(mcpp)** instead of **Fe(pdp)** complex increases the preference for C1 up to 17:1. In this case steric effects in both the substrate and the catalyst cooperate to discriminate between C1 and C8. The opposite selectivity is observed on the same menthol derivative in the case of C-H azidation, carried out employing an iron catalyst and a hypervalent iodine reagent.[49] This different selectivity can be tentatively explained on the basis of the greatest conformational flexibility of the isopropyl side chain.

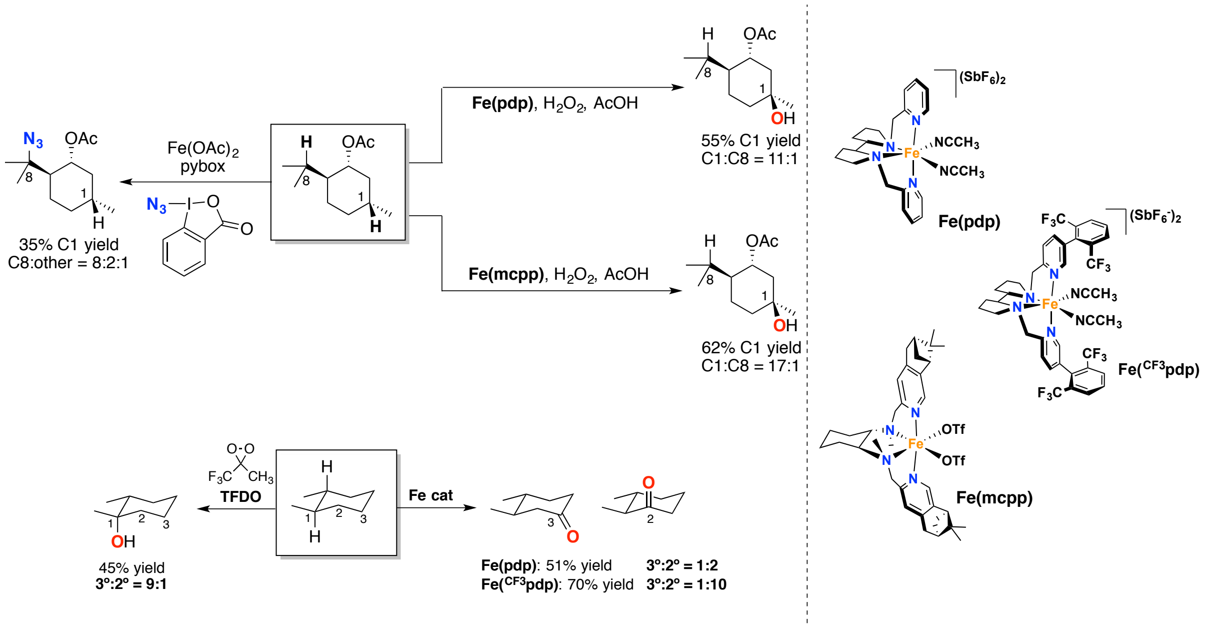
N3
OAc
8
1
H
35% C1 yield
C8:other = 8:2:1
Fe(OAc)2
pybox
N3—I—O
O
H
OAc
8
1
H
Fe(pdp), H2O2, AcOH
Fe(mcpp), H2O2, AcOH
H
OAc
8
1
OH
55% C1 yield
C1:C8 = 11:1
H
OAc
8
1
OH
62% C1 yield
C1:C8 = 17:1
(SbF6)2
N
NCCH3
NCCH3
Fe
Fe(pdp)
F3C
(SbF6-)2
CF3
CF3
F3C
Fe(CF3pdp)
OTf
OTf
Fe(mcpp)
O-O
F3C
CH3
TFDO
H
1
2
3
H
1
2
3
OH
45% yield
3º:2º = 9:1
Fe cat
3
O
O
2
Fe(pdp): 51% yield
Fe(CF3pdp): 70% yield
3º:2º = 1:2
3º:2º = 1:10

Scheme I.6. Steric effects on C-H oxidation reactions of simple substrates.

Another example of the effect of the steric environment of the reagent or the catalyst on site selectivity has been observed in the oxidation of *trans*-1,2-dimethylcyclohexane.[5, 17, 50] The preference for the tertiary C-H bond displayed by TFDO is underlined in the case of this substrate, indeed C1 is oxidized preferentially with a 3º:2º ratio of 9:1.[5] A different behavior is observed when the reactions are carried out employing the **Fe(pdp)** complex.[17] In this case the strong preference for hydroxylation at the weaker tertiary C-H bond is overcome by the bulky nature of the oxidant formed with the iron catalyst, which directs oxidation towards the stronger but sterically more accessible methylenic sites (3º:2º ratio of 1:2). Further increase in the 3º:2º ratio up to 1:10 is observed with the bulkier **Fe(^{CF3}pdp)** catalyst.

I.2.4. Directing Groups

Directed oxidation represents an excellent opportunity to oxidize a particular C-H bond overriding the presence of electronic, steric and stereoelectronic factors. On the basis of the role of acetic acid on the catalytic activity of **Fe(pdp)**, White and coworkers employed a carboxylic acid group on the substrate to direct the oxidation towards a specific site (Scheme I.7.).[16, 51] The hexanoic acid derivative gave the corresponding five-membered ring lactone as unique product in high yield, while the oxidation of the ester derivative gave the ketone derived from oxidation of a remote methylenic group as mayor product. The second example reported in Scheme I.7., shows the ability of the carboxylic group to override electronic effects, resulting from the presence of the acetoxy group, directing instead oxidation toward relatively electron poor sites. The methyl esters are oxidized to give the lactone product. Moreover, as the EWG group is moved away from the tertiary site, the substrate becomes more reactive (from 26% to 35% yield). Instead, the carboxylic acid derivatives were oxidized more efficiently providing much better yields (from 50% to 63% yield).

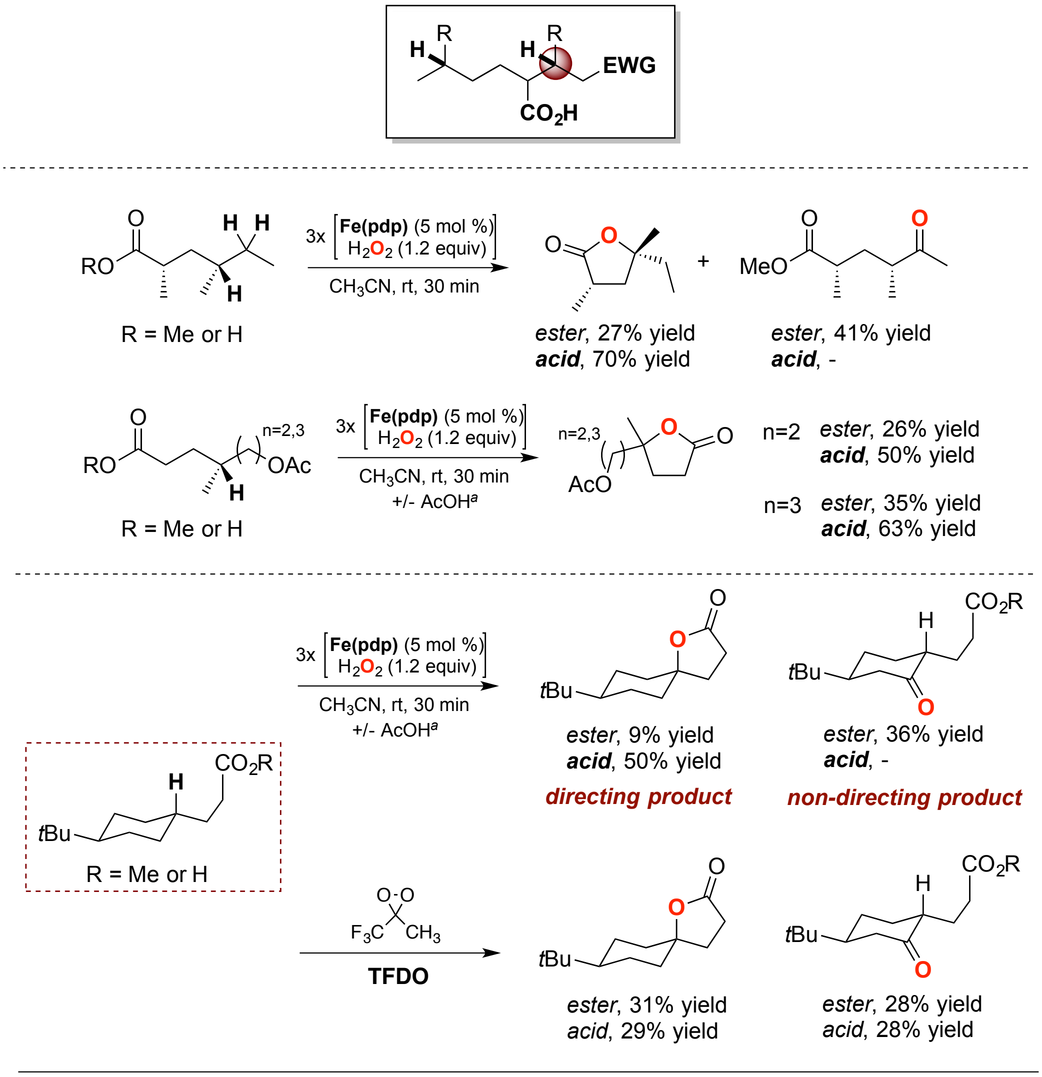
EWG
CO_2H
3x [Fe(pdp) (5 mol %) H_2O_2 (1.2 equiv)]
CH_3CN, rt, 30 min
R = Me or H
ester, 27% yield
acid, 70% yield
ester, 41% yield
acid, -
n=2,3
OAc
+/- AcOH[a]
AcO
n=2 ester, 26% yield
acid, 50% yield
n=3 ester, 35% yield
acid, 63% yield
tBu
CO_2R
ester, 9% yield
acid, 50% yield
directing product
ester, 36% yield
acid, -
non-directing product
F_3C CH_3
TFDO
ester, 31% yield
acid, 29% yield
ester, 28% yield
acid, 28% yield

[a]Reactions of methyl esters included 3 x 50 mol % AcOH.

Scheme I.7. Representative examples in which steric and electronic effects are overridden by the presence of a carboxylic acid directing group.

The oxidation of a *tert*-butylcyclohexane derived ester and corresponding acid derivative were also studied (Scheme I.7.). The ester affords the lactone product in 9% yield, while the mayor product is the ketone arising from oxidation of a less sterically hindered secondary site on the cyclohexyl ring. In contrast, the carboxylic acid derivative provides exclusively the lactone product in 50% yield. The use of the electrophilic reagent TFDO to perform the oxidation of the same substrates, shows no directing effect. In fact, similar yields (1:1 ratio) for the two oxidation products were obtained for both the ester and carboxylic acid derivatives.

I.2.5. Stereoelectronic Effects

I.2.5.1 Hyperconjugation Effects

Hyperconjugative effects represents another form to achieve selective C-H bond oxidation. Groups capable to donate electron density from a filled orbital to the antibonding orbital of a C-H bond can be used to activate this C-H bond toward oxidation. For example, it has been found that the cyclopropane ring, having a *p*-character in the C-C bonding orbitals, can populate σ* orbitals of adjacent C-H bonds, weakening these bonds and activating them towards oxidation.[52-54]

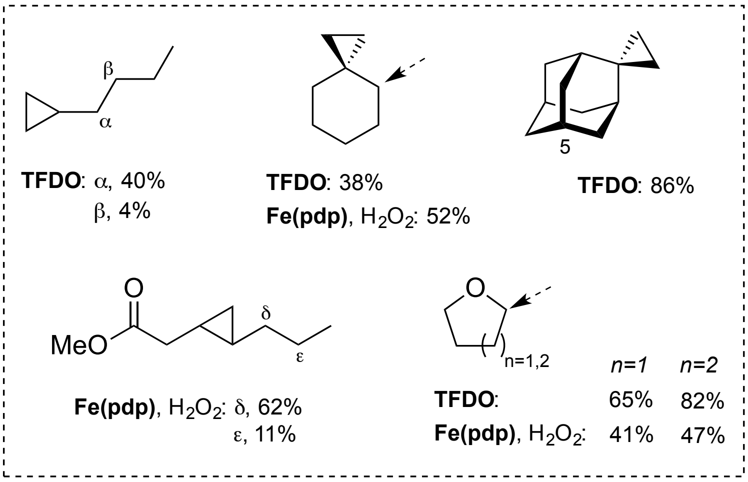

Scheme I.8. Hyperconjugation by cyclopropanes and heteroatoms activates vicinal C-H bonds.

In the case of butylcyclopropane, oxidation occurs at the methylenic position α to the cyclopropane group.[55] Oxidation of spiro[2.5]octane also occurs on the position that is vicinal to the cyclopropane ring.[55] When the **Fe(pdp)** catalyst is used to oxidize the same substrate, the presence of the cyclopropane ring permits to override steric effects, displaying the same site-selectivity.[17] Spiro-[cyclopropane-1,2'-adamantane] is particularly interesting, in this case hydroxylation occurs only at C5.[55] The proximal positions are deactivated because their *p*-orbital component is forced to lay in an unfavorable perpendicular conformation with respect to the cyclopropane ring. By installing a cyclopropane group on the side chain, the selectivity in the oxidation of methylheptanoate can be changed in favor of the δ position, usually deactivated by the electronic effect of the ester group.[17] Finally, hyperconjugative activation can be also exerted by an heteroatom such as an oxygen atom of an ether. Although the oxygen atom can exert an electron withdrawing inductive effect, the lone-pair electrons of an ethereal oxygen can donate electron density to the adjacent C-H bonds through hyperconjugative overlap, activating these positions. The electronic activating effect of the oxygen atom enables the selective oxidation of tetrahydrofuran and tetrahydropyran to give the corresponding lactone products.[17, 56]

I.2.5.2 Strain Release

This subtle effect has attracted increasing attention in recent years and is now recognized as an important factor to be considered for the selective C-H bond oxidation of cyclic substrates. Strain release was initially proposed by Eschenmoser and Schreiber in 1955 in the study of the oxidation of steroidal alcohols. It was observed that axial alcohols reacted faster than the corresponding equatorial ones.[57] They hypothesized that the release of 1,3-diaxial strain in the transition state, for the case of the axial alcohol results in a decrease in the activation barrier and an increase in reactivity. Later on, this important effect was highlighted by Baran in the oxidation of the 2,2,2-trifluoroethyl carbamate of the eudesmane terpene dihydrojunenol (Scheme I.9.).[58]

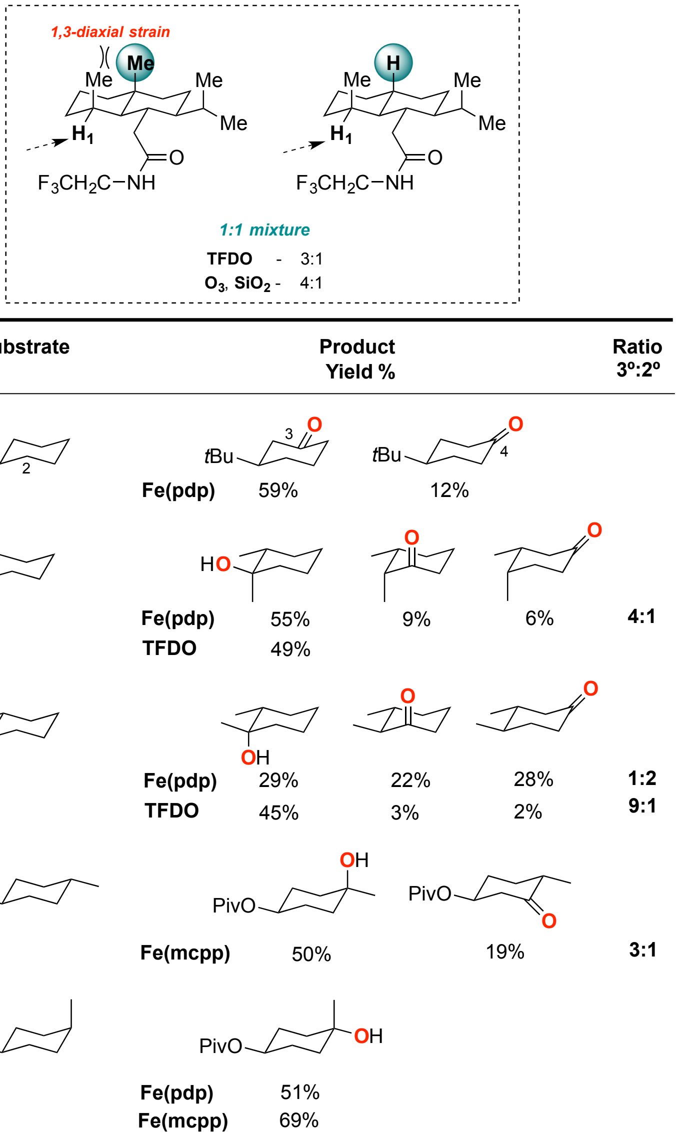
1,3-diaxial strain
Me
Me
Me
Me
H1
F3CH2C−NH
O
H
Me
Me
Me
H1
F3CH2C−NH
O
1:1 mixture
TFDO - 3:1
O3, SiO2 - 4:1
Entry
Substrate
Product Yield %
Ratio 3º:2º
1
tBu
2
Fe(pdp) 59%
3
O
tBu
12%
4
2
3
Fe(pdp) 55% 9% 6% 4:1
TFDO 49%
HO
4
5
Fe(pdp) 29% 22% 28% 1:2
TFDO 45% 3% 2% 9:1
OH
6
PivO
Fe(mcpp) 50% 19% 3:1
OH
7
8
Fe(pdp) 51%
Fe(mcpp) 69%

Scheme I.9. Strain release as an important factor in controlling site selectivity in C-H bond oxidation reactions.

Among the five tertiary C-H bonds present in the later molecule, selective oxidation of the equatorial C-H_1 was observed. The two derivatives shown in Scheme I.9, differing only for the presence of an axial methyl group, display identical conformations in the solid state and almost identical ^{13}C-NMR chemical shifts, strongly indicating that the electronic and steric reactivity factors are almost identical for the two molecules. When a 1:1 mixture of these two compounds were subjected to oxidation with two different oxidants, (to confirm that the reactivity is not reagent-specific), the substrate that contains the axial methyl group displayed a 3- or 4-fold higher reactivity as compared to the derivative bearing an axial hydrogen atom. This reactivity factor can be clearly attributed to strain release, since both steric and electronic effects are identical at the reaction site.

Some relevant examples of the selectivity observed in the C-H oxidation by TFDO and bioinspired iron complexes of cyclic compounds are reported in Scheme I.9.[5, 16-17, 48] In all the examples reported in Scheme I.9. tertiary equatorial C-H bonds display a higher reactivity compared to the corresponding tertiary axial C-H bonds.

The pattern of products observed in the oxidation of *tert*-butylcyclohexane suggests that the torsional strain between the axial hydrogen on C1 and the axial hydrogen on C3, generated the unfavorable 1,3-diaxial interaction, is alleviated by oxidation of C3. The same behavior is observed for the oxidation of *cis*- and *trans*-1,2-dimethylcyclohexane, where the *cis* derivative displays a higher reactivity and selectivity for the oxidation of the tertiary C-H bond in equatorial conformation. Also in the case of *cis*- and *trans*-(4-methyl)cyclohexylpivalate, exclusive oxidation of the equatorial tertiary C-H bond was observed for the *cis* isomer, while for the *trans* isomer, competitive oxidation at the adjacent methylenic site was also observed.

I.2.6 Control over Oxidation in Complex Molecules

The understanding of the individual steric, electronic, hyperconjugative and stereoelectronic effects or the sum of some of them can be smartly applied to predict site selectivity in late-stage oxidation reactions on complex molecules, such as natural products, where the multitude of different C-H bond makes site selective oxidation particularly difficult. Some examples are shown in Scheme I.10.[16-17]

Oxidation of the α-ethereal (–)-ambroxide (**a**), furnished (+)-(3*R*)-sclareolide in 80% yield. The presence of hyperconjugative activation determined by the presence of the ether motifs led to the formation of only one product, even if several other electronically and steric accessible secondary and tertiary sites are present. The newly installed ketone moiety now deactivates by electronic effects ring B and C. C2 oxidation is now favored on the basis of the release of 1,3-diaxial interactions and accordingly the product deriving from oxidation at this site represents the major oxidation product. Employing pleuromutilin derivative (**b**) as substrate, the glycolic chain is not touched during oxidation, even in the presence of a primary alcohol because of to the EWG character of the ester and ketone groups. The major oxidation product results from oxidation of the equatorial C7 C-H bond, rationalized on the basis of a release of 1,3-diaxial interaction between the axial C-H bond at C7 and the C9 group.

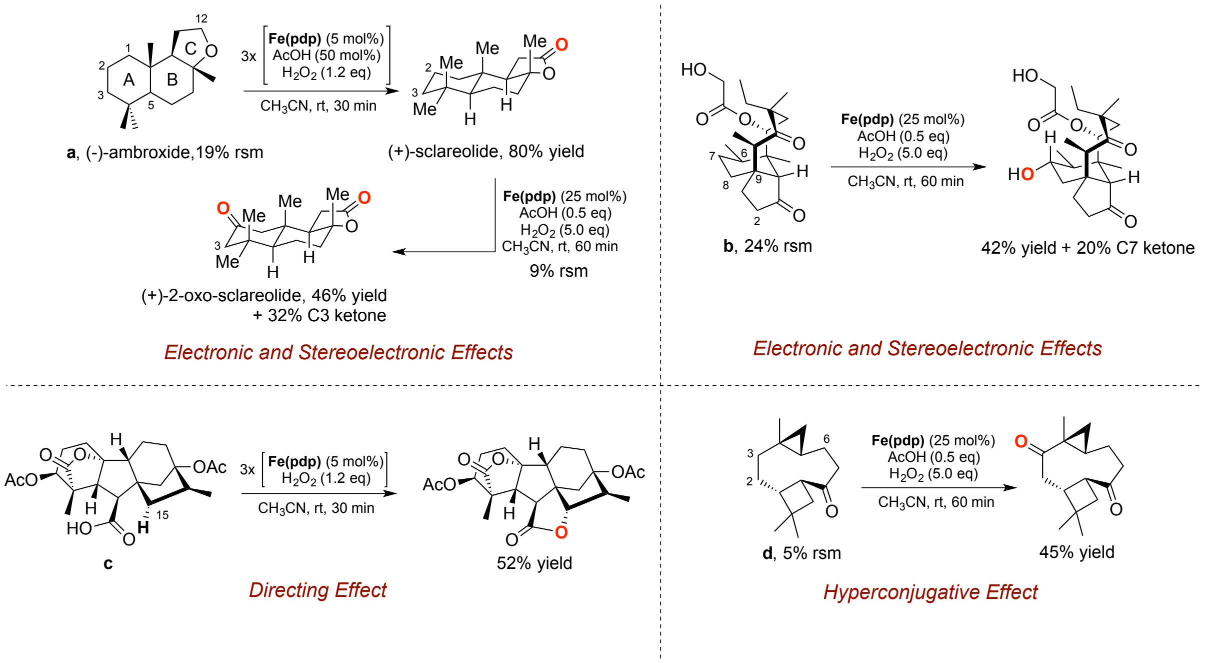
a, (-)-ambroxide,19% rsm
3x Fe(pdp) (5 mol%) AcOH (50 mol%) H_2O_2 (1.2 eq)
CH_3CN, rt, 30 min
(+)-sclareolide, 80% yield
Fe(pdp) (25 mol%) AcOH (0.5 eq) H_2O_2 (5.0 eq) CH_3CN, rt, 60 min
9% rsm
(+)-2-oxo-sclareolide, 46% yield + 32% C3 ketone
Electronic and Stereoelectronic Effects
b, 24% rsm
Fe(pdp) (25 mol%) AcOH (0.5 eq) H_2O_2 (5.0 eq)
CH_3CN, rt, 60 min
42% yield + 20% C7 ketone
Electronic and Stereoelectronic Effects
c
3x Fe(pdp) (5 mol%) H_2O_2 (1.2 eq)
CH_3CN, rt, 30 min
52% yield
Directing Effect
d, 5% rsm
Fe(pdp) (25 mol%) AcOH (0.5 eq) H_2O_2 (5.0 eq)
CH_3CN, rt, 60 min
45% yield
Hyperconjugative Effect

Scheme I.10. Late-stage C-H bond oxidation reactions.

A powerful application of the directing effect by a carboxylic acid group is shows in the oxidation of compound **c**. The carboxylate moiety directs the five-membered ring lactonization in 52% yield. Hyperconjugative activation is demonstrated for the oxidation of the terpenoid derivative **d**, affording only one oxidation product. The cyclopropane moiety is capable to override steric effects by activating the C3 methylene groups, while the C6 accessible site is deactivated by the ketone moiety.

I.3 Enantioselective Aliphatic C-H Bond Oxidations

I.3.1 Introduction

Besides the difficulty to control site selectivity in the oxidation reactions of aliphatic C-H bonds, additional challenges are encountered in enantioselective C-H bond oxidations.[59] Reagents that are both chiral and capable of oxidizing inherently strong aliphatic C-H bonds are rare, and the easy overoxidation of the first formed secondary alcohol product, resulting from hydroxylation of a methylenic site, into ketone eliminates the chirality. As a consequence, enantioselective aliphatic C-H bond oxidation remains a standing problem in organic synthesis. On the other hand, enantioselective C-H oxidation is a very common reaction in enzymes,[60-63] where the generation of highly reactive C-H oxidizing species is combined with the fine control of substrate approach to the active site. Formation of the oxidizing species is exquisitely harmonized with the presence of the substrate, limiting both oxidative damage at the active site, and overoxidation of the first formed product. For this reason, metalloenzymes are currently employed as biotechnological tools for performing these reactions with preparative scope.[60-66] Most usually, iron dependent metalloenzymes are prevalent among the proteins that catalyze C-H oxidations. Some representative examples of enantioselective C-H oxidations carried out by iron enzymes are reported in Schemes I.11., I.12. and I.13.

Cytochrome P450 is a family of iron enzymes ubiquitous in life forms, from bacteria to humans.[67-69] These enzymes catalyze the O_2-mediated hydroxylation of complex compounds such as terpenes, alkaloids and steroids in many cases with high selectivity.[67, 70] For this reason, the use of cytochrome P450 variants as catalysts for site-selective and enantioselective C-H oxidation is currently being pursued.[60-63] The active site and the oxidation reaction mechanism of Cyt P450 enzymes have been well established (Scheme I.11.).[69, 71] The active site consists of a single ferric heme coordinated to a cysteinate sulfur residue of the protein at one of the axial positions of the iron center, and the other axial site is occupied by a water molecule or by an hydroxide ligand. As shown in Scheme I.11., after oxidation of the iron center by dioxygen to form hydroperoxoiron(III) complex, the species undergoes proton assisted O-O heterolytic bond cleavage to generate a high-valent oxo-Fe^{IV}-porphyryl radical cation. The oxygen atom is transferred from this oxo complex to the substrate through a two-step process, first a HAT from the substrate to the oxo center, followed by fast rebound of the hydroxyl group to the substrate carbon radical. As a representative example, wild-type cytochrome P450 BM-3 catalyzes alkane hydroxylation with good enantioselectivity (Scheme I.11.).[72] In particular the oxidation of nonane produces 2-nonanol with high enantiomeric excess (83% ee).

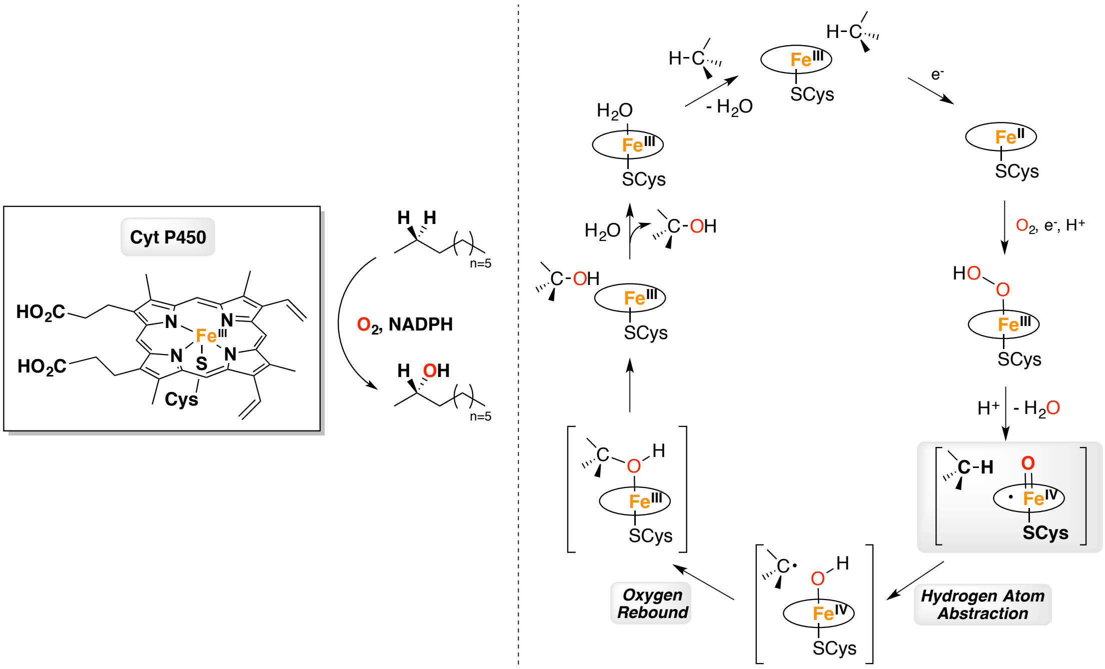
Cyt P450
HO2C
HO2C
N
N
N
N
Fe III
S
Cys
H H
n=5
O2, NADPH
H OH
n=5
H2O
Fe III
SCys
H-C
- H2O
Fe III
SCys
H-C
e-
Fe II
SCys
O2, e-, H+
HO
O
Fe III
SCys
H+
- H2O
C-H
O
Fe IV
SCys
Hydrogen Atom Abstraction
C•
O
H
Fe IV
SCys
Oxygen Rebound
C
O
H
Fe III
SCys
C-OH
Fe III
SCys
H2O
C-OH

Scheme I.11. Representative scheme of the active site of Cyt P450 BM3 and proposed catalytic cycle for alkane hydroxylation.

Bacterial enzymes such as Rieske oxygenases contain a non heme iron center at their active site (Scheme I.12.) and have been shown to catalyze the selective C-H hydroxylation and stereo- and enantioselective *cis*-dihydroxylation of arenes and olefins.[73-74] From the crystal structure of naphthalene 1,2-dioxygenase (NDO), it has been possible to identify two components (Scheme I.12.): the oxygenase component characterized by an octahedral mononuclear nonheme iron(II) center that interacts with the substrate molecule and O_2, and the Fe_2S_2 Rieske-type cluster that acts as reductase and mediates electron transfer from NAD(P)H to the oxygenase site. An aspartate group has also been shown to bind to these two components. A catalytic cycle, for *cis*-dihydroxylation of naphthalene, was proposed as show in Scheme I.12.[73-74] The catalytic cycle is initiated by reaction of O_2 and an electron with the iron center to form an iron(III)-peroxo complex that, after the O-O cleavage, leads to the formation of a $Fe^V(O)(OH)$ species. Also for this active site, a putative Fe-oxo intermediate $Fe^V(O)$ is proposed as the active oxidant, able to promote formation of the *syn*-diol product. Besides of naphthalene, NDO can oxidize the benzylic C-H bonds of indane in a stereoselective manner (up to 92% ee) to give enantioenriched 1-indanol (Scheme I.12.).[75]

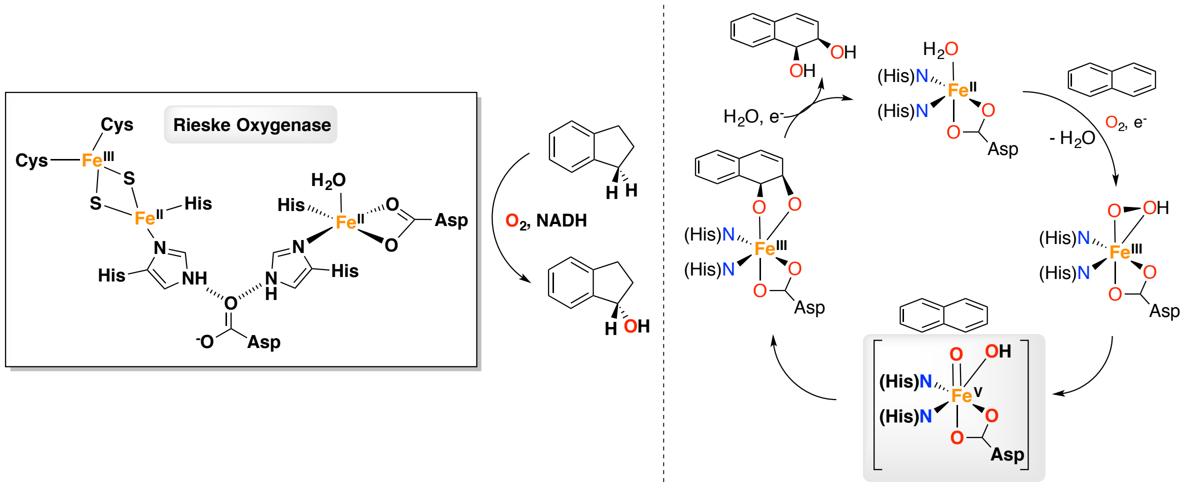

Scheme I.12. Active Site of Naphthalene 1,2-Dioxygenase (NDO) and Proposed Catalytic Cycle.

Prolyl 4-hydroxylase (P4H) is a member of the α-ketoglutarate-dependent, nonheme iron(II) oxygenase family of enzymes.[76] This enzyme performs the oxidation of a proline residue, in a enantioselective manner, to give an enantiopure 4-hydroxyproline product (Scheme I.13.).[77-78] In order to function, these enzymes require iron(II), α-ketoglutarate and O_2. Also in this case, as show in Scheme I.13., in order to perform challenging C-H bond oxidation reactions, this enzyme forms in the catalytic cycle a highly reactive iron(IV)-oxo species, via an oxidative decarboxylation of α-ketoglutarate and formation of succinate and CO_2.[79-81] This species is responsible for the abstraction of the 4-proR hydrogen atom from proline substrate followed by the transfer the hydroxyl group to the carbon radical species finally leading to the oxidized 4-hydroxyproline product.[82]

The mechanism of C-H oxidation taking place in the three examples discussed above can be considered representative for the majority of mononuclear transition metal dependent aliphatic C-H hydroxylases.[81, 83-84] It involves an initial HAT from the substrate to a high valent metal-oxo species, to give a carbon centered radical and the corresponding one-electron reduced metal-hydroxide species. Then, the hydroxyl ligand is transferred to the radical, generating the corresponding alcohol product, and the further one-electron reduced metal center. Alkane hydroxylases that contain dimetallic species in the active site often follow the same mechanism, but the reactive oxo unit is a bridged ligand, and the formal two-electron reduction of the active center results in a single electron reduction of each of the two metal ions.[85] The lifetime of the carbon centered radical depends on the nature of the enzyme. For example, in P-450, it is extraordinarily short lived, and does not abandon the solvent cage, overall resulting in an almost stereoretentive hydroxylation.[86] In Rieske dioxygenases, the radical has a longer lifetime,[84] and in the case of diiron alkane oxygenase AlkB, it can even diffuse from the active center.[87] However, there is a growing body of evidence that the trajectory of these radicals is influenced by the chemical and structural nature of the enzyme active site.

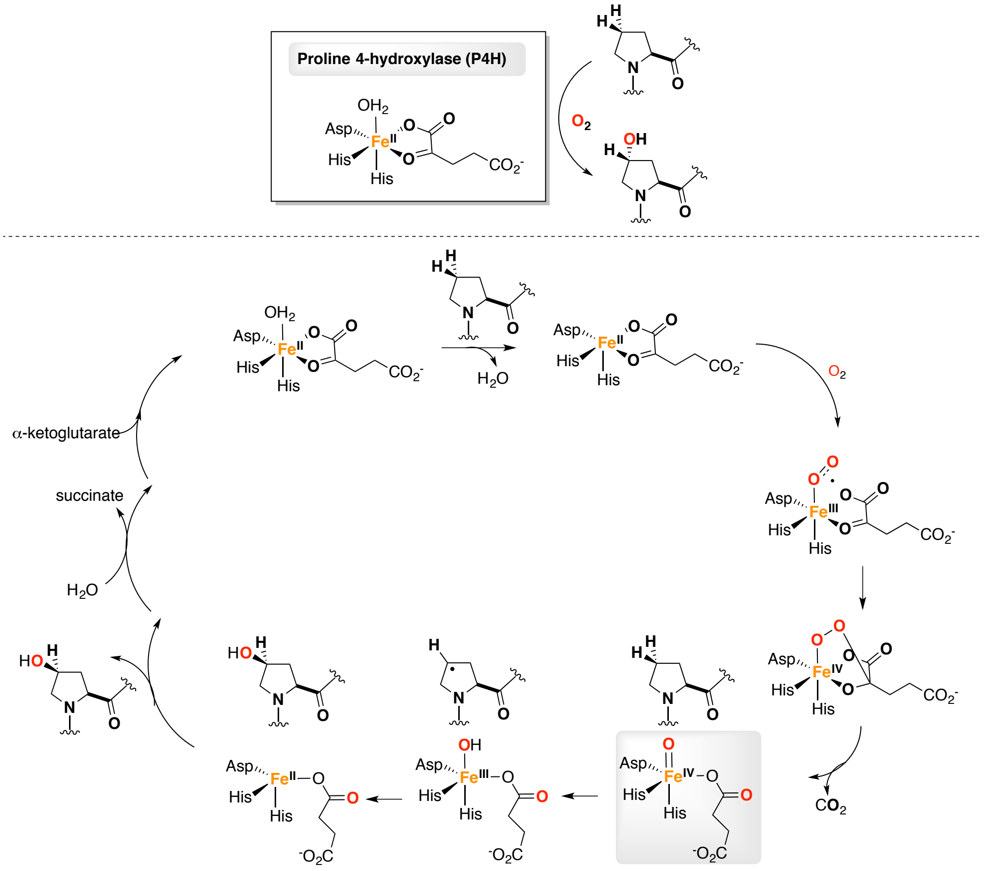

Scheme I.13. Proposed mechanism of proline hydroxylation catalyzed by human P4H.

I.3.2. Origin of Stereoselection in C-H Oxidation

The enantioselective differentiation in C-H oxidation reactions can derive from one of the two elementary steps that participate in a common hydroxylation reaction through a HAT process. Enantioselectivity can result from the transfer of a hydroxyl group belonging to a chiral metal-OH unit to one of the two faces of a long lived and planarized carbon centered radical (Scheme I.14., a) or from the first C-H cleaving step by a chiral metal-oxo species (Scheme I.14., b). Radicals formed after HAT from activated C-H bonds, such as benzylic, allylic or adjacent to heteroatom, are relatively stable and long lived, and are susceptible to embrace in the former mechanism. Instead the high reactivity of alkyl radicals seems a priori incompatible with their use as radical relays. Accordingly, with these assumptions, enantioselective C-H oxidation in alkanes thus needs to originate from an enantiodiscriminating HAT step.

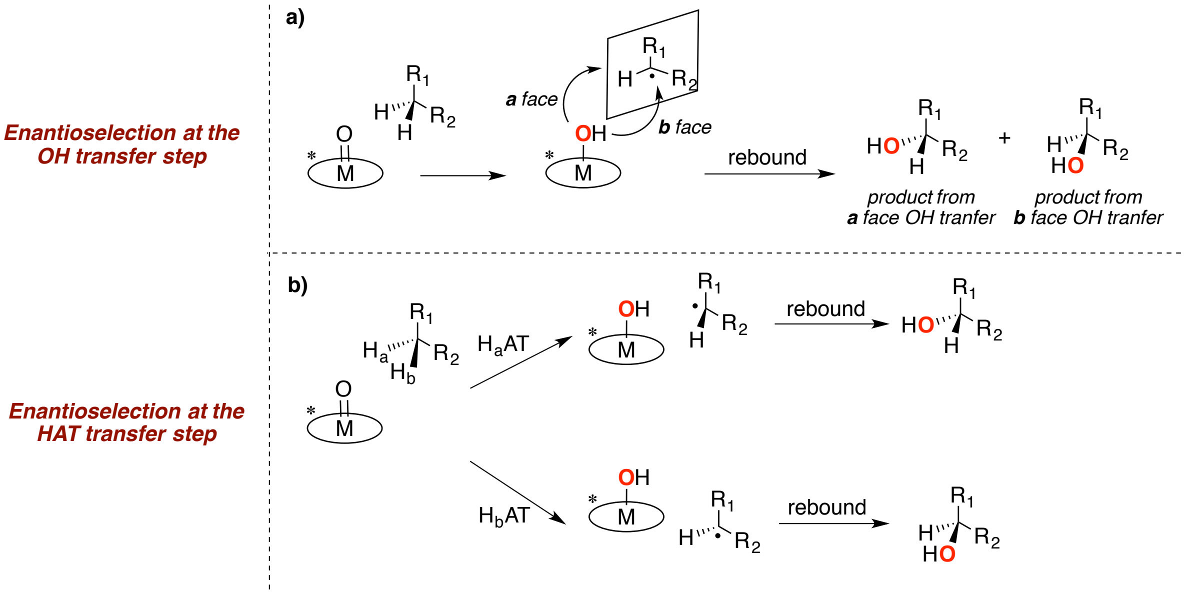
Enantioselection at the OH transfer step
a)
a face
b face
rebound
product from a face OH tranfer
product from b face OH tranfer
Enantioselection at the HAT transfer step
b)
H_aAT
H_bAT
rebound
rebound

Scheme I.14. Description of the possible mechanism at the origin of enantioselectivity.

I.3.3. Typology of Enantioselective C-H Oxidation Reaction

I.3.3.1 Enantioselective Desymmetrization of Alkanes

Aliphatic C-H bonds that are α- to an OH group are typically activated toward HAT-based oxidants. Along this line, one approach to circumvent the problem of overoxidation of the first formed alcohol product is to develop a desymmetrization reaction through C-H bond oxidation. Enantioselective desymmetrization converts an achiral or *meso* compound to a chiral product by the destruction of one symmetry element, provided that the point of reaction does not lie on that symmetry element (Scheme I.15.).[88-89] In this case, the formation of a ketone after overoxidation of the first formed secondary alcohol does not destroy the new chiral center formed after the initial oxidation.

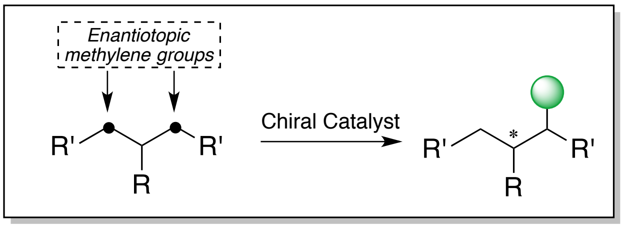

Scheme I.15. Representative scheme of desymmetrization reaction with a chiral catalyst.

The first examples of metal-catalyzed desymmetrization reactions based on the oxidation of activated C-H bonds such as benzylic or α to an heteroatom, were proposed by Katsuki, Murahashi and co-workers.[90-93] In these reactions (salen)manganese(III) complexes were employed as catalysts for the enantioselective oxidation of C-H bonds (oxidation of compounds **5**, **9**, **11** and **13**, Scheme I.16.).[90] The oxidation of 4-*tert*-butyltetrahydropyran (**5**) was studied with chiral Mn-salen complexes (**1**-**4**, Scheme I.16.) using iodosobenzene as oxidant. The reactions afforded a mixture of the lactol **6** and lactone **7** products. The mixture was then treated with diisobutylaluminium hydride (DiBAlH) to achieve only the lactol **6** which was eventually converted into the corresponding *trans* and *cis*-benzyl acetals (**8**). Under the best conditions, enatioselectivity increased up to 48% ee, accompanied however by a modest 13% yield. Differently from the oxidation of **5**, oxidation of the more rigid and planar 3-oxabicyclo[3.3.0]octane (**9**) gave lactol **10** as the mayor product in 59% isolated yield with 82% ee. Also, the oxidation of compounds **11** and **13** proceeded with high enantioselectivity (89 and 90% ee respectively), giving the corresponding hydroxylated product in good isolated yield (41% and 61%, respectively).

Katsuki et al. also reported desymmetrization reactions on *meso*-pyrrolidine derivatives (oxidation of compounds **15** and **18**, Scheme I.16.).[91-92] The oxidation of **15** catalyzed by Mn(salen) complex (**4**) occurs at the carbon α to the nitrogen atom affording the chiral 2-hydroxypyrrolidine derivative (**16**) which is oxidized by the Jones reagent to give the chiral imide **17**, a moderate enantioselectivity (64% ee) was obtained. To evaluate the effect of the amino-protecting group on the enantioselectivity of the reaction, the oxidation of a series of *N*-protected 8-azabicyclo[4.3.0]nonanes (**18**) was studied, employing complex **4** as catalyst and pentafluoroiodosylbenzene as the oxidant (entries 1-9, Scheme I.16.). Among the substrates employed, a relatively good enantioselectivity was only observed with *N*-phenylacetylpyrrolidine (76% ee, entry 7). Finally, the oxidation of *N*-phenylacetyl protected 3,4-dimethyl pyrrolidine (**21**) and 7-azabicyclo[3.3.0]octane (**22**) occurred on the carbon α to the nitrogen atom to give the corresponding chiral hydroxypyrrolidine derivatives that provided chiral imides (**23** and **24**) in 49% and 48% isolated yield and high enantioselectivity (84% and 75% ee).

Murahashi et al. have reported the asymmetric oxidation of alkanes catalyzed by Mn-salen complexes to give chiral ketones (Scheme I.16.).[93] By using complex **25**, PhIO in excess as oxidant in the presence of 4-phenylpyridine-*N*-oxide, desymmetrization of 2-methyl-1,3-diphenylpropane (**27**), that exhibits two symmetric benzylic positions, gave chiral 2-methyl-1,3-diphenyl-1-propanone (**28**) with low enantioselectivity (22% ee). The same authors have also reported the α-C-H oxidation of silyl ethers like 2-*tert*-butyldimethylsiloxyindane (**29**), that provided α-ketone **30** with high enantioselectivity (70% ee) but in poor yield (Scheme I.16.).[94]

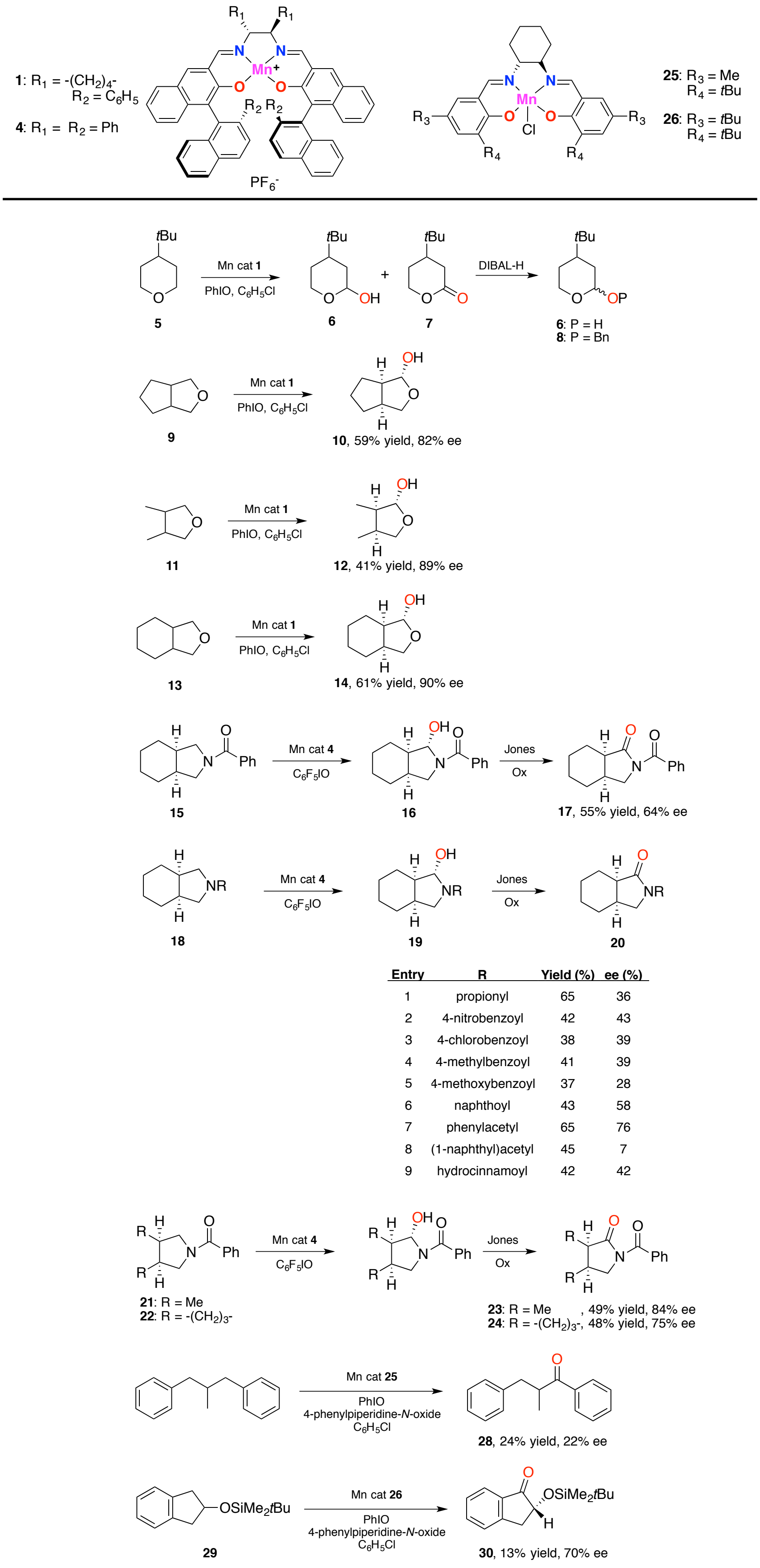
1: R1 = -(CH2)4-
R2 = C6H5
4: R1 = R2 = Ph
PF6-
25: R3 = Me
R4 = tBu
26: R3 = tBu
R4 = tBu
Mn cat 1
PhIO, C6H5Cl
DIBAL-H
5
6
7
6: P = H
8: P = Bn
9
10, 59% yield, 82% ee
11
12, 41% yield, 89% ee
13
14, 61% yield, 90% ee
Mn cat 4
C6F5IO
Jones
Ox
15
16
17, 55% yield, 64% ee
18
19
20
21: R = Me
22: R = -(CH2)3-
23: R = Me , 49% yield, 84% ee
24: R = -(CH2)3-, 48% yield, 75% ee
Mn cat 25
PhIO
4-phenylpiperidine-N-oxide
C6H5Cl
28, 24% yield, 22% ee
Mn cat 26
29
30, 13% yield, 70% ee

Entry	R	Yield (%)	ee (%)
1	propionyl	65	36
2	4-nitrobenzoyl	42	43
3	4-chlorobenzoyl	38	39
4	4-methylbenzoyl	41	39
5	4-methoxybenzoyl	37	28
6	naphthoyl	43	58
7	phenylacetyl	65	76
8	(1-naphthyl)acetyl	45	7
9	hydrocinnamoyl	42	42

Scheme I.16. Oxidative desymmetrization using Mn-salen complexes as catalysts.

An elegant approach based on the supramolecular recognition of the substrate by a chiral ruthenium porphyrin has been recently disclosed by Bach and co-workers to achieve enantiotopic selective C-H oxygenation on spirocyclic oxindoles compounds.[95] These compounds present enantiotopic methylene groups and the oxidation favors one of these two sites on the indane system. The results obtained in the oxidation of different spirocyclic oxindoles derivatives are displayed in Scheme I.17. Despite of the high conversion of **38** under the optimized conditions (60% conv, 90% ee) the desired ketone **38a** was isolated in a modest 20% yield (method **A**, Scheme I.17.). This observation suggested that the intermediate alcohol was not completely oxidized to the ketone. To promote alcohol oxidation, the crude reaction mixture obtained after C-H oxidation was submitted to pyridinium chlorochromate (PCC) or Swern conditions. This procedure provided an improved yield of **38a** (70%) and a relatively high enantiomeric excess of 80% (method **B**, Scheme I.17.). Substrates bearing methyl or methoxy substituents on the indane aromatic ring provided ketones **39a** and **40a** in excellent ee (92% and 94% ee, Scheme I.17.). Substitution at C6 of the oxindole by Br, Cl and CN (**41a**, **42a** and **43a**) also led to high enantiomeric excesses (82% to 90% ee). Instead, substitution at C5 led to larger differences in enantioselectivity, with the ee that decreased on going from CN (**44a**, 80% ee), to Cl and CF_3 (**45a**, 60% ee and **46a**, 44% ee).

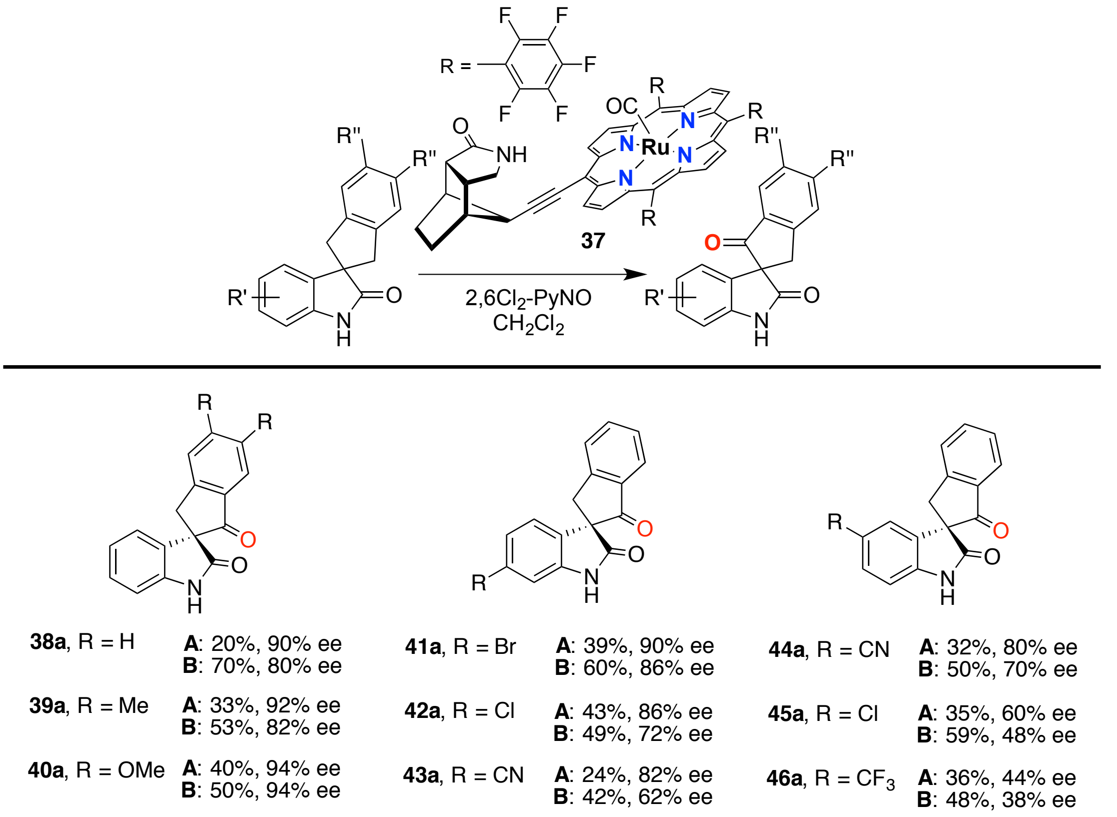

38a, R = H	**A**: 20%, 90% ee **B**: 70%, 80% ee	**41a**, R = Br	**A**: 39%, 90% ee **B**: 60%, 86% ee	**44a**, R = CN	**A**: 32%, 80% ee **B**: 50%, 70% ee
39a, R = Me	**A**: 33%, 92% ee **B**: 53%, 82% ee	**42a**, R = Cl	**A**: 43%, 86% ee **B**: 49%, 72% ee	**45a**, R = Cl	**A**: 35%, 60% ee **B**: 59%, 48% ee
40a, R = OMe	**A**: 40%, 94% ee **B**: 50%, 94% ee	**43a**, R = CN	**A**: 24%, 82% ee **B**: 42%, 62% ee	**46a**, R = CF_3	**A**: 36%, 44% ee **B**: 48%, 38% ee

Isolated yields. Method **A**: substrate (1.0 equiv), Ru catalyst (1 mol %), 2,6-dichloropyridine *N*-oxide (2.2 equiv), CH_2Cl_2, 50 °C, 20 h. Method **B**: Yield end e.r. following submission of the crude material (from step **A**) to either Swern or PCC oxidation conditions.

Scheme I.17. Enantioselective oxidation of spirocyclic oxindoles derivatives by Ru-complex.

Sun, Nam and co-workers have also described the desymmetrization of spirocyclic compounds in particular spirocyclic tetralone and indanone derivatives catalyzed by aminopyridine manganese complexes with H_2O_2 as the oxidant in the presence of 2,2-dimethylbutanoic acid (DMBA) (Scheme I.18.).[96] The substrate is initially oxidized to the alcohol product that, after overoxidation leads to β,β'-diketones in high yield and excellent enantioselectivity. Some relevant examples are reported in Scheme I.18. Manganese complex (**47**) based on chiral diamine ligands derived from proline and two benzimidazoles as sp^2 nitrogen units resulted to be very efficient in terms of yield and enantioselectivity. Different functional groups on the aromatic ring were tolerated such as methoxy, dimethoxy, halogens and the oxidized products were obtained in moderate to good isolated yields in all of the reactions. Moreover, enantioselectivities were excellent, up to 94% ee for the oxidation of spirocyclic tetralone derivatives and up to 98% ee when spirocyclic indanone derivatives were used as substrates.

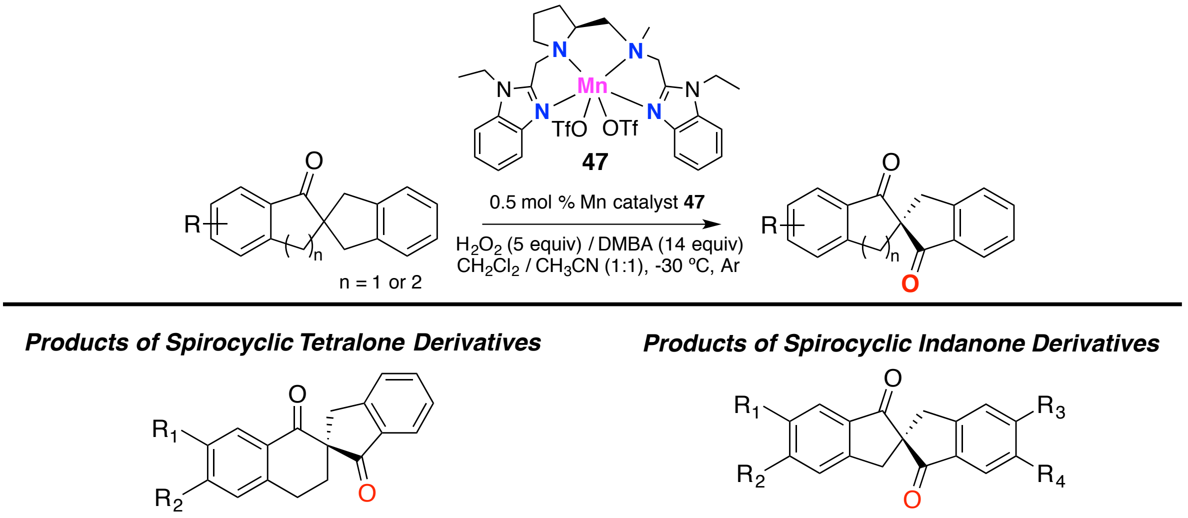
N
N
N
N
N
N
Mn
TfO OTf
47
O
R
n
n = 1 or 2
0.5 mol % Mn catalyst 47
H2O2 (5 equiv) / DMBA (14 equiv)
CH2Cl2 / CH3CN (1:1), -30 °C, Ar
O
R
n
O
Products of Spirocyclic Tetralone Derivatives
Products of Spirocyclic Indanone Derivatives
R1
R2
O
O
R1
R2
O
O
R3
R4

48a, R_1=R_2=H	80%, 94% ee
49a, R_1=MeO, R_2=H	63%, 92% ee
50a, R_1=H, R_2=MeO	68%, 92% ee
51a, R_1=MeO, R_2=MeO	63%, 94% ee
52a, R_1=F, R_2=H	57%, 89% ee

54a, R_1=R_2=H R_3=R_4=H	94%, 85% ee
55a, R_1=MeO, R_2=MeO R_3=R_4=H	51%, 92% ee
56a, R_1=H, R_2=Br R_3=R_4=H	67%, 98% ee
57a, R_1=H, R_2=Cl R_3=R_4=H	64%, 92% ee
58a, R_1=H, R_2=MeO R_3=R_4=MeO	53%, 93% ee

Scheme I.18. Oxidations of spyrocyclic tetralone and indanone derivatives catalyzed by manganese complex.

I.3.3.2 Enantioselective C-H Bond Hydroxylation

Enantioselective hydroxylation of methylene groups still remains a very difficult reaction. To achieve this goal overoxidation of the first formed alcohol product has to be avoided in order to preserve chirality. The works by Groves and Viski described the use of chiral metalloporphyrins as hydroxylating and epoxidizing catalysts, mimicking the activity of the heme site of P-450's.[97-98] Iron catalyst **64**, (Scheme I.19.) performs alkane hydroxylation and alkene epoxidation reactions in the presence of iodosobenzene employed as oxidant. Interestingly, the chiral cavity of the porphyrins can induce enantioselectivity in the oxidation reactions. As reported in Scheme I.19., hydroxylation of a series of benzylic compounds proceeded with 19-72% yield with respect to the oxidant. More significant, modest to good ee's were observed up to 72%. For each of the substrates investigated, variable amounts of the corresponding ketone product were also observed (alcohol/ketone ratio between 0.2 and 20.1), deriving from overoxidation of the first formed alcohol product by the active oxidizing species. As previously described by the author,[99] a mechanism proceeding through initial HAT from the substrate to an oxidized iron porphyrin species, followed by OH transfer to the carbon radical to give the alcohol product was proposed.

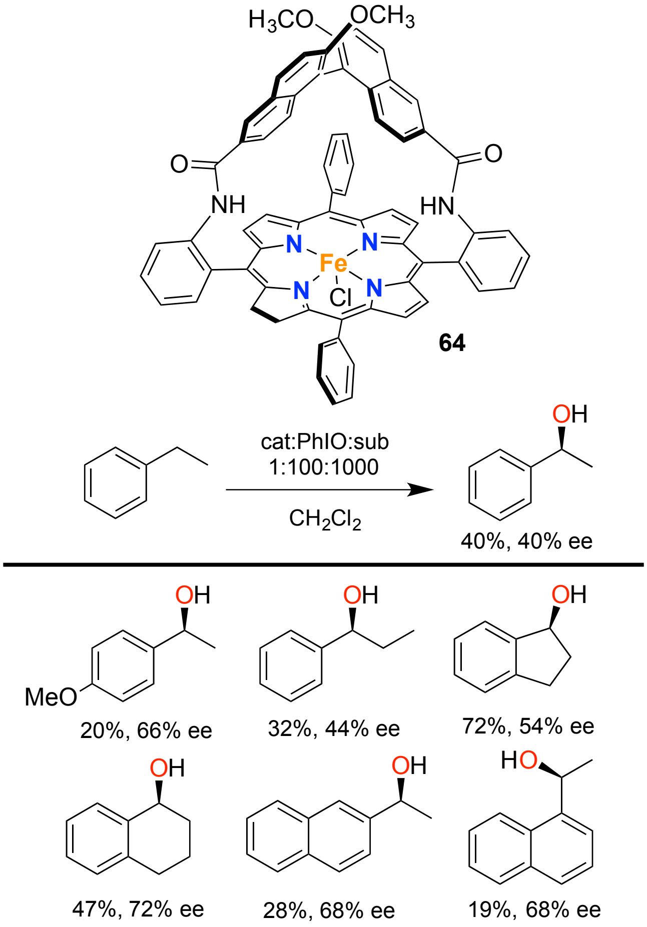

Yields determined by GC analysis and referred to the amount of oxidant.

Scheme I.19. Hydroxylation catalyzed by Fe catalyst **64**.

Inspired by the work of Groves, Katsuki and co-workers described enatioselective benzylic oxidation catalyzed by Mn-salen complexes (**65**, **66** and **67**) as reported in Scheme I.20.[100-101] All the substrates examined under optimized conditions, namely ethylbenzene, 4-methoxyethylbenzene, tetrahydronaphthalene, 1,2,3,4-tetrahydro-1,1-dimethylnaphthalene and 1,1-dimethylindane, gave the corresponding chiral benzylic alcohol in modest yield and relatively good to high enantiomeric excess (6-28% yield and 56-90% ee).

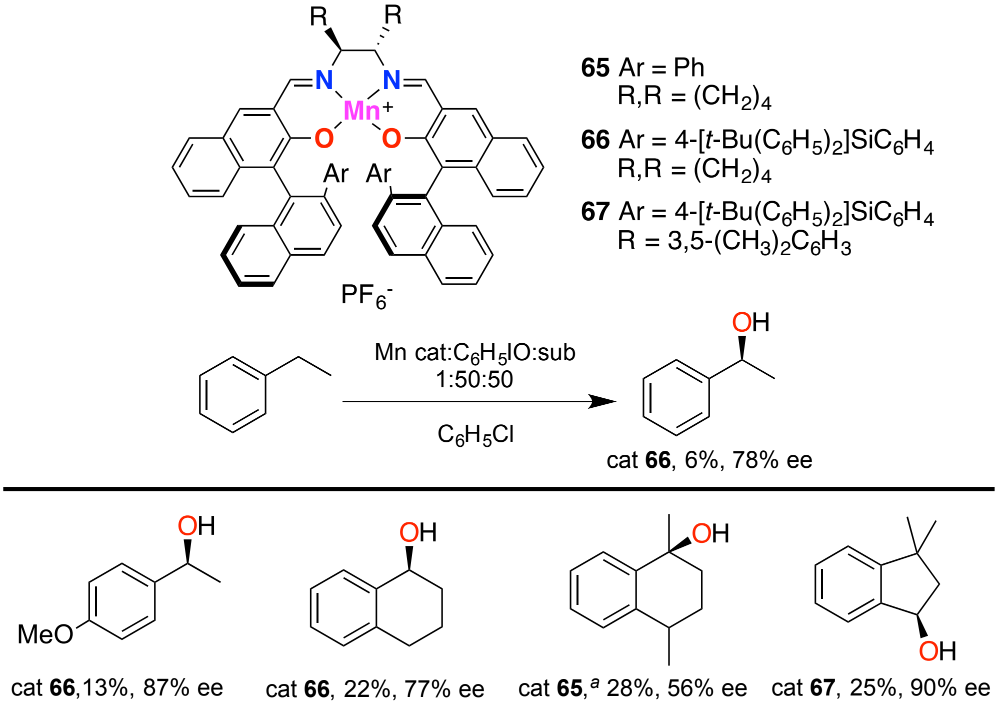
R
R
N
N
Mn+
O
O
Ar
Ar
PF6-
65 Ar = Ph
R,R = (CH2)4
66 Ar = 4-[t-Bu(C6H5)2]SiC6H4
R,R = (CH2)4
67 Ar = 4-[t-Bu(C6H5)2]SiC6H4
R = 3,5-(CH3)2C6H3
Mn cat:C6H5IO:sub
1:50:50
C6H5Cl
OH
cat 66, 6%, 78% ee
OH
MeO
cat 66,13%, 87% ee
OH
cat 66, 22%, 77% ee
OH
cat 65,a 28%, 56% ee
OH
cat 67, 25%, 90% ee

Yields determined by GC analysis. [a]Isolated yield.

Scheme I.20. Asymmetric oxidation using salen manganese catalysts.

Gross and co-workers reported the synthesis of double-side protected ruthenium porphyrins with D_2 symmetry to achieve epoxidation of olefins by *N*-oxides.[102] To improve the enantioselectivity in the oxidation of alkenes and alkanes, they also synthetized a new ruthenium porphyrin complex (**68**), modifying the porphyrin core, the structure for which is shown in Scheme I.21.[103] They employed the new ruthenium complex for the resolution of a racemic mixture of chiral alkylbenzenes via catalytic asymmetric hydroxylation of tertiary benzylic C-H bonds. However, the alcohol product was formed with moderate enantiomeric excess (16% ee for 2-phenylhexane and 38% ee for 2-phenylbutane).

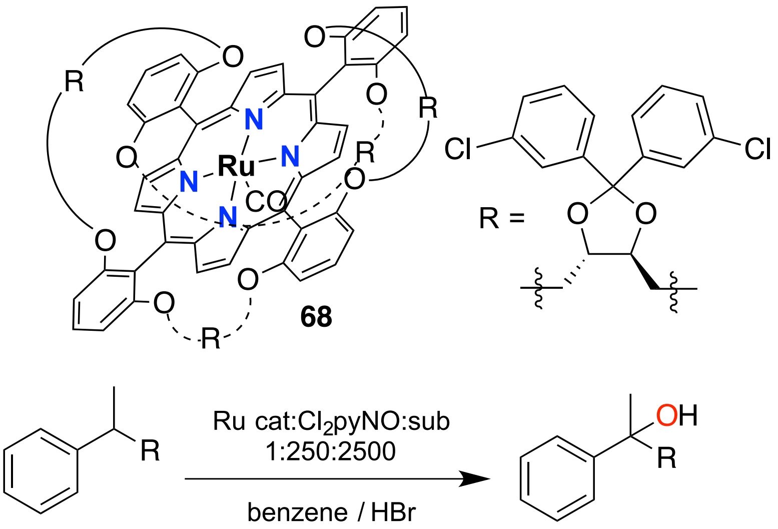

R	Yield (%)	ee (%)
Bu	41	16
Et	23	38

Yields determined by GC analysis and referred to the amount of oxidant.

Scheme I.21. Catalytic asymmetric hydroxylation of tertiary alkanes.

Murahashi et al. proposed a bridged (salen)manganese complex (**69**, Scheme I.22.) characterized by a strapping unit for the generation of oxo-manganese species in a cage, that was able to carry out enantioselective alkane hydroxylation and alkene epoxidation.[104] The asymmetric hydroxylation of indane by using PhIO as oxidant and Mn-salen catalyst **69** gave (*S*)-1-indanol with 34% ee together with a small amount of indanone (Scheme I.22.). It was proposed that the coordination of an auxiliary axial ligand can occur inside or outside the cavity. A bulky auxiliary ligand favors coordination to the opposite site of the strapped unit, resulting in the formation of the oxo manganese species in the chiral cavity. Without the auxiliary ligand, the Mn(salen) complex **67** gave 1-indanol with only 5% ee. When imidazole was used as the ligand, the enantioselectivity was not influenced (8% ee of 1-indanol). On the other hand, when 1,5-dicyclohexylimidazole was used the enatioselectivity improved up to 25% ee. Furthermore, the ee increased to 34% ee when the reaction was performed at low temperature (-30 ºC). Under these conditions, the bulky auxiliary ligand binds at the opposite side of the cavity with the substrate that can approach the cage defined by the naphthyl groups.

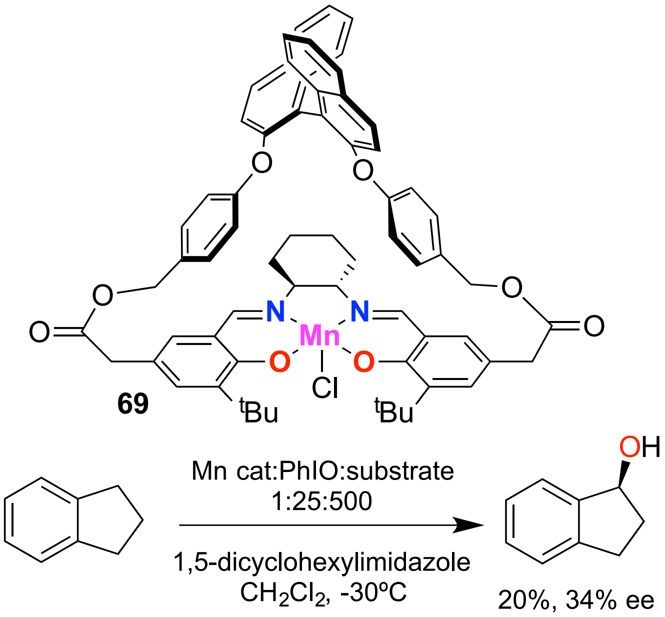

Scheme I.22. Enantioselective oxidation of indane with Mn(salen) catalyst **69**.

Another system based on a D_4-symmetric chiral ruthenium porphyrin that can perform catalytic enantioselective hydroxylation of benzylic C-H bonds to give enantioenriched alcohols, has been reported by Che and co-workers.[105-106] The oxidations were catalyzed by ruthenium complex **70** (Scheme I.23.) with 2,6-dichloropyridine *N*-oxide (Cl_2pyNO) as terminal oxidant. Although low to modest conversions were reported (11-54%) good levels of enantioselectivity were obtained (up to 76% ee, Scheme I.23.). *para*-Substituted ethylbenzenes (R = H, Me, F, Cl, Br, OMe) were effective substrates for the ruthenium-catalyzed asymmetric hydroxylation, and the corresponding 1-arylethanols were produced in notable ee's between 62-76% ee with alcohol over ketone ratios in agreement with literature values. When 2-ethylnaphthalene was employed as a substrate the corresponding alcohol was obtained with 75% ee. Indane was instead observed to be a poor substrate for this reaction as shown by the low enantioselectivity obtained after oxidation (12% ee). On the other hand, with 1,1-diethylindane, the Ru-catalyzed oxidation reaction gave the indanol product in 76% ee. The oxidation of benzylcyclopropane gave the corresponding benzylic alcohol with 76% ee. Notably, no ring opened products were detected, suggesting a fast hydroxyl rebound following HAT.

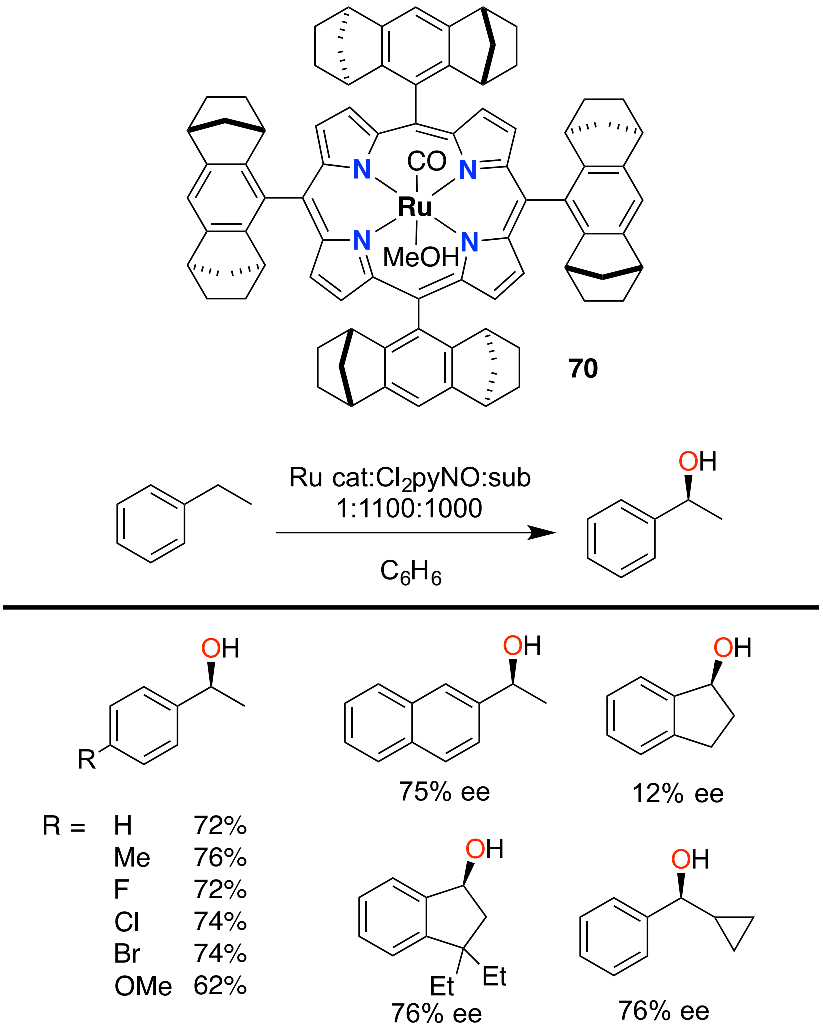
70

Scheme I.23. Ruthenium catalyzed asymmetric alkane oxidation.

Chiral manganese and iron porphyrin complexes have been recently reported by Simonneaux and co-workers.[107-108] Enantioselective alkene epoxidation ad aliphatic hydroxylation were achieved using H_2O_2 and $PhI(OAc)_2$ as oxidants for water-soluble manganese and iron porphyrins respectively (**71** and **72**, Scheme I.24.). The substrates employed in the hydroxylation reactions, all characterized by the presence of benzylic C-H bonds, include ethylbenzenes, indane and tetrahydronaphtalene, the structures for which are reported in Scheme I.24. In most cases higher enantiomeric excesses were observed with the iron porphyrins as compared to the manganese one, approaching 76% ee in the reaction of 4-bromoethylbenzene. Higher substrate:oxidant ratios were however required with the iron system accompanied by lower conversions (between 24-80% with respect to the oxidant), as compared to the manganese system (88-100%).

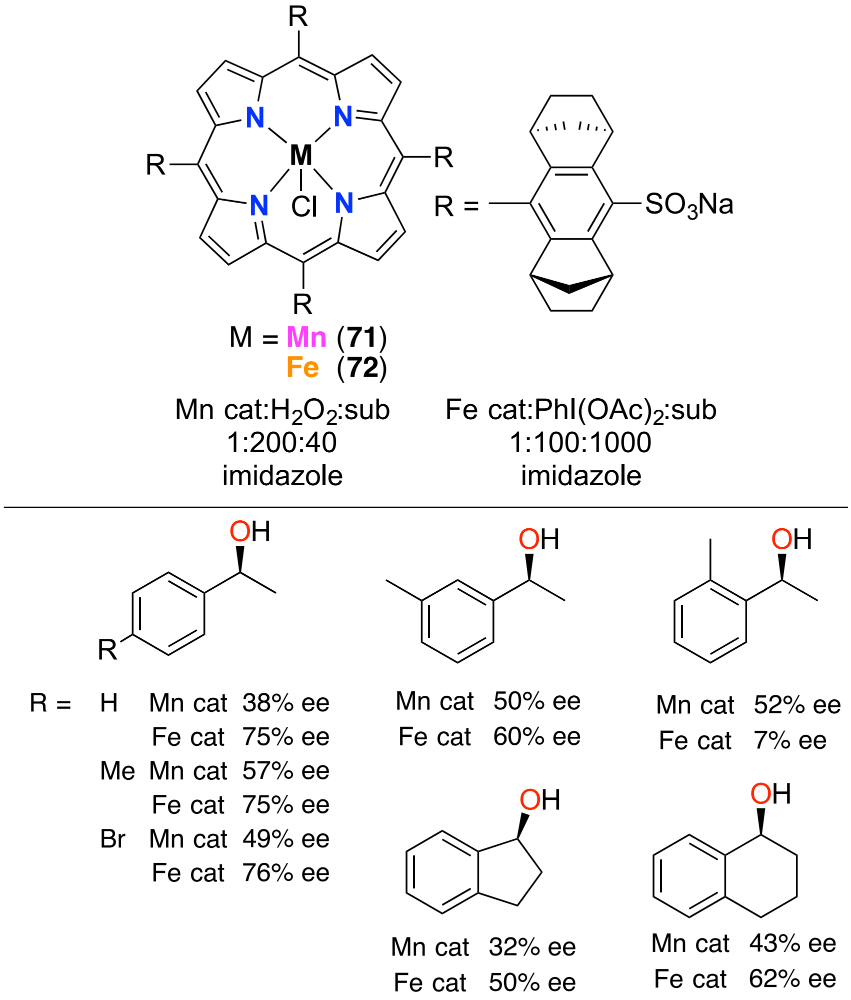
R
N
M
Cl
R =
SO3Na
M = Mn (71)
Fe (72)
Mn cat:H2O2:sub
1:200:40
imidazole
Fe cat:PhI(OAc)2:sub
1:100:1000
imidazole
OH
R
R = H Mn cat 38% ee
Fe cat 75% ee
Me Mn cat 57% ee
Fe cat 75% ee
Br Mn cat 49% ee
Fe cat 76% ee
Mn cat 50% ee
Fe cat 60% ee
Mn cat 52% ee
Fe cat 7% ee
Mn cat 32% ee
Fe cat 50% ee
Mn cat 43% ee
Fe cat 62% ee

Scheme I.24. Asymmetric hydroxylation catalyzed by Mn or Fe porphyrin systems.

In the last decade one of the mayor trends has been represented by the design of different bioinspired transition metal catalyst (Fe- and Mn-based) bearing aminopyridine ligands.[16-17, 51] The easy modification of these ligands, for example its steric bulk and electronic properties, enable to manipulate the reactivity of the active species, site selectivity and moreover the stereoselectivity in the oxidation of a large variety of substrates including complex molecules such as steroids, with the environmentally benign oxidant H_2O_2.[109-112] Bryliakov and co-workers reported on the enantioselective benzylic C-H bond oxidation using manganese catalyst (**74**) the structure for which is displayed in Scheme I.25., and H_2O_2 as oxidant in the presence of different carboxylic acids.[113-114] With ethylbenzene, among the different carboxylic acids employed, the best result, in terms of enantioselecitvity, was obtained employing the amino acid *N*-Boc-L-Pro (76% ee, Scheme I.25.). Although product yields and selectivities were relatively low, ethylbenzene derivatives such as 4-methylethylbenzene and 4-bromoethylbenzene gave the highest levels of enantioselectivity (86% and 78% ee, respectively).

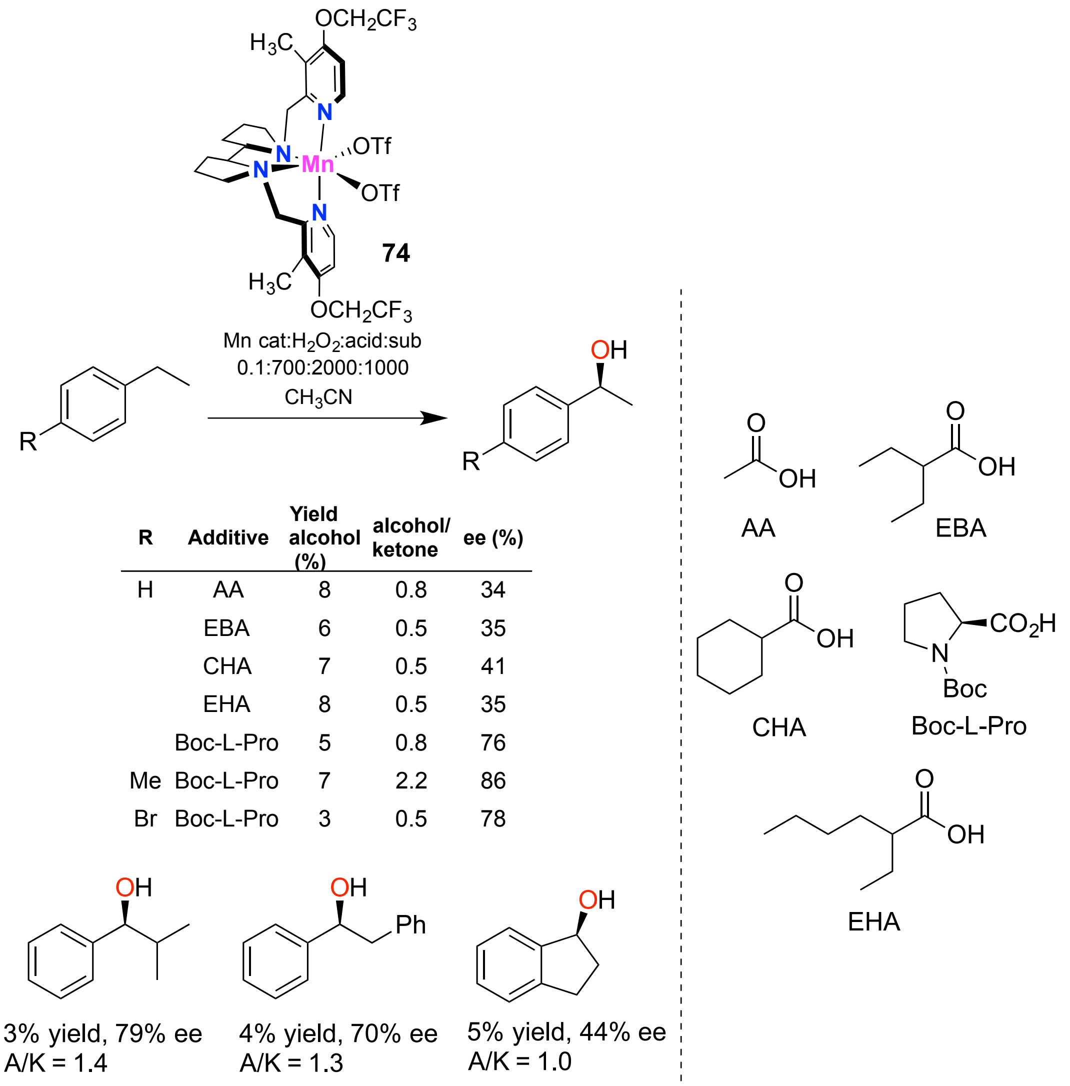
OCH2CF3
H3C
N
N
N
Mn
OTf
OTf
N
74
H3C
OCH2CF3
Mn cat:H2O2:acid:sub
0.1:700:2000:1000
CH3CN
R
OH
R
O
OH
AA
O
OH
EBA
O
OH
CHA
CO2H
N
Boc
Boc-L-Pro
O
OH
EHA
OH
OH
Ph
OH
3% yield, 79% ee
A/K = 1.4
4% yield, 70% ee
A/K = 1.3
5% yield, 44% ee
A/K = 1.0

R	Additive	Yield alcohol (%)	alcohol/ ketone	ee (%)
H	AA	8	0.8	34
	EBA	6	0.5	35
	CHA	7	0.5	41
	EHA	8	0.5	35
	Boc-L-Pro	5	0.8	76
Me	Boc-L-Pro	7	2.2	86
Br	Boc-L-Pro	3	0.5	78

Scheme I.25. Benzylic oxidation reactions in the presence of manganese complex.

Improved yields of the alcohol could be obtained carrying out the reactions in fluorinated alcohol solvents. These are powerful hydrogen bond donors, and can induce a polarity reversal that deactivates the alcohol toward further oxidation.[115] As reported in Scheme I.26., oxidation of ethylbenzene with 1 mol % catalyst, 0.5 equiv of H_2O_2 and 2.0 equiv of 2-ethylhexanoic acid (2-eha) in trifluoroethanol (TFE) led to the formation of the corresponding benzylic alcohol with 99% hydroxylation selectivity and good enantiomeric excess. Catalyst screening and optimization of the temperature led to an increase in enantioselectivity, while the hydroxylation selectivity was kept above 90%. The best result was obtained employing the **Mn(^{dMM}pdp)** (**75**) catalyst at -35 ºC, and from 1-phenylpropane, 1-phenyl-1-propanol was obtained with 66% ee. The results obtained clearly indicate that the use of fluorinated alcohols such as TFE, preserve the first formed chiral benzylic alcohol against overoxidation, avoiding the use of a large excess of substrate.

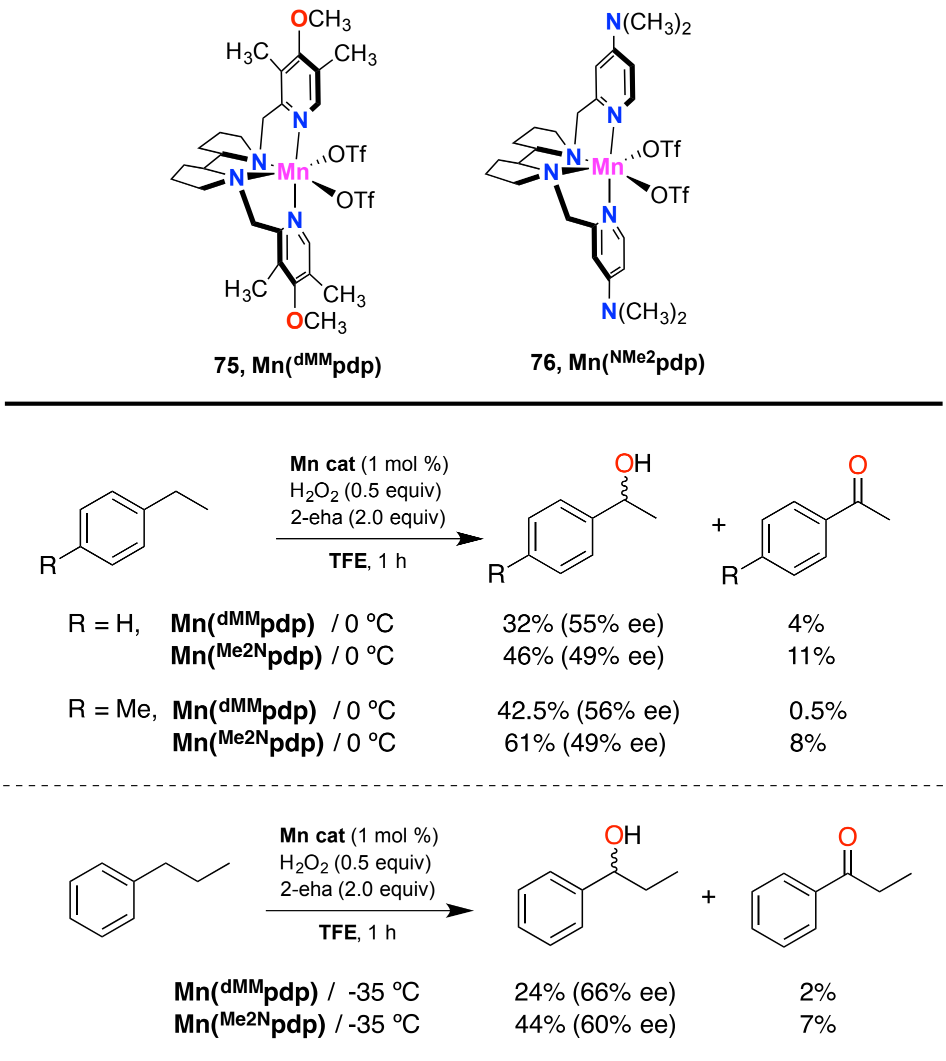

75, Mn(^{dMM}pdp)

76, Mn(^{NMe2}pdp)

	Catalyst / T	Alcohol	Ketone
R = H,	**Mn(^{dMM}pdp)** / 0 °C	32% (55% ee)	4%
	Mn(^{Me2N}pdp) / 0 °C	46% (49% ee)	11%
R = Me,	**Mn(^{dMM}pdp)** / 0 °C	42.5% (56% ee)	0.5%
	Mn(^{Me2N}pdp) / 0 °C	61% (49% ee)	8%

Catalyst / T	Alcohol	Ketone
Mn(^{dMM}pdp) / -35 °C	24% (66% ee)	2%
Mn(^{Me2N}pdp) / -35 °C	44% (60% ee)	7%

Yields calculated with respect to the amount of H_2O_2 determined by GC analysis. 2-eha = 2-ethylhexanoic acid.

Scheme I.26. Oxidation of ethylbenzene, 4-methylethylbenzene and propylbenzene in TFE with different manganese catalysts.

Most interestingly, Bach and coworkers reported on the catalytic C-H bond oxidation of 3,4-dihydroquinolones through supramolecular recognition of the substrate by manganese porphyrin complex **77** (Scheme I.27.).[116] The desired oxygenated product was obtained thanks to two-point hydrogen bonding between the substrate and the supramolecular catalyst leading to excellent site selectivity and enantioselectivity (Scheme I.27.). Substituents in positions C3 and C7 have an impact on the isolated yield and enantioselectivity. Oxidation occurs selectively at the C4 methylene group with outstanding enantioselectivity (87-99% ee). The reaction tolerates different functional groups on the aromatic ring (X = Me, Et, OMe, OBn, Cl, OTf). Analogous results were obtained changing the methyl groups α to the carbonyl group with spyro cyclopropyl and cyclopentyl groups. It is particularly interesting to notice the unusual product chemoselectivity of the system, since overoxidation of the alcohol to the corresponding ketone is modest. This behavior may be related to the steric encumbrance of the *ipso* C-H bond of the alcohols. In keeping with the results discussed above on the enantioselective C-H bond oxidation of spirocyclic oxyndoles catalyzed by a ruthenium porphyrin complex (Scheme I.27.),[95] the mechanistic picture proposed by the authors consists in a Mn^V oxo species as the active oxidant, with substrate oxidation being directed by two complementary hydrogen bond interactions between the substrate and the catalyst, in particular at the pro-*S* hydrogen atom at C4 as described in Scheme I.27., below. The results clearly indicate that in these reactions enantioselectivity originates from the HAT step, as discussed above in Scheme I.14. The proposed hydrogen bond interactions are also supported by the observation that when the reaction was carried out on the *N*-methylathed derivative of substrate **78** only a small amount of oxidation product was observed with very low enantioselectivity (15% yield, 5% ee). After stereoselective HAT from the substrate to the Mn^V oxo intermediate, a fast hydroxyl rebound leads to the formation of the enantioenriched hydroxylated product.

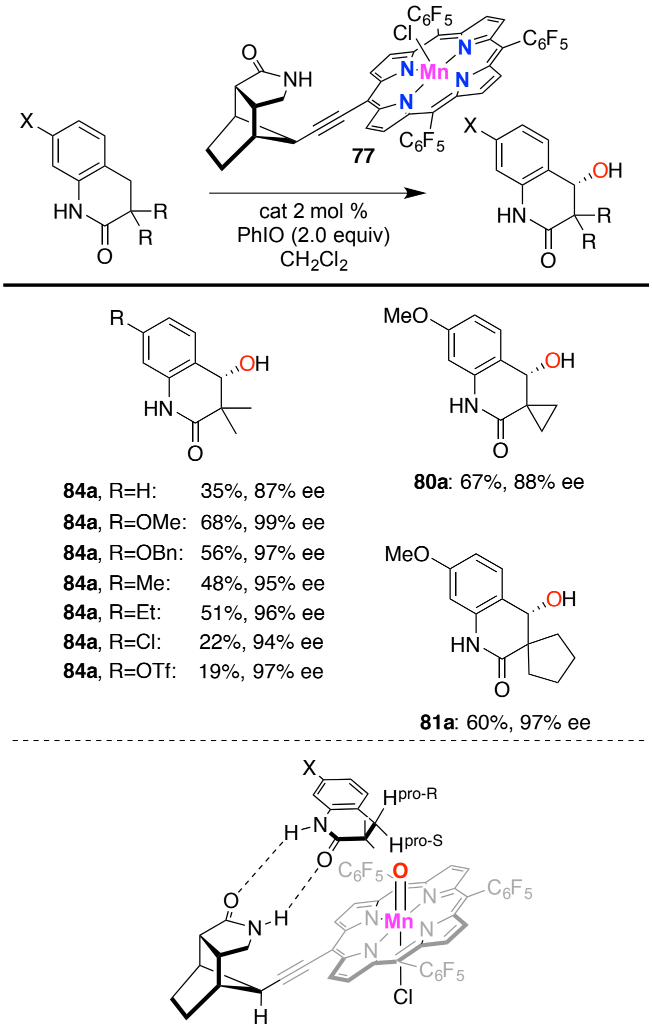
77
cat 2 mol %
PhIO (2.0 equiv)
CH2Cl2
84a, R=H: 35%, 87% ee
84a, R=OMe: 68%, 99% ee
84a, R=OBn: 56%, 97% ee
84a, R=Me: 48%, 95% ee
84a, R=Et: 51%, 96% ee
84a, R=Cl: 22%, 94% ee
84a, R=OTf: 19%, 97% ee
80a: 67%, 88% ee
81a: 60%, 97% ee
Hpro-R
Hpro-S

Scheme I.27. Effects of substituents X and R on the catalytic enantioselective hydroxylation of 3,4-dihydroquinolones and interaction between the active species deriving from complex and substrate.

I.4. References

1. Oloo, W. N.; Que, L., *Acc. Chem. Res.* **2015,** *48*, 2612-2621.
2. Huang, X.; Groves, J. T., *J. Biol. Inorg. Chem.* **2017,** *22*, 185-207.
3. Murray, R. W.; Jeyaraman, R.; Mohan, L., *J. Am. Chem. Soc.* **1986,** *108*, 2470-2472.
4. Curci, R.; Dinoi, A.; Rubino, M. F., Dioxirane oxidations: Taming the reactivity-selectivity principle. In *Pure and Applied Chemistry*, 1995; Vol. 67, p 811.
5. Mello, R.; Fiorentino, M.; Fusco, C.; Curci, R., *J. Am. Chem. Soc.* **1989,** *111*, 6749-6757.
6. Curci, R.; D'Accolti, L.; Fusco, C., *Acc. Chem. Res.* **2006,** *39*, 1-9.
7. Bovicelli, P.; Lupattelli, P.; Mincione, E.; Prencipe, T.; Curci, R., *J. Org. Chem.* **1992,** *57*, 5052-5054.
8. Murray, R. W.; Singh, M.; Jeyaraman, R., *J. Am. Chem. Soc.* **1992,** *114*, 1346-1351.
9. Minisci, F.; Zhao, L.; Fontana, F.; Bravo, A., *Tetrahedron Lett.* **1995,** *36*, 1697-1700.
10. Bravo, A.; Bjorsvik, H.-R.; Fontana, F.; Minisci, F.; Serri, A., *J. Org. Chem.* **1996,** *61*, 9409-9416.
11. Glukhovtsev, M. N.; Canepa, C.; Bach, R. D., *J. Am. Chem. Soc.* **1998,** *120*, 10528-10533.
12. Du, X.; Houk, K. N., *J. Org. Chem.* **1998,** *63*, 6480-6483.
13. Zou, L.; Paton, R. S.; Eschenmoser, A.; Newhouse, T. R.; Baran, P. S.; Houk, K. N., *J. Org. Chem.* **2013,** *78*, 4037-4048.
14. Yang, Z.; Yu, P.; Houk, K. N., *J. Am. Chem. Soc.* **2016,** *138*, 4237-4242.
15. Luo, Y., *Handbook of Bond Dissociation Energies in Organic Compounds*. 2002.
16. Chen, M. S.; White, M. C., *Science* **2007,** *318*, 783-787.
17. Chen, M. S.; White, M. C., *Science* **2010,** *327*, 566-571.
18. Asensio, G.; Castellano, G.; Mello, R.; González Núñez, M. E., *J. Org. Chem.* **1996,** *61*, 5564-5566.
19. Schmidt, V. A.; Quinn, R. K.; Brusoe, A. T.; Alexanian, E. J., *J. Am. Chem. Soc.* **2014,** *136*, 14389-14392.
20. White, M. C.; Doyle, A. G.; Jacobsen, E. N., *J. Am. Chem. Soc.* **2001,** *123*, 7194-7195.
21. Mas-Balleste, R.; Que, L., Jr., *J. Am. Chem. Soc.* **2007,** *129*, 15964-15972.
22. Cussó, O.; Garcia-Bosch, I.; Font, D.; Ribas, X.; Lloret-Fillol, J.; Costas, M., *Org. Lett.* **2013,** *15*, 6158-6161.
23. Lyakin, O. Y.; Ottenbacher, R. V.; Bryliakov, K. P.; Talsi, E. P., *ACS Catal.* **2012,** *2*, 1196-1202.
24. Cussó, O.; Garcia-Bosch, I.; Ribas, X.; Lloret-Fillol, J.; Costas, M., *J. Am. Chem. Soc.* **2013,** *135*, 14871-14878.
25. Ottenbacher, R. V.; Talsi, E. P.; Bryliakov, K. P., *ACS Catal.* **2015,** *5*, 39-44.
26. Ottenbacher, R. V.; Samsonenko, D. G.; Talsi, E. P.; Bryliakov, K. P., *ACS Catal.* **2014,** *4*, 1599-1606.
27. Murray, R. W., *Chem. Rev.* **1989,** *89*, 1187-1201.
28. Adam, W.; Curci, R.; Edwards, J. O., *Acc. Chem. Res.* **1989,** *22*, 205-211.
29. Vitaku, E.; Smith, D. T.; Njardarson, J. T., *J. Med. Chem.* **2014,** *57*, 10257-10274.
30. Nam, W.; Lee, Y.-M.; Fukuzumi, S., *Acc. Chem. Res.* **2014,** *47*, 1146-1154.
31. Kim, S.; Ginsbach, J. W.; Lee, J. Y.; Peterson, R. L.; Liu, J. J.; Siegler, M. A.; Sarjeant, A. A.; Solomon, E. I.; Karlin, K. D., *J. Am. Chem. Soc.* **2015,** *137*, 2867-2874.
32. Genovino, J.; Lütz, S.; Sames, D.; Touré, B. B., *J. Am. Chem. Soc.* **2013,** *135*, 12346-12352.
33. Ling, Z.; Yun, L.; Liu, L.; Wu, B.; Fu, X., *Chem. Comm.* **2013,** *49*, 4214-4216.

34. Park, J.; Morimoto, Y.; Lee, Y.-M.; You, Y.; Nam, W.; Fukuzumi, S., *Inorg. Chem.* **2011,** *50*, 11612-11622.
35. Murahashi, S.; Naota, T.; Yonemura, K., *J. Am. Chem. Soc.* **1988,** *110*, 8256-8258.
36. Zaitsev, V. G.; Shabashov, D.; Daugulis, O., *J. Am. Chem. Soc.* **2005,** *127*, 13154-13155.
37. Zhang, S.-Y.; He, G.; Zhao, Y.; Wright, K.; Nack, W. A.; Chen, G., *J. Am. Chem. Soc.* **2012,** *134*, 7313-7316.
38. Chan, K. S. L.; Wasa, M.; Chu, L.; Laforteza, B. N.; Miura, M.; Yu, J.-Q., *Nat. Chem.* **2014,** *6*, 146.
39. Asensio, G.; Gonzalez-Nunez, M. E.; Bernardini, C. B.; Mello, R.; Adam, W., *J. Am. Chem. Soc.* **1993,** *115*, 7250-7253.
40. Lee, M.; Sanford, M. S., *J. Am. Chem. Soc.* **2015,** *137*, 12796-12799.
41. Mbofana, C. T.; Chong, E.; Lawniczak, J.; Sanford, M. S., *Org. Lett.* **2016,** *18*, 4258-4261.
42. Lee, M.; Sanford, M. S., *Org. Lett.* **2017,** *19*, 572-575.
43. Lersch, M.; Tilset, M., *Chem. Rev.* **2005,** *105*, 2471-2526.
44. Stahl, S. S.; Labinger, J. A.; Bercaw, J. E., *Angew. Chem. Int. Ed.* **1998,** *37*, 2180-2192.
45. Shilov, A. E.; Shteinman, A. A., *Coord. Chem. Rev.* **1977,** *24*, 97-143.
46. Labinger, J. A.; Herring, A. M.; Bercaw, J. E., *J. Am. Chem. Soc.* **1990,** *112*, 5628-5629.
47. Howell, J. M.; Feng, K.; Clark, J. R.; Trzepkowski, L. J.; White, M. C., *J. Am. Chem. Soc.* **2015,** *137*, 14590-14593.
48. Gomez, L.; Garcia-Bosch, I.; Company, A.; Benet-Buchholz, J.; Polo, A.; Sala, X.; Ribas, X.; Costas, M., *Angew. Chem. Int. Ed.* **2009,** *48*, 5720-5723.
49. Sharma, A.; Hartwig, J. F., *Nature* **2015,** *517*, 600.
50. Gormisky, P. E.; White, M. C., *J. Am. Chem. Soc.* **2013,** *135*, 14052-14055.
51. Bigi, M. A.; Reed, S. A.; White, M. C., *J. Am. Chem. Soc.* **2012,** *134*, 9721-9726.
52. Olah, G. A.; Reddy, V. P.; Prakash, G. K. S., *Chem. Rev.* **1992,** *92*, 69-95.
53. Hehre, W. J., *Acc. Chem. Res.* **1975,** *8*, 369-376.
54. Armin, d. M., *Angew. Chem. Int. Ed.* **1979,** *18*, 809-826.
55. D'Accolti, L.; Dinoi, A.; Fusco, C.; Russo, A.; Curci, R., *J. Org. Chem.* **2003,** *68*, 7806-7810.
56. Curci, R.; D'Accolti, L.; Fiorentino, M.; Fusco, C.; Adam, W.; González-Nu~nez, M. E.; Mello, R., *Tetrahedron Lett.* **1992,** *33*, 4225-4228.
57. J., S.; A., E., *Helv. Chim. Acta* **1955,** *38*, 1529-1536.
58. Chen, K.; Eschenmoser, A.; Baran, P. S., *Angew. Chem. Int. Ed.* **2009,** *48*, 9705-9708.
59. Zheng, C.; You, S.-L., *RSC Adv.* **2014,** *4*, 6173-6214.
60. Kille, S.; Zilly, F. E.; Acevedo, J. P.; Reetz, M. T., *Nat. Chem.* **2011,** *3*, 738–743.
61. Narayan, A. R. H.; Jimenez-Oses, G.; Liu, P.; Negretti, S.; Zhao, W.; Gilbert, M. M.; Ramabhadran, R. O.; Yang, Y.-F.; Furan, L. R.; Li, Z.; Podust, L. M.; Montgomery, J.; Houk, K. N.; Sherman, D. H., *Nat. Chem.* **2015,** *7*, 653-660.
62. Roiban, G.-D.; Agudo, R.; Reetz, M. T., *Angew. Chem. Int. Ed.* **2014,** *53*, 8659-8663.
63. Zhang, K.; Shafer, B. M.; Matthew D. Demars, I.; Stern, H. A.; Fasan, R., *J. Am. Chem. Soc* **2012,** *134*, 18695–18704.
64. Lewis, J. C.; Coelho, P. S.; Arnold, F. H., *Chem. Soc. Rev.* **2011,** *40*, 2003-2021.
65. King-Smith, E.; Zwick, C. R.; Renata, H., *Biochemistry* **2018,** *57*, 403-412.
66. Zwick, C. R.; Renata, H., *J. Am. Chem. Soc.* **2018,** *140*, 1165-1169.
67. Ortiz de Montellano, P. R., *Cytochrome P450: Structure, Mechanism and Biochemistry*. 3rd ed.; Kluwer Academic/Plenum Publishers: New York, 2005.
68. Meunier, B.; Bernadou, J., *Struct. Bonding* **2000,** *97*, 1-35.

69. Meunier, B.; de Visser, S. P.; Shaik, S., *Chem. Rev.* **2004,** *104*, 3947-3980.

70. Gotor, V. A., I.; Garcia-Urdiales, E. Asymmetric Organic Synthesis with Enzymes (Wiley-VCH) **2008**.

71. Schlichting, I.; Berendzen, J.; Chu, K.; Stock, A. M.; Maves, S. A.; Benson, D. E.; Sweet, R. M.; Ringe, D.; Petsko, G. A.; Sligar, S. G., *Science* **2000,** *287*, 1615-1622.

72. Peters, M. W.; Meinhold, P.; Glieder, A.; Arnold, F. H., *J. Am. Chem. Soc.* **2003,** *125*, 13442-13450.

73. Barry, S. M.; Challis, G. L., *ACS Catal.* **2013,** *3*, 2362-2370.

74. Karlsson, A.; Parales, J. V.; Parales, R. E.; Gibson, D. T.; Eklund, H.; Ramaswamy, S., *Science* **2003,** *299*, 1039-1042.

75. Wackett, L. P.; Kwart, L. D.; Gibson, D. T., *Biochemistry* **1988,** *27*, 1360-1367.

76. N.A. Guzman (Ed.), P. H., Protein Disulfide Isomerase, and Other; Structurally Related Proteins, D., New York, , **1998**.

77. Gorres, K. L.; Raines, R. T., *Anal. Biochem.* **2009,** *386*, 181-185.

78. Collagen Hydroxylases and the Protein Disulfide Isomerase Subunit of Prolyl 4-Hydroxylases. In *Advances in Enzymology and Related Areas of Molecular Biology: Amino Acid Metabolism, Part A*.

79. Rhoads, R. E.; Udenfriend, S., *Proceedings of the National Academy of Sciences* **1968,** *60*, 1473-1478.

80. Costas, M.; Mehn, M. P.; Jensen, M. P.; Que, L., Jr., *Chem. Rev.* **2004,** *104*, 939-986.

81. Hoffart, L. M.; Barr, E. W.; Guyer, R. B.; J. M. Bollinger, J.; Krebs, C., *Proc. Natl. Acad. Sci. USA* **2006,** *103*, 14738.

82. Fujita, Y.; Gottlieb, A.; Peterkofsky, B.; Udenfriend, S.; Witkop, B., *J. Am. Chem. Soc.* **1964,** *86*, 4709-4716.

83. Huang, X.; Groves, J. T., *Chem. Rev.* **2018,** *118*, 2491-2553.

84. Chakrabarty, S.; Austin, R. N.; Deng, D.; Groves, J. T.; Lipscomb, J. D., *J. Am. Chem. Soc.* **2007,** *129*, 3514-3515.

85. Jasniewski, A. J.; Que, L., *Chem. Rev.* **2018,** *118*, 2554-2592.

86. Auclair, K.; Hu, Z. B.; Little, D. M.; Ortiz de Montellano, P. R.; Groves, J. T., *J. Am. Chem. Soc.* **2002,** *124*, 6020-6027.

87. Austin, R. N.; Luddy, K.; Erickson, K.; Pender-Cudlip, M.; Bertrand, E.; Deng, D.; Buzdygon, R. S.; Beilen, J. B. v.; Groves, J. T., *Angew. Chem., Int. Ed.* **2008,** *47*, 5232–5234.

88. Saint-Denis, T. G.; Zhu, R.-Y.; Chen, G.; Wu, Q.-F.; Yu, J.-Q., *Science* **2018,** *359*.

89. Herrmann, P.; Bach, T., *Chem. Soc. Rev.* **2011,** *40*, 2022-2038.

90. Miyafuji, A.; Katsuki, T., *Tetrahedron* **1998,** *54*, 10339-10348.

91. Punniyamurthy, T.; Miyafuji, A.; Katsuki, T., *Tetrahedron Lett.* **1998,** *39*, 8295-8298.

92. Punniyamurthy, T.; Katsuki, T., *Tetrahedron* **1999,** *55*, 9439-9454.

93. Komiya, N.; Noji, S.; Murahashi, S.-I., *Tetrahedron Lett.* **1998,** *39*, 7921-7924.

94. Murahashi, S.-I.; Noji, S.; Hirabayashi, T.; Komiya, N., *Tetrahedron: Asymmetry* **2005,** *16*, 3527-3535.

95. Frost, J. R.; Huber, S. M.; Breitenlechner, S.; Bannwarth, C.; Bach, T., *Angew. Chem. Int. Ed.* **2015,** *54*, 691-695.

96. Qiu, B.; Xu, D.; Sun, Q.; Miao, C.; Lee, Y.-M.; Li, X.-X.; Nam, W.; Sun, W., *ACS Catal.* **2018**, 2479-2487.

97. Groves, J. T.; Viski, P., *J. Am. Chem. Soc.* **1989,** *111*, 8537-8538.

98. Groves, J. T.; Viski, P., *J. Org. Chem.* **1990,** *55*, 3628-3634.

99. Groves, J. T.; Nemo, T. E., *J. Am. Chem. Soc.* **1983,** *105*, 6243-6248.

100. Hamachi, K.; Irie, R.; Katsuki, T., *Tet. Lett.* **1996,** *37*, 4979-4982.
101. Hamada, T.; Irie, R.; Mihara, J.; Hamachi, K.; Katsuki, T., *Tetrahedron* **1998,** *54*, 10017-10028.
102. Ini, S.; Kapon, M.; Cohen, S.; Gross, Z., *Tetrahedron: Asymmetry* **1996,** *7*, 659-662.
103. Gross, Z.; Ini, S., *Org. Lett.* **1999,** *1*, 2077-2080.
104. Murahashi, S.-I.; Noji, S.; Komiya, N., *Adv. Synth. Catal.* **2004,** *346*, 195-198.
105. Zhang, R.; Yu, W.-Y.; Che, C.-M., *Tetrahedron Asymmetry* **2005,** *16*, 3520-3526.
106. Zhang, R.; Yu, W. Y.; Lai, T. S.; Che, C.-M., *Chem. Commun.* **1999**, 1791-1792.
107. Maux, P. L.; Srour, H. F.; Simonneaux, G., *Tetrahedron* **2012,** *68*, 5824-5828.
108. Srour, H.; Maux, P. L.; Simonneaux, G., *Inorg. Chem.* **2012,** *51*, 5850-5856.
109. Gomez, L.; Canta, M.; Font, D.; Prat, I.; Ribas, X.; Costas, M., *J. Org. Chem.* **2013,** *78*, 1421-33.
110. Prat, I.; Gomez, L.; Canta, M.; Ribas, X.; Costas, M., *Chemistry (Weinheim an der Bergstrasse, Germany)* **2013,** *19*, 1908-13.
111. Font, D.; Canta, M.; Milan, M.; Cusso, O.; Ribas, X.; Gebbink, R.; Costas, M., *Angew. Chem. Int. Ed.* **2016,** *55*, 5776-5779.
112. Ottenbacher, R. V.; Samsonenko, D. G.; Talsi, E. P.; Bryliakov, K. P., *Org. Lett.* **2012,** *14*, 4310–4313.
113. Talsi, E. P.; Samsonenko, D. G.; Ottenbacher, R. V.; Bryliakov, K. P., *ChemCatChem* **2017,** *9*, 4580-4586.
114. Talsi, E. P.; Samsonenko, D. G.; Bryliakov, K. P., *ChemCatChem* **2017,** *9*, 2599-2607.
115. Dantignana, V.; Milan, M.; Cussó, O.; Company, A.; Bietti, M.; Costas, M., *ACS Cent. Sci.* **2017**.
116. Burg, F.; Gicquel, M.; Breitenlechner, S.; Pöthig, A.; Bach, T., *Angew. Chem. Int. Ed.* **2018,** *57*, 2953-2957.

Chapter II

Objectives

Metalloenzymes involved in oxidation reactions can override the limitations found in conventional synthetic oxidation protocols, operating with high efficiency and in a selective manner. For this reason, small molecules capable to operate like metalloenzymes, have the potential to be employed as catalysts in novel synthetically useful oxidation procedures. Considering the excellent efficiency, selectivity and soft conditions of oxidation reactions catalyzed by enzymes such as heme and non-heme oxygenases, and inspired by their mechanisms of action, in this thesis we target **the development of biologically inspired manganese and iron tetradentate complexes as catalysts for C-H oxidation reactions**.

In particular, we focused our attention on chiral manganese and iron complexes with the general formula $[M(CF_3SO_3)_2(L)]$ (L = mcp and pdp, mcp = *N,N'*-dimethyl *N,N'*-bis(2-pyridylmethyl)-2,2'-bipyrrolidine). This class of complexes has been widely used in aliphatic C-H bond oxidation, asymmetric olefin epoxidation and *cis*-dihydroxylation. **Our aim in this thesis is to achieve high levels of site-selectivity for C-H bond oxidation reactions on aliphatic sites**. Moreover, we also focused our attention on the asymmetric oxidation of nonactivated aliphatic C-H bonds.

Two strategies to achieve those goals have been pursued in this thesis.

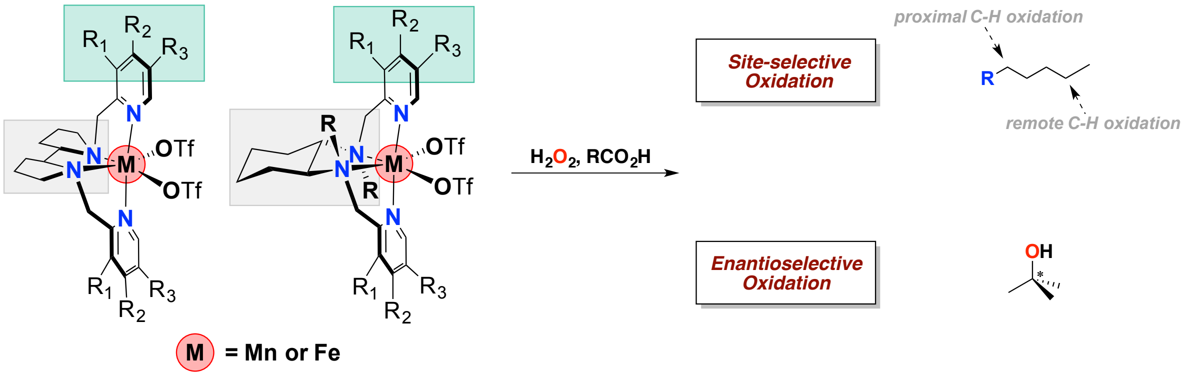

Scheme II.1. General scheme of the objectives.

The first strategy consists in the development of the catalysts reported in Scheme II.1, including their preparation, characterization and study in catalytic C-H oxidation reactions. We envisioned that modification of both the backbone and the substituents on the pyridine rings would lead to a higher control of the site- and the enantioselectivity of the C-H bond oxidation reaction. To design the catalysts, we take as starting point previous catalysts reported in the literature. In particular, we focused our attention on the mcp backbone system. The development of new catalysts is proposed by modification of the electronic and steric properties of the substituents on position 2, 3 and 4 of the pyridine rings. Moreover, different ligands based on the mcp backbone, but differing in the nature of the *N*-alkyl group (R in Scheme II.1.) are also targeted. The role of different carboxylic acids on the reaction site- and enantioselectivity s will be also investigated.

The second strategy pursued will be to explore the possibility of controlling the site-selectivity of C-H oxidation reactions by changing the electronic and steric properties of functional groups present in the substrate. In particular, stereoelectronic effects will be explored as site directing elements. Studies will be focused in substrates containing the amide functional group, which represents an especially important functionality in organic chemistry, present in a variety of natural products, bioactive molecules and organic materials.

Chapter III

Tuning Selectivity in Aliphatic C–H Bond Oxygenation of *N*-Alkylamides and Phthalimides Catalyzed by Manganese Complexes

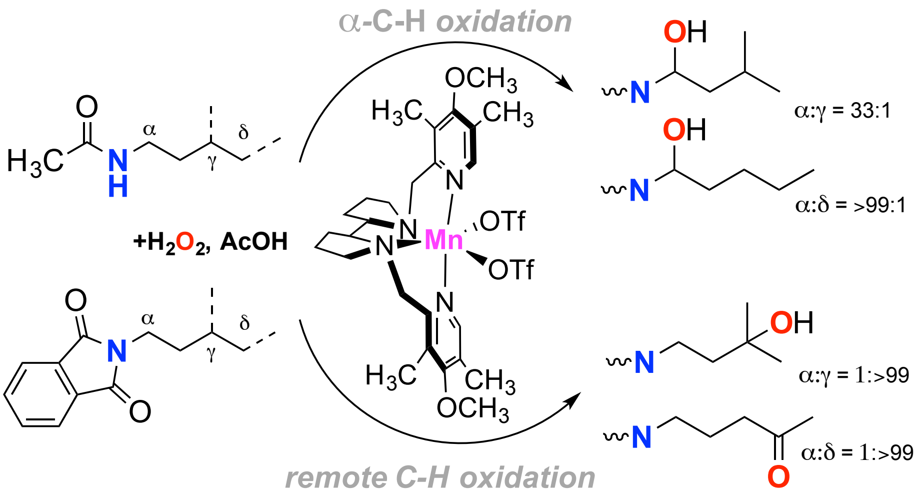
α-C-H oxidation
H3C
O
N
H
α
γ
δ
+H2O2, AcOH
O
N
O
α
γ
δ
OCH3
H3C
CH3
N
N
N
Mn
OTf
OTf
N
H3C
CH3
OCH3
OH
N
α:γ = 33:1
OH
N
α:δ = >99:1
N
OH
α:γ = 1:>99
N
O
α:δ = 1:>99
remote C-H oxidation

This chapter correspond to the following publication:

Milan, M.; Carboni, G.; Salamone, M.; Costas, M.; Bietti, M. *ACS Catal.* **2017**, *7*, 5903-5911

Reproduced with permission from:

Milan, M.; Carboni, G.; Salamone, M.; Costas, M.; Bietti, M. *A CSCatal.* 2017, *7*, 5903-5911

http://dx.doi.org/10.1021/acscatal.7b02151
ACS Catal. 2017, 7, 5903−5911

Copyright © 2017 American Chemical Society

ACS Catalysis

Research Article

pubs.acs.org/acscatalysis

Tuning Selectivity in Aliphatic C−H Bond Oxidation of *N*-Alkylamides and Phthalimides Catalyzed by Manganese Complexes

Michela Milan,[†] Giulia Carboni,[‡] Michela Salamone,[‡] Miquel Costas,*,[†] and Massimo Bietti*,[‡]

[†]QBIS Research Group, Institut de Química Computacional i Catàlisi (IQCC) and Departament de Química, Universitat de Girona, Campus Montilivi, Girona, E-17071 Catalonia, Spain

[‡]Dipartimento di Scienze e Tecnologie Chimiche, Università "Tor Vergata", Via della Ricerca Scientifica, 1 I-00133 Rome, Italy

Supporting Information

ABSTRACT: Site selective C−H oxidation of *N*-alkylamides and phthalimides with aqueous hydrogen peroxide catalyzed by manganese complexes is described. These catalysts are shown to exhibit substantially improved performance in product yields and substrate scope in comparison with their iron counterparts. The nature of the amide and imide group and of the *N*-alkyl moiety are shown to be effective tools in order to finely tune site selectivity between proximal (adjacent to the nitrogen) and remote C−H bonds on the basis of steric, electronic, and stereoelectronic effects. Moreover, formation of the α-hydroxyalkyl product in good yield and with excellent product chemoselectivity was observed in the reactions of the pivalamide and acetamide derivatives bearing an α-CH_2 group, pointing again toward an important role played by stereoelectronic effects and supporting the hypothesis that these oxidations proceed via hydrogen atom transfer (HAT) to a high-valent manganese−oxo species. Good product yields and mass balances are obtained in short reaction times and under mild experimental conditions when relatively low loadings of an electron-rich manganese catalyst are used. The potential utility of these reactions for preparative purposes is highlighted in the site-selective oxidation of the pivalamide and phthalimide derivatives of substrates of pharmaceutical interest.

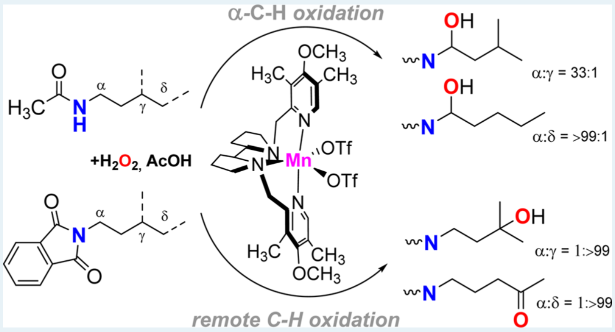

KEYWORDS: *C−H oxidation, manganese and iron catalysts, hydrogen atom transfer, stereoelectronic effects, selectivity, amides, phthalimides*

INTRODUCTION

The selective functionalization of aliphatic C−H bonds in organic molecules represents one of the main challenges of modern synthetic organic chemistry because of their inert character and because selectivity is hampered by the multitude of C−H bonds that differ only slightly in terms of their electronic and steric properties. Increasing efforts have been devoted toward meeting this rewarding research goal, by pursuing metal-catalyzed reactions that could implement site selectivity in C−H functionalization reactions.[1−6]

A breakthrough toward the development of selective aliphatic C−H oxidation methodologies for organic synthesis was disclosed in the studies of White and co-workers, using non-heme nitrogen-ligated iron coordination complexes as catalysts and hydrogen peroxide as oxidant.[7,8] Selectivity rules for the C−H oxidation reaction were clearly defined on the basis of steric, electronic, and stereoelectronic effects, and a reaction mechanism proceeding through an initial hydrogen abstraction step was proposed.[9,10] When these elements were taken into consideration, a reliable prediction of oxidation sites could be deduced in several substrates, including complex natural products. Related manganese complexes have been more recently shown to follow the same selectivity patterns, but their use remains much less explored.[11,12] Catalyst-dependent selectivity distinct from the innate relative reactivity of C−H bonds can also be introduced by employing highly structured catalysts.[13−16] On one hand, sterically crowded catalysts favor oxidation of secondary over tertiary C−H bonds because, despite being weaker, the latter are sterically more demanding.[13−15] On the other hand, chiral bulky catalysts can also exhibit chirality-dependent site selectivity in the oxidation of steroids.[13]

Amines represent an especially important class of organic compounds, which serve in particular as the basic structure of a variety of natural products, bioactive molecules, and organic materials. The tolerance of this functional group to metal-catalyzed oxidation reactions is particularly critical, however. In addition to their strong tendency to bind and deactivate metal centers, amines can also be easily oxidized.[17] Quite importantly, functionalization of amine substrates, when achieved, selectively occurs at the strongly activated C−H that is α to the nitrogen center.[18−30] Remote aliphatic C−H bond oxidation of amines with iron and manganese catalysts was recently reported.[31−33]

Received: July 1, 2017
Published: July 25, 2017

© XXXX American Chemical Society

DOI: 10.1021/acscatal.7b02151
ACS Catal. 2017, 7, 5903−5911

In these works protonation of the amine, or formation of Lewis acid−base amine−BF_3 adducts, electronically deactivated the amine moiety and the C−H bonds that are adjacent to the nitrogen center, favoring selective oxidation at remote positions (Scheme 1a).

Scheme 1. Influence of (a) Medium and (b) Structural Effects on Site Selectivity in Aliphatic C−H Bond Functionalization of Amine and Amine-Derived Substrates

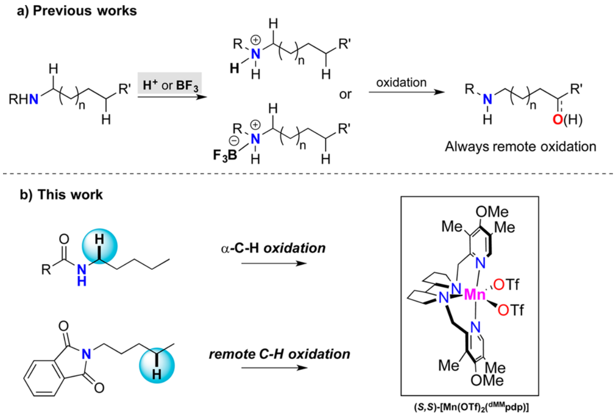

Along this vein, amide functionalities are also very interesting because, by decreasing nucleophilicity at the nitrogen center, they can be employed as protecting groups for primary and secondary amines, and the functionalization of these substrates can thus expand the structural elaboration of amine-containing targets. Moreover, highly efficient C−H oxidation of monosubstituted cyclohexanes has been recently described with manganese catalysts, where an *N*-cyclohexylamide moiety was the key to enable high levels of regio- and enantioselectivity,[34] highlighting a very powerful role of this functional group in defining selective C−H oxidation reactions. In this study it was proposed that enantioselectivity arises in the C−H cleavage step via hydrogen atom transfer (HAT) to a chiral high-valent manganese−oxo species, followed by a fast hydroxyl rebound toward the incipient carbon-centered radical.

In addition to the utility of the amide moiety as an amine protecting group, selective oxidation of the aliphatic C−H bonds of these substrates is also of considerable interest in modern organic synthesis. With secondary and tertiary amides bearing *N*-alkyl groups and with *N*-acyl cyclic amines, oxidation generally occurs at the C−H bonds that are α to nitrogen, yielding α-hydroxylated products that are rapidly converted into imides, a useful functional group that has multiple applications.[26,35−40] Quite importantly, isolation of the first-formed α-hydroxy derivatives was only achieved in a very limited number of cases,[41−43] despite the fact that such products can represent versatile intermediates for further synthetic elaboration.[44] Therefore, amide substrates constitute a very promising platform for the development of selective C−H oxidation procedures, where control over site (intramolecular) and product (intermolecular) selectivity can be particularly challenging but highly rewarding.

Within this framework, we reasoned that amide moieties have the potential to be developed into powerful directing groups for site-selective C−H functionalization because their electronic properties and steric demands can be uniquely tuned. For example, the acyl moiety can be changed from a strongly electron withdrawing group such as trifluoroacetyl to the weaker acetyl group, and the electron-withdrawing character can be further increased by conversion into an imide derivative. On the other hand, sterically demanding acyl moieties, such as pivaloyl, can be envisioned to affect the accessibility of the different C−H bonds of the substrate, translating into site selectivity. With these considerations in mind, in this work aliphatic C−H bond oxidation of *N*-alkylpivalamides, acetamides, trifluoroacetamides, and phthalimides bearing 1-pentyl, 2-(5-methylhexyl), and 1-(3-methylbutyl) groups bound to nitrogen (structures **S1−S12** displayed below in Table 1) has been explored using iron and manganese catalysts and hydrogen peroxide as the oxidant. The three series of substrates were chosen in order to allow a thorough evaluation of the role of structural and electronic effects on the C−H functionalization selectivity, taking advantage of the methylenic C−H bonds present in the *N*-pentyl derivatives (**S1−S4**), the combination of a tertiary α-C−H bond with a tertiary δ-C−H bond in the *N*-2-(5-methylhexyl) derivatives (**S5−S8**), and the combination of an α-CH_2 group with a tertiary γ-C−H bond in the *N*-1-(3-methylbutyl) derivatives (**S9−S12**).

Table 1. Oxidation of *N*-Pentylpivalamide (S1) with Different Catalysts

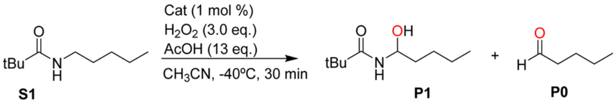

entry	catalyst	conversn, %[a]	yield of **P1**, %[a]	yield of **P0**, %[a]
1[b]	**Fe(pdp)**	<2%		
2	**Mn(pdp)**	64	41	15
3[b]	**Fe(mcp)**	10		
4	**Mn(mcp)**	36	10	4
5[b]	**Fe(^{dMM}pdp)**	15	6	5
6	**Mn(^{dMM}pdp)**	**99**	**60**	**11**
7	**Mn(^{dMM}mcp)**	97	42	10
8	**Mn(^{Cl}mcp)**	22	8	11
9[b]	**Fe(^{Me2N}pdp)**	4		
10	**Mn(^{Me2N}pdp)**	60	14	12
11[b]	**Fe(^{TIPS}mcp)**	11		
12	**Mn(^{TIPS}mcp)**	65	58	4
13	**Mn(^{TIPS}pdp)**	52	31	13
14	**Mn(^{BzIm}pdp)**	98	40	10
15	**Mn(^{CF3}mcp)**	63	15	12
16[c]	**Mn(^{dMM}pdp)**	60	45	12

[a] Conversions and yields determined from crude reaction mixtures by GC or ^{1}H NMR. [b] Reaction conditions: Fe catalyst (3 mol %), H_2O_2 (2.5 equiv), AcOH (1.5 equiv) in CH_3CN at 0 °C for 30 min. [c] Cyclopropanecarboxylic acid was used instead of acetic acid.

The results obtained show that with manganese catalysts the nature of the amide and imide group and of the *N*-alkyl moiety effectively tunes site selectivity between proximal (adjacent to the nitrogen) and remote C−H bonds on the basis of steric, electronic, and stereoelectronic effects (Scheme 1b). Good product yields and mass balances are obtained in short reaction times and under mild experimental conditions when relatively low loadings of an electron-rich manganese catalyst are used, highlighting the potential utility of these reactions for preparative purposes. Quite importantly, in the reactions of the pivalamide and acetamide derivatives bearing a CH_2 group

Scheme 2. Diagram of the Iron and Manganese Complexes Studied[a]

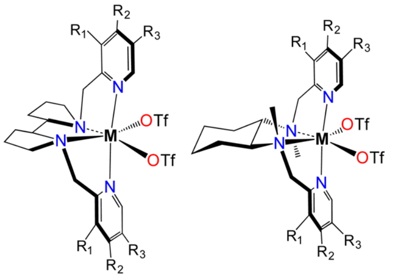

M(^{X}pdp) M(^{X}mcp)

M^{x}	R_1	R_2	R_3
Fe(pdp)	-H	-H	-H
Mn(pdp)	-H	-H	-H
Fe(mcp)	-H	-H	-H
Mn(mcp)	-H	-H	-H
Fe(^{dMM}pdp)	-Me	-OMe	-Me
Mn(^{dMM}pdp)	-Me	-OMe	-Me
Mn(^{dMM}mcp)	-Me	-OMe	-Me
Mn(^{Cl}mcp)	-H	-Cl	-H
Fe(^{Me2N}pdp)	-H	-NMe_2	-H
Mn(^{Me2N}pdp)	-H	-NMe_2	-H
Fe(^{TIPS}mcp)	-H	-H	-Si(^{i}Pr)$_3$
Mn(^{TIPS}mcp)	-H	-H	-Si(^{i}Pr)$_3$
Mn(^{TIPS}pdp)	-H	-H	-Si(^{i}Pr)$_3$
Mn(^{BzIm}pdp)	-BzIm[a]		
Mn(^{CF3}mcp)	-H	-H	-Ph(CF_3)$_2$

[a] *N*-Methylbenzimidazole instead of pyridine.

α to nitrogen, good yields and excellent selectivities were observed for the formation of the α-hydroxyalkyl product.

RESULTS AND DISCUSSION

The oxidation of *N*-pentylpivalamide (**S1**) with hydrogen peroxide catalyzed by different iron and manganese complexes was initially explored. The catalysts tested are based on chiral iron and manganese complexes bearing tetradentate ligands and have the general formula [M(CF_3SO_3)$_2$(L)] (L = mcp, pdp; mcp = *N,N′*-dimethyl *N,N′*-bis(2-pyridylmethyl)-1,2-*trans*-diaminocyclohexane, pdp = *N,N′*-bis(2-pyridylmethyl)-2,2′-bipyrrolidine); their structures are displayed in Scheme 2, all of which have been recently described to be particularly efficient in aliphatic C−H oxidation reactions.[7,8,11−13,16,34,45−48] The results of these reactions are shown in Table 1.

Standard conditions for the reactions catalyzed by the manganese complexes involved syringe pump delivery of H_2O_2 (3.0 equiv) to an acetonitrile solution of the catalyst (1 mol %) and AcOH (13 equiv) in CH_3CN at −40 °C over 30 min. Exploration of the simplest catalysts of the series, **Fe(pdp)**, **Mn(pdp)**, **Fe(mcp)**, and **Mn(mcp)** (Table 1, entries 1−4), reveals that only the manganese catalysts oxidize the substrate, with the bipyrrolidine **Mn(pdp)** catalyst being more efficient than the cyclohexanediamine **Mn(mcp)** catalyst. The negligible conversion observed with **Fe(pdp)** and **Fe(mcp)** highlights the challenge that these substrates represent for the iron complexes. With the two manganese catalysts the product derived from C−H hydroxylation α to nitrogen (**P1**) was obtained in poor (10%, entry 4) to moderate (41%, entry 2) yield, together with smaller amounts of pentanal. Despite the electron-withdrawing character of the amide group, the nitrogen atom in pivalamide **S1** is still sufficiently electron rich to activate the α-C−H bonds. No products deriving from oxidation at C2−C5 or from oxidation of the primary *t*-Bu C−H bonds were observed. Remarkably, no evidence for the formation of the corresponding imide, which is the most common product resulting from oxidation of the C−H bonds that are α to nitrogen in *N*-alkylamides,[38] was observed. Pentanal presumably arises from oxidative C−N bond cleavage. Control experiments showed that **P1** does not convert into pentanal under the reaction conditions, indicating that the latter is formed via a path that competes with α-C−H hydroxylation.[49] Improved yields, from moderate to good, were obtained when electron-donating methyl and methoxy groups (**Mn(^{dMM}pdp)** and **Mn(^{dMM}mcp)**) were introduced at pyridine positions 3, 4, and 5 of the manganese complexes (entries 6 and 7). Making the catalyst more electron rich partially rescues activity also in the case of iron catalysts; thus, **Fe(^{dMM}pdp)** provides oxidation products but in low yield (entry 5), far from the values obtained with the manganese analogue (entry 6). On the other hand, the more electron poor catalyst **Mn(^{Cl}mcp)** delivered only very low product yields (entry 8). This apparent correlation between catalytic activity and electron-donating ability of the ligand follows that observed in epoxidation reactions.[50,51] However, the use of the electron-rich **Fe(^{Me2N}pdp)** and **Mn(^{Me2N}pdp)** catalysts, which have proven particularly active in olefin epoxidation reactions[51] but are quite sensitive to harsh oxidation conditions, affords no product or only 14% of the α-C−H hydroxylation product (entries 9 and 10). Improvement in product yield was also observed by the use of manganese catalysts, where bulky groups such as triisopropylsilyl (TIPS) were introduced at positions 3 of the pyridine rings (entries 12 and 13). In this case, the cyclohexanediamine system **Mn(^{TIPS}mcp)** performs substantially better than the bipyrrolidine system **Mn(^{TIPS}pdp)**, in line with our previous observations on the oxidation of *N*-cyclohexylamides.[34] In addition, other manganese complexes were included in the catalyst screening: namely, **Mn(^{BzIm}pdp)**, where the pyridine rings were replaced by *N*-methylbenzimidazole (BzIm) rings, and **Mn(^{CF3}mcp)**, where 2,6-bis(trifluoromethyl)phenyl groups were appended to position 3 of the pyridines of the mcp ligand (entries 14 and 15). None of these catalysts improved the outcome of the reaction. Finally, cyclopropanecarboxylic acid was used instead of acetic acid in reactions with the **Mn(^{dMM}pdp)** catalyst (entry 16). This acid is sterically more demanding than acetic acid and has recently proven particularly effective in regio- and enantioselective C−H oxidation of *N*-cyclohexylamides with similar manganese catalysts.[34] In comparison to acetic acid, the reaction furnished reduced yields of **P1** and pentanal as the only products, in similar relative ratios, although the mass balance of the reaction was particularly good. Therefore, on the basis of this screening, **Mn(^{dMM}pdp)** in combination with acetic acid was selected as the catalyst and carboxylic acid partner of choice for the oxidation of the three series of *N*-alkylamide and phthalimide substrates, in order to study in detail the effect of *N*-alkyl structure and of functional group structure and electronics on

Table 2. Oxidation of Different *N*-Pentyl Derivatives

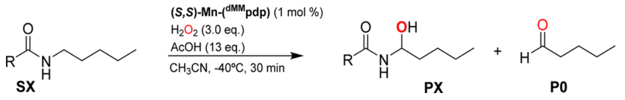
(*S*,*S*)-Mn-(dMMpdp) (1 mol %)
H2O2 (3.0 eq.)
AcOH (13 eq.)
CH3CN, -40ºC, 30 min
R
O
N
H
OH
+
SX
PX
P0

Entry/ Substrate (SX)		Conv %[a]	Yield PX %[a] (Isolated)	Yield P0 %[a]
1	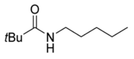 **S1**	99	60 (48)	11
2	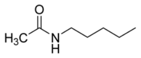 **S2**	89	40[b]	13
3	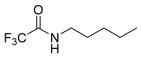 **S3**	64	26	6

Entry 4

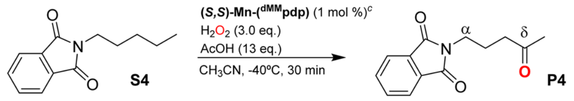
(*S*,*S*)-Mn-(dMMpdp) (1 mol %)c
H2O2 (3.0 eq.)
AcOH (13 eq.)
CH3CN, -40ºC, 30 min
O
N
α
δ
S4
P4

61% conv

45[a] (41) % yield
<1:99 α:δ

[a]Conversions and yields determined from crude reaction mixtures by GC or ^{1}H NMR. [b]In a larger scale catalysis experiment driven to complete substrate conversion, 36% yield of product **P2** and 36% yield of the overoxidized imide product were isolated together with pentanal (determined by GC) in 11% yield. [c]Iterative addition (2×): cat. (1 mol %), H_2O_2 (3.0 equiv), AcOH (13 equiv) in CH_3CN at −40 °C for 30 min.

Table 3. Oxidation of Different *N*-2-(5-Methylhexyl) Derivatives

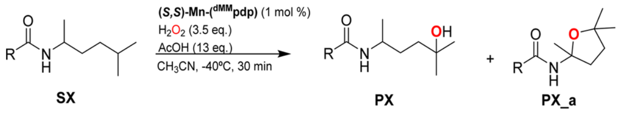
(*S*,*S*)-Mn-(dMMpdp) (1 mol %)
H2O2 (3.5 eq.)
AcOH (13 eq.)
CH3CN, -40ºC, 30 min
R
O
N
H
OH
+
SX
PX
PX_a

Entry	Substrate	Conv %[a]	Yield PX %[a] (isolated)	Yield PX_a %[a] (isolated)
1	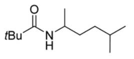 **S5**	93	77 (52)	13
2	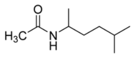 **S6**	99	41 (36)	34 (33)[b]
3	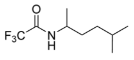 **S7**	90	84 (58)	2

Entry 4

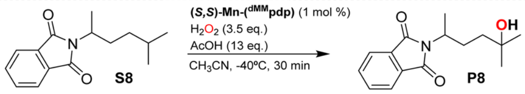
(*S*,*S*)-Mn-(dMMpdp) (1 mol %)
H2O2 (3.5 eq.)
AcOH (13 eq.)
CH3CN, -40ºC, 30 min
O
N
OH
S8
P8

>99% conv

84[a] (83) % yield

[a]Conversions and yields determined from crude reaction mixtures by GC or ^{1}H NMR. [b]**P6_a** was isolated with 11% yield of a nonidentified impurity that could not be separated.

the yield and site selectivity of the reaction. The product distributions observed in the oxidation of the *N*-pentyl (**S1**−**S4**), *N*-2-(5-methylhexyl) (**S5**−**S8**) and *N*-1-(3-methylbutyl) derivatives (**S9**−**S12**) catalyzed by **Mn(**$^{\mathbf{dMM}}$**pdp)** are displayed in Tables 2−4, respectively.

Starting from the reactions of the *N*-pentyl derivatives, the results displayed in Table 2 show that replacement of the sterically demanding pivaloyl (**S1**) for acetyl (**S2**) and for the more electron withdrawing trifluoroacetyl (**S3**) (Table 2, entries 1−3) did not alter site selectivity, as clearly shown for all three substrates by the formation of products **P1**−**P3**, respectively, derived from *α*-C−H bond hydroxylation. Interestingly, the imide product was only observed in the oxidation of **S2**, when the reaction was driven to full substrate conversion. Under these conditions formation of the *α*-hydroxylation and imide products in a 1:1 ratio was observed, supporting the hypothesis of a higher reactivity of the substrate **S2** in comparison to the first formed product **P2** in the **Mn(**$^{\mathbf{dMM}}$**pdp)** catalyzed reaction and indicating that the imide product is derived from overoxidation of **P2**. Pentanal, which as mentioned above is presumably derived from oxidative C−N bond cleavage, was again identified in the reaction mixtures as a

DOI: 10.1021/acscatal.7b02151
ACS Catal. 2017, 7, 5903−5911

side product. The decrease in conversion and product yield observed on going from **S1** and **S2** to **S3** is in line with the electrophilic character of the intermediate manganese oxo complex and the electron-withdrawing effect of the CF_3 group that, in comparison to *t*-Bu and Me groups, deactivates the *α*-C−H bonds toward oxidation.

Most interestingly, on going from the *N*-pentylamides to *N*-pentylphthalimide (**S4**), a dramatic change in site selectivity was observed in the reactions catalyzed by **Mn(**$^{\mathbf{dMM}}$**pdp)** (Table 2, entry 4), where exclusive formation of the *δ*-ketoamide product resulting from oxidation at the most remote methylene site of the pentyl moiety was detected. This behavior can be explained on the basis of the increased electron-withdrawing ability of the phthalimido group that, in comparison to the acyl groups, strongly deactivates the *α*-C−H bonds, as well as the *β* and *γ* bonds, toward oxidation, showing in particular that in these reactions site selectivity can be drastically changed through a simple synthetic modification of a parent amine substrate. The remote functionalization observed in the reaction of **S4** is in agreement with the results of recent studies on aliphatic C−H bond oxidation of *N*-pentyl, *N*-cyclohexyl, and *N*-cycloheptyl derivatives, where in all cases the phthalimido group provided the highest selectivity for the most remote methylene group.[34,52−54] However, in partial contrast to the present study, Alexanian and co-workers have recently shown that sterically demanding amidyl radicals, generated photochemically from *N*-bromo- and *N*-chloroamides, react with *N*-pentylphthalimide leading, in addition to the *δ*-haloimide, to the formation of sizable amounts (18−19%) of products derived from halogenation at other sites.[52,53] This comparison points toward an important role of the **Mn(**$^{\mathbf{dMM}}$**pdp)** catalyst in defining this exquisite C−H oxidation selectivity that may reflect a higher steric demand of the reactive manganese−oxo species in comparison to the amidyl radicals, but it may also denote a higher and less discriminate HAT reactivity of the latter, a hypothesis that is well supported by the observation of small amounts of products derived from halogenation of the terminal methyl group.[52,53]

Moving then to the oxidation of the *N*-2-(5-methylhexyl) derivatives (**S5**−**S8**), characterized by the presence of a tertiary *α*-C−H bond and a tertiary C−H bond at the remote *δ* position, the main product observed is in all cases the hydroxylated product **PX** that is derived from oxidation at the *δ*-C−H bond (Table 3, entries 1−4). This result is in sharp contrast with the oxidations of **S1**−**S3**, which selectively occurred at the proximal *α*-methylene site (Table 2, entries 1−3). A second compound, **PX_a**, appears as a significant side product in the reactions of the least deactivated pivalamide (**S5**) and acetamide (**S6**) substrates and as a minor product in the reaction of the trifluoroacetamide substrate (**S7**). Formation of this cyclic product can be explained on the basis of *α*-C−H oxidation of the first-formed product **PX** followed by cyclization. The observation that the relative importance of product **PX_a** over **PX** increases with increasing conversion, together with the increased yield in **PX_a** observed on going from **S5** to **S6**, and the very low yield or lack of this product observed in the reactions of **S7** and **S8**, respectively, strongly supports this hypothesis, reflecting the contribution of steric (faster *α*-C−H oxidation of **P6** in comparison to **P5**) and electronic effects (slower *α*-C−H oxidation of **P7** in comparison to **P5** and **P6**) on the formation of this product.

The lack of products derived from tertiary *α*-C−H bond oxidation in **S5**−**S7** can be reasonably explained on the basis of the operation of stereoelectronic effects. As described in a recent time-resolved kinetic study on HAT from *N*-alkylamides to a representative oxygen-centered radical such as cumyloxyl ($CumO^\bullet$), an ∼9-fold decrease in the k_H value for HAT from the *α*-C−H bonds was measured on going from *N*-ethylpivalamide to *N*-isopropylpivalamide.[55] It was proposed that the introduction of a methyl group on the *α*-carbon increases the energy barrier required to reach the most suitable conformation for HAT where the *α*-C−H bonds are aligned with the amide *π* system (structure **A** in Scheme 3), accounting for the observed decrease in reactivity.

Scheme 3. Conformational Equilibrium for Rotation around the N−CH(CH$_3$)$_2$ Bond in *N*-Isopropylpivalamide

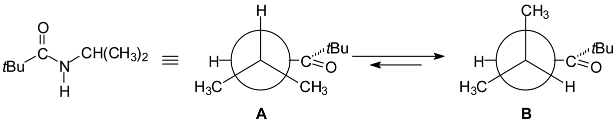

Along these lines, a similar explanation can be put forward to account for the regioselectivity observed in the present study in the **Mn(**$^{\mathbf{dMM}}$**pdp)**-catalyzed oxidation of **S5**−**S7**. Quite importantly, this observation supports the hypothesis that the reactions of alkanamides with $CumO^\bullet$ and the oxidations catalyzed by manganese complexes described in this work involve a common HAT step.

Of note, an analogous regioselective oxidation of a trifluoroacetamide substrate strictly related to **S7**, namely *N*-(2-(6-methylheptyl)trifluoroacetamide, with the $[Fe(pdp)(CH_3CN)_2](SbF_6)_2$ catalyst was previously described and rationalized on the basis of the electron-withdrawing *α*-C−H deactivation determined by the trifluoroacetyl group.[7] The current results indicate instead that stereoelectronic effects are at the basis of the observed regioselectivity.

Along the same vein, a very recent study on the aliphatic *α*-C−H functionalization of *N*-Boc-protected ethylmethylamine and isopropylmethylamine via a combination of photoredox, nickel, and HAT catalysis pointed toward steric effects as a rationale for the predominant alkylation of the primary *α*-C−H bonds of the methyl groups over the weaker secondary and tertiary bonds.[56] Also in this case, stereoelectronic effects can be reasonably invoked to account for this peculiar selectivity, pointing once again toward the very important role played by these effects in governing site selectivity in HAT-based functionalization of aliphatic C−H bonds that are *α* to sp^2 nitrogen atoms, such as those of amide and carbamate substrates.

Particularly relevant in the context of the oxidation of *N*-2-(5-methylhexyl) derivatives is the observation that with the phthalimide derivative **S8** the reaction progresses with excellent yield and mass balance (Table 3, entry 4), leading to exclusive oxidation at the remote tertiary position, with no formation of the secondary oxidation product **P8_a**.

Finally, the oxidation of *N*-1-(3-methyl)butyl derivatives **S9**−**S12** was evaluated. In this case, the proximal position is a methylenic site, which was envisioned to compete with the oxidation of a tertiary C−H bond at a remote *γ*-position. In line with the previous observations (Tables 2 and 3), in the reactions of the pivalamide (**S9**) and acetamide (**S10**) derivatives the *α*-CH_2 position is activated toward oxidation, and the proximal hydroxylated products **P9_b** and **P10_b** were preferentially obtained in good isolated yield (Table 4, entries 1

Table 4. Oxidation of Different *N*-1-(3-Methylbutyl) Derivatives

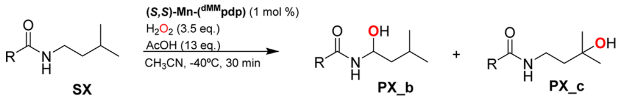

Entry	Substrate	Conv %[a]	Yield PX_b %[a] (isolated)	Yield PX_c %[a] (isolated)	Selectivity PX_b / PX_c[b]
1	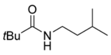 **S9**	93	66 (64)	7	4.7:1
2[c]	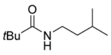 **S9**	<2	-	-	-
3	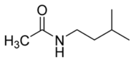 **S10**	95	66 (65)	1	33:1
4[c]	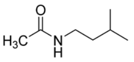 **S10**	<2	-	-	-
5	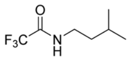 **S11**	91	7	77 (48)	1:22
6[c]	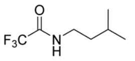 **S11**	55	11	36	1:6.5

Entry 7

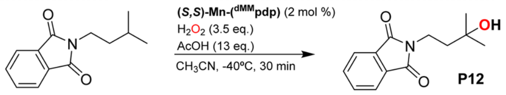

S12 73% conv

P12 68[a] (65) % yield
<1:99 α:γ

[a]Conversions and yields determined from crude reaction mixtures by GC or ^{1}H NMR. [b]Normalized ratio. [c]Reaction conditions: **Fe(pdp)** (3 mol %), H_2O_2 (2.5 equiv), AcOH (1.5 equiv) in CH_3CN at 0 °C for 30 min.

and 3), while the remote oxidized products **P9_c** and **P10_c** were observed only in low or very low amount. This can be explained on the basis of a stronger activation of the α-C−H bonds in comparison to the remote tertiary C−H bonds determined by the presence of the amide nitrogen atom. It is possible to notice that the presence of the bulkier pivaloyl group in comparison to acetyl can reduce the extent of α-oxidation; however, a good to excellent selectivity for this oxidation site was observed for both substrates (**PX_b**:**PX_c** = 4.7:1 and 33:1; Table 4, entries 1 and 3, respectively). The formation of **P9_b** and **P10_b**, with no evidence of overoxidation to the corresponding imide products, highlights once again the ability of this catalyst to perform oxidation of amide C−H bonds with very high levels of product selectivity. The origin of this unusual chemoselectivity can be explained on the basis of the stereoelectronic effects discussed above (see Scheme 3), where α-hydroxylation increases the energy barrier required to reach the most suitable conformation for HAT from this position where the α-C−H bonds are aligned with the amide π system. It can also be proposed that intramolecular hydrogen bonding between the α-hydroxyl and carbonyl groups plays a role in this respect, preventing optimal overlap of the α-C−H bond with the amide π system.

On the other hand, the presence of EWG groups led to a dramatic change in site selectivity. The predominant or exclusive formation of the product derived from remote tertiary C−H bond hydroxylation, **PX_c**, was obtained with the trifluoroacetamide and phthalimide substrates (**S11** and **S12**, respectively; Table 4, entries 5 and 7) with modest to good isolated yields and very good to outstanding levels of selectivity (**PX_b**:**PX_c** from 1:22 to <1:99; Table 4, entries 5 and 7, respectively). Very striking is the observation that the phthalimide derivative **S12** undergoes exclusive oxidation at the remote position, highlighting once again the powerful role of this functional group in governing site selectivity.

Finally, the poor performance of the iron analogues of the **Mn(pdp)** and **Mn($^{\mathrm{dMM}}$pdp)** catalysts was further investigated. It was noticed that with the **Fe(pdp)** and **Fe($^{\mathrm{dMM}}$pdp)** catalysts catalytic oxidation of amide substrates bearing activated α-C−H bonds (**S1**, **S9**, and **S10**) did not proceed or provided very low product yields (Table 1, entries 1 and 5; Table 4, entries 2 and 4). Instead, oxidation of amide substrates where oxidation takes place preferentially at remote positions (**S4**, see the Supporting Information; **S11**, see Table 4, entry 6) occurred with improved (albeit still modest) yields. We reasoned that the α-hydroxylated product may inhibit the catalyst, presumably by chelation through the carbonyl and α-OH groups. Consistent with this proposal, no oxidation products were obtained when a typical catalytic oxidation reaction of **S10** (50 equiv with respect to the catalyst) with **Fe(pdp)** was performed in the presence of **P10** (50 equiv with respect to the catalyst). Furthermore, reaction mixtures of the oxidation of **S1**, **S9**, and **S10** with the iron catalysts rapidly turned intense purple-blue following addition of hydrogen peroxide, suggesting the immediate formation of iron species that exhibit low-energy charge transfer transitions. Charge transfer from extended π

Scheme 4. Oxidation of Bioactive Molecules[a]

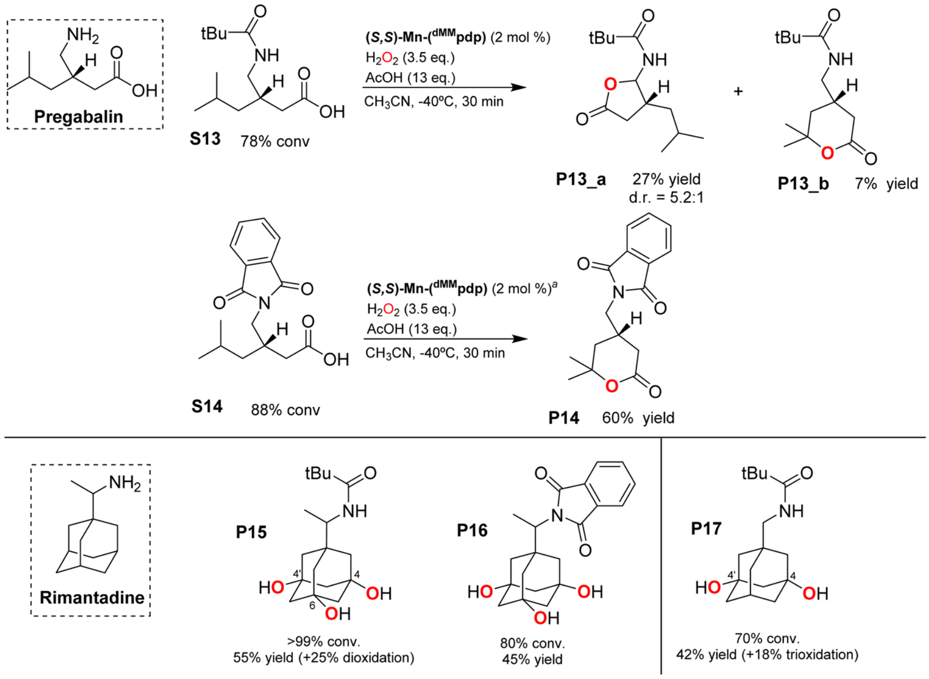

[a]Iterative addition (3×): cat. (2 mol %), H_2O_2 (3.5 equiv), AcOH (13 equiv) in CH_3CN at −40 °C for 30 min. Isolated yields.

systems of the ligand to a Fe^{III} center are usually associated with these spectroscopic features.[57−61] In addition, high-resolution mass spectrometry monitoring of the reaction of **Fe(pdp)** with **S10** under standard conditions showed cluster ions at *m*/*z* 261.1294 that can be assigned to $\{[Fe(pdp)(\mathbf{S10}) + O{-}H]\}^{2+}$ ions. Taken together, these observations suggest that **P10** chelates and effectively deactivates the iron catalysts, while manganese counterparts do not appear to be affected, suggesting that they are more labile and less sensitive to chelation.

With these results in hand, we decided to probe the versatility of this approach in the oxidation of more complex bioactive molecules bearing primary amine moieties as a main structural feature. For this purpose, pivalamide and phthalimide derivatives of drug molecules such as pregabalin (Lyrica) and the antiviral drug rimantadine (Flumadine), whose structures are shown in Scheme 4, were chosen as substrates.

As expected, the **Mn(^{dMM}pdp)** catalyst performs the oxidation of these molecules in satisfactory yields, with site selectivity that can be predicted on the basis of the amine derivatization. In line with the results shown in Table 4, oxidation of the pivalamide derivative of pregabalin (**S13**, Scheme 4) occurs preferentially at the most activated CH_2 position that is α to nitrogen, yielding amido γ-lactone compound **P13_a** derived from cyclization of the first-formed product, that results from hydroxylation at this methylenic site, with the carboxylic group.

The oxidized amido δ-lactone product resulting from hydroxylation at the remote tertiary C−H site (**P13_b**) was observed only in lower amount (**P13_a**/**P13_b** = 3.9). No evidence for functionalization at the tertiary C−H bond that is β to both the amido and carboxyl groups was observed, in line with the deactivation of this site determined by the presence of the latter group. On the other hand, when pregabalin is derivatized with the strongly electron withdrawing phthalimido group (**S14**, Scheme 4), oxidation catalyzed by **Mn(^{dMM}pdp)** provides exclusively the amido δ-lactone product (**P14**) derived from remote tertiary C−H hydroxylation, in good isolated yield (60%). On the other hand, the nature of the amine protecting group did not alter site selectivity in the oxidation of rimantadine derivatives **S15** and **S16** (Scheme 4). In both cases, products derived from hydroxylation of two and/or three tertiary C−H bonds of the adamantane skeleton were observed. Moreover, removal of the methyl group that is α to nitrogen (**S17**, Scheme 4) did not change the reaction regioselectivity. Product **P17**, resulting from hydroxylation of two adamantane tertiary C−H bonds, is the major product, along with a smaller amount of the trihydroxylated species. Products derived from oxidation at the α-C−H bonds were not observed, pointing toward the strong activation of adamantane tertiary C−H bonds and suggesting moreover an important contribution of steric and stereoelectronic effects imposed by the presence of the bulky adamanane moiety toward deactivation of the α-CH_2 site.

■ CONCLUSIONS

The present work describes the oxidation of aliphatic amides and phthalimides with aqueous H_2O_2 using manganese catalysts. Amides are demonstrated to be superior functional groups for modulating site selectivity in these reactions, playing an activating or deactivating role on proximal C−H bonds on the basis of electronic, steric, and stereoelectronic factors. The phthalimido group constitutes a unique case because its powerful electron-withdrawing character strongly deactivates proximal C−H bonds and consistently directs oxidation toward the most remote position. Also remarkably, amides that present a methylenic site that is α to nitrogen are hydroxylated at this position with excellent product chemoselectivity, providing a straightforward entry into this challenging class of molecules. This hydroxylation reaction is remarkable because most oxidation methods reported in the literature consistently lead to the imide product, and it highlights in particular the powerful role of the manganese catalyst in governing selectivity. Presumably, the HAT nature of the current reactions and the associated stereoelectronic effects lay at the basis of this unusual chemoselectivity. Taken together, the current work discloses a site- and product-selective and predictable C−H oxidation methodology with potential applicability to molecules of interest in modern organic chemistry, including substrate platforms of pharmaceutical relevance.

■ ASSOCIATED CONTENT

Ⓢ Supporting Information

The Supporting Information is available free of charge on the ACS Publications website at DOI: 10.1021/acscatal.7b02151.

> Experimental details on the preparation and characterization of the catalysts, experimental procedures for the catalytic reactions, and spectroscopic data for the products (PDF)

■ AUTHOR INFORMATION

Corresponding Authors

*E-mail for M.C.: miquel.costas@udg.edu.
*E-mail for M.B.: bietti@uniroma2.it.

ORCID

Miquel Costas: 0000-0001-6326-8299
Massimo Bietti: 0000-0001-5880-7614

Notes

The authors declare no competing financial interest.

■ ACKNOWLEDGMENTS

M.C. acknowledges financial support from the MINECO of Spain (CTQ2015-70795-P) and the Catalan DIUE of the Generalitat de Catalunya (2009SGR637). M.C. acknowledges an ICREA-Academia award.

■ REFERENCES

(1) Newhouse, T.; Baran, P. S. *Angew. Chem., Int. Ed.* **2011**, *50*, 3362−3374.

(2) Brückl, T.; Baxter, R. D.; Ishihara, Y.; Baran, P. S. *Acc. Chem. Res.* **2012**, *45*, 826−839.

(3) Sun, C.-L.; Li, B.-J.; Shi, Z.-J. *Chem. Rev.* **2011**, *111*, 1293−1314.

(4) Cernak, T.; Dykstra, K. D.; Tyagarajan, S.; Vachal, P.; Krska, S. W. *Chem. Soc. Rev.* **2016**, *45*, 546−576.

(5) Liu, W.; Groves, J. T. *Acc. Chem. Res.* **2015**, *48*, 1727−1735.

(6) Hartwig, J. F.; Larsen, M. A. *ACS Cent. Sci.* **2016**, *2*, 281−292.

(7) Chen, M. S.; White, M. C. *Science* **2007**, *318*, 783−787.

(8) Chen, M. S.; White, M. C. *Science* **2010**, *327*, 566−571.

(9) Bigi, M. A.; Reed, S. A.; White, M. C. *Nat. Chem.* **2011**, *3*, 218−224.

(10) Bigi, M. A.; Reed, S. A.; White, M. C. *J. Am. Chem. Soc.* **2012**, *134*, 9721−9726.

(11) Ottenbacher, R. V.; Samsonenko, D. G.; Talsi, E. P.; Bryliakov, K. P. *Org. Lett.* **2012**, *14*, 4310−4313.

(12) Shen, D. Y.; Miao, C. X.; Xu, D. Q.; Xia, C. G.; Sun, W. *Org. Lett.* **2015**, *17*, 54−57.

(13) Font, D.; Canta, M.; Milan, M.; Cussó, O.; Ribas, X.; Klein Gebbink, R. J. M.; Costas, M. *Angew. Chem., Int. Ed.* **2016**, *55*, 5776−5779.

(14) Prat, I.; Gomez, L.; Canta, M.; Ribas, X.; Costas, M. *Chem. - Eur. J.* **2013**, *19*, 1908−13.

(15) Gormisky, P. E.; White, M. C. *J. Am. Chem. Soc.* **2013**, *135*, 14052−14055.

(16) Gomez, L.; Canta, M.; Font, D.; Prat, I.; Ribas, X.; Costas, M. *J. Org. Chem.* **2013**, *78*, 1421−33.

(17) Topczewski, J. J.; Cabrera, P. J.; Saper, N. I.; Sanford, M. S. *Nature* **2016**, *531*, 220−224.

(18) Khusnutdinova, J. R.; Ben-David, Y.; Milstein, D. *J. Am. Chem. Soc.* **2014**, *136*, 2998−3001.

(19) Legacy, C. J.; Wang, A.; O'Day, B. J.; Emmert, M. H. *Angew. Chem., Int. Ed.* **2015**, *54*, 14907−14910.

(20) Wu, X.-F.; Bheeter, C. B.; Neumann, H.; Dixneuf, P. H.; Beller, M. *Chem. Commun.* **2012**, *48*, 12237−12239.

(21) Xu, W.; Jiang, Y.; Fu, H. *Synlett* **2012**, *23*, 801−804.

(22) Preedasuriyachai, P.; Chavasiri, W.; Sakurai, H. *Synlett* **2011**, *2011*, 1121−1124.

(23) Kim, J. W.; Yamaguchi, K.; Mizuno, N. *Angew. Chem., Int. Ed.* **2008**, *47*, 9249−9251.

(24) Klobukowski, E. R.; Mueller, M. L.; Angelici, R. J.; Woo, L. K. *ACS Catal.* **2011**, *1*, 703−708.

(25) Genovino, J.; Lütz, S.; Sames, D.; Touré, B. B. *J. Am. Chem. Soc.* **2013**, *135*, 12346−12352.

(26) Liu, P.; Liu, Y.; Wong, E. L.-M.; Xiang, S.; Che, C.-M. *Chem. Sci.* **2011**, *2*, 2187−2195.

(27) Murahashi, S.; Naota, T.; Yonemura, K. *J. Am. Chem. Soc.* **1988**, *110*, 8256−8258.

(28) Mitchell, E. A.; Peschiulli, A.; Lefevre, N.; Meerpoel, L.; Maes, B. U. W. *Chem. - Eur. J.* **2012**, *18*, 10092−10142.

(29) Griffiths, R. J.; Burley, G. A.; Talbot, E. P. A. *Org. Lett.* **2017**, *19*, 870−873.

(30) Milan, M.; Salamone, M.; Bietti, M. *J. Org. Chem.* **2014**, *79*, 5710−5716.

(31) Lee, M.; Sanford, M. S. *J. Am. Chem. Soc.* **2015**, *137*, 12796−12799.

(32) Howell, J. M.; Feng, K.; Clark, J. R.; Trzepkowski, L. J.; White, M. C. *J. Am. Chem. Soc.* **2015**, *137*, 14590−14593.

(33) Mbofana, C. T.; Chong, E.; Lawniczak, J.; Sanford, M. S. *Org. Lett.* **2016**, *18*, 4258−4261.

(34) Milan, M.; Bietti, M.; Costas, M. *ACS Cent. Sci.* **2017**, *3*, 196−204.

(35) Nicolaou, K. C.; Mathison, C. J. N. *Angew. Chem., Int. Ed.* **2005**, *44*, 5992−5997.

(36) Bjorsvik, H.-R.; Fontana, F.; Liguori, L.; Minisci, F. *Chem. Commun.* **2001**, *0*, 523−524.

(37) Itoh, I.; Matsusaki, Y.; Fujiya, A.; Tada, N.; Miura, T.; Itoh, A. *Tetrahedron Lett.* **2014**, *55*, 3160−3162.

(38) Sperry, J. *Synthesis* **2011**, *2011*, 3569−3580.

(39) Minisci, F.; Punta, C.; Recupero, F.; Fontana, F.; Pedulli, G. F. *J. Org. Chem.* **2002**, *67*, 2671−2676.

(40) Ito, R.; Umezawa, N.; Higuchi, T. *J. Am. Chem. Soc.* **2005**, *127*, 834−835.

(41) Capdevielle, P.; Maumy, M. *Tetrahedron Lett.* **1991**, *32*, 3831−3834.

(42) Ivashkin, P. E.; Lukyanov, K. A.; Lukyanov, S.; Yampolsky, I. V. *J. Org. Chem.* **2011**, *76*, 2782−2791.

(43) Braña, M. F.; Rodriquez, M. L. L. *J. Heterocycl. Chem.* **1981**, *18*, 869−871.

(44) Osberger, T. J.; Rogness, D. C.; Kohrt, J. T.; Stepan, A. F.; White, M. C. *Nature* **2016**, *537*, 214−219.

(45) Adams, A. M.; Du Bois, J.; Malik, H. A. *Org. Lett.* **2015**, *17*, 6066−6069.

(46) Murphy, A.; Dubois, G.; Stack, T. D. P. *J. Am. Chem. Soc.* **2003**, *125*, 5250−5251.

(47) Shen, D.; Miao, C.; Wang, S.; Xia, C.; Sun, W. *Org. Lett.* **2014**, *16*, 1108−1111.

(48) Canta, M.; Font, D.; Gómez, L.; Ribas, X.; Costas, M. *Adv. Synth. Catal.* **2014**, *356*, 818−830.

(49) Hull, J. F.; Balcells, D.; Sauer, E. L. O.; Raynaud, C.; Brudvig, G. W.; Crabtree, R. H.; Eisenstein, O. *J. Am. Chem. Soc.* **2010**, *132*, 7605−7616.

(50) Cussó, O.; Garcia-Bosch, I.; Ribas, X.; Lloret-Fillol, J.; Costas, M. *J. Am. Chem. Soc.* **2013**, *135*, 14871−14878.

(51) Cussó, O.; Garcia-Bosch, I.; Font, D.; Ribas, X.; Lloret-Fillol, J.; Costas, M. *Org. Lett.* **2013**, *15*, 6158−6161.

(52) Schmidt, V. A.; Quinn, R. K.; Brusoe, A. T.; Alexanian, E. J. *J. Am. Chem. Soc.* **2014**, *136*, 14389−14392.

(53) Quinn, R. K.; Könst, Z. A.; Michalak, S. E.; Schmidt, Y.; Szklarski, A. R.; Flores, A. R.; Nam, S.; Horne, D. A.; Vanderwal, C. D.; Alexanian, E. J. *J. Am. Chem. Soc.* **2016**, *138*, 696−702.

(54) Kawamata, Y.; Yan, M.; Liu, Z.; Bao, D.-H.; Chen, J.; Starr, J. T.; Baran, P. S. *J. Am. Chem. Soc.* **2017**, *139*, 7448−7451.

(55) Salamone, M.; Basili, F.; Mele, R.; Cianfanelli, M.; Bietti, M. *Org. Lett.* **2014**, *16*, 6444−6447.

(56) Le, C.; Liang, Y.; Evans, R. W.; Li, X.; MacMillan, D. W. C. *Nature* **2017**, *547*, 79.

(57) Cox, D. D.; Benkovic, S. J.; Bloom, L. M.; Bradley, F. C.; Nelson, M. J.; Que, L., Jr.; Wallick, D. E. *J. Am. Chem. Soc.* **1988**, *110*, 2026−2032.

(58) Mehn, M. P.; Fujisawa, K.; Hegg, E. L.; Que, L., Jr. *J. Am. Chem. Soc.* **2003**, *125*, 7828−7842.

(59) Solomon, E. I.; Brunold, T. C.; Davis, M. I.; Kemsley, J. N.; Lee, S.-K.; Lehnert, N.; Neese, F.; Skulan, A. J.; Yang, Y.-S.; Zhou, J. *Chem. Rev.* **2000**, *100*, 235−349.

(60) Makhlynets, O. V.; Rybak-Akimova, E. V. *Chem. - Eur. J.* **2010**, *16*, 13995−14006.

(61) Serrano-Plana, J.; Oloo, W. N.; Acosta-Rueda, L.; Meier, K. K.; Verdejo, B.; García-España, E.; Basallote, M. G.; Münck, E.; Que, L.; Company, A.; Costas, M. *J. Am. Chem. Soc.* **2015**, *137*, 15833−15842.

Chapter IV

Highly Enantioselective Oxidation of Nonactivated Aliphatic C–H Bonds with Hydrogen Peroxide Catalyzed by Manganese Complexes

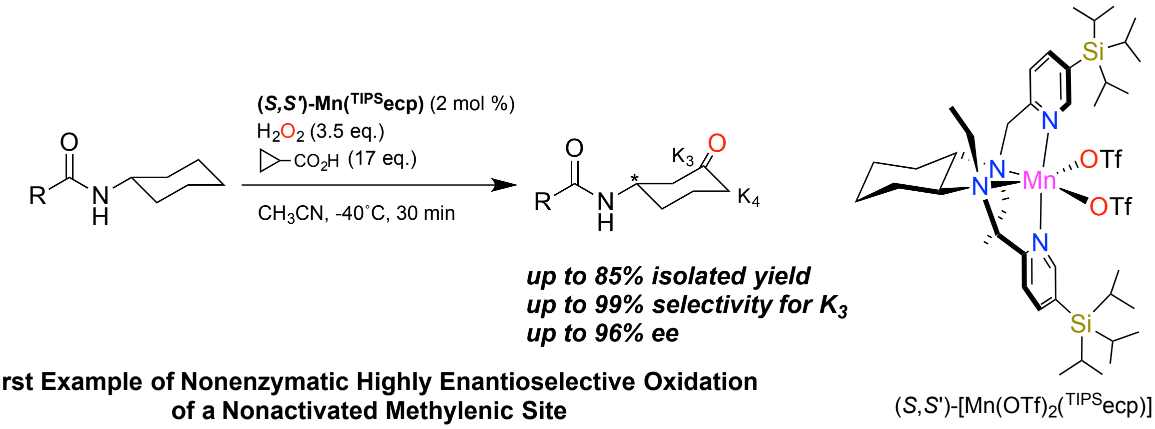
(S,S')-Mn(TIPSecp) (2 mol %)
H2O2 (3.5 eq.)
CO2H (17 eq.)
CH3CN, -40˚C, 30 min
R
O
N
H
K3
K4
*
Si
N
Mn
OTf
OTf

up to 85% isolated yield
up to 99% selectivity for K_3
up to 96% ee

First Example of Nonenzymatic Highly Enantioselective Oxidation of a Nonactivated Methylenic Site

(S,S')-[Mn(OTf)$_2$(^{TIPS}ecp)]

This chapter correspond to the following publication:

Milan, M.; Bietti, M.; Costas, M. *ACS Cent. Sci.* **2017**, 3, 196-204

This is an open access article published under an ACS AuthorChoice License, which permits copying and redistribution of the article or any adaptations for non-commercial purposes.

ACS central science

Research Article

http://pubs.acs.org/journal/acscii

Highly Enantioselective Oxidation of Nonactivated Aliphatic C−H Bonds with Hydrogen Peroxide Catalyzed by Manganese Complexes

Michela Milan,[†] Massimo Bietti,*,[‡] and Miquel Costas*,[†]

[†]QBIS Research Group, Institut de Química Computacional i Catàlisi (IQCC) and Departament de Química, Universitat de Girona, Campus Montilivi, Girona E-17071, Catalonia, Spain

[‡]Dipartimento di Scienze e Tecnologie Chimiche, Università "Tor Vergata", Via della Ricerca Scientifica, 1, I-00133 Rome, Italy

Supporting Information

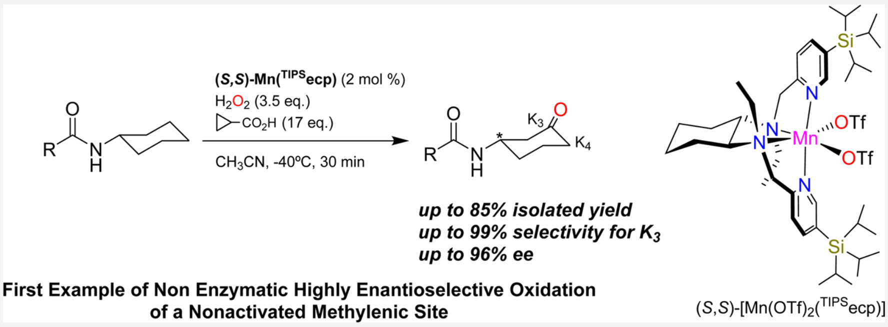
(S,S)-Mn(TIPSecp) (2 mol %)
H2O2 (3.5 eq.)
CO2H (17 eq.)
CH3CN, -40ºC, 30 min
R
N
H
O
K3
K4
*
up to 85% isolated yield
up to 99% selectivity for K3
up to 96% ee
First Example of Non Enzymatic Highly Enantioselective Oxidation of a Nonactivated Methylenic Site
Si
N
Mn
OTf
(S,S)-[Mn(OTf)2(TIPSecp)]

ABSTRACT: Monosubstituted cycloalkanes undergo regio- and enantioselective aliphatic C−H oxidation with H_2O_2 catalyzed by biologically inspired manganese catalysts. The reaction furnishes the corresponding ketones resulting from oxidation at C3 and C4 methylenic sites (K_3 and K_4, respectively) leading to a chiral desymmetrization that proceeds with remarkable enantioselectivity (64% ee) but modest regioselectivity at C3 ($K_3/K_4 \approx 2$) for *tert*-butylcyclohexane, and with up to 96% ee and exquisite regioselectity toward C3 (up to $K_3/K_4 > 99$) when *N*-cyclohexylalkanamides are employed as substrates. Efficient H_2O_2 activation, high yield, and highly enantioselective C−H oxidation rely on the synergistic cooperation of a sterically bulky manganese catalyst and an oxidatively robust alkanoic acid. This represents the first example of nonenzymatic highly enantioselective oxidation of nonactivated methylenic sites. Furthermore, the principles of catalyst design disclosed in this work constitute a unique platform for further development of stereoselective C−H oxidation reactions.

■ INTRODUCTION

The oxidation of nonactivated aliphatic C−H bonds is a very powerful reaction because it can transform the inert C−H bond, ubiquitous in organic molecules, into a suitable site for further chemical elaboration.[1,2] However, it also represents one of the most challenging reactions in modern synthetic organic chemistry because the multitude of aliphatic C−H bonds in a molecule makes site selective oxidation particularly difficult. This is further accentuated because of the high reactivity of the oxidizing species capable of breaking these bonds, often incompatible with chemo- and regioselective transformations. Additional challenges are encountered in enantioselective C−H oxidations.[3] In the first place, reagents that are both chiral and capable of oxygenating aliphatic C−H bonds via mechanisms potentially susceptible to induce enantioselectivity are scarce. In addition, the more facile overoxidation of secondary alcohols with respect to the C−H precursor usually eliminates the chirality. Instead, enantioselective C−H oxidation is common in enzymes, where the combination of subtle interactions in the active site governs substrate orientation, and formation of the oxidizing species is finely triggered. Not surprisingly, examples of enantioselective sp^3 C−H oxidation with nonenzymatic systems are rare and limited to relatively weak C−H bonds (benzylic, allylic, and adjacent to heteroatom) most commonly with low substrate conversion (Scheme 1).[4−18] Examples of enantioselective oxidation of nonactivated aliphatic C−H bonds remain exclusive to enzymes.[19−22]

Oxidation of nonactivated aliphatic C−H bonds with biologically inspired transition metal catalysts that form high valent metal-oxo species may constitute a promising option to pursue asymmetric C−H oxidation. This class of complexes has been recently applied successfully in asymmetric olefin epoxidation[23−25] and *cis*-dihydroxylation,[26,27] but to date asymmetric C−H bond oxidation has not been described. Most interestingly, these species can hydroxylate C−H bonds with stereospecificity,[28−32] and the steric and chiral properties of the first coordination sphere of the metal site have been shown to impact the C−H site selectivity of chiral molecules.[33,34]

Herein we describe the development of chiral manganese complexes with sterically demanding tetradentate amino-

Received: December 1, 2016
Published: February 8, 2017

© 2017 American Chemical Society

DOI: 10.1021/acscentsci.6b00368
ACS Cent. Sci. 2017, 3, 196−204

Scheme 1. Selected Precedents of Asymmetric C−H Oxidation: (a) Ref 16 (b) Ref 7 (c) Ref 5, and (d) Ref 8

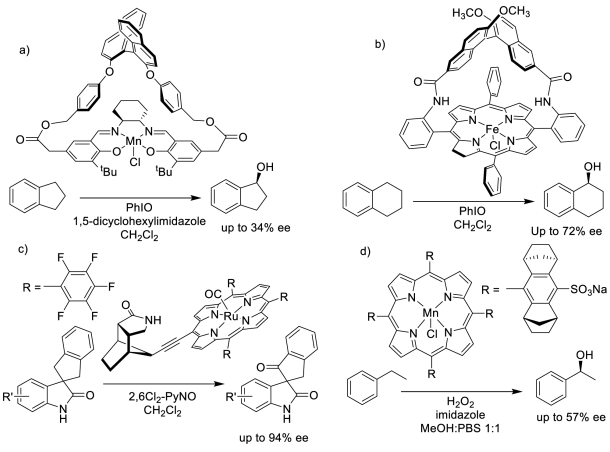

Scheme 2. Diagram of the Iron and Manganese Complexes Studied[a]

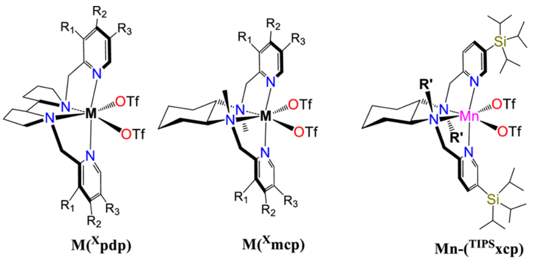

M^x	R_1	R_2	R_3
Fe(pdp)	-H	-H	-H
Fe(mcp)	-H	-H	-H
Fe(TIPSpdp)	-H	-H	-Si(^{i}Pr)$_3$
Fe(TIPSmcp)	-H	-H	-Si(^{i}Pr)$_3$
Mn(pdp)	-H	-H	-H
Mn(mcp)	-H	-H	-H
Mn(Me2Npdp)	-H	-NMe$_2$	-H
Mn(BzImpdp)	-BzIm[a]		
Mn(dMMmcp)	-Me	-OMe	-Me
Mn(CF3mcp)	-H	-H	-Ph(CF$_3$)$_2$
Mn(TIPSpdp)	-H	-H	-Si(^{i}Pr)$_3$
Mn(TIPSmcp)	-H	-H	-Si(^{i}Pr)$_3$

Mn-(TIPSecp) **R'** = $-CH_2CH_3$
Mn-(TIPScpcp) **R'** = $-CH_2c-(C_3H_5)$
Mn-(TIPSchcp) **R'** = $-CH_2c-(C_6H_{11})$
Mn-(TIPStBucp) **R'** = $-CH_2CH_2C(CH_3)_3$

[a]Benzimidazole instead of pyridine.

Table 1. Oxidation of *tert*-Butylcyclohexane (S1) with Different Catalysts

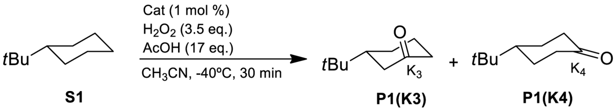

entry	cat	conv (%)[a]	yield (%)[a] K_3 (K_4)	K_3/K_4[b]	Ee (K_3) (%)
1[c]	**Fe(mcp)**	62	37 (9)	2.1	2
2[c]	**Fe(pdp)**	48	25 (6)	2.0	6
3	**Mn(mcp)**	46	32 (7)	2.3	9
4	**Mn(pdp)**	86	56 (13)	2.2	3
5[c]	**Fe(TIPSmcp)**	73	61 (10)	3.1	33
6[c]	**Fe(TIPSpdp)**	88	53 (17)	1.6	15
7	**Mn(Me2Npdp)**	37	13 (3)	2.2	8
8	**Mn(dMMpdp)**	93	50 (11)	2.3	8
9	**Mn(BzImpdp)**	79	50 (11)	2.3	11
10	**Mn(CF3mcp)**	55	22 (5)	2.2	2
11	**Mn(TIPSmcp)**	77	**53 (19)**	**1.4**	**44**
12	**Mn(TIPSpdp)**	51	22 (7)	1.6	34
13[d]	**Mn(TIPSecp)**	87	**51 (15)**	**1.7**	**43**
14	**Mn(TIPScpcp)**	68	32 (12)	1.3	32
15	**Mn(TIPSchcp)**	45	10 (6)	1.0	6
16	**Mn(TIPStBucp)**	48	8 (5)	1.0	Rac

[a]Conversions and yields determined from crude reaction mixtures by GC. Ee's determined by GC with chiral stationary phase. [b]Normalized ratio. [c]Reaction conditions: Fe catalyst (3 mol %), H_2O_2 (2.5 equiv), AcOH (1.5 equiv) in CH_3CN at 0 °C during 30 min. [d]**(*S*,*S*)-Mn-(TIPSecp)** (2 mol %).

pyridine ligands that catalyze the regio- and enantioselective oxidation of methylenic groups in monosubstituted cyclohexanes using H_2O_2 as oxidant. Oxidation occurs at positions C3 and C4 of the cyclohexane ring, producing a chiral desymmetrization in the former product, with outstanding levels of regioselectivity (>99:1 for C3 over C4) and enantioselectivity (up to 96% ee) in the reactions of *N*-cyclohexylalkanamides. To the best of our knowledge the current report constitutes the first example of enantioselective oxidation of a nonactivated aliphatic C−H bond by a nonenzymatic system.

RESULTS AND DISCUSSION

Chirality at the metal iron complexes bearing tetradentate ligands has been recently shown to exhibit site selectivity in the oxidation of methylenic units of chiral substrates, depending on the chirality of the complex.[33] Therefore, we sought to explore their ability to engage in enantioselective C−H oxidation. Since secondary alcohols are rapidly oxidized by these catalysts to the corresponding achiral ketones,[34] we explored the C−H oxidation of substrates that will result in an asymmetric desymmetrization.[35] Parent manganese complexes have recently shown excellent catalytic activity in related aliphatic C−H oxidation reactions,[36,37] and consequently, they were also included in the study. In particular chiral iron and manganese tetradentate complexes of general formula $[M(CF_3SO_3)_2(L)]$ (L = mcp, and pdp, mcp = *N*,*N*′-dimethyl *N*,*N*′-bis(2-pyridylmethyl)-1,2-*trans*-diamino cyclohexane, pdp = *N*,*N*′-bis(2-pyridylmethyl)-2,2′-bipyrrolidine, Scheme 2, complexes **Fe(mcp)**, **Fe(pdp)**, **Mn(mcp)**, and **Mn(pdp)**, respectively)[32,33,38,39] were tested as catalysts in the oxidation of *tert*-butylcyclohexane (**S1**). Results are shown in Table 1 (entries 1−4). Standard conditions involved syringe pump delivery of H_2O_2 (3.5 equiv) to an acetonitrile solution of the catalyst (1 mol %) and AcOH (17 equiv) in CH_3CN at −40 °C during 30 min. For all the catalysts oxidation of **S1** occurs preferentially at C3 over C4 methylene sites to produce the corresponding ketone products (**P1(K_3)** and **P1(K_4)**, respectively) in moderate to good product yields (31−69%). No products arising from C1 and C2 oxidation, nor from oxidation of the primary *t*-Bu C−H bonds were observed. Products are formed via initial hydrogen atom transfer (HAT) mediated C−H hydroxylation, followed by fast oxidation of the resulting secondary alcohol.[40−42] Regioselectivity, quantified on the basis of the normalized product ratio (K_3/K_4), is comprised between 2.0 and 2.3, in line with the results of previous studies on the oxidation of **S1** with HAT reagents such as iron and manganese complexes (K_3/K_4 = 1.9−2.5),[41,43] methyl(trifluoromethyl)-dioxirane (K_3/K_4 = 1.8),[44] and iodanyl radicals (K_3/K_4 = 1.4−2.3).[45,46] Poor enantioselectivities were obtained with these catalysts (<10% ee, entries 1−4), but when bulky groups like *tris*-(isopropyl)silyl (TIPS) were introduced at position 3 of the pyridine rings in the iron catalysts (entries 5–6), both yield and enantioselectivity increased significantly (70–71% yield, 33 and 15% ee for **Fe(**$^{\mathrm{TIPS}}$**mcp)** and **Fe(**$^{\mathrm{TIPS}}$**pdp)**, respectively), while retaining regioselectivity (K_3/K_4 = 1.6–3.1).

Most interestingly, use of the parent manganese complexes **Mn(**$^{\mathrm{TIPS}}$**mcp)** and **Mn(**$^{\mathrm{TIPS}}$**pdp)** (entries 11–12, full details on the synthesis and characterization of the complexes are provided in the Supporting Information) led to modest to good product yields but improved levels of enantioselectivity in ketone **P1(K$_3$)** (up to 44% ee). On the other hand, the use of electron-rich manganese catalysts (**Mn(**$^{\mathrm{Me2N}}$**pdp)** and **Mn-(**$^{\mathrm{dMM}}$**pdp)**), which have been recently shown to lead to high ee's in epoxidation reactions,[47,48] provided only low ee's (entries 7–8), suggesting that the steric demand imposed by the TIPS group is the basis of the improved enantioselectivity. Further catalyst screening included related manganese complexes where the pyridine rings were replaced by benzylimidazole (BzIm) rings[49] and the use of a 2,6-*bis*-trifluoromethylphenyl substituted mcp ligand[50] (entries 9 and 10, respectively). In all the latter cases (entries 7–10), lower enantioselectivities were obtained as compared to the TIPS based catalysts. Then, different manganese catalysts based on the mcp backbone, but differing in the nature of the *N*-alkyl group (R′ in Scheme 2, entries 13–16 in Table 1) were prepared and tested in the model reaction. This study led to the identification of the ethyl substituted catalyst **(*S,S*)-Mn-(**$^{\mathrm{TIPS}}$**ecp)**, ecp = *N,N*′-diethyl *N,N*′-bis(2-pyridylmethyl)-1,2-*trans*-diamino cyclohexane, as also particularly efficient in terms of product yield and enantioselectivity (entry 13). For the particular case of **S1**, **(*S,S*)-Mn(**$^{\mathrm{TIPS}}$**ecp)** and **(*S,S*)-Mn-(**$^{\mathrm{TIPS}}$**mcp)** provided analogous ee's, but significant improvements in enantioselectivity were observed for other substrates (see below). As expected, the use of the enantiomerically related catalyst **(*R,R*)-Mn(**$^{\mathrm{TIPS}}$**mcp)** provides the oxidation product with comparable ee but with opposite absolute configuration.

The X-ray determined molecular structure of **(*S,S*)-Mn-(**$^{\mathrm{TIPS}}$**ecp)** is shown in Scheme 3. The complex is structurally very similar to the parent **Mn(pdp)**[51] and the related **Fe(**$^{\mathrm{TIPS}}$**mcp)** complexes.[33] Bond distances and angles are collected in the Supporting Information. The manganese center adopts a C_2-symmetric *cis-α* topology, with the two pyridines *trans* to each other. The complex exhibits chirality at the metal (Λ and Δ), in turn determined by the chirality of the cyclohexanediamine backbone (*S,S* and *R,R*, respectively). Most interestingly, TIPS groups determine a well-defined chiral clef occupied by the triflate ions, that bind *cis* to each other at the manganese center, *trans* to the two aliphatic amine sites. These sites are labile and are the place where H_2O_2 presumably binds and is activated, forming a high valent manganese oxo species responsible for the C–H oxidation reaction.[30] Of notice is also the proximity of the *N*-ethyl groups to the triflate ions, suggesting that these groups can also contribute significantly in defining the structure of the C–H oxidation site.

Scheme 3. Schematic Diagram (Left) and ORTEP Diagram (Right) of the Single-Crystal X-ray Determined Structure of (*S,S*)-Mn($^{\mathrm{TIPS}}$**ecp)**[a]

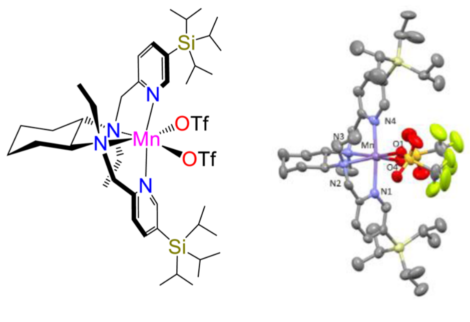

[a] List of selected distances (Å); Mn–O(4) 2.151(6), Mn–O(1) 2.151(5), Mn–N(4) 2.186(6), Mn–N(1) 2.213(7), Mn–N(2) 2.327(7), Mn–N(3) 2.365(7).

Table 2. Oxidation of Different Cyclohexane Derivatives

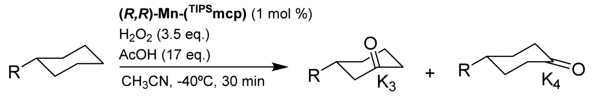

entry	R	conv (%)[a]	yield (%)[a] $K_3(K_4)$	K_3/K_4[b]	Ee (K_3) (%)
1	-*t*-Bu (**S1**)	77	53 (19)	1.4	44
2	-OPiv (**S2**)	80	41 (10)	2.0	54
3	-Si(Me)$_3$ (**S3**)	95	42 (13)	1.6	23
4[c]	-CO$_2$CH$_3$ (**S4**)	88	47 (20)	1.2	11
5	-CO$_2$H (**S5**)	45	20 (11)	0.9	9[e]
6[c]	-COCH$_3$ (**S6**)	95	47 (19)	1.2	8
7	-NHCOCH$_3$ (**S7**)	93	74 (3)	12	(+)63[f]
8[c]	-NHCOCH$_3$ (**S7**)	94	75 (3)	12	(−)78
9	-NHCO*t*Bu (**S8**)	**>99**	**90 (1)**	**45**	**(+)76**
10[d]	-NHCO*t*Bu (**S8**)	**>99**	**90 (1)**	**45**	**(−)76**
11[c]	-NHCO*t*Bu (**S8**)	**>99**	**90 (1)**	**45**	**(−)85**

[a] Conversions and yields determined from crude reaction mixtures by GC or ^{1}H NMR. [b] Normalized ratio. [c] **(*S,S*)-Mn-(**$^{\mathrm{TIPS}}$**ecp)** (2 mol %). [d] **(*S,S*)-Mn-(**$^{\mathrm{TIPS}}$**mcp)**. [e] Ee's determined after esterification of isolated products. [f] Absolute configuration was determined on the basis of the crystal structure of the product obtained from **S10** (see Table 4 and Supporting Information). Ee's determined by GC with chiral stationary phase.

On the basis of these results, catalyst **Mn(**$^{\mathrm{TIPS}}$**mcp)** was chosen for the oxidation of a series of monosubstituted cyclohexanes in order to estimate the effect of the substituent on yield, regioselectivity, and enantioselectivity of the reaction (Table 2). Consideration of the elements that determine regioselectivity in the oxidation of *tert*-butylcyclohexane (**S1**) serves to provide an understanding of the changes observed upon replacement of the *t*-Bu group for other groups. With **S1**, regioselectivity can be understood by considering the relative reactivity of the C–H bonds of this substrate in HAT reactions. Primary and tertiary C–H bonds of **S1** are not reactive because of the high bond dissociation energy in the former, and of steric and torsional effects in the latter where in particular substrate conformation places this bond in an axial position. Tertiary axial C–H bond deactivation has been recently explained in terms of an increase in torsional strain in the HAT transition state, where planarization of the incipient carbon radical forces the bulky *t*-Bu group toward an unfavorable eclipsed interaction with the equatorial C–H groups on the adjacent positions.[52,53] Along the same line, oxidation at C2 of **S1** is disfavored because planarization of the incipient carbon radical formed following

DOI: 10.1021/acscentsci.6b00368
ACS Cent. Sci. 2017, 3, 196–204

HAT forces the remaining C−H bond toward an unfavorable eclipsed interaction with the adjacent *t*-Bu group.[52]

The results of previous studies on the oxidation of monosubstituted cyclohexanes with methyl(trifluoromethyl)-dioxirane have suggested that the K_3/K_4 regioselectivity observed in these reactions reflects the electronic effect of the substituent, with C3 oxidation over C4 being favored by electron releasing groups (K_3/K_4 = 1.8 for **S1**) and C4 over C3 by electron withdrawing groups (K_3/K_4 = 0.3 for trifluoromethylcyclohexane).[44] Along this line, the regioselectivity observed in the oxidation of **S1** catalyzed by **Mn($^{\text{TIPS}}$mcp)** (Table 2, entry 1: K_3/K_4 = 1.4) can be explained accordingly on the basis of the electron donating ability of the *t*-Bu group that activates C3 over C4 toward the electrophilic manganese-oxo species.

When the *t*-Bu group was replaced by a pivalate (cyclohexylpivalate (**S2**), Table 2, entry 2), comparable product yields and regioselectivity toward C3 (K_3/K_4 = 2.0) are observed, and the enantioselectivity increases up to 54% ee. Use of a trimethylsilyl (TMS) substituent as in **S3** provides moderate yields and reduced enantioselectivity (ee = 23%, entry 3). Regioselectivity is not changed significantly with regard to **S1** (K_3/K_4 = 1.6 and 1.4, for **S3** and **S1**, respectively), in accordance with the similar electron donating abilities of the two substituents. On the other hand, with cyclohexanes bearing electron withdrawing substituents such as methyl cyclohexanecarboxylate (**S4**), cyclohexane carboxylic acid (**S5**), and cyclohexyl methyl ketone (**S6**) (entries 4−6, respectively), a slight decrease in the normalized K_3/K_4 ratio is observed (K_3/K_4 between 0.9 and 1.2), still reflecting however the formation of ketone K_3 as the major product. This observation appears to be, at least to a certain extent, in contrast with the explanation given above, indicating that in addition to electronic effects other factors also contribute in defining regioselectivity. Very remarkably, as compared to **S1** and **S2**, a sharp decrease in enantioselectivity is observed with the latter three substrates (**S4**-**S6**, entries 4−6, ee's between 8 and 11%), indicating that the presence of electron withdrawing substituents can strongly influence the interaction of the substrate with the electrophilic C−H oxidation site.

Most interestingly, in the presence of a strongly Lewis basic amide substituent, as in *N*-cyclohexylacetamide (**S7**), the reaction proceeds with excellent yield, strongly improved regioselectivity toward C3 (K_3/K_4 = 12), and good enantioselectivity (63% ee, entry 7). Furthermore, an exquisite regioselectivity (K_3/K_4 = 45) and very good enantioselectivity (76% ee) are observed on moving to an amide substrate characterized by a bulky acyl moiety such as *N*-cyclohexylpivalamide (**S8**, entry 9).

These results point toward a strong interaction of these substrates with the manganese-oxo species, where substrate Lewis basicity and the presence of a bulky aliphatic group both appear to play a key role in providing an optimal substrate orientation for regioselective and enantioselective C−H oxidation. Most interestingly, with **S7** and **S8** enantioselectivity could be further improved to 78 and 85% ee, respectively, while retaining the excellent yield and regioselectivity, by using (***S***,***S***)-**Mn($^{\text{TIPS}}$ecp)** as catalyst, where the *N*-methyl groups of the cyclohexanediamine backbone have been replaced by ethyl groups (entries 8 and 11).

The highly regioselective oxidation of **S8** requires further consideration. It is well established that in the reaction of cyclohexyl amine with electrophilic HAT reagents such as oxygen centered radicals, reaction occurs selectively from the strongly activated α-C-H bond.[54] Transformation of the NH_2 group into a bulky amide moiety reduces the extent of activation at C1, increasing in the same time the importance of the conformation that places the tertiary C−H bond in an axial position, thus deactivating both C1 and C2 toward oxidation (see above), providing a highly efficient method for site-selective functionalization at a nonactivated methylene position.

Carboxylic acids have been recently shown to strongly impact the stereoselectivity of Mn and Fe catalyzed epoxidation reactions with related catalysts.[47,51,55] These acids bind to the metal center, *cis* to the site where H_2O_2 is activated, and contribute in defining the active site.[30,48] Thus, their assistance was explored in the current C−H oxidation reactions. Using (***R***,***R***)-**Mn($^{\text{TIPS}}$mcp)** as catalyst and amide **S8** as substrate, the effect of different alkanoic acids is shown in Table 3. Almost exclusive formation of ketone K_3 was observed, with the yield of ketone K_4 being in all cases <1%. With the exclusion of 2-chloroethanoic acid (entry 6), cyclohexanecarboxylic acid (**S5**, entry 10) and carboxylic acids containing relatively long and branched alkyl chains such as 4-methylpentanoic and 2-ethylhexanoic acid (entries 11 and 12), comparable ee's comprised between 73 and 82% were obtained for all the acids investigated. The significantly lower enantioselectivity observed with 2-chloroethanoic acid (55% ee, entry 6) reasonably reflects the electron withdrawing character of the chlorine substituent that makes this acid less prone to bind to the manganese center. The lack of or marginal conversion obtained with the latter three acids can be explained in terms of a favorable competition with the amide substrate for the oxidizing species, as specifically shown above for the case of cyclohexanecarboxylic acid (**S5**) (Table 2, entry 5) that is efficiently oxidized under these experimental conditions,[56] clearly indicating that in order to obtain highly enantioselective C−H oxidations easily oxidizable carboxylic acids must be avoided. A chiral carboxylic acid was also studied with the aim to explore matching−mismatching effects between the chiralities of catalyst and carboxylic acid. The combination of (***R***,***R***)-**Mn($^{\text{TIPS}}$mcp)** and (***S***,***S***)-**Mn($^{\text{TIPS}}$mcp)** with (*S*)-(+)-2-methylbutanoic acid provided virtually identical enantioselectivities but reduced product yields (entries 15−16).

Interestingly, as shown for the oxidatively robust acetic, propanoic, and cycloproanecarboxylic acids (entries 2, 5, and 14, respectively), by using (***S***,***S***)-**Mn($^{\text{TIPS}}$ecp)** as catalyst a substantial increase in enantioselectivity was obtained (85−90% ee) while retaining the excellent yield and regioselectivity, with the rigid cyclopropanecarboxylic acid that provides the highest ee of the series (entry 14, 90% yield, 90% ee). Structural rigidity and stability toward oxidation make this acid particularly suitable to combine with the highly structured and sterically demanding, while oxidatively resistant, site of the **Mn($^{\text{TIPS}}$ecp)** catalyst in order to create an outstandingly robust site capable of promoting a highly enantioselective oxidation of the strong aliphatic C−H bond of a nonactivated methylene group.

The role of the structure and electronic properties of the amide substrate on the regio- and enantioselectivity of the reaction was then explored under optimized conditions, using (***S***,***S***)-**Mn($^{\text{TIPS}}$ecp)** as the catalyst and cyclopropanecarboxylic or acetic acid (17 equiv) as the acids of choice (Table 4). Secondary amides that present aliphatic acyl groups show in the most of cases high isolated yields, from good to excellent regioselectivities for oxidation at C3 and excellent ee's (up to 96% ee, entry 5). It is possible to notice that the systematic

DOI: 10.1021/acscentsci.6b00368
ACS Cent. Sci. 2017, 3, 196−204

Table 3. C−H Oxidation Reactions Using Different Carboxylic Acids and *N*-Cyclohexylpivalamide (S8)

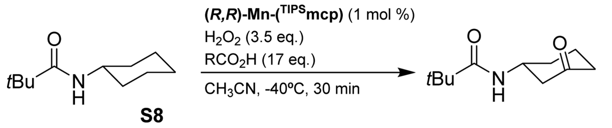

Entry	RCO₂H	Conv.(yield)(%)[a]	(ee)%
1	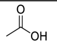	**>99 (90)**	**79**
2[b]	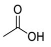	**>99 (90)**	**85**
3	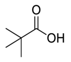	88 (51)	75
4	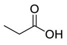	**97 (70)**	**81**
5[b]	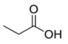	**90 (79)**	**89**
6	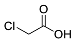	98 (86)	55
7	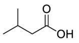	58 (42)	81
8	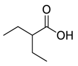	50 (38)	80
9	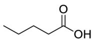	86 (73)	78
10	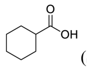 (S5)	8 (5)	-
11	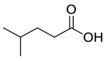	0 (-)	-
12	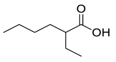	0 (-)	-
13	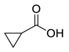	**91 (80)**	**73**
14[b]	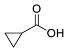	**99 (90)**	**90**
15	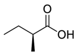	68 (41)	81
16[c]	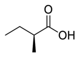	62 (25)	82

[a] Conversions and yields (in parentheses) determined by GC. [b] **(*S*,*S*)-Mn($^{\text{TIPS}}$ecp)** (2 mol %). [c] **(*S*,*S*)-Mn($^{\text{TIPS}}$mcp)**. Ee's determined by chiral GC.

Table 4. Impact of the Structure of the Acyl Moiety in Regio- and Enantioselective C−H Oxidation of *N*-Cyclohexyl Amides with (*S*,*S*)-Mn($^{\text{TIPS}}$ecp) as Catalyst

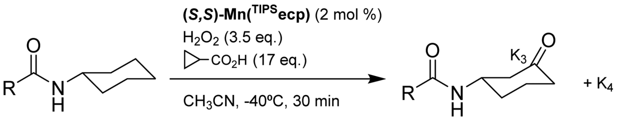

Entry	Substrate	Isol. yield (%) K₃	Norm K₃ / K₄[a,b]	(ee)% K₃
1	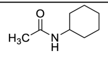 (S7)	61	12	(-)78
2	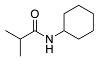 (S9)	60	9	(-)88
3	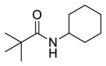 (S8)	**84**	**45**	**(-)91**
4	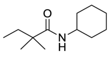 (S10)	**85**	**43**	**(-)94**
5	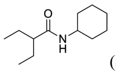 (S11)	45	23	**(-)96**
6[c]	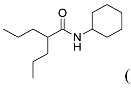 (S12)	8	4	**(-)90**
7	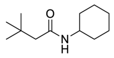 (S13)	69	>99	**(-)94**
8	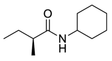 (S14)	50, 61[d]	25	**(+)91**, (-)86[d]
9[e]	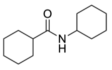 (S15)	**75**	**38**	**(-)91**
10	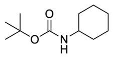 (S16)	66[f]	8.2	(-)65
11	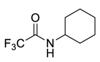 (S17)	65	2	(-)65
12	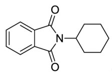 (S18)	37[g]	0.8	62
13	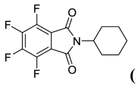 (S19)	40[g]	0.6	-[h]

[a] Normalized ratio. [b] K_4 yields determined by GC. [c] Recovered starting material = 78%. [d] **(*R*,*R*)-Mn($^{\text{TIPS}}$ecp)**. [e] Acetic acid (17 equiv) instead of cyclopropanecarboxylic acid. [f] Yield determined by GC. [g] Products isolated as mixture of (K_3 + K_4). [h] Ee not determined. Ee's determined by chiral GC and HPLC.

increase in steric hindrance of the acyl group, when going from acetyl to 2-methylpropanoyl and 2,2-dimethylpropanoyl (entries 1−3), results in an increase in the enantioselectivity, which remains very high (>90% ee) as long as this group contains sterically demanding alkyl moieties (entries 3−9). A truly remarkable behavior is displayed by *N*-cyclohexyl-2,2-dimethylbutanamide (**S10**, entry 4), which combines high isolated yield (85% for product K_3), excellent regioselectivity (K_3/K_4 = 43), and enantioselectivity (94% ee). Low yield was obtained only in the case of **S12** (entry 6), suggesting that for this substrate the exceedingly high steric bulk of the acyl moiety prevents efficient oxidation. The use of an amide substrate that bears a chiral center (**S14**, entry 8) does not lead to any improvement in enantioselectivity; however the ee's obtained with both **(*S*,*S*)-Mn($^{\text{TIPS}}$ecp)** and **(*R*,*R*)-Mn($^{\text{TIPS}}$ecp)** are excellent (91% and 86% ee, respectively). A remarkable demonstration of the important role played by electronic and steric effects in determining an optimal substrate orientation for highly regio and enantioselective C−H oxidation is provided by *N*-cyclohexylcyclohexanecarboxamide (**S15**, entry 9). Oxidation of this substrate occurs selectively at the *N*-cyclohexyl ring with excellent isolated yield (75%), exquisite regioselectivity ($K_3/K_4 = 38$), and very high enantioselectivity (91% ee).

Increasing the electron withdrawing ability of the R group (**S16**-**S19**, entries 10−13) progressively decreases the K_3/K_4 ratio due to deactivation of proximal positions (C3) as compared to remote ones (C4), with the lowest regioselectivities for oxidation at C3 ($K_3/K_4 = 0.6$) being observed with *N*-cyclohexylphthalimide (**S18**) and *N*-cyclohexyltetrafluorophthalimide (**S19**) (K_3/K_4 = 0.8 and 0.6, respectively). These findings are in full agreement with the results of recent studies on the HAT-based aliphatic C−H halogenation of pentyl derivatives, where, among different electron withdrawing substituents, the phthalimido one provided the highest selectivity for the most remote methylene group.[57,58] Decreased levels of enantioselectivity are also observed with these substrates (ee's between 62 and 68%), in line with the discussion outlined above on the role played by substrate Lewis basicity on the C−H oxidation enantioselectivity.

Finally, under the optimized conditions, *N*-cyclohexyl amides bearing methyl substituents on the cyclohexane ring were evaluated (Scheme 4). *N*-(4,4-Dimethylcyclohexyl)pivalamide **S20** was oxidized with excellent regioselectivity and 76% ee, while blocking positions 3 and 5 with methyl groups (*N*-(3,3,5,5-tetramethylcyclohexyl)pivalamide, **S22**) results in an inert substrate under the experimental conditions. Oxidation of a racemic mixture of *N*-(3,3-dimethylcyclohexyl)pivalamide **S21** results in a chiral resolution, providing the ketone K_3 in 39% isolated yield and 55% ee, while the starting amide is enantiomerically enriched to a moderate extent (38% ee). Under optimized conditions *tert*-butylcyclohexane (**S1**) and cyclohexyl pivalate (**S2**) were also oxidized in good yields and with remarkable ee's (64 and 61% ee, respectively). The results obtained in the oxidation of **S1** are particularly interesting because this substrate is characterized by a simple cycloalkane skeleton devoid of any functionality, and the relatively high enantioselectivity must be mostly based on sterics.

Scheme 4[a]

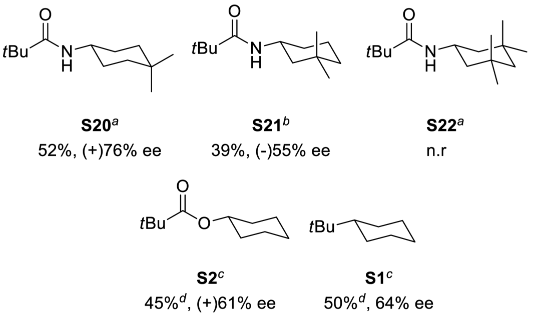

S20[a] 52%, (+)76% ee

S21[b] 39%, (-)55% ee

S22[a] n.r

S2[c] 45%[d], (+)61% ee

S1[c] 50%[d], 64% ee

[a](a) **(*R*,*R*)-Mn-($^{\text{TIPS}}$mcp)** and acetic acid. (b) **(*S*,*S*)-Mn($^{\text{TIPS}}$ecp)** and acetic acid. (c) **(*R*,*R*)-Mn-($^{\text{TIPS}}$mcp)** and cyclopropanecarboxylic acid. (d) Sum of $K_3 + K_4$. Isolated yields.

The significance of the levels of regio- and enantioselectivity exhibited in the current reactions must be considered in context. Cyclohexane scaffolds have been used as model substrates in studies aimed at clarifying the factors that govern selectivity in C−H oxidation. Trends in regioselectivity related to those observed for the current Mn-catalyzed oxidations, entailing preferential oxidation at C3 and C4 have been observed in the oxidation of **S1** with hypervalent iodine reagents,[45,46] dioxiranes,[44] alkoxyl radicals,[52] and iron and manganese catalysts.[41,43] However, the outstanding directing role of the amide moiety is unprecedented and provides an excellent tool to consider in governing site-selectivity in C−H oxidation.

The levels of enantioselectivity observed in the current reactions deserve special discussion. To the best of our knowledge, the reactions described herein represent the first example of an enantioselective C−H oxidation of a nonactivated C−H bond carried out by a nonenzymatic system. Indeed, the current reactions are focused on methylenic sites, that, as compared to tertiary sites, are characterized by significantly stronger C−H bonds, and for which viable oxidants are limited. Previous chiral oxidations of a cyclohexane moiety have been described only after systematic mutations of a P450 enzyme,[21] where enantioselective hydroxylation at C2 was obtained.

Scheme 5. Description of the Possible Mechanisms at the Origin of the Enantioselectivity

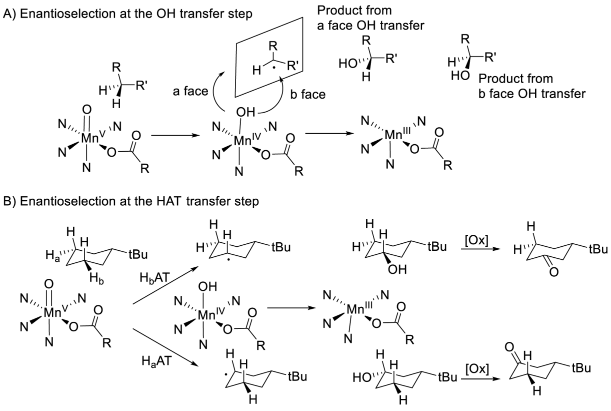
A) Enantioselection at the OH transfer step
Product from a face OH transfer
Product from b face OH transfer
a face
b face
R
H
R'
HO
OH
N
Mn^{V}
Mn^{IV}
Mn^{III}
O
R
B) Enantioselection at the HAT transfer step
H$_a$
H$_b$
H$_b$AT
H$_a$AT
tBu
OH
HO
[Ox]

The origin of the enantioselective discrimination in the current reactions also deserves a comment. Enantioselectivity can originate from the transfer of a hydroxyl ligand belonging to a chiral Mn−OH complex to a long-lived and planar carbon centered radical (Scheme 5A) or from the initial C−H cleaving step by a chiral metal-oxo species (Scheme 5B). The high reactivity of alkyl radicals seems a priori incompatible with their use as radical relays, in a similar way as done in recent benzylic C−H functionalization reactions.[17] More definitively, however, this latter mechanism is incompatible with the desymmetrization reactions described herein. In the current reactions enantioselectivity must be necessarily introduced in the C−H lysis step, which has been previously established to entail HAT from the aliphatic C−H bond to a high valent manganese-oxo species Mn^{V}(O) (carboxylate) moiety, followed by a fast hydroxyl rebound toward the incipient carbon centered radical.[30] Therefore, the current reactions capture the mechanistic essence of stereoselective aliphatic C−H oxidation reactions taking place at P450 cpdI.[59] Careful design of the chiral $Mn^V(O)$ (carboxylate) site is necessary for reaching good product yields and high levels of stereoselection in the oxidation of these strong C−H bonds. This is achieved by embedding the manganese center in a chiral robust cavity defined by bulky TIPS groups of the ligand and the assistance of an oxidatively robust carboxylic acid. In this scenario, it must be recognized that the extraordinary role of the basic amide moiety in dictating regio- and enantioselectivity is not completely understood. The most obvious binding of the Lewis basic carbonyl moiety to the $Mn^V(O)$ (carboxylate) site will require the unlikely formation of a seven coordinate manganese species. Other possibilities to consider may be the presence of a partially protonated oxo or carboxylate ligand, introducing an acidic site susceptible to engage in H-bonding with the incoming amide substrate. Precedents for a basic high valent iron-oxo species exist for chloroperoxidase.[60] Elucidation of these possibilities will require a more precise understanding of the nature of the active species, maybe only possible via computational methods. On the other hand, it must be noticed that the current reactions entail breakage of strong C−H bonds, but they occur at low temperature in a remarkably efficient manner. This implies that the active species must be extraordinarily reactive, and activation barriers for the reactions must be small. Introduction of stereoselectivity in these conditions is particularly challenging, and therefore it is not surprising that ee's appear to be quite sensitive to small changes in the nature of the catalyst, carboxylic acid, and substrate. Particular optimizations may be necessary. Indeed, we notice that structural specificity in stereoselective aliphatic C−H oxidation is a common feature of enzymatic systems and may be a fundamental drawback of this type of reaction.

■ CONCLUSIONS

The present work describes unique examples of regio- and enantioselective oxidation of nonactivated aliphatic C−H bonds with small molecule manganese catalysts using hydrogen peroxide as the oxidant. A chiral sterically demanding and oxidatively robust active center can be built via careful tuning of the manganese ligands. These results represent the first examples of highly enantioselective nonenzymatic oxidation of nonactivated methylenic sites. The principles of catalyst design disclosed in this work constitute a very solid platform for further development of stereoselective C−H oxidation reactions in terms of substrate scope, but we also envision their straightforward application to other asymmetric oxygen atom transfer reactions (to olefins, amines, or sulfides, for example). Not less important, the current oxidation reactions are based on the use of an abundant first row transition metal and hydrogen peroxide as the oxidant. Therefore, they are also particularly interesting from a sustainable perspective.

■ ASSOCIATED CONTENT

Supporting Information

The Supporting Information is available free of charge on the ACS Publications website at DOI: 10.1021/acscentsci.6b00368.

> Experimental details for the preparation and characterization of ligands and metal complexes. Experimental details of catalytic reactions, and spectroscopic data for product characterization (PDF)
>
> Crystallographic information files (CIF1, CIF2)

■ AUTHOR INFORMATION

Corresponding Authors

*(M.C.) Tel: +34-972419842. E-mail: miquel.costas@udg.edu.
*(M.B.) E-mail: bietti@uniroma2.it.

ORCID

Massimo Bietti: 0000-0001-5880-7614
Miquel Costas: 0000-0001-6326-8299

Notes

The authors declare no competing financial interest.

■ ACKNOWLEDGMENTS

We acknowledge financial support from MINECO of Spain (CTQ2015-70795-P) and the Catalan DIUE of the Generalitat de Catalunya (2009SGR637). M.C. thanks an ICREA-Academia award. We thank STR from UdG and Gabriel Peris from UJI by Xray diffraction analyses. We thank Prof. Antoni Riera from UB for kindly providing access to a polarimeter.

■ REFERENCES

(1) Newhouse, T.; Baran, P. S. If C-H Bonds Could Talk: Selective C-H Bond Oxidation. *Angew. Chem., Int. Ed.* **2011**, *50*, 3362−3374.

(2) Cernak, T.; Dykstra, K. D.; Tyagarajan, S.; Vachal, P.; Krska, S. W. The medicinal chemist's toolbox for late stage functionalization of drug-like molecules. *Chem. Soc. Rev.* **2016**, *45*, 546−576.

(3) Zheng, C.; You, S.-L. Recent development of direct asymmetric functionalization of inert C-H bonds. *RSC Adv.* **2014**, *4*, 6173−6214.

(4) Miyafuji, A.; Katsuki, T. Asymmetric desymmetrization of meso-tetrahydrofuran derivatives by highly enantiotopic selective C-H oxidation. *Tetrahedron* **1998**, *54*, 10339−10348.

(5) Frost, J. R.; Huber, S. M.; Breitenlechner, S.; Bannwarth, C.; Bach, T. Enantiotopos-Selective C-H Oxygenation Catalyzed by a Supramolecular Ruthenium Complex. *Angew. Chem., Int. Ed.* **2015**, *54*, 691−695.

(6) Groves, J. T.; Viski, P. Asymmetric hydroxylation, epoxidation, and sulfoxidation catalyzed by vaulted binaphthyl metalloporphyrins. *J. Org. Chem.* **1990**, *55*, 3628−3634.

(7) Groves, J. T.; Viski, P. Asymmetric hydroxylation by a chiral iron porphyrin. *J. Am. Chem. Soc.* **1989**, *111*, 8537−8538.

(8) Srour, H.; Maux, P. L.; Simonneaux, G. Enantioselective Manganese-Porphyrin-Catalyzed Epoxidation and C−H Hydroxylation with Hydrogen Peroxide in Water/Methanol Solutions. *Inorg. Chem.* **2012**, *51*, 5850−5856.

(9) Maux, P. L.; Srour, H. F.; Simonneaux, G. Enantioselective water-soluble iron−porphyrin-catalyzed epoxidation with aqueous hydrogen peroxide and hydroxylation with iodobenzene diacetate. *Tetrahedron* **2012**, *68*, 5824−5828.

(10) Zhang, R.; Yu, W. Y.; Lai, T. S.; Che, C.-M. Enantioselective hydroxylation of benzylic C-H bonds by D-4-symmetric chiral oxoruthenium porphyrins. *Chem. Commun.* **1999**, 1791−1792.

(11) Zhang, R.; Yu, W.-Y.; Che, C.-M. Catalytic enantioselective oxidation of aromatic hydrocarbons with D4-symmetric chiral ruthenium porphyrin catalysts. *Tetrahedron: Asymmetry* **2005**, *16*, 3520−3526.

(12) Hamada, T.; Irie, R.; Mihara, J.; Hamachi, K.; Katsuki, T. Highly enantioselective benzylic hydroxylation with concave type of (salen)-manganese(III) complex. *Tetrahedron* **1998**, *54*, 10017−10028.

(13) Hamachi, K.; Irie, R.; Katsuki, T. Asymmetric benzylic Oxidation Using a Mn-Salen Complex as Catalyst. *Tetrahedron Lett.* **1996**, *37*, 4979−4982.

(14) Komiya, N.; Noji, S.; Murahashi, S.-I. Manganese catalyzed asymmetric oxidation of alkanes to optically active ketones bearing asymmetric center at the α-position. *Tetrahedron Lett.* **1998**, *39*, 7921−7924.

(15) Murahashi, S.-I.; Noji, S.; Hirabayashi, T.; Komiya, N. Manganese-catalyzed enantioselective oxidation of C−H bonds of alkanes and silyl ethers to optically active ketones. *Tetrahedron: Asymmetry* **2005**, *16*, 3527−3535.

(16) Murahashi, S.-I.; Noji, S.; Komiya, N. Catalytic Enantioselective Oxidation of Alkanes and Alkenes Using (Salen)Manganese Complexes Bearing a Chiral Binaphthyl Strapping Unit. *Adv. Synth. Catal.* **2004**, *346*, 195−198.

(17) Zhang, W.; Wang, F.; McCann, S. D.; Wang, D.; Chen, P.; Stahl, S. S.; Liu, G. Enantioselective cyanation of benzylic C−H bonds via copper-catalyzed radical relay. *Science* **2016**, *353*, 1014−1018.

(18) Wang, F.; Wang, D.; Wan, X.; Wu, L.; Chen, P.; Liu, G. Enantioselective Copper-Catalyzed Intermolecular Cyanotrifluoromethylation of Alkenes via Radical Process. *J. Am. Chem. Soc.* **2016**, *138*, 15547−15550.

(19) Kille, S.; Zilly, F. E.; Acevedo, J. P.; Reetz, M. T. Regio- and stereoselectivity of P450-catalysed hydroxylation of steroids controlled by laboratory evolution. *Nat. Chem.* **2011**, *3*, 738−743.

(20) Narayan, A. R. H.; Jimenez-Oses, G.; Liu, P.; Negretti, S.; Zhao, W.; Gilbert, M. M.; Ramabhadran, R. O.; Yang, Y.-F.; Furan, L. R.; Li, Z.; Podust, L. M.; Montgomery, J.; Houk, K. N.; Sherman, D. H. Enzymatic hydroxylation of an unactivated methylene C-H bond guided by molecular dynamics simulations. *Nat. Chem.* **2015**, *7*, 653−660.

(21) Roiban, G.-D.; Agudo, R.; Reetz, M. T. Cytochrome P450 Catalyzed Oxidative Hydroxylation of Achiral Organic Compounds with Simultaneous Creation of Two Chirality Centers in a Single C-H Activation Step. *Angew. Chem., Int. Ed.* **2014**, *53*, 8659−8663.

(22) Zhang, K.; Shafer, B. M.; Matthew, D.; Demars, I.; Stern, H. A.; Fasan, R. Controlled Oxidation of Remote sp^3 C-H Bonds in Artemisinin via P450 Catalysts with Fine-Tuned Regio- and Stereoselectivity. *J. Am. Chem. Soc.* **2012**, *134*, 18695−18704.

(23) Cussó, O.; Ribas, X.; Costas, M. Biologically inspired non-heme iron-catalysts for asymmetric epoxidation; design principles and perspectives. *Chem. Commun.* **2015**, *51*, 14285−14298.

(24) Wang, C.; Yamamoto, H. Asymmetric Epoxidation Using Hydrogen Peroxide as Oxidant. *Chem. - Asian J.* **2015**, *10*, 2056−2068.

(25) Bryliakov, K. P.; Talsi, E. P. Active sites and mechanisms of bioinspired oxidation with H_2O_2, catalyzed by non-heme Fe and related Mn complexes. *Coord. Chem. Rev.* **2014**, *276*, 73−96.

(26) Zang, C.; Liu, Y.; Xu, Z.-J.; Tse, C.-W.; Guan, X.; Wei, J.; Huang, J.-S.; Che, C.-M. Highly Enantioselective Iron-Catalyzed cis-Dihydroxylation of Alkenes with Hydrogen Peroxide Oxidant via an FeIII-OOH Reactive Intermediate. *Angew. Chem., Int. Ed.* **2016**, *55*, 10253−10257.

(27) Chow, T. W.-S.; Liu, Y.; Che, C.-M. Practical manganese-catalysed highly enantioselective cis-dihydroxylation of electron-deficient alkenes and detection of a cis-dioxomanganese(v) intermediate by high resolution ESI-MS analysis. *Chem. Commun.* **2011**, *47*, 11204−11206.

(28) Costas, M.; Olivo, G.; Cussó, O. Biologically Inspired C-H and C═C Oxidations with H_2O_2 Catalyzed by Iron Coordination Complexes. *Chem. - Asian J.* **2016**, *11*, 3148−3158.

(29) Oloo, W. N.; Que, L. Bioinspired Nonheme Iron Catalysts for C−H and C═C Bond Oxidation: Insights into the Nature of the Metal-Based Oxidants. *Acc. Chem. Res.* **2015**, *48*, 2612−2621.

(30) Ottenbacher, R. V.; Talsi, E. P.; Bryliakov, K. P. Mechanism of Selective C-H Hydroxylation Mediated by Manganese Aminopyridine Enzyme Models. *ACS Catal.* **2015**, *5*, 39−44.

(31) White, M. C. Adding Aliphatic C-H Bond Oxidations to Synthesis. *Science* **2012**, *335*, 807−809.

(32) Chen, M. S.; White, M. C. A Predictably Selective Aliphatic C-H Oxidation Reaction for Complex Molecule Synthesis. *Science* **2007**, *318*, 783−787.

(33) Font, D.; Canta, M.; Milan, M.; Cussó, O.; Ribas, X.; Klein Gebbink, R. J. M.; Costas, M. Readily Accessible Bulky Iron Catalysts exhibiting Site Selectivity in the Oxidation of Steroidal Substrates. *Angew. Chem., Int. Ed.* **2016**, *55*, 5776−5779.

(34) Gomez, L.; Canta, M.; Font, D.; Prat, I.; Ribas, X.; Costas, M. Regioselective oxidation of nonactivated alkyl C-H groups using highly structured non-heme iron catalysts. *J. Org. Chem.* **2013**, *78*, 1421−33.

(35) Borissov, A.; Davies, T. Q.; Ellis, S. R.; Fleming, T. A.; Richardson, M. S. W.; Dixon, D. J. Organocatalytic enantioselective desymmetrisation. *Chem. Soc. Rev.* **2016**, *45*, 5474−5540.

(36) Ottenbacher, R. V.; Samsonenko, D. G.; Talsi, E. P.; Bryliakov, K. P. Highly Efficient, Regioselective, and Stereospecific Oxidation of Aliphatic C-H Groups with H_2O_2, Catalyzed by Aminopyridine Manganese Complexes. *Org. Lett.* **2012**, *14*, 4310−4313.

(37) Adams, A. M.; Du Bois, J.; Malik, H. A. Comparative Study of the Limitations and Challenges in Atom-Transfer C−H Oxidations. *Org. Lett.* **2015**, *17*, 6066−6069.

(38) Canta, M.; Font, D.; Gómez, L.; Ribas, X.; Costas, M. The Iron(II) Complex $[Fe(CF_3SO_3)_2(mcp)]$ as a Convenient, Readily Available Catalyst for the Selective Oxidation of Methylenic Sites in Alkanes. *Adv. Synth. Catal.* **2014**, *356*, 818−830.

(39) Murphy, A.; Dubois, G.; Stack, T. D. P. Efficient Epoxidation of Electron-Deficient Olefins with a Cationic Manganese Complex. *J. Am. Chem. Soc.* **2003**, *125*, 5250−5251.

(40) Chen, K.; Que, L. Stereospecific alkane hydroxylation by non-heme iron catalysts: Mechanistic evidence for an Fe^V=O active species. *J. Am. Chem. Soc.* **2001**, *123*, 6327−6337.

(41) Chen, M. S.; White, M. C. Combined Effects on Selectivity in Fe-Catalyzed Methylene Oxidation. *Science* **2010**, *327*, 566−571.

(42) Shen, D. Y.; Miao, C. X.; Xu, D. Q.; Xia, C. G.; Sun, W. Highly Efficient Oxidation of Secondary Alcohols to Ketones Catalyzed by Manganese Complexes of N-4 Ligands with H_2O_2. *Org. Lett.* **2015**, *17*, 54−57.

(43) Shen, D.; Miao, C.; Wang, S.; Xia, C.; Sun, W. Efficient Benzylic and Aliphatic C−H Oxidation with Selectivity for Methylenic Sites Catalyzed by a Bioinspired Manganese Complex. *Org. Lett.* **2014**, *16*, 1108−1111.

(44) González-Núñez, M. E.; Castellano, G.; Andreu, C.; Royo, J.; Báguena, M.; Mello, R.; Asensio, G. Influence of Remote Substituents on the Equatorial/Axial Selectivity in the Monooxygenation of Methylene C−H Bonds of Substituted Cyclohexanes. *J. Am. Chem. Soc.* **2001**, *123*, 7487−7491.

(45) Moteki, S. A.; Usui, A.; Zhang, T.; Solorio Alvarado, C. R.; Maruoka, K. Site-Selective Oxidation of Unactivated C-H Bonds with Hypervalent Iodine(III) Reagents. *Angew. Chem., Int. Ed.* **2013**, *52*, 8657−8660.

(46) Moteki, S. A.; Selvakumar, S.; Zhang, T.; Usui, A.; Maruoka, K. A Practical Approach for the Oxidation of Unactivated Csp^3-H Bonds with o-Nitro(diacetoxyiodo)benzene as an Efficient Hypervalent Iodine(III)-Based Oxidizing Agent. *Asian J. Org. Chem.* **2014**, *3*, 932−935.

(47) Cussó, O.; Garcia-Bosch, I.; Font, D.; Ribas, X.; Lloret-Fillol, J.; Costas, M. Highly Stereoselective Epoxidation with H_2O_2 Catalyzed by Electron-Rich Aminopyridine Manganese Catalysts. *Org. Lett.* **2013**, *15*, 6158−6161.

(48) Ottenbacher, R. V.; Samsonenko, D. G.; Talsi, E. P.; Bryliakov, K. P. Highly Enantioselective Bioinspired Epoxidation of Electron-Deficient Olefins with H_2O_2 on Aminopyridine Mn Catalysts. *ACS Catal.* **2014**, *4*, 1599−1606.

(49) Wang, X.; Miao, C. X.; Wang, S. F.; Xia, C. G.; Sun, W. Bioinspired Manganese and Iron Complexes with Tetradentate N Ligands for the Asymmetric Epoxidation of Olefins. *ChemCatChem* **2013**, *5*, 2489−2494.

(50) Gormisky, P. E.; White, M. C. Catalyst-Controlled Aliphatic C−H Oxidations with a Predictive Model for Site-Selectivity. *J. Am. Chem. Soc.* **2013**, *135*, 14052−14055.

(51) Lyakin, O. Y.; Ottenbacher, R. V.; Bryliakov, K. P.; Talsi, E. P. Asymmetric Epoxidations with H_2O_2 on Fe and Mn Aminopyridine Catalysts: Probing the Nature of Active Species by Combined Electron Paramagnetic Resonance and Enantioselectivity Study. *ACS Catal.* **2012**, *2*, 1196−1202.

(52) Salamone, M.; Ortega, V. B.; Bietti, M. Enhanced Reactivity in Hydrogen Atom Transfer from Tertiary Sites of Cyclohexanes and

Decalins via Strain Release: Equatorial C−H Activation vs Axial C−H Deactivation. *J. Org. Chem.* **2015**, *80*, 4710−4715.

(53) Zou, L.; Paton, R. S.; Eschenmoser, A.; Newhouse, T. R.; Baran, P. S.; Houk, K. N. Enhanced Reactivity in Dioxirane C−H Oxidations via Strain Release: A Computational and Experimental Study. *J. Org. Chem.* **2013**, *78*, 4037−4048.

(54) Salamone, M.; Carboni, G.; Bietti, M. Fine Control over Site and Substrate Selectivity in Hydrogen Atom Transfer-Based Functionalization of Aliphatic C−H Bonds. *J. Org. Chem.* **2016**, *81*, 9269−9278.

(55) Cussó, O.; Garcia-Bosch, I.; Ribas, X.; Lloret-Fillol, J.; Costas, M. Asymmetric Epoxidation with H_2O_2 by Manipulating the Electronic Properties of Non-heme Iron Catalysts. *J. Am. Chem. Soc.* **2013**, *135*, 14871−14878.

(56) Bigi, M. A.; Reed, S. A.; White, M. C. Directed Metal (Oxo) Aliphatic C−H Hydroxylations: Overriding Substrate Bias. *J. Am. Chem. Soc.* **2012**, *134*, 9721−9726.

(57) Quinn, R. K.; Könst, Z. A.; Michalak, S. E.; Schmidt, Y.; Szklarski, A. R.; Flores, A. R.; Nam, S.; Horne, D. A.; Vanderwal, C. D.; Alexanian, E. J. Site-Selective Aliphatic C−H Chlorination Using N-Chloroamides Enables a Synthesis of Chlorolissoclimide. *J. Am. Chem. Soc.* **2016**, *138*, 696−702.

(58) Schmidt, V. A.; Quinn, R. K.; Brusoe, A. T.; Alexanian, E. J. Site-Selective Aliphatic C−H Bromination Using N-Bromoamides and Visible Light. *J. Am. Chem. Soc.* **2014**, *136*, 14389−14392.

(59) Ortiz de Montellano, P. R. Hydrocarbon Hydroxylation by Cytochrome P450 Enzymes. *Chem. Rev.* **2010**, *110*, 932−948.

(60) Green, M. T.; Dawson, J. H.; Gray, H. B. Oxoiron(IV) in Chloroperoxidase Compound II Is Basic: Implications for P450 Chemistry. *Science* **2004**, *304*, 1653−1656.

■ NOTE ADDED AFTER ASAP PUBLICATION

This article was published on February 8, 2017. Corrections to stereochemical designations in the article and the Supporting Information were made on February 23, 2017.

Chapter V

Aliphatic C–H Bond Oxidation with Hydrogen Peroxide Catalyzed by Manganese Complexes: Directing Selectivity through Torsional Effects

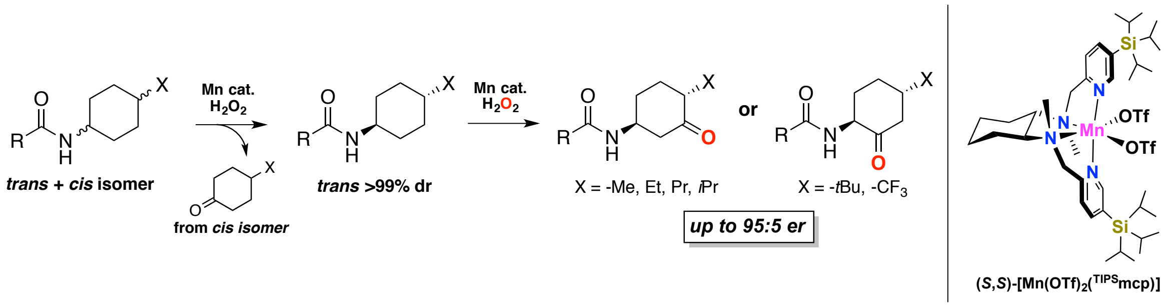
Mn cat.
H2O2
trans + cis isomer
from cis isomer
trans >99% dr
or
X = -Me, Et, Pr, iPr
X = -tBu, -CF3
up to 95:5 er
OTf
OTf
(S,S)-[Mn(OTf)2(TIPSmcp)]

This chapter correspond to the following publication:

Milan, M.; Bietti, M.; Costas, M. *Org. Lett.* **2018**, *20*, 2720-2723

Reproduced with permission from:

Milan, M.; Bietti, M.; Costas, M. *Org. Lett.* 2018, *20*, 2720-2723

http://dx.doi.org/10.1021/acs.orglett.8b00929

Copyright © 2018 American Chemical Society

Organic LETTERS
Cite This: Org. Lett. 2018, 20, 2720−2723
Letter
pubs.acs.org/OrgLett

Aliphatic C−H Bond Oxidation with Hydrogen Peroxide Catalyzed by Manganese Complexes: Directing Selectivity through Torsional Effects

Michela Milan,[†] Massimo Bietti,*,[‡] and Miquel Costas*,[†]

[†]Institut de Química Computational i Catàlisi, IQCC and Departament de Química, Universitat de Girona, Campus de Montilivi, 17003 Girona, Spain

[‡]Dipartimento di Scienze e Tecnologie Chimiche, Università"Tor Vergata", Via della Ricerca Scientifica, 1, I-00133 Rome, Italy

Supporting Information

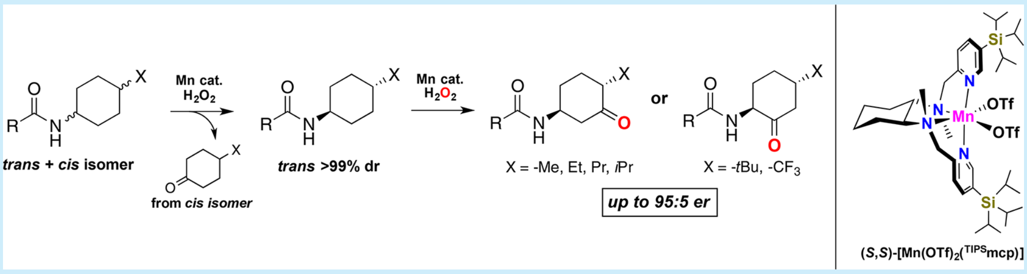

ABSTRACT: Substituted *N*-cyclohexyl amides undergo aliphatic C−H bond oxidation with H_2O_2 catalyzed by manganese complexes. The reactions are directed by torsional effects leading to site-selective oxidation of *cis*-1,4-, *trans*-1,3-, and *cis*-1,2-cyclohexanediamides. The corresponding diastereoisomers are unreactive under the same conditions. Competitive oxidation of *cis*−*trans* mixtures of 4-substituted *N*-cyclohexylamides leads to quantitative conversion of the *cis*-isomers, allowing isolation and successive conversion of the *trans*-isomers into densely functionalized oxidation products with excellent site selectivity and good enantioselectivity.

The development of oxidation methodologies that can selectively target nonactivated aliphatic C−H bonds and discriminate among them within the same substrate would provide very valuable tools in organic synthesis that can rapidly expand product diversity and build chemical complexity in a single step from relatively simple and readily available substrates.[1−9] The factors that govern the relative reactivity of C−H bonds against different oxidants have been extensively scrutinized, with the final goal of setting predictability in C−H oxidation reactions of complex substrates. Bond strengths as well as electronic, steric, stereoelectronic, and torsional effects have been recognized as innate C−H relative reactivity determining factors.[1,3,10] Medium effects have also been shown to play an important role.[11−15] In cases where these elements synergistically cooperate, site selective oxidation of complex organic molecules has been accomplished.[16] In this context, we have recently shown that amide functionalities constitute a powerful handle to direct site selectivity in C−H oxidation reactions by means of steric, electronic, and stereoelectronic effects.[17,18] Herein, we disclose site selective and enantioselective oxidation of a series of *N*-cyclohexyl amides and diamides catalyzed by manganese complexes. We show moreover that torsional effects enable the unprecedented resolution of mixtures of *cis*- and *trans*-1,4-disubstituted *N*-cyclohexyl amides via C−H bond oxidation, selectively providing the oxidation products derived from the *cis* isomer, allowing the recovery of the unreacted *trans* one in good to excellent yield. Subsequent methylene oxidation in the latter isomers yields enantioenriched ketoamide products via site and enantioselective C−H oxidation. By virtue of these reactions, *cis*−*trans* mixtures of *N*-cyclohexyl amides substituted at C-4 are converted into precious chiral and densely functionalized building blocks. The current reactions are remarkable because amides, besides their inherent interest, can be readily converted into amines, one of the most important classes of organic compounds.[19] Furthermore, to the best of our knowledge, the current report pioneers the use of selective C−H bond oxidation of cyclohexane derivatives, in the current case guided by torsional effects, as a synthetic tool for resolving diastereoisomeric mixtures.

Chiral manganese complexes, which have been recently shown to display an excellent catalytic activity in the selective oxidation of aliphatic C−H bonds,[15,17,18,20−22] and with the general formula [Mn(CF_3SO_3)$_2$(L)] (L = pdp and mcp, pdp = *N,N*′-bis(2-pyridylmethyl)-2,2′-bipyrrolidine, mcp = *N,N*′-dimethyl *N,N*′-bis(2-pyridylmethyl)-1,2-*trans*-diamino cyclohexane, ecp = *N,N*′-diethyl *N,N*′-bis(2-pyridylmethyl)-1,2-*trans*-diamino cyclohexane Scheme 1; **Mn(pdp)**, **Mn(^{TIPS}mcp)**, and **Mn(^{TIPS}ecp)**) were used in this work. The oxidation of *cis* and

Received: March 21, 2018
Published: April 20, 2018

© 2018 American Chemical Society

DOI: 10.1021/acs.orglett.8b00929
Org. Lett. 2018, 20, 2720−2723

Scheme 1. General Scheme of the Reactions and the Catalysts Used in This Work

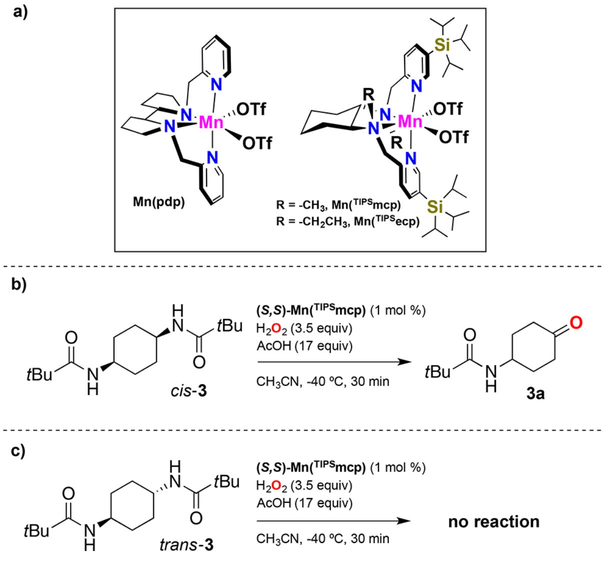

Scheme 2. Transition Structures for HAT from Tertiary Equatorial and Axial C−H Bonds of Z-Disubstituted Cyclohexanes to a Generic Radical X$^{\bullet}$ Showing the Release of 1,3-Diaxial Strain (A) and the Increase in Torsional Strain (B) Associated to HAT

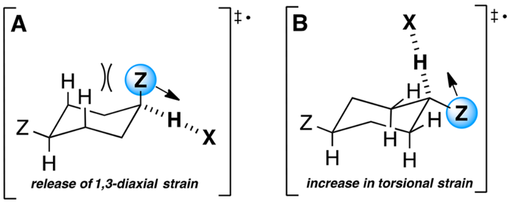

trans diamides derived from 1,2-, 1,3-, and 1,4-cyclohexanediamines was initially studied in order to evaluate the effect of substrate structure on selectivity.

Reactions were conducted employing an acetonitrile solution of the catalyst **Mn(pdp)** or **Mn(^{TIPS}mcp)** (1−3 mol %) and the substrate, delivering H_2O_2 (2.0−4.5 equiv) via syringe pump during 30 min at −40 °C under air.

Starting from the pivaldiamides derived from *cis*- and *trans*-1,4-cyclohexanediamine (Scheme 1, *cis*-**3** and *trans*-**3**, respectively), oxidation of *cis*-**3** led to the formation of *N*-(4-oxocyclohexyl)-pivalamide (**3a**) (63% conversion, 51% yield, Scheme 1b) as the exclusive oxidation product. Formation of **3a** can be rationalized by considering an initial tertiary equatorial C−H bond hydroxylation via hydrogen atom transfer (HAT) from this bond to a high valent manganese-oxo species, followed by a hydroxyl rebound to give an α-hydroxo-amide product that then undergoes hydrolytic cleavage. Under identical conditions, no reaction was observed for *trans*-**3**, which was instead quantitatively recovered from the reaction mixture pointing toward a low reactivity of both the tertiary axial and secondary C−H bonds of this substrate. These findings are in full agreement with the results of previous studies on cyclohexane derivatives[23,24] that have clearly shown that, while tertiary equatorial C−H bonds are activated toward abstraction, the opposite holds for tertiary axial C−H bonds that are instead deactivated. This behavior has been rationalized in terms of torsional effects associated with the planarization of an incipient carbon radical in the HAT transition state. Tertiary equatorial C−H bond activation is a well-established concept in these processes and has been explained on the basis of a release of 1,3-diaxial strain in the HAT transition state (Scheme 2A).[23−25]

The concept of tertiary axial C−H bond deactivation has received instead less attention and has been rationalized in terms of an increase in torsional strain in the HAT transition state where the substituent is forced toward an eclipsed interaction with the equatorial C−H bonds on the adjacent positions (Scheme 2B).[23,26] It is worth mentioning that a very recent kinetic study has pointed out that the latter effect can override favorable C−H BDEs, representing an important contributor in governing the functionalization selectivity of monosubstituted cyclohexanes.[27] A striking example of this deactivation is provided by phenylcyclohexane that, despite of the presence of a relatively weak tertiary benzylic C−H bond (BDE = 85.2 kcal mol^{-1}),[28] undergoes selective functionalization at C-3 and C-4 in its reactions with a variety of HAT reagents.[29−33]

Scheme 3. Oxidation Reactions of Cyclohexane-Derived Pivaldiamides

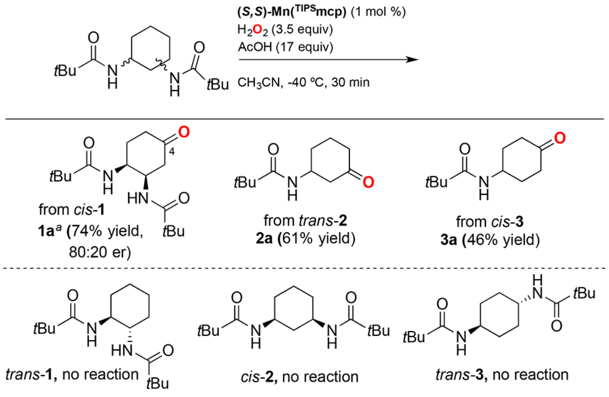

^{a}Iterative addition (2×): cat. (1 mol %), H_2O_2 (4.5 equiv). Isolated yields.

In the studies described above,[23−33] it was also proposed that bulky equatorial substituents deactivate the C−H bonds of the adjacent secondary sites via planarization of an incipient carbon radical in the HAT transition state that forces the remaining C−H bond toward an eclipsed interaction with the ring substituent.[17,23,27] Results on the oxidation of 1,2- and 1,3-cyclohexanediamides following analogous procedures are collected in Scheme 3. Oxidation of the pivaldiamide derived from *trans*-1,3-cyclohexanediamine (*trans*-**2**) led to the formation of *N*-(3-oxocyclohexyl) pivalamide (**2a**) as the exclusive oxidation product (61% isolated yield) following HAT from the tertiary equatorial C−H bond, as described above for the oxidation of *cis*-**3**. The corresponding cis isomer (*cis*-**2**) and the pivaldiamide derived from *trans*-1,2-cyclohexanediamine (*trans*-**1**), characterized by the presence of two tertiary axial C−H bonds, proved instead unreactive, in keeping with the results discussed above on the oxidation of *trans*-**3**. Oxidation of the pivaldiamide derived from *cis*-1,2-cyclohexanediamine (*cis*-**1**) took place selectively at position 4 and not at the tertiary equatorial C−H bond, providing keto diamide **1a** in 74% isolated yield and a 80:20 enantiomeric ratio (er). The lack of reaction at the latter position can be again rationalized in terms of an increase in torsional strain in the HAT transition state, where planarization of an incipient tertiary radical forces the two bulky pivalamido groups toward an unfavorable eclipsed interaction, directing HAT to C-4. The lack of reactivity of *trans*-**1**, *cis*-**2**, and *trans*-**3** deserves special consideration. As mentioned above, the tertiary axial and adjacent secondary C−H bonds are deactivated toward HAT, but in addition it appears that these substrates can also inhibit the oxidizing ability of the manganese catalyst, probably through chelation of the metal by the two amide groups. This hypothesis is supported by the observation that, while oxidation of *N*-cyclohexylpivalamide catalyzed by **Mn-(^{TIPS}mcp)** led to the formation of *N*-(3-oxocyclohexyl)-pivalamide in 90% isolated yield,[17] only small amounts (between 10 and 37%) of this product were observed when *N*-cyclohexylpivalamide was oxidized in the presence of an equimolar amount of *trans*-**1**, *cis*-**2**, or *trans*-**3**. Full details of these experiments are provided in the Supporting Information (SI).

These results suggest that resolution of *cis* and *trans* couples of *N*-cyclohexylamide derivatives bearing a substituent at C-4 may be possible on the basis of their distinct reactivity patterns in Mn-catalyzed C−H oxidation. Selective oxidation of the *cis* isomer, characterized by the presence of an activated tertiary equatorial C−H bond, should leave the *trans* isomer unreacted, allowing facile separation. For this purpose, a series of *cis*−*trans* isomeric mixtures of 4-X substituted *N*-cyclohexylamides (X = Et, *i*Pr, *t*-Bu, CF_3) differing in isomeric composition (details see the SI) were subjected to standard oxidation conditions, taking particular advantage of the lower conformational energy of the amido group, as compared to the selected X substituents.[34] The results are reported in Scheme 4. As predicted, after optimization, the *cis* isomers are quantitatively converted to the 4-X-substituted cyclohexanone product. The valuable *trans* isomers (*trans*-**5**−*trans*-**9**) are recovered in good to excellent yield (66−96%) and can thus be isolated from different *cis*−*trans* mixtures obtained from commercially available starting materials with a relatively low material loss (see SI). To the best of our knowledge, the diastereomerically pure *trans*-amides and derived *trans*-amines are currently not accessible by other methods. The intramolecular and intermolecular selectivity observed in these reactions is quite striking, if one considers in particular that substrate couples **5**, **6**, and **7** also display exocyclic secondary and tertiary C−H bonds. The lack or low amount of products deriving from oxidation at these sites in the *cis* and *trans* isomers, respectively, clearly indicates that tertiary equatorial C−H bond activation is so strong as to minimize competitive oxidation at other sites.

Scheme 4. Oxidation Reactions of *cis*−*trans* Mixtures of 4-X-Substituted *N*-Cyclohexyl Amides

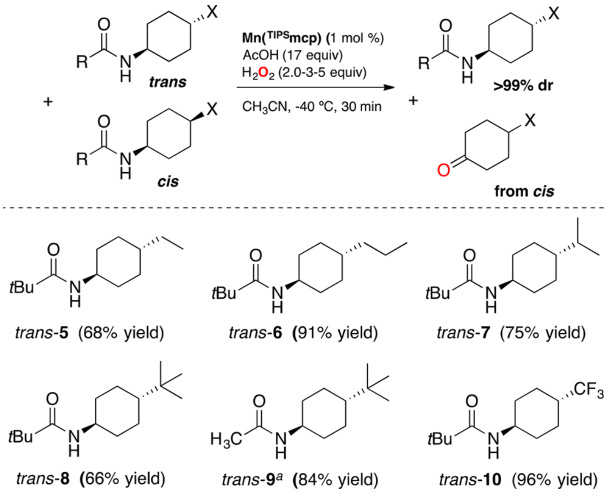

[a] (*S*,*S*)-**Mn(^{TIPS}ecp)** and cyclopropanecarboxylic acid. Isolated yields.

On the basis of these findings, we considered the possibility of further elaborating the *trans* isomers of **5**−**9** into valuable chiral products. Much to our delight, oxidation of these substrates resulted in products where a methylene site is oxidized with excellent site-selectivity and moderate to good enantioselectivity (Scheme 5). Substituents at C-4 have a profound effect on the reaction selectivity. The presence of a methyl, ethyl, or propyl group as in *trans*-**4**, *trans*-**5**, and *trans*-**6** provides good isolated yields of the product deriving from oxidation at C-3 and remarkable enantioselectivity (**4a** (78% yield, 89:11 er), **5a** (65% yield, 93:7 er), and **6a** (42% yield, 95:5 er), respectively). Oxidation of the tertiary axial C−H bond at C-4 to give hydroxyamide **4b** is only observed as a minor side reaction (14%) in the case of *trans*-**4**, indicating that with this substrate the tertiary C−H bond activation determined by the methyl substituent competes with the deactivating torsional effects. With *trans*-**5** and *trans*-**6**, smaller amounts of products deriving from oxidation at the secondary exocyclic C−H bonds were also observed (**5b** and **6b**, 13% and 4% yield, respectively). The presence of an isopropyl group at C-4 as in *trans*-**7** results in a change in site-selectivity, with C−H bond oxidation that now takes place preferentially at the most activated tertiary isopropyl C−H bond to give product **7a** in 45% yield, while a lower amount of product **7b** in an unexpected nearly racemic form (14% yield, 52:48 er) resulting from oxidation at C-3 was obtained. In keeping with the discussion outlined above, the product

Scheme 5. Enantioselective Oxidation Reactions of *trans*-4-X-Substituted *N*-Cyclohexyl Amides

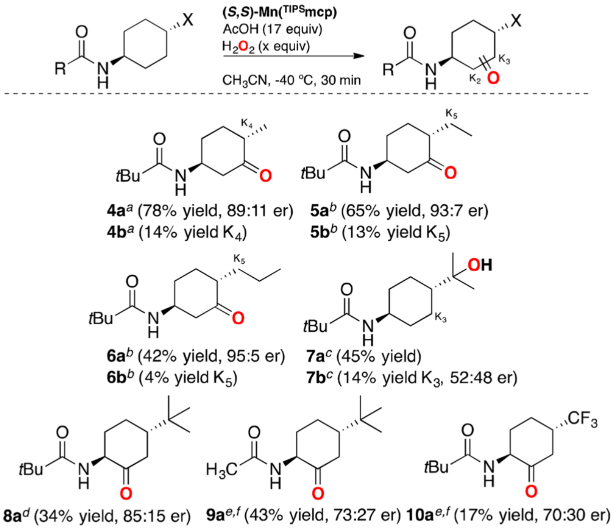

[a] Iterative addition (2×): cat. (1 mol %), H_2O_2 (3.5 equiv). [b] Cat. (3 mol %), H_2O_2 (3.5 equiv). [c] Cat. (3 mol %), H_2O_2 (3.5 equiv). [d] **(*S*,*S*)-Mn(pdp)** (1 mol %), H_2O_2 (4.5 equiv). [e] Iterative addition (3×): cat. (1 mol %), H_2O_2 (3.5 equiv). [f] Yield determined by ^1H NMR analysis. er's determined by GC with chiral stationary phase.

distributions observed with *trans*-**4**, *trans*-**5**, *trans*-**6**, and *trans*-**7**, indicative of strong tertiary axial C—H bond deactivation, coupled to the selective tertiary equatorial C—H bond oxidation of the corresponding *cis* isomers, point toward torsional effects as a determinant contributor in governing the functionalization selectivity of cyclohexane derivatives. Interestingly, an increase in steric hindrance of the ring substituent, i.e., on going from isopropyl to *tert*-butyl (*trans*-**8**), results in a drastic change in site-selectivity. The presence of the bulky *tert*-butyl group at C-4 strongly deactivates the C—H bonds at C-3, directing oxidation at C-2. The 2-keto amide product was obtained in modest to good isolated yield and er both for the pivalamide and acetamide derivatives (**8a** and **9a**). Furthermore, the use of the electron-withdrawing trifluoromethyl group as in *trans*-**10** also directs oxidation toward C-2, presumably by electronic deactivation of the proximal position (C-3), providing the corresponding 2-keto amide-product **10a** with modest yield and er (17% yield, 70:30 er, Scheme 5). We notice that this result is in full agreement with those recently obtained for the C—H bond oxidation reactions of monosubstituted cyclohexanes catalyzed by manganese catalyst, where the presence of an EWG substituent strongly affects the interaction of the substrate with an electrophilic oxidizing species.[17]

In summary, we have shown that C—H bond oxidation directed by torsional effects can be successfully employed to selectively oxidize *cis*-1,4-, *trans*-1,3-, and *cis*-1,2-cyclohexanediamides over the corresponding diastereoisomers. As a consequence, competitive oxidation of *cis*—*trans* mixtures of 4-substituted *N*-cyclohexylamides leads to quantitative conversion of the *cis*-isomers, allowing isolation of the *trans*-isomers in good to excellent yield, which can in turn be converted into densely functionalized oxidation products with excellent site-selectivity and good enantioselectivity. Overall, the current report discloses kinetic resolution in C—H bond oxidation of cyclohexane derivatives as a novel tool for organic synthesis, and exemplifies a rapid building up on chemical complexity and functionality on the basis of site selective and enantioselective aliphatic C—H bond oxidation guided by torsional effects.

■ ASSOCIATED CONTENT

Ⓢ Supporting Information

The Supporting Information is available free of charge on the ACS Publications website at DOI: 10.1021/acs.orglett.8b00929.

Complete experimental details and characterization data (PDF)

■ AUTHOR INFORMATION

Corresponding Authors

*E-mail: miquel.costas@udg.edu.
*E-mail: bietti@uniroma2.it.

ORCID

Massimo Bietti: 0000-0001-5880-7614
Miquel Costas: 0000-0001-6326-8299

Notes

The authors declare no competing financial interest.

■ ACKNOWLEDGMENTS

M.C. acknowledges the MINECO of Spain (CTQ2015-70795-P) and the Catalan DIUE (2017 SGR 264 ICREA Academia award).

■ REFERENCES

(1) Newhouse, T.; Baran, P. S. *Angew. Chem., Int. Ed.* **2011**, *50*, 3362—3374.

(2) Cernak, T.; Dykstra, K. D.; Tyagarajan, S.; Vachal, P.; Krska, S. W. *Chem. Soc. Rev.* **2016**, *45*, 546.

(3) White, M. C. *Science* **2012**, *335*, 807—809.

(4) Hartwig, J. F.; Larsen, M. A. *ACS Cent. Sci.* **2016**, *2*, 281—292.

(5) Davies, H. M. L.; Morton, D. *ACS Cent. Sci.* **2017**, *3*, 936—943.

(6) Liu, W.; Groves, J. T. *Acc. Chem. Res.* **2015**, *48*, 1727—1735.

(7) Olivo, G.; Cussó, O.; Borrell, M.; Costas, M. *JBIC, J. Biol. Inorg. Chem.* **2017**, *22*, 425—452.

(8) Que, L.; Tolman, W. B. *Nature* **2008**, *455*, 333—340.

(9) Talsi, E. P.; Bryliakov, K. P. *Coord. Chem. Rev.* **2012**, *256*, 1418—1434.

(10) Brückl, T.; Baxter, R. D.; Ishihara, Y.; Baran, P. S. *Acc. Chem. Res.* **2012**, *45*, 826—839.

(11) Salamone, M.; Bietti, M. *Acc. Chem. Res.* **2015**, *48*, 2895—2903.

(12) Mack, J. B. C.; Gipson, J. D.; Du Bois, J.; Sigman, M. S. *J. Am. Chem. Soc.* **2017**, *139*, 9503—9506.

(13) Lee, M.; Sanford, M. S. *Org. Lett.* **2017**, *19*, 572—575.

(14) Howell, J. M.; Feng, K. B.; Clark, J. R.; Trzepkowski, L. J.; White, M. C. *J. Am. Chem. Soc.* **2015**, *137*, 14590—14593.

(15) Dantignana, V.; Milan, M.; Cussó, O.; Company, A.; Bietti, M.; Costas, M. *ACS Cent. Sci.* **2017**, *3*, 1350.

(16) Chen, M. S.; White, M. C. *Science* **2010**, *327*, 566—571.

(17) Milan, M.; Bietti, M.; Costas, M. *ACS Cent. Sci.* **2017**, *3*, 196—204.

(18) Milan, M.; Carboni, G.; Salamone, M.; Costas, M.; Bietti, M. *ACS Catal.* **2017**, *7*, 5903—5911.

(19) Pellissier, H. *Adv. Synth. Catal.* **2011**, *353*, 1613—1666.

(20) (a) Ottenbacher, R. V.; Talsi, E. P.; Bryliakov, K. P. *ACS Catal.* **2015**, *5*, 39—44. (b) Ottenbacher, R. V.; Samsonenko, D. G.; Talsi, E. P.; Bryliakov, K. P. *Org. Lett.* **2012**, *14*, 4310—4313.

(21) (a) Shen, D.; Miao, C.; Wang, S.; Xia, C.; Sun, W. *Org. Lett.* **2014**, *16*, 1108—1111. (b) Qiu, B.; Xu, D.; Sun, Q.; Miao, C.; Lee, Y.-M.; Li, X.-X.; Nam, W.; Sun, W. *ACS Catal.* **2018**, *8*, 2479—2487.

(22) Murphy, A.; Dubois, G.; Stack, T. D. P. *J. Am. Chem. Soc.* **2003**, *125*, 5250—5251.

(23) Salamone, M.; Ortega, V. B.; Bietti, M. *J. Org. Chem.* **2015**, *80*, 4710—4715.

(24) Chen, K.; Eschenmoser, A.; Baran, P. S. *Angew. Chem., Int. Ed.* **2009**, *48*, 9705—9708.

(25) Zou, L.; Paton, R. S.; Eschenmoser, A.; Newhouse, T. R.; Baran, P. S.; Houk, K. N. *J. Org. Chem.* **2013**, *78*, 4037—4048.

(26) Damm, W.; Giese, B.; Hartung, J.; Hasskerl, T.; Houk, K. N.; Hueter, O.; Zipse, H. *J. Am. Chem. Soc.* **1992**, *114*, 4067—4079.

(27) Salamone, M.; Martin, T.; Milan, M.; Costas, M.; Bietti, M. *J. Org. Chem.* **2017**, *82*, 13542—13549.

(28) Luo, Y.-R. *Comprehensive Handbook of Chemical Bond Energies*; CRC Press: Boca Raton, FL, 2001.

(29) Moteki, S. A.; Selvakumar, S.; Zhang, T.; Usui, A.; Maruoka, K. *Asian J. Org. Chem.* **2014**, *3*, 932—935.

(30) Moteki, S. A.; Usui, A.; Zhang, T.; Solorio Alvarado, C. R.; Maruoka, K. *Angew. Chem., Int. Ed.* **2013**, *52*, 8657—8660.

(31) Ravelli, D.; Fagnoni, M.; Fukuyama, T.; Nishikawa, T.; Ryu, I. *ACS Catal.* **2018**, *8*, 701—713.

(32) Ni, L.; Ni, J.; Lv, Y.; Yang, P.; Cao, Y. *Chem. Commun.* **2009**, 2171—2173.

(33) England, P. A.; Rouch, D. A.; Westlake, A. C. G.; Bell, S. G.; Nickerson, D. P.; Webberley, M.; Flitsch, S. L.; Wong, L.-L. *Chem. Commun.* **1996**, 357—358.

(34) Eliel, E. L.; Wilen, S. H.; Doyle, M. P. *Basic Organic Stereochemistry*; Wiley-Interscience: New York, 2001; p 203.

Chapter VI

Results and Discussion

VI.1. Tuning Selectivity in Aliphatic C–H Bond Oxidation of *N*-Alkylamides and Phthalimides Catalyzed by Manganese Complexes

Amines represent an especially important class of organic compounds, with this functional group being represented in a wide variety of natural products, bioactive molecules and organic materials. However, the tolerance of this group to metal-catalyzed oxidation reactions is particularly critical. Amines can be easily oxidized, and display moreover a strong tendency to bind and deactivate metal centers.[1] More importantly, C-H functionalization of amine containing substrates, when achieved, selectively occurs at the strongly activated C-H that is in α to the nitrogen atom center.[2-14] Remote aliphatic C-H bond oxidation of amines with iron and manganese catalysts was recently reported.[15-17] Remote oxidation was obtained through protonation of the amine, or formation of Lewis acid-base amine-BF_3 adducts that electronically deactivated the amine moiety and the C-H bonds that are adjacent to the nitrogen center. Along this line, amide functional groups are also very interesting because they can be used as protecting groups for primary and secondary amines, with the possibility to expand the structural elaboration of amine-containing targets. With secondary and tertiary amides oxidation occurs at the C-H bond that is α to nitrogen, giving the α-hydroxylated product, that can be rapidly converted into imides.[10]

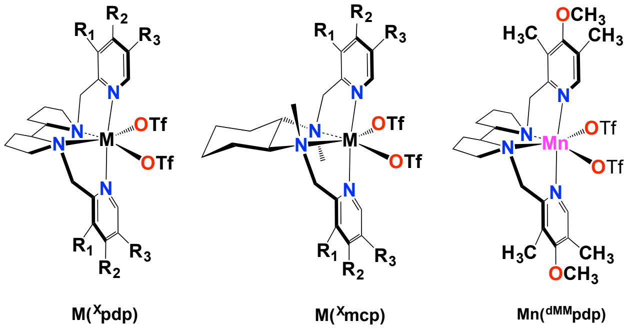

M^x	R_1	R_2	R_3
Fe(pdp)	-H	-H	-H
Mn(pdp)	-H	-H	-H
Fe(mcp)	-H	-H	-H
Mn(mcp)	-H	-H	-H
Fe(^{dMM}pdp)	-Me	-OMe	-Me
Mn(^{dMM}pdp)	-Me	-OMe	-Me
Mn(^{dMM}mcp)	-Me	-OMe	-Me
Mn(^{Cl}mcp)	-H	-Cl	-H
Fe(^{Me2N}pdp)	-H	-NMe_2	-H
Mn(^{Me2N}pdp)	-H	-NMe_2	-H
Fe(^{TIPS}mcp)	-H	-H	-Si(^{i}Pr)$_3$
Mn(^{TIPS}mcp)	-H	-H	-Si(^{i}Pr)$_3$
Mn(^{TIPS}pdp)	-H	-H	-Si(^{i}Pr)$_3$
Mn(^{BzIm}pdp)	-BzIm[a]		
Mn(^{CF3}mcp)	-H	-H	-Ph(CF_3)$_2$

Figure VI.1. Structures of the iron and manganese complexes studied. [a]*N*-methylbenzoimidazole instead of pyridine.

Our work has been focused on the development amide moieties as directing groups for selective C-H oxidation because their electronic and steric properties can be easily tuned. Reaction optimization was carried out on *N*-pentylpivalamide (**S1**) using different iron and manganese catalyst bearing tetradentate ligand of the general formula, $[M(CF_3SO_3)_2(L)]$ (L = mcp, pdp; mcp = *N,N*′-dimethyl *N,N*′-bis(2-pyridylmethyl)-1,2-*trans*-diaminocyclohexane, pdp = *N,N*′-bis(2-pyridylmethyl)-2,2′-bipyrrolidine); the structure for which is reported in Figure VI.1. The complexes present different electronic and steric features, bearing in some cases hindering groups in position 3 or 4 of the pyridine ring. Standard conditions for the reaction with manganese complexes involve syringe pump delivery of H_2O_2 (3.0 equiv) to a CH_3CN solution of the catalyst (1 mol %) and AcOH (13 equiv) at -40 ºC during 30 min. Standard conditions for the reaction with iron complexes involve syringe pump delivery of H_2O_2 (2.5 equiv) to a CH_3CN solution of the catalyst (3 mol %) and AcOH (1.5 equiv) at 0 ºC during 30 min. Results are reported in Table VI.1.

Table VI.1. Oxidation of *N*-pentylpivalamide (**S1**) with different catalysts.

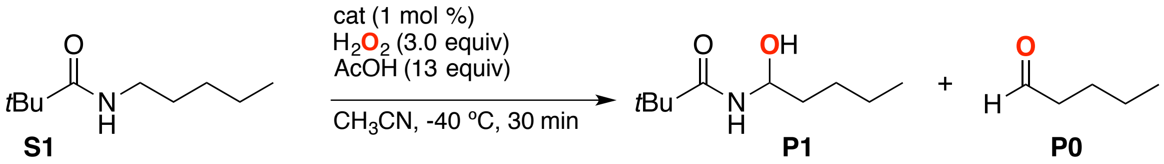

Entry	Catalysts	Conv %[a]	Yield P1 %[a]	Yield P0 %[a]
1	**Fe (pdp)**	< 2	-	-
2	**Mn (pdp)**	64	41	15
3	**Fe (mcp)**	10	-	-
4	**Mn (mcp)**	36	10	4
5	**Fe (^{dMM}pdp)**	15	6	5
6	**Mn (^{dMM}pdp)**	**99**	**60**	**11**
7	**Mn (^{dMM}mcp)**	97	42	10
8	**Mn (^{Cl}mcp)**	22	8	11
9	**Fe (^{Me2N}pdp)**	4	-	-
10	**Mn (^{Me2N}pdp)**	60	14	12
11	**Fe (^{TIPS}mcp)**	11	-	-
12	**Mn (^{TIPS}mcp)**	65	58	4
13	**Mn (^{TIPS}pdp)**	52	31	13
14	**Mn (^{BzIm}pdp)**	98	40	10
15	**Mn (^{CF3}mcp)**	63	15	12
16[b]	**Mn (^{dMM}pdp)**	60	45	12

[a]Conversions and yields determined from crude reaction mixtures by GC or ^{1}H NMR. [b]Cyclopropanecarboxylic acid was used instead of acetic acid.

We first explored the oxidation activity of the simpler catalysts of the series, **Fe(pdp)**, **Mn(pdp)**, **Fe(mcp)** and **Mn(mcp)** (Table VI.1., entries 1-4). The results reveal that only the manganese catalysts oxidize the substrate with the most efficient catalyst being represented by **Mn(pdp)**. Two oxidation products were obtained: α-hydroxyamide (**P1**) deriving from C-H bond hydroxylation α to nitrogen, together with a smaller amount of pentanal (**P0**) arising from oxidative C-N bond cleavage. Control experiments showed that pentanal does not derive from the oxidation of **P1** under the experimental conditions employed, suggesting formation through a different pathway.[18] No products deriving from C2-C5 oxidation were observed. The best yields (42% and 60%, Table VI.1., entries 6 and 7) were obtained when electron-donating methyl and methoxy groups (**Mn(^{dMM}pdp)** and **Mn(^{dMM}mcp)**) were introduced at pyridine position 3, 4 and 5 of the manganese complexes making the active species more electron rich. Electron poor catalyst such as **Mn(^{Cl}mcp)** gave instead lower amounts of oxidation products. **Mn(^{Me2N}pdp)** and **Mn(^{Me2N}mcp)** that have been shown to be excellent catalysts for epoxidation reactions,[19] did not work efficiently in C-H bond oxidation. Improvement in yield was obtained using manganese catalysts where bulky groups such as *tris*-(isopropyl)silyl (TIPS) were introduced on the pyridine ring (entries 12-13). In addition, the use of **Mn(^{CF3}mcp)** and **Mn(^{BzIm}mcp)** catalysts did not improve product yields. On the basis of this screening, **Mn(^{dMM}pdp)** was selected as the catalyst of choice for oxidation of the other substrates. Unfortunately, the α-hydroxyamide product (**P1**) is obtained as a racemic mixture (enantiomeric excess was determined after methylation of the hydroxyl group of **P1**).

The oxidation of a series of *N*-alkylamide and *N*-alkylphthalimide derivatives was then investigated, in order to evaluate the effect of substrate structure on the reaction site-selectivity. The oxidation products obtained with the *N*-pentyl derivatives **S1**-**S4** are reported in Scheme VI.1. The results show that replacement of the pivaloyl group does not affect site-selectivity. The decrease in the yield of product **PX** observed on going from **S1** to **S3** is in line with the electrophilic character of the active oxidant, indicating that the trifluoroacetyl groups deactivates the α-C-H bonds toward oxidation.

Scheme VI.1. Oxidation of different *N*-pentyl derivatives.

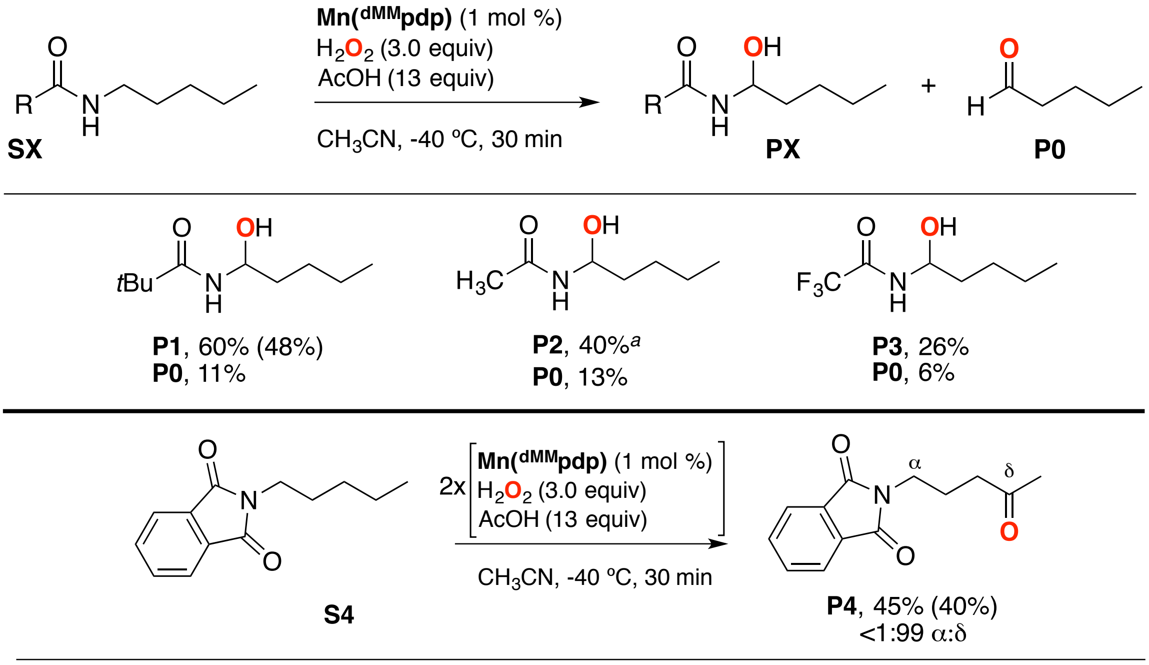

Yields determined from crude reaction mixtures by GC or ^{1}H NMR, isolated yields in parentheses. [a]In a larger scale catalysis experiment driven to complete substrate conversion, 36% yield of product **P2** and 36% yield of the overoxidized imide product were isolated together with pentanal (determined by GC) in 11% yield.

Very interestingly, the presence of the phthalimido moiety dramatically changed site selectivity, and only the γ-ketoamide product derived from remote C-H bond oxidation was detected. This behavior can be explained on the basis of the strong electron-withdrawing ability of the phthalimido group.

Moving to the oxidation of the *N*-2-(5-methylhexyl) derivatives, characterized by the presence of two tertiary C-H bonds (**S5-S8**, Scheme VI.2.), the hydroxyamide derived from δ-C-H oxidation (**P5**-**P8**) is the predominant product, isolated in moderate to high yield (up to 83% for **P8**). A second compound also appears as a minor product in the oxidation of substrates **S5-S7**. Formation of the latter product can be explained on the bases of α-C-H oxidation of the first-formed δ-hydroxyamide followed by cyclization. The increase of the amount of the cyclic product in the order **S7** < **S5** < **S6** reflects the contribution of steric and electronic effects.

Scheme VI.2. Oxidation of different *N*-2-(5-methylhexyl) derivatives.

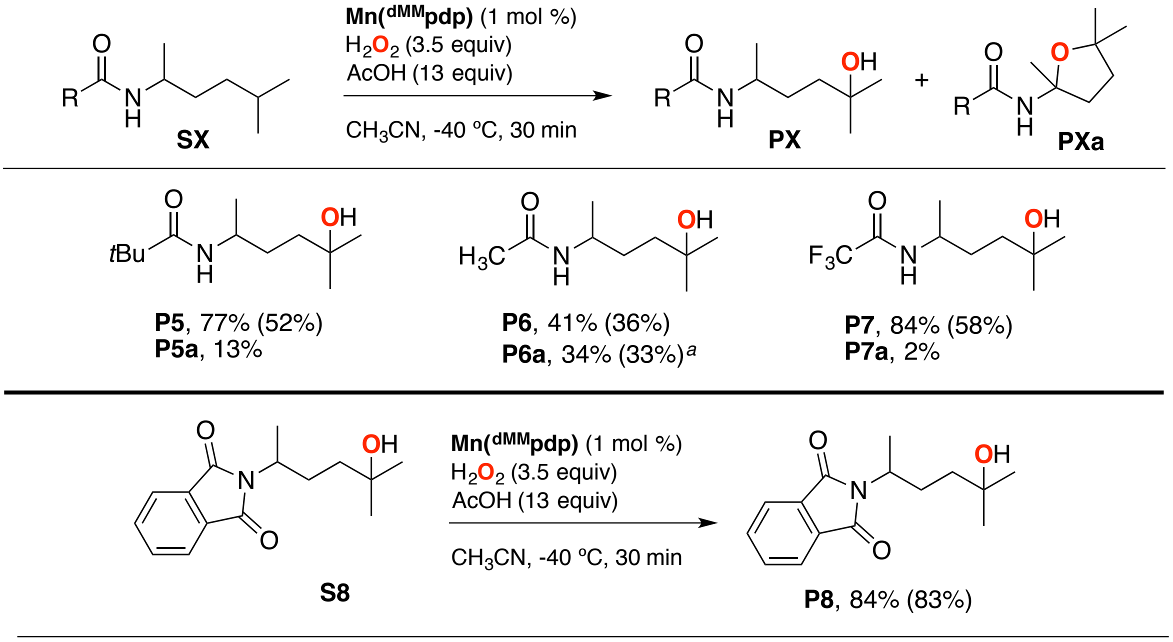
Mn(dMMpdp) (1 mol %)
H2O2 (3.5 equiv)
AcOH (13 equiv)
CH3CN, -40 ºC, 30 min
SX
PX
PXa
R
tBu
H3C
F3C
OH
S8
P5, 77% (52%)
P5a, 13%
P6, 41% (36%)
P6a, 34% (33%)a
P7, 84% (58%)
P7a, 2%
P8, 84% (83%)

Yields determined from crude reaction mixtures by GC or ^{1}H NMR, isolated yields in parentheses. [a]**P6a** was isolated with 11% yield of a non-identified impurity that could not be separated.

The lack of products derived from α-C-H oxidation can be explained on the basis of the operation of stereoelectronic effects. Taking into account recent time-resolved kinetic studies on HAT reactions from *N*-alkylamides to the cumyloxyl radical,[20] we propose that the introduction of a methyl group on the α-carbon increases the energy barrier required to reach the most suitable conformation for HAT, where the α-C-H bond is aligned with the amide π system (structure **A** in Scheme VI.3.).

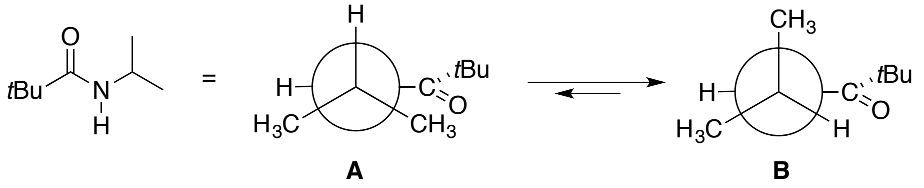
tBu
=
H
H3C
CH3
C
O
A
B

Scheme VI.3. Conformational equilibrium for rotation around the N-CH(CH$_3$)$_2$ bond in *N*-isopropylpivalamide.

Finally, we evaluated the oxidation of the *N*-1-(3-methylbutyl) derivatives. In this series of compounds, oxidation can occur from two different sites: the methylene group α to nitrogen and the remote tertiary γ-C-H bond. With the pivalamide (**S9**) and acetamide (**S10**) derivatives, the α-hydroxylated product was obtained in good isolated yield, accompanied by the formation of very low amounts of the product deriving from remote oxidation. This behavior can be explained on the basis of a stronger activation of the α-C-H bond as compared to the remote tertiary γ-C-H bond. The different proximal/remote ratios obtained for substrates **S9** and **S10** (4.7:1 and 33:1, respectively, normalized for the different number of hydrogens, Scheme VI.4.) reflects the steric hindrance of the *t*Bu group as compared to the methyl one. Very interestingly, the presence of an EWG group on the amide moiety led to a dramatic change in selectivity. With the trifluoroacetamide and phthalimide substrates, **S1** and **S12,** predominant or exclusive formation of the product derived from remote oxidation was obtained in moderate to good isolated yield and good to outstanding selectivity (1:22 and <1:99, for **S11** and **S12**, respectively).

Scheme VI.4. Oxidation of different *N*-1-(3-methylbutyl) derivatives**.**

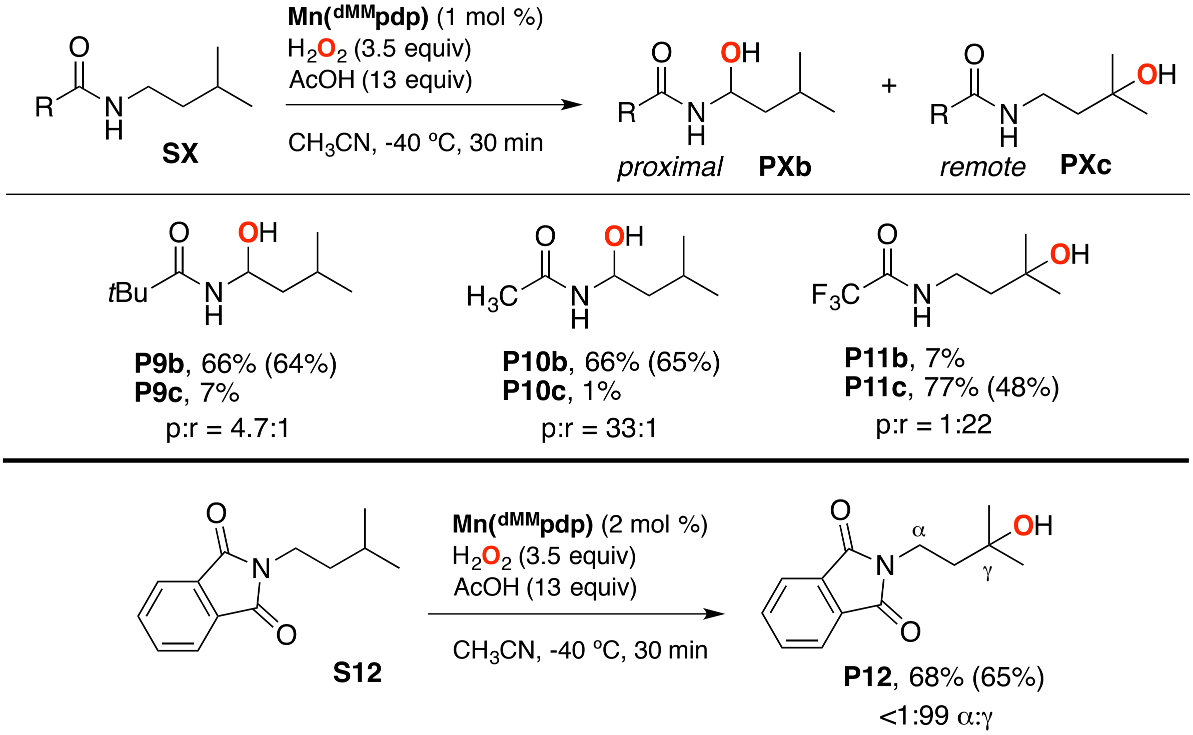
O
R
N
H
SX
Mn(dMMpdp) (1 mol %)
H2O2 (3.5 equiv)
AcOH (13 equiv)
CH3CN, -40 °C, 30 min
O
OH
R
N
H
proximal
PXb
+
O
R
N
H
OH
remote
PXc
O
OH
tBu
N
H
P9b, 66% (64%)
P9c, 7%
p:r = 4.7:1
O
OH
H3C
N
H
P10b, 66% (65%)
P10c, 1%
p:r = 33:1
O
F3C
N
H
OH
P11b, 7%
P11c, 77% (48%)
p:r = 1:22
O
N
O
S12
Mn(dMMpdp) (2 mol %)
H2O2 (3.5 equiv)
AcOH (13 equiv)
CH3CN, -40 °C, 30 min
O
N
O
α
γ
OH
P12, 68% (65%)
<1:99 α:γ

Yields determined from crude reaction mixtures by GC or ^{1}H NMR, isolated yields in parentheses.

Finally, the poor reactivity obtained with the iron complexes was further investigated (Scheme VI.5.). Oxidation of the amide substrates where oxidation takes place at the remote position occurred with improved yields (Scheme VI.5., entries 1 and 4). We hypothesized that the α-hydroxylated product may inhibit the catalyst through chelation via the carbonyl and the α-OH group. Following this hypothesis, no oxidation products were observed when substrate **S10** (50 equiv) and product **P10** (50 equiv) were submitted to oxidation in the presence of **Fe(pdp)**. Furthermore, the reaction mixture of the oxidation of substrates **S1**, **S9** and **S10** with **Fe(pdp)** turned intense purple-blue after addition of H_2O_2, suggesting the formation of an iron species that exhibits low-energy charge transfer transitions.[21-25]

Scheme VI.5. Oxidation reactions with **Fe(pdp)** complex.

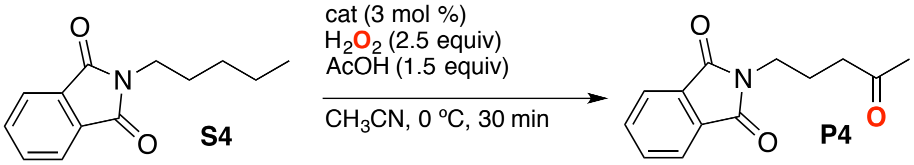
cat (3 mol %)
H2O2 (2.5 equiv)
AcOH (1.5 equiv)
CH3CN, 0 ºC, 30 min
S4
P4
O
N

Entry	Substrate	Conv (%)[a]	Yield (%)[a]
1	**S4**	10	8

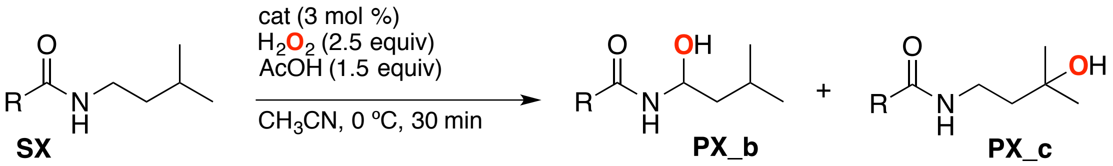
cat (3 mol %)
H2O2 (2.5 equiv)
AcOH (1.5 equiv)
CH3CN, 0 ºC, 30 min
R
N
H
O
OH
+
SX
PX_b
PX_c

Entry	Substrate	Conv (%)[a]	Yield (%)[a] PX_b	Yield (%)[a] PX_c
2	**S9**	<2	-	-
3	**S10**	<2	-	-
4	**S11**	55	11	36

[a]Conversions and yields determined from crude reaction mixtures by GC and ^{1}H-NMR.

High-resolution mass spectrometry monitoring of the reaction of **S10** with **Fe(pdp)** under standard conditions showed cluster ions at *m/z* 261.1294 that can be assigned to [**Fe(pdp)**(**S10**) + O-H]$^{2+}$ ions (Figure VI.2.).

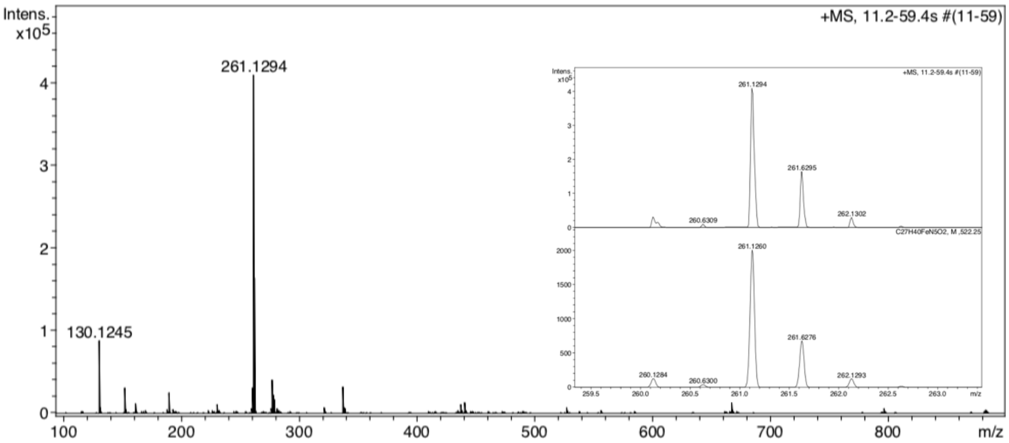

Figure VI.2. ESI-MS spectrum of [**Fe(pdp)**(**S10**)+O-H]$^{2+}$.The spectrum was obtained by adding a solution of H_2O_2 in CH_3CN (1.0 equiv) to an acetonitrile solution at 0 ºC of **S10** (1 equiv), **Fe(pdp)** (1 mol %) and AcOH (13 equiv). Sample was taken after 10 minutes of peroxide addition, and analyzed by high resolution mass spectroscopy (HRMS).

With these results in hand, we applied the reaction protocol to the oxidation of amide and phthalimide derivatives of more complex bioactive molecules characterized by the presence of primary amine functionalities, such as pregabalin (Lyrica) and antiviral drug rimantadine (Flumadine) (Scheme VI.6). Oxidation of the pivalamide derivative of pregabalin occurred preferentially at the more activated α position yielding amido γ-lactone (**P13_a**), while the amido δ-lactone (**P13_b**) resulting from the remote tertiary C-H bond was recovered in lower amount. When the pivaloyl moiety was replaced with the more electron-withdrawing phthalimido group only remote oxidation occurred (**P14**) in good yield (60%). On the other hand, the nature of the amine protecting group did not affect the site selectivity of rimantadine derivatives (**P15**, **P16** and **P17**).

Scheme VI.6. Oxidation of bioactive molecules.

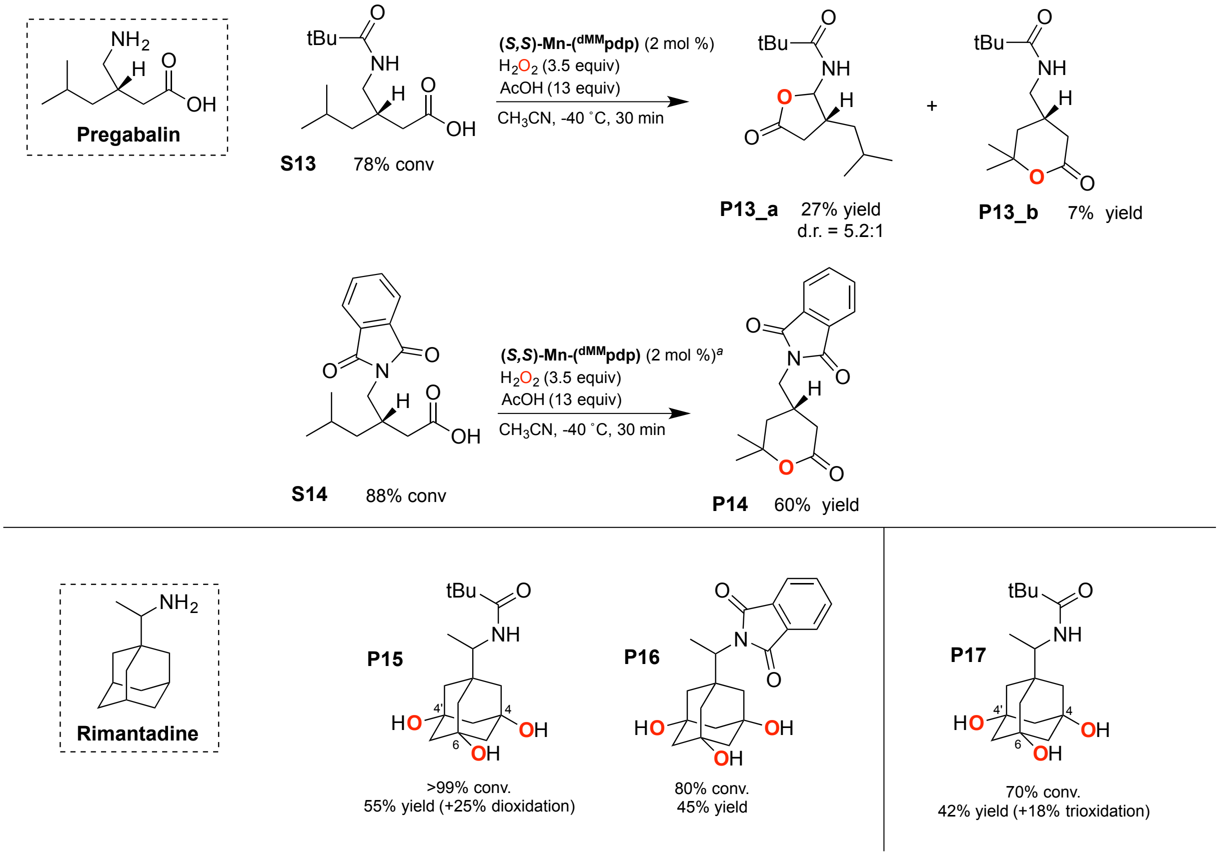

Pregabalin
S13 78% conv
(S,S)-Mn-(dMMpdp) (2 mol %)
H2O2 (3.5 equiv)
AcOH (13 equiv)
CH3CN, -40 °C, 30 min
P13_a 27% yield
d.r. = 5.2:1
+
P13_b 7% yield
S14 88% conv
(S,S)-Mn-(dMMpdp) (2 mol %)a
H2O2 (3.5 equiv)
AcOH (13 equiv)
CH3CN, -40 °C, 30 min
P14 60% yield
Rimantadine
P15
>99% conv.
55% yield (+25% dioxidation)
P16
80% conv.
45% yield
P17
70% conv.
42% yield (+18% trioxidation)

[a] Iterative addition (3x): cat (2 mol %), H_2O_2 (3.5 equiv), AcOH (13 equiv) in CH_3CN at -40 °C during 30 min. Isolated yields.

VI.2. Highly Enantioselective Oxidation of Nonactivated Aliphatic C–H Bonds with Hydrogen Peroxide Catalyzed by Manganese Complexes

As discussed in the introduction, examples of enantioselective sp^3 C-H oxidation with non-enzymatic systems are rare and limited to weak C-H bonds (benzylic, allylic and adjacent to heteroatom) commonly with low substrate conversion.[26-39] Moreover examples of enantioselective oxidation of nonactivated aliphatic C-H bonds remain exclusive to enzymes.[40-43] To achieve this challenging goal, we developed biologically inspired transition metal catalysts with sterically demanding tetradentate amino-pyridine ligands, that, in the presence of suitable oxidants, form high valent metal-oxo species. This approach was based in the fact that during the last decade this class of complexes have been applied successfully in asymmetric epoxidation[44-46] and *cis*-dihydroxylation.[47-48] Figure VI.3. displays the iron and manganese complexes employed in the oxidation reactions. Taking the pyridine characterized by the presence of bulky group like *tris*-(isopropyl)silyl (TIPS) on position 3 as the basic structural motif, we synthesized different manganese complexes modifying the mcp backbone, in particular the *N*-alkyl group (Figure VI.4.).

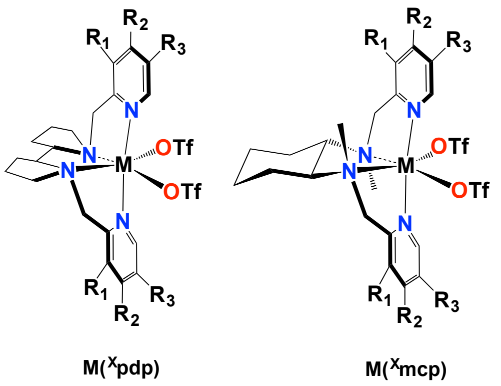

M^x	R$_1$	R$_2$	R$_3$
Fe(pdp)	-H	-H	-H
Mn(pdp)	-H	-H	-H
Fe(mcp)	-H	-H	-H
Mn(mcp)	-H	-H	-H
Mn(^{dMM}mcp)	-Me	-OMe	-Me
Mn(^{Cl}mcp)	-H	-Cl	-H
Mn(^{Me2N}pdp)	-H	-NMe$_2$	-H
Fe(^{TIPS}mcp)	-H	-H	-Si(^{i}Pr)$_3$
Mn(^{TIPS}mcp)	-H	-H	-Si(^{i}Pr)$_3$
Mn(^{TIPS}pdp)	-H	-H	-Si(^{i}Pr)$_3$
Mn(^{BzIm}pdp)	-BzIm^a		
Mn(^{CF3}mcp)	-H	-H	-Ph(CF$_3$)$_2$

Figure VI.3. Structures of the iron and manganese complexes studied. ^{a}Benzimidazole instead of pyridine.

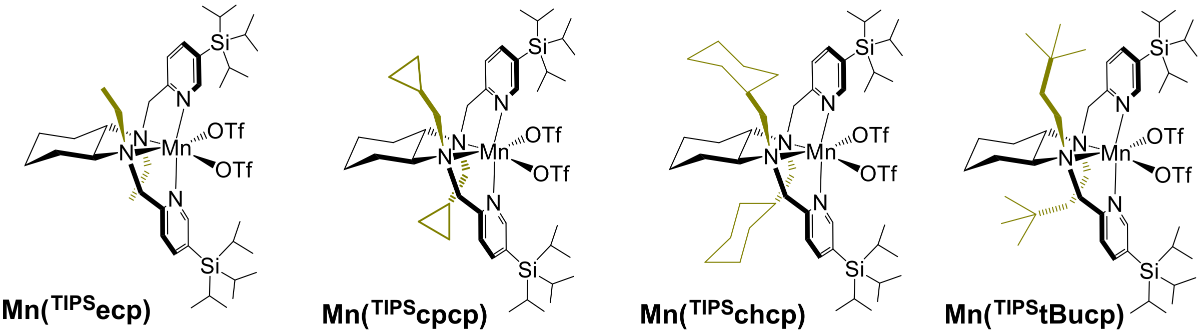

Figure VI.4. Structures of the manganese complexes studied changing the mcp backbone.

The screening of the different catalysts for the oxidation of *tert*-butylcyclohexane (**S1**) is shown in Table VI.2. Site-selectivity, quantified on the basis of the normalized product ratio (K_3/K_4) is also reported. Standard conditions involved syringe pump delivery of H_2O_2 (3.5 equiv) to a CH_3CN solution of the catalyst (1 mol %) and AcOH (17 equiv) at -40 ºC during 30 min. For all catalysts oxidation occurred preferentially at C3 over C4 methylene sites to produce the corresponding ketone products, formed via initial hydrogen atom transfer (HAT) mediated C-H hydroxylation, followed by fast oxidation of the resulting secondary alcohol.[49-51] Using the catalysts bearing unsubstituted pyridine rings, moderate to good yields and poor enantioselectivities were obtained (Table VI.2., entries 1-4). K_3/K_4 product ratios, comprised between 2.0 and 2.3, are in line with previously reported values.[50, 52-55] The best results were obtained introducing the bulky TIPS on the pyridine ring of the complex, in particular in the case of **Mn(^{TIPS}mcp)**, improving the level of enantioselectivity up to 44% ee (Table VI.2., entry 11). This behavior suggests that the steric demand imposed by the TIPS groups is at the basis of the improved enantioselectivity. Similar results have been obtained with **Mn(^{TIPS}ecp)**.

Table VI.2. Oxidation of *tert*-butylcyclohexane (**S1**) with different catalysts.

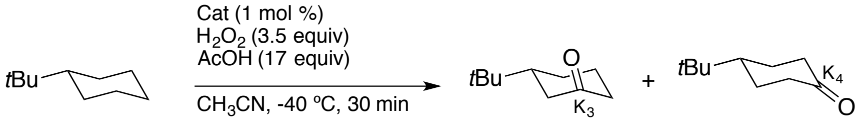

S1 **P1(K_3)** **P1(K_3)**

Entry	Cat	Conv (%)[a]	Yield (%)[a] K_3 (K_4)	K_3/K_4[b]	Ee (K_3) (%)
1[c]	**Fe(mcp)**	62	37 (9)	2.1	2
2[c]	**Fe(pdp)**	48	25 (6)	2.0	6
3	**Mn(mcp)**	46	32 (7)	2.3	9
4	**Mn(pdp)**	86	56 (13)	2.2	3
5[c]	**Fe(^{TIPS}mcp)**	73	61 (10)	3.1	33
6[c]	**Fe(^{TIPS}pdp)**	88	53 (17)	1.6	15
7	**Mn(^{Me2N}pdp)**	37	13 (3)	2.2	8
8	**Mn(^{dMM}pdp)**	93	50 (11)	2.3	8
9	**Mn(^{BzIm}pdp)**	79	50 (11)	2.3	11
10	**Mn(^{CF3}mcp)**	55	22 (5)	2.2	2
11	**Mn(^{TIPS}mcp)**	**77**	**53 (19)**	**1.4**	**44**
12	**Mn(^{TIPS}pdp)**	51	22 (7)	1.6	34
13[d]	**Mn(^{TIPS}ecp)**	**87**	**51 (15)**	**1.7**	**43**
14	**Mn(^{TIPS}cpcp)**	68	32 (12)	1.3	32
15	**Mn(^{TIPS}chcp)**	45	10 (6)	1.0	6
16	**Mn(^{TIPS}tBucp)**	48	8 (5)	1.0	Rac

[a] Conversions and yields determined from crude reaction mixtures by GC. Ee's determined by GC with chiral stationary phase. [b] Normalized ratio. [c] Reaction conditions: **Fe** catalyst (3 mol %), H_2O_2 (2.5 eq.), AcOH (1.5 eq.) in CH_3CN at 0 °C during 30 min. [d] **(*S,S'*)-Mn-(^{TIPS}ecp)** (2 mol %).

On the basis of these results, **Mn(^{TIPS}mcp)** was selected as the catalyst of choice for the oxidation of a series of monosubstituted cyclohexanes, in order to evaluate the effect of the substituent on the reaction yield, site-selectivity and enantioselectivity. When the *t*Bu is replaced by a pivalate group (**S2**) comparable yields and site-selectivity were observed (K_3/K_4 = 2.0, entry 2, Table VI.3.), and ee's increased up 54% ee. The use of **S3**, characterized by the presence of trimethylsilyl substituent, provides moderate yields and lower enantioselectivity (23% ee, entry 3, Table VI.3.). As compared to *tert*-butylcyclohexane (**S1**), with cyclohexanes bearing electron withdrawing substituents such as methyl cyclohexanecarboxylate (**S4**), cyclohexanecarboxylic acid (**S5**) and cyclohexyl methyl ketone (**S6**), a decrease in the K_3/K_4 ratio was observed, indicating that such substituents can strongly influence the interaction of the substrate with the electrophilic active oxidizing species. Interestingly, in the presence of an amide substituent, such as acetamido (**S7**), the reaction proceeded with excellent yield, strongly improved selectivity towards C3 (K_3/K_4 = 12) and good enantioselectivity (63% ee, entry 7). Furthermore, an exquisite site-selectivity (K_3/K_4 = 45) and very good enantioselectivity (76% ee) were observed on moving to an amide substrate characterized by a bulky acyl moiety such as *N*-cyclohexylpivalamide (**S8**, entry 9). These results suggest the occurrence of a strong interaction of these amide substrates with the manganese-oxo species, where the substrate Lewis basicity plays a role in providing the optimal substrate orientation for site-selective and enantioselective C-H oxidation. The enantioselectivity was further improved by using **Mn(^{TIPS}ecp)** as catalyst (entries 8 and 11, for **S7** and **S8**, respectively).

Table VI.3. Oxidation of different cyclohexane derivatives.

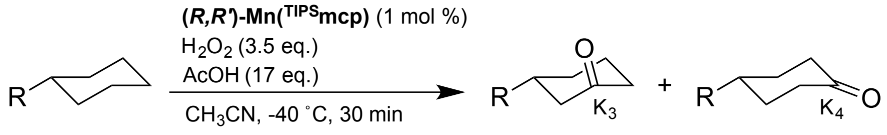

Entry	R	Conv (%)[a]	Yield (%)[a] K_3 (K_4)	K_3/K_4[b]	Ee (K_3) (%)
1	-*t*-Bu (**S1**)	77	53 (19)	1.4	44
2	-OPiv (**S2**)	80	41 (10)	2.0	54
3	-Si(Me)$_3$ (**S3**)	95	42 (13)	1.6	23
4[c]	-CO_2CH_3 (**S4**)	88	47 (20)	1.2	11
5	-CO_2H (**S5**)	45	20 (11)	0.9	9[e]
6[c]	-$COCH_3$ (**S6**)	95	47 (19)	1.2	8
7	-$NHCOCH_3$ (**S7**)	93	74 (3)	12	(+)63[f]
8[c]	-$NHCOCH_3$ (**S7**)	94	75 (3)	12	(-)78
9	-NHCO*t*Bu (**S8**)	**>99**	**90 (1)**	**45**	**(+)76**
10[d]	-NHCO*t*Bu (**S8**)	**>99**	**90 (1)**	**45**	**(-)76**
11[c]	-NHCO*t*Bu (**S8**)	**>99**	**90 (1)**	**45**	**(-)85**

[a] Conversions and yields determined from crude reaction mixtures by GC or ^{1}H-NMR. [b] Normalized ratio. [c] **(*S,S*)-Mn-(^{TIPS}ecp)** (2 mol %). [d] **(*S,S*)-Mn-(^{TIPS}mcp)**. [e] Ee's determined after esterification of isolated products. [f] Absolute configuration was determined on the basis of the crystal structure of the product obtained from **S10** (see Digital Supporting Info) and optical rotation (see Experimental Section). Ee's determined by GC with chiral stationary phase.

We also carried out the screening of different carboxylic acids, to obtain information on the impact of acid structure on the reaction stereoselectivity, using *N*-cyclohexylpivalamide (**S8**) as the substrate and **Mn(^{tips}mcp)** as catalyst (Scheme VI.7.). With the exclusion of 2-chloroethanoic acid, cyclohexanecarboxylic acid and acids containing long alkyl chains, comparable ee's between 73% and 81% were obtained. The lower enantioselectivity observed with 2-chloroethanoic acid (55% ee), presumably reflects a weaker interaction of the acid to the metal center due to the electron withdrawing character of the chlorine substituent. The lack of or very low conversion obtained in the last three examples reported in Scheme VI.7., can be explained in terms of a favorable competition with the substrate for the oxidizing species, as show above in Table VI.3., entry 5, for the case of cyclohexanecarboxylic acid, that is oxidized under the experimental conditions.[56] To explore matching-mismatching effects between the chirality of the catalyst and carboxylic acid, (*S*)-(+)-2-methylbutanoic acid was also studied. The combination of this acid with **(*R,R*)-Mn(^{tips}mcp)** and **(*S,S*)-Mn(^{tips}mcp)** provided similar ee's but decreased product yields. More interestingly, by using **Mn(^{tips}ecp)** as catalyst in combination with acetic, propanoic or cyclopropanecarboxylic acid a substantial increase in enantioselectivity was observed (85-90% ee), while retaining the excellent yield. The rigid cyclopropanecarboxylic acid provides the best results (90% yield, 90% ee). Considering that high valent species [Mn(O)(O_2CR)] are likely the C-H cleaving agents (see below), we can speculate that the combination of the rigidity of this acid and the highly structured and sterically demanding cavity of the **Mn(^{tips}ecp)** catalyst can create a robust oxidation site capable of carrying out highly enantioselective oxidation of the strong aliphatic C-H bond of nonactivated methylene groups.

Scheme VI.7. C-H oxidation reactions using different carboxylic acids and *N*-cyclohexylpivalamide (**S8**).

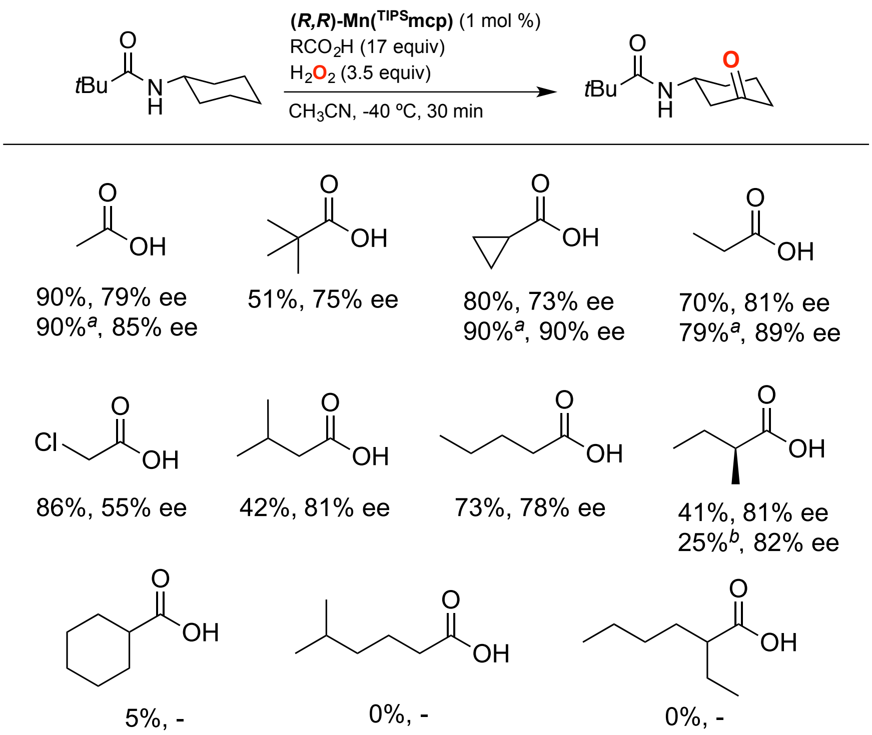

Yields determined by GC analysis. [a]**(*S,S*)-Mn($^{\text{TIPS}}$ecp)** (2 mol %). [b]**(*S,S*)-Mn($^{\text{TIPS}}$mcp)**. Ee's determined by chiral GC. K_4 yield is in all the cases <1%.

Finally, we explored the role of the structure and electronic properties of the amide substrate on the site-selectivity and enantioselectivity of the reaction (Scheme VI.8.). Excellent isolated yields and outstanding ee's (up to 96%) have been obtained (**P11**, Scheme VI.8.). The use of an amide substrate that bears a chiral center (**S14**) does not lead to any improvement in enantioselectivity, however the ee's obtained with both **(*S,S*)-Mn($^{\text{TIPS}}$ecp)** and **(*R,R*)-Mn($^{\text{TIPS}}$ecp)** are excellent (91% and 86% ee, respectively). Increasing the electron withdrawing ability of the amide group (**S16**-**S19**, Scheme VI.8.) led to a decrease in the K_3/K_4 product ratio due to the electronic deactivation of the proximal C3 position (with *N*-cyclohexyltrifluoroacetamide and *N*-cyclohexylphthalimide: K_3/K_4 = 2 and 0.8 respectively, Scheme VI.8.). A decrease in enantioselectivity was also observed with these two substrates (65 and 62% ee, respectively). Interestingly, oxidation of a racemic mixture of **S21** (Scheme VI.8.), results in a chiral resolution, giving product K_3 in 39% isolated yield and 55% ee, accompanied by recovery of the enantiomerically enriched (38% ee) starting substrate. Unfortunately, a decrease in isolated yield and enantioselectivity was observed by using *N*-cyclopentyl derivative **P22** as substrate (Scheme VI.8.), highlighting the sensitivity of the reactions to the ring size.

Scheme VI.8. Impact of the structure of the acyl moiety in site-selective and enantioselective C-H oxidation of *N*-cyclohexyl amides with **(*S,S'*)-Mn(^{TIPS}ecp)** as catalyst.

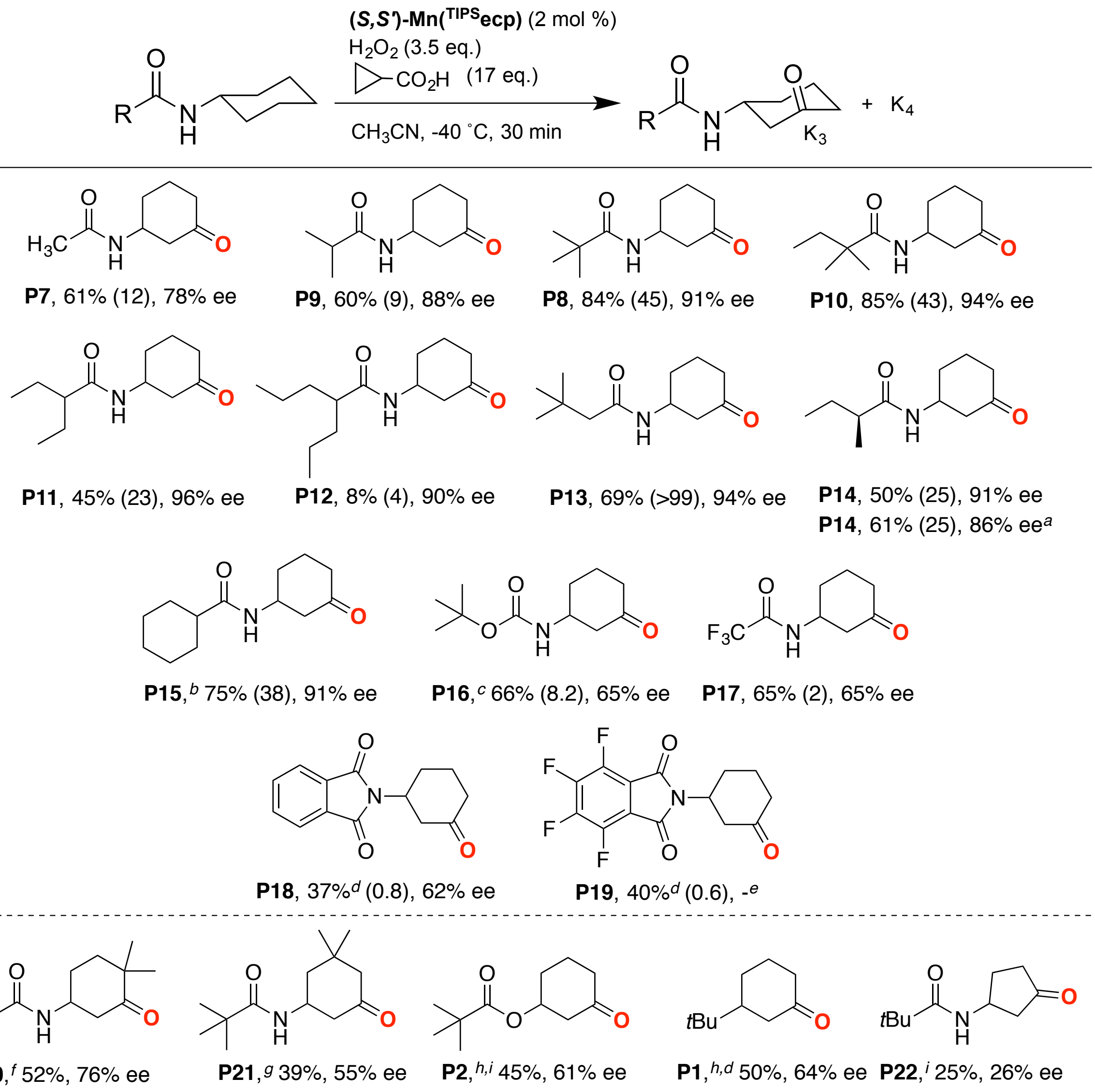
(S,S')-Mn(TIPSecp) (2 mol %)
H2O2 (3.5 eq.)
CO2H (17 eq.)
CH3CN, -40 ˚C, 30 min
R
N
H
O
K3
+ K4
H3C
F3C
F
tBu
P7, 61% (12), 78% ee
P9, 60% (9), 88% ee
P8, 84% (45), 91% ee
P10, 85% (43), 94% ee
P11, 45% (23), 96% ee
P12, 8% (4), 90% ee
P13, 69% (>99), 94% ee
P14, 50% (25), 91% ee
P14, 61% (25), 86% ee[a]
P15,[b] 75% (38), 91% ee
P16,[c] 66% (8.2), 65% ee
P17, 65% (2), 65% ee
P18, 37%[d] (0.8), 62% ee
P19, 40%[d] (0.6), -[e]
P20,[f] 52%, 76% ee
P21,[g] 39%, 55% ee
P2,[h,i] 45%, 61% ee
P1,[h,d] 50%, 64% ee
P22,[i] 25%, 26% ee

Isolated yields and normalized ratio (K_3/K_4) in parentheses. [a]**(*R,R*)-Mn(^{TIPS}ecp)**. [b]Acetic acid (17 eq.) instead of cyclopropanecarboxylic acid. [c]Yield determined by GC. [d]Products isolated as mixture of (K_3+K_4). [e]Ee not determined. [f]**(*S,S*)-Mn(^{TIPS}ecp)** (2 mol %). [g]**(*S,S*)-Mn(^{TIPS}mcp)**. [g]**(*S,S*)-Mn(^{TIPS}ecp)** and acetic acid. [h]**(*R,R*)-Mn-(^{TIPS}mcp)** and cyclopropanecarboxylic acid. [i]**(*R,R*)-Mn-(^{TIPS}mcp)** and acetic acid. Ee's determined by chiral GC and HPLC.

VI.3. Aliphatic C–H Bond Oxidation with Hydrogen Peroxide Catalyzed by Manganese Complexes: Directing Selectivity through Torsional Effects

In this work, it was explored the site selective and enantioselective oxidation of a series of *N*-cyclohexyl amides and diamides catalyzed by manganese complexes, taking into account the influence of electronic, steric, stereoelectronic and torsional effects, highlighting in particular the role of this latter effect. The chiral complexes used in this work, namely **Mn(pdp)**, **Mn(^{TIPS}mcp)** and **Mn(^{TIPS}ecp)** are displayed in Figure VI.5. The oxidation of *cis* and *trans* diamides derived from 1,2-, 1,3- and 1,4-cyclohexanediamides was initially studied in order to evaluate the effect of substrate structure on selectivity (Scheme VI.9.).

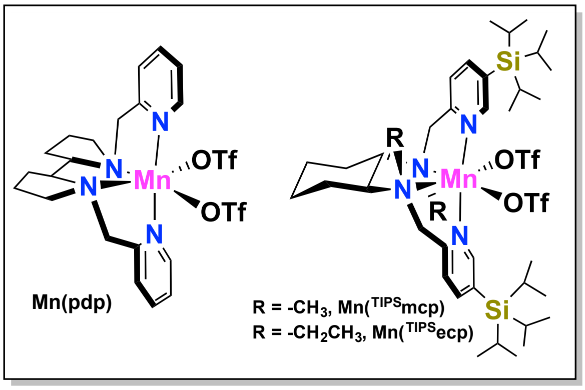

Figure VI.5. Structures of the catalysts used.

Results of previous studies on HAT-based functionalization of cyclohexane derivatives,[57-58] have shown that tertiary equatorial C-H bonds are activated toward abstraction, while tertiary axial C-H bonds are deactivated. This behavior has been rationalized in terms of torsional effects associated to the planarization of an incipient carbon radical in the HAT transition state. The activation of tertiary equatorial C-H bonds is a well-known concept that has been explained on the basis of a release of 1,3-diaxial strain in the HAT transition state as reported in Figure VI.6.**A**.[57, 59] The concept of tertiary axial C-H bond deactivation has been instead rationalized in terms of an increase in torsional strain in the HAT transition state where the substituent is forced toward an eclipsed interaction with the equatorial C-H bonds on the adjacent positions (Figure VI.6.**B**).[57, 60] Such deactivation depends on the steric hindrance of the substituent and also extends to the adjacent secondary positions, where planarization associated to HAT from this position forces the remaining C-H bond toward an eclipsed interaction with the substituent (Figure VI.6.**C**).

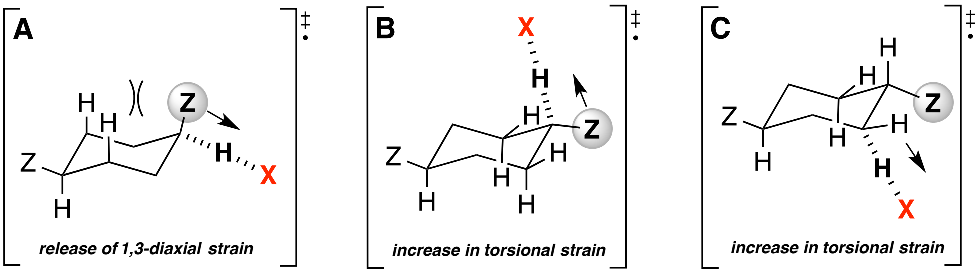
A
H
H
Z
Z
H
X
H
release of 1,3-diaxial strain
B
X
H
H
Z
Z
H
H
H
H
increase in torsional strain
C
H
H
Z
Z
H
H
H
H
X
increase in torsional strain
‡

Figure VI.6. Transition structures for HAT from tertiary equatorial and axial C-H bonds of disubstituted cyclohexanes to a generic HAT reagent X$^•$.

Standard conditions involved syringe pump delivery of H_2O_2 (2.0-4.5 equiv) to a CH_3CN solution of the catalyst **Mn(pdp)** or **Mn(^{TIPS}mcp)** (1-3 mol %) and AcOH (17 equiv) at -40 ºC during 30 min. Starting from the pivaldiamides derived from *cis*- and *trans*-1,4-cyclohexanediamine (Scheme VI.14., *cis*-**3** and *trans*-**3**, respectively), oxidation of *cis*-**3** led to the formation of *N*-(4-oxocyclohexyl)pivalamide (**3a**) (63% conversion, 51% yield, Scheme VI.9., **a**) as the exclusive oxidation product. Formation of **3a** can be rationalized by considering an initial tertiary equatorial C-H bond hydroxylation via HAT from this bond to a high valent manganese-oxo species, followed by a hydroxyl rebound to give an α-hydroxo-amide product, that then undergoes hydrolytic cleavage. In contrast, no reaction was observed for *trans*-**3** that was instead quantitatively recovered from the reaction mixture pointing toward a low reactivity of both the tertiary axial and secondary C-H bonds of this substrate.

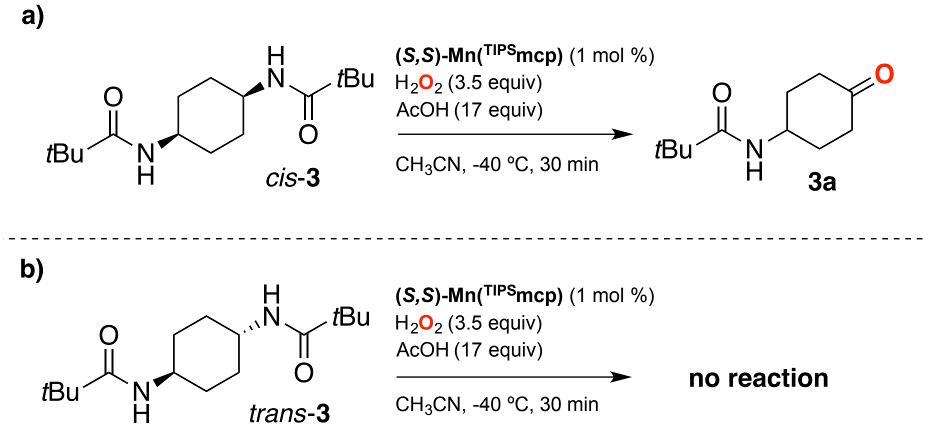
a)
tBu
O
N
H
H
N
tBu
O
cis-3
(S,S)-Mn(TIPSmcp) (1 mol %)
H2O2 (3.5 equiv)
AcOH (17 equiv)
CH3CN, -40 ºC, 30 min
O
tBu
N
H
O
3a
b)
tBu
O
N
H
H
N
tBu
O
trans-3
(S,S)-Mn(TIPSmcp) (1 mol %)
H2O2 (3.5 equiv)
AcOH (17 equiv)
CH3CN, -40 ºC, 30 min
no reaction

Scheme VI.9. Oxidation of *cis* and *trans* 1,2-cyclohexanediamides.

We then analyzed the oxidation of 1,2- and 1,3-cyclohexanediamides following analogous procedures (Scheme VI.10.). Oxidation of the pivaldiamide derived from *trans*-1,3-cyclohexanediamine (*trans*-**2**), led to the formation of *N*-(3-oxocyclohexyl) pivalamide (**2a**) as the exclusive oxidation product in 61% isolated yield, following HAT from the tertiary equatorial C-H bond. The corresponding *cis* isomer (*cis*-**2**) and the pivaldiamide derived from *trans*-1,2-cyclohexanediamine (*trans*-**1**), characterized by the presence of two tertiary axial C-H bonds, were also unreactive, in line with the results discussed above on the oxidation of *trans*-**3**. Oxidation of the pivaldiamide derived from *cis*-1,2-cyclohexanediamine, *cis*-**1**, took place selectively at position 4 and not at the tertiary equatorial C-H bond, providing **1a** in 74% isolated yield and 80:20 enantiomeric ratio (er). The lack of reaction at the tertiary position can be again rationalized in terms of an increase in torsional strain in the HAT transition state, where planarization of an incipient tertiary radical would force the two bulky pivalamido groups toward an unfavorable eclipsed interaction. The lack of reactivity of *trans*-**1**, *cis*-**2** and *trans*-**3**, deserves special consideration. It has been observed that while oxidation of *N*-cyclohexylpivalamide catalyzed by **Mn(^{TIPS}mcp)** led to the formation of *N*-(3-oxocyclohexyl)pivalamide in 84% isolated yield (see above, Scheme VI.10.),[61] only small amounts of this product were observed when *N*-cyclohexylpivalamide was oxidized in the presence of an equimolar amount of *trans*-**1**, *cis*-**2** or *trans*-**3** (Scheme VI.10.). On the basis of these results, it seems reasonable to propose that these substrates can inhibit the oxidizing ability of the manganese catalyst, probably through chelation of the metal by the two amide groups (see Experimental Section for additional information).

Scheme VI.10. Oxidation reactions of cyclohexane-derived pivaldiamides.

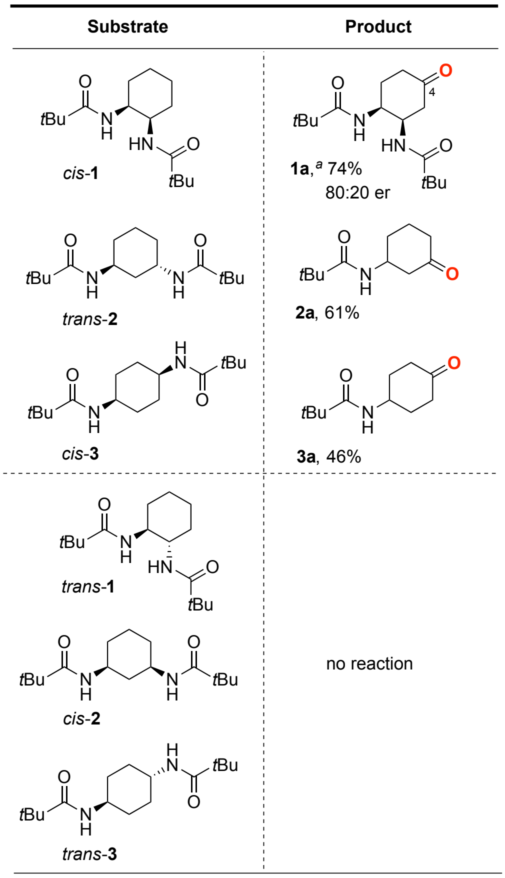

[a]Iterative addition (2x): cat. (1 mol %), H_2O_2 (4.5 equiv). Isolated yields.

The results displayed in Scheme VI.10. suggest that resolution of *cis* and *trans* couples of *N*-cyclohexylamide derivatives bearing a substituent at C4 may be possible on the basis of their distinct reactivity patterns in Mn-catalyzed C-H oxidation. For this purpose, a series of *cis*-*trans* mixtures of 4-X-substituted *N*-cyclohexylamides (X = Et, Pr, *i*Pr, *t*Bu, CF_3) were oxidized under standard conditions. As mentioned above, the *cis* isomers are converted to the 4-X-substituted cyclohexanone product and the valuable *trans* isomers are recovered in good to excellent yield (66-96%, Scheme VI.11.).

Scheme VI.11. Oxidation Reactions of *cis:trans* mixtures of 4-X substituted *N*-cyclohexyl amides.

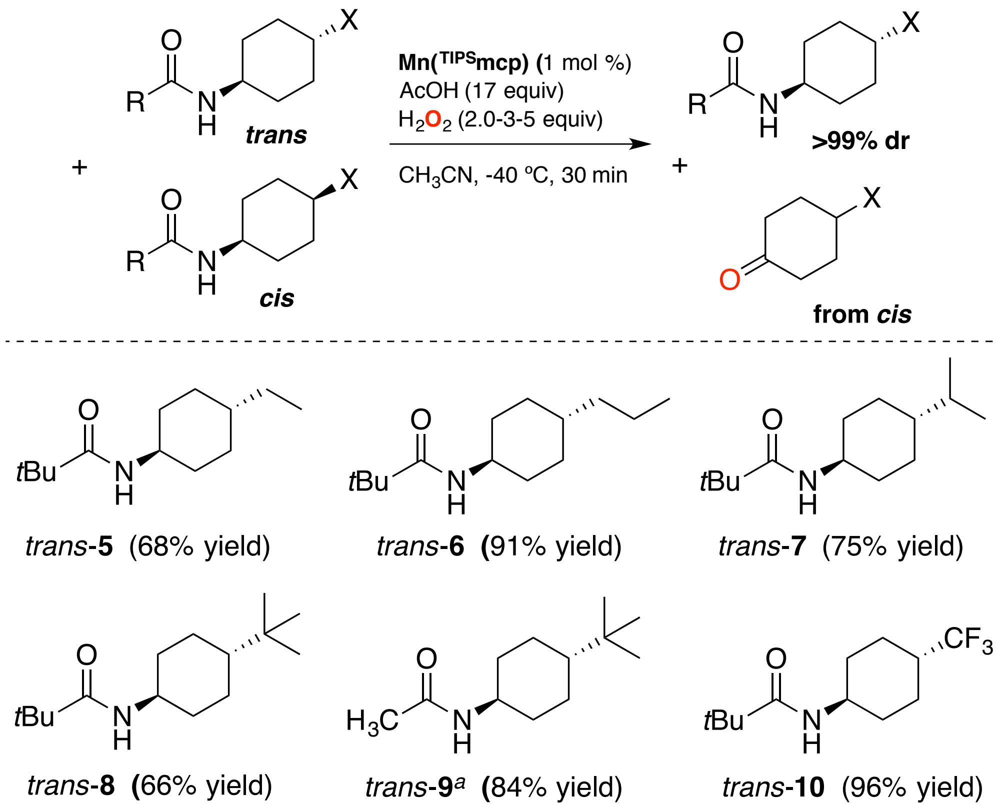
trans
cis
Mn(TIPSmcp) (1 mol %)
AcOH (17 equiv)
H2O2 (2.0-3-5 equiv)
CH3CN, -40 °C, 30 min
>99% dr
from cis
trans-5 (68% yield)
trans-6 (91% yield)
trans-7 (75% yield)
trans-8 (66% yield)
trans-9a (84% yield)
trans-10 (96% yield)

[a] **(*S,S*)-Mn(^{TIPS}ecp)** and cyclopropanecarboxylic acid. Isolated yields.

We also observed that substituents at C4 of a cyclohexane ring can have a profound effect on the reaction selectivity (Scheme VI.12.). The presence of a methyl, ethyl or propyl group provides good isolated yields of the ketone product deriving from oxidation at C3 and remarkable enantioselectivity (**4a** (78% yield, 89:11 er), **5a** (65% yield, 93:7 er) and **6a** (42% yield, 95:5 er), respectively). Oxidation of the tertiary axial C-H bond at the remote position **4b** is only observed as a minor product (14%) for X = methyl, indicating that with this substrate tertiary C-H bond activation determined by the substituent competes with deactivating torsional effects. In the presence of ethyl and propyl groups at C4, very small amounts of products deriving from oxidation at the secondary exocyclic C-H bonds were also observed

(**5b** and **6b**, 13% and 4% yield, respectively). The presence of an isopropyl group at C4 results in a change in site-selectivity, with C-H bond oxidation that now takes place preferentially at the most activated tertiary isopropyl C-H bond to give product **7a** in 45% yield, accompanied by a lower amount of product **7b** (14% yield) resulting from oxidation at C3. More interestingly, the presence of the bulky *tert*-butyl group at C4, drastically changed the site-selectivity, deactivating the C-H bonds at C3 and directing oxidation at C2. The product was obtained in good isolated yield and er both for the pivalamide and acetamide derivatives (**8a** and **9a**). Furthermore, the presence of the electron withdrawing trifluoromethyl group also directs oxidation towards C2 position, presumably by electronic deactivation of the proximal position (C3), providing the corresponding product **10a** with modest yield and er (17% yield, 70:30 er).

Scheme VI.12. Enantioselective oxidation of *trans*-4-X substituted *N*-cyclohexyl amides.

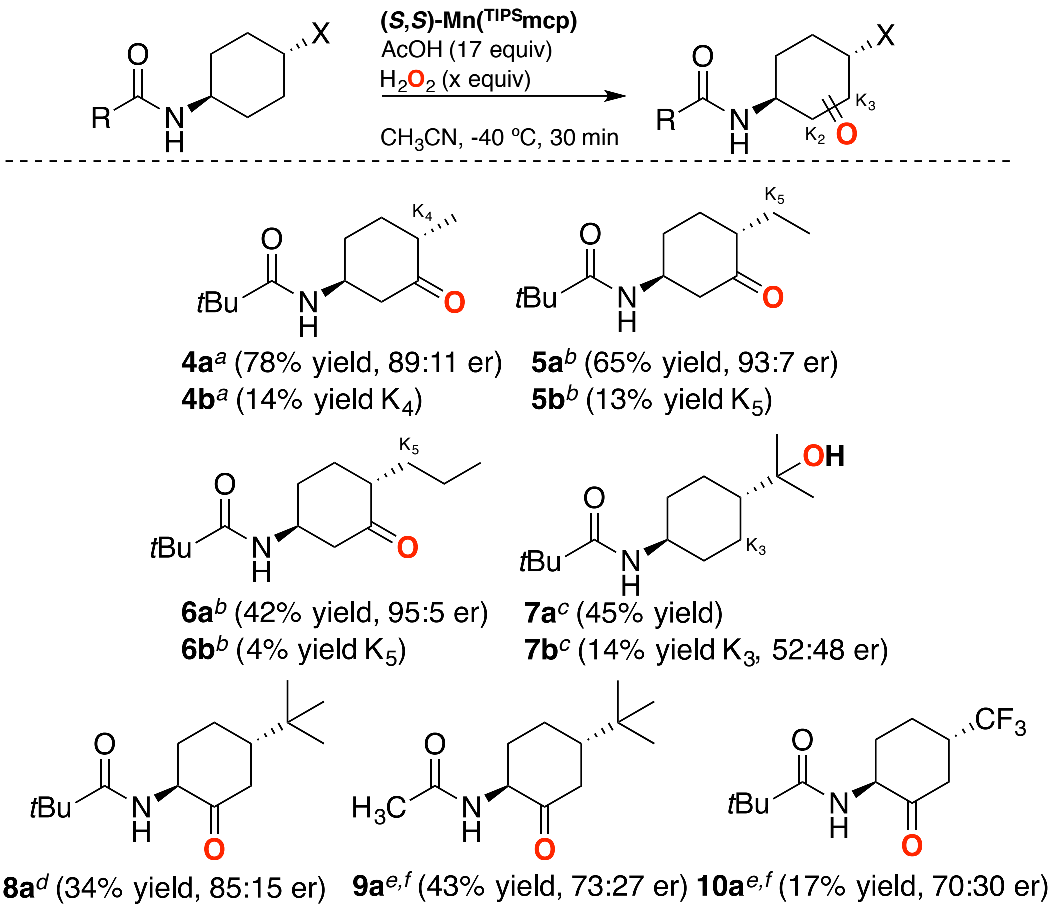
(S,S)-Mn(TIPSmcp)
AcOH (17 equiv)
H2O2 (x equiv)
CH3CN, -40 ºC, 30 min
R
O
N
H
X
K3
K2
K4
K5
tBu
OH
CF3
H3C
4a^a (78% yield, 89:11 er)
4b^a (14% yield K4)
5a^b (65% yield, 93:7 er)
5b^b (13% yield K5)
6a^b (42% yield, 95:5 er)
6b^b (4% yield K5)
7a^c (45% yield)
7b^c (14% yield K3, 52:48 er)
8a^d (34% yield, 85:15 er)
9a^e,f (43% yield, 73:27 er)
10a^e,f (17% yield, 70:30 er)

[a] Iterative addition (2x): cat. (1 mol %), H_2O_2 (3.5 equiv). [b] cat. (3 mol %), H_2O_2 (3.5 equiv). [c] cat. (3 mol %), H_2O_2 (3.5 equiv). [d] **(*S,S*)-Mn(pdp)** (1 mol %), H_2O_2 (4.5 equiv). [e] Iterative addition (3x): cat. (1 mol %), H_2O_2 (3.5 equiv). [f] Yield determined by ^{1}H-NMR analysis. Er's determined by GC with chiral stationary phase.

VI.4. References

1. Topczewski, J. J.; Cabrera, P. J.; Saper, N. I.; Sanford, M. S., *Nature* **2016,** *531*, 220-224.
2. Khusnutdinova, J. R.; Ben-David, Y.; Milstein, D., *J. Am. Chem. Soc.* **2014,** *136*, 2998-3001.
3. Legacy, C. J.; Wang, A.; O'Day, B. J.; Emmert, M. H., *Angew. Chem. Int. Ed.* **2015,** *54*, 14907-14910.
4. Wu, X.-F.; Bheeter, C. B.; Neumann, H.; Dixneuf, P. H.; Beller, M., *Chem. Comm.* **2012,** *48*, 12237-12239.
5. Xu, W.; Jiang, Y.; Fu, H., *Synlett* **2012,** *23*, 801-804.
6. Preedasuriyachai, P.; Chavasiri, W.; Sakurai, H., *Synlett* **2011,** *2011*, 1121-1124.
7. Kim, J. W.; Yamaguchi, K.; Mizuno, N., *Angew. Chem. Int. Ed.* **2008,** *47*, 9249-9251.
8. Klobukowski, E. R.; Mueller, M. L.; Angelici, R. J.; Woo, L. K., *ACS Catal.* **2011,** *1*, 703-708.
9. Genovino, J.; Lütz, S.; Sames, D.; Touré, B. B., *J. Am. Chem. Soc.* **2013,** *135*, 12346-12352.
10. Liu, P.; Liu, Y.; Wong, E. L.-M.; Xiang, S.; Che, C.-M., *Chem. Sci.* **2011,** *2*, 2187-2195.
11. Murahashi, S.; Naota, T.; Yonemura, K., *J. Am. Chem. Soc.* **1988,** *110*, 8256-8258.
12. Mitchell, E. A.; Peschiulli, A.; Lefevre, N.; Meerpoel, L.; Maes, B. U. W., *Chem. Eur. J.* **2012,** *18*, 10092-10142.
13. Griffiths, R. J.; Burley, G. A.; Talbot, E. P. A., *Org. Lett.* **2017,** *19*, 870-873.
14. Milan, M.; Salamone, M.; Bietti, M., *J. Org. Chem.* **2014,** *79*, 5710-5716.
15. Lee, M.; Sanford, M. S., *J. Am. Chem. Soc.* **2015,** *137*, 12796-12799.
16. Howell, J. M.; Feng, K. B.; Clark, J. R.; Trzepkowski, L. J.; White, M. C., *J. Am. Chem. Soc.* **2015,** *137*, 14590-14593.
17. Mbofana, C. T.; Chong, E.; Lawniczak, J.; Sanford, M. S., *Org. Lett.* **2016,** *18*, 4258-4261.
18. Hull, J. F.; Balcells, D.; Sauer, E. L. O.; Raynaud, C.; Brudvig, G. W.; Crabtree, R. H.; Eisenstein, O., *J. Am. Chem. Soc.* **2010,** *132*, 7605.
19. Cussó, O.; Garcia-Bosch, I.; Font, D.; Ribas, X.; Lloret-Fillol, J.; Costas, M., *Org. Lett.* **2013,** *15*, 6158-6161.
20. Salamone, M.; Basili, F.; Mele, R.; Cianfanelli, M.; Bietti, M., *Org. Lett.* **2014,** *16*, 6444-6447.
21. Cox, D. D.; Que, L., Jr., *J. Am. Chem. Soc.* **1988,** *110*, 8085-8092.
22. Jensen, M. P.; Lange, S. J.; Mehn, M. P.; Que, E. L.; Que, L., Jr., *J. Am. Chem. Soc.* **2003,** *125*, 2113-2128.
23. Solomon, E. I.; Brunold, T. C.; Davis, M. I.; Kemsley, J. N.; Lee, S.-K.; Lehnert, N.; Neese, F.; Skulan, A. J.; Yang, Y.-S.; Zhou, J., *Chem. Rev.* **2000,** *100*, 235-349.
24. Makhlynets, O. V.; Rybak-Akimova, E. V., *Chem. Eur. J.* **2010,** *16*, 13995-14006.
25. Serrano-Plana, J.; Oloo, W. N.; Acosta-Rueda, L.; Meier, K. K.; Verdejo, B.; García-España, E.; Basallote, M. G.; Münck, E.; Que, L.; Company, A.; Costas, M., *J. Am. Chem. Soc.* **2015,** *137*, 15833-15842.
26. Miyafuji, A.; Katsuki, T., *Tetrahedron* **1998,** *54*, 10339-10348.
27. Frost, J. R.; Huber, S. M.; Breitenlechner, S.; Bannwarth, C.; Bach, T., *Angew. Chem. Int. Ed.* **2015,** *54*, 691-695.
28. Groves, J. T.; Viski, P., *J. Org. Chem* **1990,** *55*, 3628-3634.
29. Srour, H.; Maux, P. L.; Simonneaux, G., *Inorg. Chem.* **2012,** *51*, 5850-5856.
30. Maux, P. L.; Srour, H. F.; Simonneaux, G., *Tetrahedron* **2012,** *68*, 5824-5828.

31. Zhang, R.; Yu, W. Y.; Lai, T. S.; Che, C.-M., *Chem. Commun.* **1999**, 1791-1792.

32. Zhang, R.; Yu, W.-Y.; Che, C.-M., *Tetrahedron: Asymmetry* **2005,** *16*, 3520-3526.

33. Hamada, T.; Irie, R.; Mihara, J.; Hamachi, K.; Katsuki, T., *Tetrahedron* **1998,** *54*, 10017-10028.

34. Hamachi, K.; Irie, R.; Katsuki, T., *Tet. Lett.* **1996,** *37*, 4979-4982.

35. Komiya, N.; Noji, S.; Murahashi, S.-I., *Tetrahedron Lett.* **1998,** *39*, 7921-7924.

36. Murahashi, S.-I.; Noji, S.; Hirabayashi, T.; Komiya, N., *Tetrahedron: Asymmetry* **2005,** *16*, 3527-3535.

37. Murahashi, S.-I.; Noji, S.; Komiya, N., *Adv. Synth. Catal.* **2004,** *346*, 195-198.

38. Zhang, W.; Wang, F.; McCann, S. D.; Wang, D.; Chen, P.; Stahl, S. S.; Liu, G., *Science* **2016,** *353*, 1014-1018.

39. Wang, F.; Wang, D.; Wan, X.; Wu, L.; Chen, P.; Liu, G., *J. Am. Chem. Soc.* **2016,** *138*, 15547-15550.

40. Kille, S.; Zilly, F. E.; Acevedo, J. P.; Reetz, M. T., *Nat. Chem.* **2011,** *3*, 738–743.

41. Narayan, A. R. H.; Jimenez-Oses, G.; Liu, P.; Negretti, S.; Zhao, W.; Gilbert, M. M.; Ramabhadran, R. O.; Yang, Y.-F.; Furan, L. R.; Li, Z.; Podust, L. M.; Montgomery, J.; Houk, K. N.; Sherman, D. H., *Nat. Chem.* **2015,** *7*, 653-660.

42. Roiban, G.-D.; Agudo, R.; Reetz, M. T., *Angew. Chem. Int. Ed.* **2014,** *53*, 8659-8663.

43. Zhang, K.; Shafer, B. M.; Matthew D. Demars, I.; Stern, H. A.; Fasan, R., *J. Am. Chem. Soc* **2012,** *134*, 18695–18704.

44. Cusso, O.; Ribas, X.; Costas, M., *Chem. Comm.* **2015,** *51*, 14285-14298.

45. Wang, C.; Yamamoto, H., *Chem. Asian J.* **2015,** *10*, 2056-2068.

46. Bryliakov, K. P.; Talsi, E. P., *Coord. Chem. Rev.* **2014,** *276*, 73-96.

47. Zang, C.; Liu, Y.; Xu, Z.-J.; Tse, C.-W.; Guan, X.; Wei, J.; Huang, J.-S.; Che, C.-M., *Angew. Chem. Int. Ed.* **2016,** *55*, 10253-10257.

48. Chow, T. W.-S.; Liu, Y.; Che, C.-M., *Chem. Comm.* **2011**, 11204-11206.

49. Chen, K.; Que, L., Jr., *J. Am. Chem. Soc.* **2001,** *123*, 6327-6337.

50. Chen, M. S.; White, M. C., *Science* **2010,** *327*, 566-571.

51. Shen, D. Y.; Miao, C. X.; Xu, D. Q.; Xia, C. G.; Sun, W., *Org. Lett.* **2015,** *17*, 54-57.

52. Shen, D.; Miao, C.; Wang, S.; Xia, C.; Sun, W., *Org. Lett.* **2014,** *16*, 1108-1111.

53. González-Núñez, M. E.; Castellano, G.; Andreu, C.; Royo, J.; Báguena, M.; Mello, R.; Asensio, G., *J. Am. Chem. Soc.* **2001,** *123*, 7487-7491.

54. Moteki, S. A.; Usui, A.; Zhang, T.; Solorio Alvarado, C. R.; Maruoka, K., *Angew. Chem. Int. Ed.* **2013,** *52*, 8657-8660.

55. Moteki, S. A.; Selvakumar, S.; Zhang, T.; Usui, A.; Maruoka, K., *Asian J. Org. Chem.* **2014,** *3*, 932-935.

56. Bigi, M. A.; Reed, S. A.; White, M. C., *J. Am. Chem. Soc.* **2012,** *134*, 9721-9726.

57. Salamone, M.; Ortega, V. B.; Bietti, M., *J. Org. Chem.* **2015,** *80*, 4710-4715.

58. Chen, K.; Eschenmoser, A.; Baran, P. S., *Angew. Chem. Int. Ed.* **2009,** *48*, 9705-9708.

59. Zou, L.; Paton, R. S.; Eschenmoser, A.; Newhouse, T. R.; Baran, P. S.; Houk, K. N., *J. Org. Chem.* **2013,** *78*, 4037-4048.

60. Damm, W.; Giese, B.; Hartung, J.; Hasskerl, T.; Houk, K. N.; Hueter, O.; Zipse, H., *J. Am. Chem. Soc.* **1992,** *114*, 4067-4079.

61. Milan, M.; Bietti, M.; Costas, M., *ACS Cent. Sci.* **2017,** *3*, 196-204.

Chapter VII

General Conclusions

In the last decade, selective oxidation reactions of aliphatic C-H bonds has substantially advanced, becoming a powerful and useful tool for organic synthesis. Instead, the enantioselective oxidation of non-activated C-H bonds still remains a challenge. In this thesis, several chiral manganese complexes have been synthetized and characterized as potential C-H oxidation catalysts. Furthermore, their activity towards aliphatic C-H oxidation has been studied. Particular interest, has been devoted to investigate the site-selectivity and enantioselectivity of their catalytic C-H oxidation reactions.

Particularly, in **Chapter III**, the oxidation of *N*-alkylamides and phthalimides with aqueous H_2O_2 using iron and manganese catalysts is described. A superior tolerance of manganese complexes in comparison with the iron parent is observed in the oxidation of substrates bearing the amide functional group. By playing on the electronic, steric and stereoelectronic properties of the amide functional group, a change in the site-selectivity of the reaction have been achieved. The higher is the electron-withdrawing ability of the amide moiety, the stronger is the deactivation of the proximal positions. In particular, the powerful electron withdrawing character of the phthalimido group, completely deactivates proximal C-H bonds and directs oxidation towards the most remote position (>99% selectivity, up to 83% isolated yield). Interestingly, considering that traditional methodologies for oxidizing the α position of the amide nitrogen atom provide imides, our method constitutes a unique tool to synthesize α-hydroxylated amides. The control over the site-selectivity disclosed in these studies, led to the site-selective oxidation of compounds with a pharmaceutical relevance, such as pregabalin (Lyrica) and rimantadine (Flumadine).

In **Chapter IV** a new family of chiral sterically demanding manganese complexes characterized by the presence of the bulky *tris*-(triisopropyl)silyl group (TIPS) on the ligand has been prepared. These oxidatively robust manganese catalysts have been studied in the oxidation of nonactivated aliphatic C-H bonds of monosubstituted cyclohexanes, using hydrogen peroxide as the oxidant in the presence of a carboxylic acid. The site-selectivity and enantioselectivity of the reaction have been investigated. In particular, it has been discovered that methylene oxidation in the presence of an amide group proceeds with impressive enantioselectivity (up to 96% ee) and exquisite site-selectivity (up to $K_3/K_4 > 99$). These results represent the first examples of highly enantioselective nonenzymatic oxidation of nonactivated methylenic sites in simple alkanes but also in molecules that contain different functional groups such as esters, carboxylic acids, ketones and amides. The principles of catalyst design disclosed in this work constitute a very solid platform for further development of stereoselective C-H oxidation reactions in terms of substrate scope.

Finally, in **Chapter V** it has been shown that the oxidation reactions of substituted *N*-cyclohexylamides are directed by torsional effects. In this way, it was possible to selectively oxidize *cis*-1,4-, *trans*-1,3-, and *cis*-1,2-cyclohexanediamides over the corresponding diastereoisomers. Taking advantage of this effect, kinetic resolution of cyclohexane derivatives by means of selective C-H oxidation has been accomplished. From competitive oxidation of *cis*-*trans* mixtures of 4- substituted *N*-cyclohexylamides quantitative conversion of the *cis*-isomers can be accomplished, allowing isolation of the *trans*-isomers in good to excellent yield. The *trans* isomers can be further converted into densely functionalized oxidation products with excellent site-selectivity and good enantioselectivity.

Experimental Section

Materials

Reagents and solvents used were of commercially available reagent quality unless stated otherwise. Solvents were purchased from SDS and Scharlab. Solvents were purified and dried by passing through an activated alumina purification system (M-Braun SPS-800) or by conventional distillation techniques.

Instrumentation

Oxidation products were identified by comparison of their GC retention times and GC/MS with those of authentic compounds, and/or by ^1H and $^{13}C\{^1H\}$-NMR analyses. Elemental analyses were performed using a CHNS-O EA-1108 elemental analyzer from Fisons. NMR spectra were taken on BrukerDPX300 and DPX400 spectrometers using standard conditions. High resolution mass spectra (HRMS) were recorded on a Bruker MicroTOF-Q IITM instrument with an ESI source at Serveis Tècnics of the University of Girona. Samples were introduced into the mass spectrometer ion source by direct infusion through a syringe pump and were externally calibrated using sodium formate. Chromatographic resolution of enantiomers was performed on an AgilentGC-7820-A chromatograph using a CYCLOSIL-B column and HPLC 1200 series Agilent technologies using CHIRALPAK-IA and CHIRALPAK-IC columns. The configuration of the major enantiomer was determined by chemical correlation.

Oxidation Reactions

Hydrogen peroxide solutions employed in the oxidation reactions were prepared by diluting commercially available hydrogen peroxide (30% H_2O_2 solution in water, Aldrich) in acetonitrile to achieve a 1.5 M final concentration. Commercially available glacial acetic acid (99-100%) purchased from Riedel-de-Haën was employed. The purity of the amide substrates synthetized as described above was in all cases >99%. Acetic acid was purchased from Aldrich.

Experimental Section: Chapter VI.1.

Tuning Selectivity in Aliphatic C–H Bond Oxidation of *N*-Alkylamides and Phthalimides Catalyzed by Manganese Complexes

1. Synthesis of the Complexes

The manganese complexes were prepared according to the reported procedures:

$[\mathrm{Fe(CF_3SO_3)_2(pdp)}]$[1]
$[\mathrm{Fe(CF_3SO_3)_2(mcp)}]$[2]
$[\mathrm{Fe(CF_3SO_3)_2(^{NMe2}pdp)}]$, $[\mathrm{Fe(CF_3SO_3)_2(^{dMM}pdp)}]$[3]
$[\mathrm{Fe(CF_3SO_3)_2(^{TIPS}mcp)}]$[4]
$[\mathrm{Mn(CF_3SO_3)_2(mcp)}]$[5]
$[\mathrm{Mn(CF_3SO_3)_2(pdp)}]$[6]
$[\mathrm{Mn(CF_3SO_3)_2(^{dMM}pdp)}]$, $[\mathrm{Mn(CF_3SO_3)_2(^{dMM}mcp)}]$, $[\mathrm{Mn(CF_3SO_3)_2(^{Cl}mcp)}]$, $[\mathrm{Mn(CF_3SO_3)_2(^{Me2N}pdp)}]$[7]
$[\mathrm{Mn(CF_3SO_3)_2(^{TIPS}pdp)}]$, $[\mathrm{Mn(CF_3SO_3)_2(^{TIPS}mcp)}]$, $[\mathrm{Mn(CF_3SO_3)_2(^{CF3}mcp)}]$[8]
$[\mathrm{Mn(CF_3SO_3)_2(^{BzIm}pdp)}]$[9]

2. Synthesis of the Substrates

The following substrates were prepared according to the reported procedures.
S16[10]

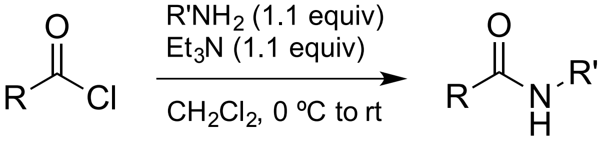

A round-bottom flask capped with a rubber septum and kept under nitrogen was charged with a 0.20 M solution of the amine (1.1 equiv) in dichloromethane and cooled to 0 °C. Triethylamine (1.1 equiv) was added to the reaction flask. The acyl chloride (1.0 equiv) was added dropwise and the reaction was stirred overnight at room temperature. At this point, a saturated aqueous Na$_2$CO$_3$ solution was added until pH~10-11 and then diluted with dichloromethane. The organic layer was separated from the basic aqueous layer. The aqueous layer was extracted with dichloromethane (2x) and the organic layers were combined. The organic layer was washed with 1N HCl and dried over anhydrous sodium sulfate (Na$_2$SO$_4$). The organic layer was evaporated to dryness and the crude amide was purified by flash chromatography over silica gel.

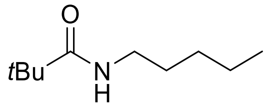

***N*-pentylpivalamide (S1):** Following the general conditions, the crude mixture was purified by flash chromatography over silica with hexane:ethyl acetate 1:1 and the product was concentrated to dryness. The product was isolated as a white solid (0.65 g, 88% yield). ^{1}H-NMR ($CDCl_3$, 400 MHz, 300K) δ, ppm: 5.74 (s, 1H), 3.19 (td, *J* = 7.2, 5.7 Hz, 2H), 1.55 – 1.40 (m, 2H), 1.36 – 1.22 (m, 4H), 1.16 (s, 9H), 0.93 – 0.80 (m, 3H). ^{13}C-NMR 178.3, 39.5, 38.6, 29.3, 29.0, 27.6, 22.3, 14.0. HRMS(ESI+) *m/z* calculated for $C_{10}H_{21}NO$ [M+Na]+ 194.1515, found 194.1515.

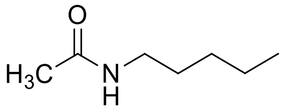

***N*-pentylacetamide (S2):** Following the general conditions, the crude mixture was purified by flash chromatography over silica with hexane:ethyl acetate 1:1 and the product was concentrated to dryness. The product was isolated as a white solid (0.53 g, 60% yield).

^{1}H-NMR ($CDCl_3$, 400 MHz, 300K) δ, ppm: 6.16 (s, 1H), 3.17 (td, *J* = 7.2, 5.7 Hz, 2H), 1.93 (s, 3H), 1.55 – 1.38 (m, 2H), 1.37 – 1.14 (m, 4H), 0.91 – 0.78 (m, 3H). ^{13}C-NMR 170.2, 39.6, 29.2, 29.0, 23.2, 22.3, 13.9. HRMS(ESI+) *m/z* calculated for $C_7H_{15}NO$ [M+Na]+ 152.1046, found 152.1047.

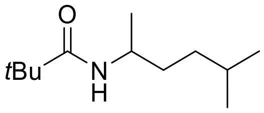

***N*-(2-(5-methylhexyl)pivalamide (S5):** Following the general conditions, the crude mixture was purified by flash chromatography over silica with hexane:ethyl acetate 1:1 and the product was concentrated to dryness. The product was isolated as a white solid (0.48 g, 85% yield). ^{1}H-NMR ($CDCl_3$, 400 MHz, 300K) δ ppm: 5.37 (s, 1H), 3.91 (dq, *J* = 8.3, 6.7 Hz, 1H), 1.51 (dq, *J* = 13.3, 6.6 Hz, 1H), 1.45 – 1.33 (m, 2H), 1.16 (s, 9H), 1.08 (d, *J* = 6.6 Hz, 3H), 0.85 (d, *J* = 6.6 Hz, 6H). ^{13}C-NMR 177.5, 45.0, 38.5, 35.1, 34.7, 27.9, 27.6, 22.5, 20.9. HRMS(ESI+) *m/z* calculated for $C_{12}H_{25}NO$ [M+Na]+ 222.1828, found 222.1832.

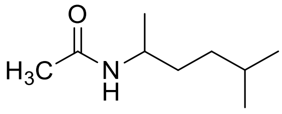

***N*-(2-(5-methylhexyl)acetamide (S6):** Following the general conditions, the crude mixture was purified by flash chromatography over silica with hexane:ethyl acetate 1:1 and the product was concentrated to dryness. The product was isolated as a white solid (0.43 g, 72% yield). ^{1}H-NMR ($CDCl_3$, 400 MHz, 300K) δ, ppm: 5.90 (s, 1H), 3.87 (d, *J* = 41.8 Hz, 1H), 1.92 (s, 3H), 1.48 (dq, *J* = 13.3, 6.6 Hz, 1H), 1.42 – 1.31 (m, 2H), 1.20 – 1.10 (m, 2H), 1.07 (d, *J* = 6.6 Hz, 3H), 0.82 (d, *J* = 6.7 Hz, 6H). ^{13}C-NMR 169.4, 45.4, 35.1, 34.6, 27.9, 23.4, 22.52, 22.50, 20.9. HRMS(ESI+) *m/z* calculated for $C_9H_{19}NO$ [M+Na]+ 180.1359, found 180.1360.

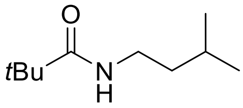

***N*-1-(3-methylbutyl)pivalamide (S9):** Following the general conditions, the crude mixture was purified by flash chromatography over silica with hexane:ethyl acetate 1:1 and the product was concentrated to dryness. The product was isolated as a white solid

(0.44 g, 64% yield). ^{1}H-NMR ($CDCl_3$, 400 MHz, 300K) δ, ppm: 5.71 (s, 1H), 3.29 – 3.16 (m, 2H), 1.57 (dp, *J* = 13.3, 6.7 Hz, 1H), 1.43 – 1.27 (m, 2H), 1.15 (s, 9H), 0.88 (d, *J* = 6.6 Hz, 6H). ^{13}C-NMR 178.3, 38.54, 38.49, 37.9, 27.6, 25.9, 22.5. HRMS(ESI+) *m/z* calculated for $C_{10}H_{21}NO$ [M+Na]+ 194.1515, found 194.1518.

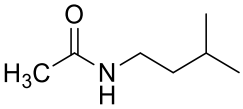

***N*-1-(3-methylbutyl)acetamide (S10):** Following the general conditions, the crude mixture was concentrated to dryness without further purification. The product was isolated as a white solid (0.65 g, 57% yield). ^{1}H-NMR ($CDCl_3$, 400 MHz, 300K) δ, ppm: 6.33 (s, 1H), 3.25 – 3.08 (m, 2H), 1.91 (s, 3H), 1.56 (dp, *J* = 13.3, 6.7 Hz, 1H), 1.33 (q, *J* = 7.1 Hz, 2H), 0.85 (d, *J* = 6.6 Hz, 6H). ^{13}C-NMR 170.3, 38.3, 37.9, 25.8, 23.1, 22.4. HRMS(ESI+) *m/z* calculated for $C_7H_{15}NO$ [M+Na]+ 152.1046, found 152.1047.

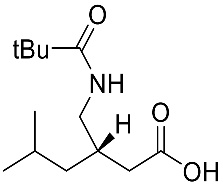

(S13): Following the general conditions, the crude mixture was purified by flash chromatography over silica with hexane:ethyl acetate 5:1 and the product was concentrated to dryness. The product was isolated as a white solid (0.19 g, 72% yield). ^{1}H-NMR ($CDCl_3$, 400 MHz, 300K) δ, ppm: 6.22 (s, 1H), 3.44 – 3.10 (m, 2H), 2.37 (dd, J = 15.0, 4.4 Hz, 1H), 2.27 (dd, J = 15.0, 7.8 Hz, 1H), 2.20 – 2.08 (m, 1H), 1.70 (dt, J = 13.4, 6.7 Hz, 1H), 1.22 (s, 9H), 1.18 (dd, J = 7.2, 1.2 Hz, 2H), 0.92 (dd, J = 9.3, 6.6 Hz, 6H). ^{13}C-NMR 179.8, 176.8, 43.4, 41.7, 38.8, 37,6, 33.4, 27.5, 25.2, 22.7, 22.6. HRMS(ESI+) *m/z* calculated for $C_{13}H_{25}NO_3$ [M+Na]+ 266.1727, found 266.1734.

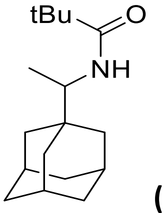

(S15): Following the general conditions, the crude mixture was purified by flash chromatography over silica with hexane:ethyl acetate 1:1 and the product was concentrated to dryness. The product was isolated as a white solid (0.99 g, 98% yield). ^{1}H-NMR ($CDCl_3$, 400 MHz, 300K) δ, ppm: 5.46 (d, J = 9.6 Hz, 1H), 3.69 (dq, J = 9.6, 6.9 Hz, 1H), 1.97 (p, J = 3.2 Hz, 3H), 1.77 – 1.56 (m, 6H), 1.55 – 1.39 (m, 6H), 1.19 (s, 9H), 0.99 (d, J = 6.9 Hz, 3H). ^{13}C-NMR 177.4, 52.3, 38.8, 38.4, 37.1, 35.9, 28.3, 27.7, 14.5. HRMS(ESI+) *m/z* calculated for $C_{17}H_{29}NO$ [M+Na]+ 286.2141, found 286.4144.

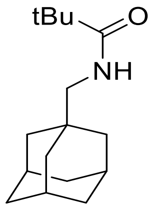

(S17): Following the general conditions, the crude mixture was purified by flash chromatography over silica with hexane:ethyl acetate 2:1 and the product was concentrated to dryness. The product was isolated as a white solid (0.42 g, 98% yield). ^{1}H-NMR ($CDCl_3$, 400 MHz, 300K) δ, ppm: 5.68 (s, 1H), 2.95 (d, J = 6.3 Hz, 2H), 1.98 (q, J = 3.2 Hz, 3H), 1.80 – 1.57 (m, 6H), 1.48 (d, J = 2.8 Hz, 6H), 1.22 (s, 9H). ^{13}C-NMR 178.3, 50.7, 40.3, 38.9, 37.0, 33.8, 28.2, 27.8. HRMS(ESI+) *m/z* calculated for $C_{16}H_{27}NO$ [M+Na]+ 272.1985, found 272.1988.

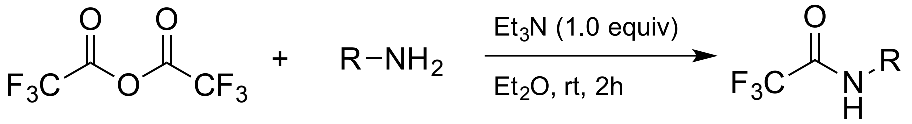

A round-bottom flask equipped with a septum and kept under nitrogen was charged with the amine (1.0 equiv) and solubilized in diethylether (1.4 M). Triethylamine (1.0 equiv) was added to the reaction flask. Trifluoroacetic anhydride (1.0 equiv) in diethylether (1.4 M) was added dropwise and the reaction was stirred for 2 hours at room temperature. At this point H_2O was added and the basic aqueous layer was separated. The organic layer was extracted with $NaHCO_3$, saturated with NH_4Cl and dried over anhydrous sodium sulfate (Na_2SO_4). The organic layer was evaporated to dryness and the crude amine was purified by flash chromatography over silica gel and the product was concentrated to dryness.

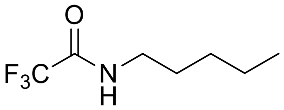

***N*-pentyltrifluoroacetamide (S3):** Following the general conditions, the crude mixture was purified by flash chromatography over silica with hexane:ethyl acetate 1:1 and the product was concentrated to dryness. The product was isolated as a white solid (0.37 g, 73% yield).

^{1}H-NMR ($CDCl_3$, 400 MHz, 300K) δ, ppm: 6.73 (s, 1H), 3.47 – 3.22 (m, 2H), 1.67 – 1.51 (m, 2H), 1.44 – 1.20 (m, 4H), 0.99 – 0.80 (m, 3H). ^{13}C-NMR 157.5, 121.6, 117.8, 114.0, 40.0, 28.7, 28.5, 22.2, 13.8. HRMS(ESI+) *m/z* calculated for $C_7H_{12}F_3NO$ [M+Na]+ 206.0763, found 206.0769.

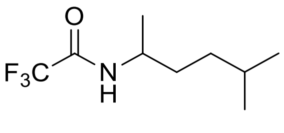

***N*-(2-(5-methylhexyl)trifluoroacetamide (S7):** Following the general conditions, the crude mixture was purified by flash chromatography over silica with hexane:ethyl acetate 1:1 and the product was concentrated to dryness. The product was isolated as a white solid (0.55 g, 64% yield). ^{1}H-NMR ($CDCl_3$, 400 MHz, 300K) δ, ppm: 6.44 (s,

1H), 4.09 – 3.87 (m, 1H), 1.53 (td, *J* = 12.7, 11.7, 7.0 Hz, 3H), 1.22 (d, *J* = 6.6 Hz, 4H), 1.17 (d, *J* = 6.7 Hz, 1H), 0.88 (d, *J* = 6.8 Hz, 6H). ^{13}C-NMR 156.8, 121.6, 117.8, 114.0, 46.8, 34.9, 34.0, 27.8, 22.4, 20.2. HRMS(ESI+) *m/z* calculated for $C_9H_{16}F_3NO$ [M+Na]+ 234.1076, found 234.1075.

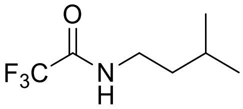

***N*-1-(3-methylbutyl)trifluoroacetamide (S11):** Following the general conditions, the crude mixture was purified by flash chromatography over silica with hexane:ethyl acetate 1:1 and the product was concentrated to dryness. The product was isolated as a white solid (0.56 g, 71% yield). ^{1}H-NMR (CDCl$_3$, 400 MHz, 300K) δ, ppm: 6.68 (s, 1H), 3.45 – 3.31 (m, 2H), 1.75 – 1.56 (m, 1H), 1.56 – 1.42 (m, 2H), 0.94 (d, *J* = 6.6 Hz, 6H). ^{13}C-NMR 157.5, 121.6, 117.8, 114.0, 38.3, 37.6, 25.7, 22.2. HRMS(ESI+) *m/z* calculated for $C_7H_{12}F_3NO$ [M+Na]+ 206.0763, found 206.0762.

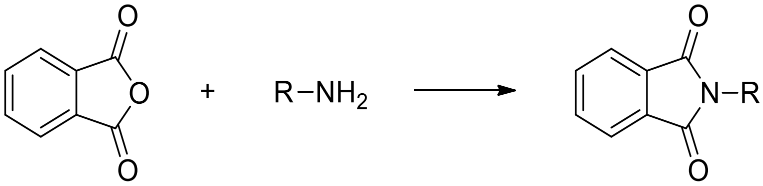

Phthalic anhydride (1.5 equiv) was added to a solution of the amine (1.0 equiv) in DMF and refluxed overnight at 155° C for 12 hours. The reaction was cooled to room temperature and poured into 50 mL of 1M HCl and extracted with Et$_2$O. The organic layer was then dried with magnesium sulfate and concentrated under reduced pressure. The crude phthalimide was purified by flash chromatography over silica gel.

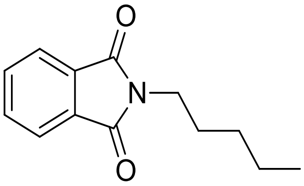

***N*-pentylphthalimide (S4):** Following the general conditions, the crude mixture was purified by flash chromatography over silica with hexane:ethyl acetate 5:1 and the product was concentrated to dryness. The product was isolated as a white solid (0.67 g, 90% yield). ^{1}H-NMR (CDCl$_3$, 400 MHz, 300K) δ, ppm: 7.86 – 7.73 (m, 2H), 7.72 – 7.59 (m, 2H), 3.72 – 3.54 (m, 2H), 1.74 – 1.54 (m, 2H), 1.37 – 1.20 (m, 4H), 0.93 – 0.73 (m, 3H). ^{13}C-NMR 168.4, 133.8, 132.1, 123.1, 38.0, 28.9, 28.2, 22.2, 13.9. HRMS(ESI+) *m/z* calculated for $C_{13}H_{15}NO_2$ [M+Na]+ 240.0995, found 240.0995.

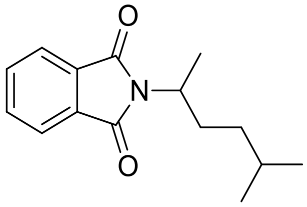

***N*-(2-(5-methylhexyl)phthalimide (S8):** Following the general conditions, the crude mixture was purified by flash chromatography over silica with hexane:ethyl acetate 5:1 and the product was concentrated to dryness. The product was isolated as a white solid (0.43 g, 95% yield). ^{1}H-NMR ($CDCl_3$, 400 MHz, 300K) δ, ppm: 7.87 – 7.73 (m, 2H), 7.76 – 7.62 (m, 2H), 4.29 (ddt, *J* = 13.0, 9.3, 6.9 Hz, 1H), 2.03 (dddd, *J* = 13.5, 11.1, 9.3, 5.1 Hz, 1H), 1.71 (dddd, *J* = 13.6, 11.3, 6.0, 5.3 Hz, 1H), 1.58 – 1.48 (m, 1H), 1.45 (d, *J* = 7.0 Hz, 3H), 1.28 – 0.96 (m, 2H), 0.82 (dd, *J* = 6.6, 3.4 Hz, 6H). ^{13}C-NMR 168.5, 133.7, 132.0, 123.0, 47.7, 35.9, 31.6, 27.8, 22.6, 22.4, 18.7. HRMS(ESI+) *m/z* calculated for $C_{15}H_{19}NO_2$ [M+Na]+ 268.1308, found 268.1309.

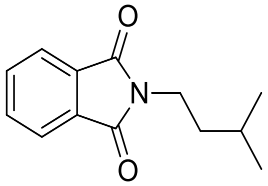

***N*-1-(3-methylbutyl)phthalimide (S12):** Following the general conditions, the crude mixture was purified by flash chromatography over silica with hexane:ethyl acetate 5:1 and the product was concentrated to dryness. The product was isolated as a white solid (0.54 g, 96% yield). ^{1}H-NMR ($CDCl_3$, 400 MHz, 300K) δ, ppm: 7.85 – 7.73 (m, 2H), 7.72 – 7.59 (m, 2H), 3.74 – 3.55 (m, 2H), 1.66 – 1.44 (m, 3H), 0.92 (d, *J* = 6.3 Hz, 6H). ^{13}C-NMR 168.3, 133.8, 132.1, 123.0, 35.3, 36.4, 25.8, 22.3. HRMS(ESI+) *m/z* calculated for $C_{13}H_{15}NO_2$ [M+Na]+ 240.0995, found 240.1003.

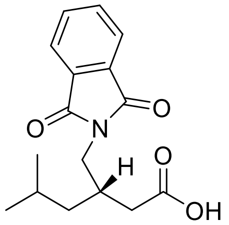

(S14): Following the general conditions, the crude mixture was purified by flash chromatography over silica with hexane:ethyl acetate 5:1 and the product was concentrated to dryness. The product was isolated as a white solid (0.29 g, 70% yield). ^{1}H-NMR ($CDCl_3$, 400 MHz, 300K) δ, ppm: 7.95 – 7.79 (m, 2H), 7.79 – 7.59 (m, 2H), 3.79 – 3.53 (m, 2H), 2.45 (dtd, J = 8.2, 6.6, 4.9 Hz, 1H), 2.40 – 2.25 (m, 2H), 1.78 (dq, J = 13.5, 6.7 Hz, 1H), 1.33 – 1.20 (m, 2H), 0.95 (dd, J = 20.5, 6.6 Hz, 6H). ^{13}C-NMR 177.2, 168.7, 134.0, 131.9, 123.3, 41.8, 41.6, 37.2, 32.7, 25.3, 22.7, 22.5. HRMS(ESI+) *m/z* calculated for $C_{16}H_{19}NO_4$ [M+Na]+ 312.1206, found 312.1213.

3. Reaction Protocol for Catalysis

An acetonitrile solution (400 µL) of the substrate (0.25 M) and the pertinent complex (2.5 mM) was prepared in a vial (10 mL) equipped with a stirring bar and cooled at -40 °C, in a CH_3CN/N_2(liq) bath. Acetic acid (13 equiv) was added directly to the solution. Then hydrogen peroxide in CH_3CN (3.5 equiv) was added by syringe pump over a period of 30 min. At this point, an internal standard was added and the solution was quickly filtered through a basic alumina plug, which was subsequently rinsed with 2 x 1 mL AcOEt. GC or ^{1}H-NMR analysis of the solution provided substrate conversions and product yields relative to the internal standard integration.

3.1 Reaction Protocol for Product Isolation

25 mL round bottom flask was charged with: catalyst (6 µmol, 1.0 mol%), substrate (1.0 equiv.), CH_3CN (3.3 mL) and a magnetic stirring bar. Acetic acid was then added (13 equiv.) and the mixture was cooled at -40 °C in an CH_3CN/N_2(liq) bath under magnetic stirring. Then, 1.4 mL of hydrogen peroxide solution in CH_3CN (3.5 equiv.) were added by syringe pump over a period of 30 min at -40 °C. At this point, 15 mL of an aqueous $NaHCO_3$ saturated solution were added to the mixture. The resultant solution was extracted with CH_2Cl_2 (3 x 10 mL). The organic fractions were combined, dried over $MgSO_4$, and the solvent was removed under reduced pressure to afford the oxidized product. This residue was filtered by silica gel column to obtain the pure product.

4. Characterization of the Isolated Products

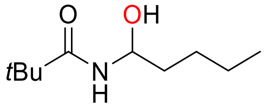

***N*-(1-hydroxy)pentylpivalamide (P1):** Following the general conditions, the crude mixture was purified by flash chromatography over silica with hexane:ethyl acetate 1:1 and the product was concentrated to dryness. The product was isolated as a white solid (61 mg, 48% yield). ^{1}H-NMR ($CDCl_3$, 400 MHz, 300K) δ, ppm: 6.26 (d, *J* = 5.2 Hz, 1H), 5.28 (q, *J* = 6.7 Hz, 1H), 4.37 (s, 1H), 1.73 – 1.61 (m, 1H), 1.55 (tdt, *J* = 11.7, 9.4, 6.2 Hz, 1H), 1.36 (tddd, *J* = 11.2, 9.4, 5.6, 2.0 Hz, 4H), 1.18 (s, 9H), 0.90 (td, *J* = 6.2, 5.5, 1.8 Hz, 3H). ^{13}C-NMR 179.7, 74.4, 38.6, 34.9, 27.3, 27.0, 22.3, 13.9. HRMS(ESI+) *m/z* calculated for $C_{10}H_{21}NO_2$ [M+Na]+ 210.1465, found 210.1468.

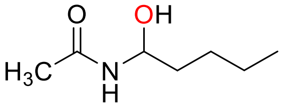

***N*-(1-hydroxy)pentylacetamide (P2):** Following the general conditions, the crude mixture was purified by flash chromatography over silica with hexane:ethyl acetate 1:1 and the product was concentrated to dryness. The product was isolated as a white solid (40 mg, 36% yield). ^{1}H-NMR ($CDCl_3$, 400 MHz, 300K) δ, ppm: 6.46 (d, J = 7.8 Hz, 1H), 5.29 (td, J = 8.6, 4.5 Hz, 1H), 4.34 (d, J = 3.5 Hz, 1H), 2.00 (s, 3H), 1.74 – 1.62 (m, 1H), 1.62 – 1.50 (m, 1H), 1.46 – 1.26 (m, 4H), 0.97 – 0.85 (m, 3H). ^{13}C-NMR 171.6, 74.3, 34.9, 27.0, 23.3, 22.3, 13.9. HRMS(ESI+) *m/z* calculated for $C_7H_{15}NO_2$ [M+Na]+ 168.0995, found 168.0991.

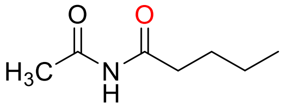

***N*-(1-oxo)pentylacetamide (P2_i):** Following the general conditions, the crude mixture was purified by flash chromatography over silica with hexane:ethyl acetate 1:1 and the product was concentrated to dryness. The product was isolated as a white solid (39 mg, 36% yield). ^{1}H-NMR ($CDCl_3$, 400 MHz, 300K) δ, ppm: 9.24 (s, 1H), 2.51 (t, J = 7.5 Hz, 2H), 2.34 (d, J = 23.9 Hz, 3H), 1.61 (p, J = 7.5 Hz, 2H), 1.35 (h, J = 7.3 Hz, 2H), 0.91 (t, J = 7.4 Hz, 3H). ^{13}C-NMR 174.3, 172.7, 37.0, 26.5, 25.1, 22.2, 13.7. HRMS(ESI+) *m/z* calculated for $C_7H_{13}NO_2$ [M+Na]+ 166.0838, found 166.0843.

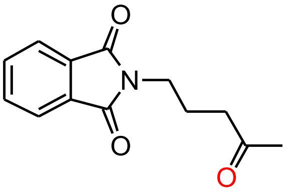

***N*-(4-oxo)penthylphthalimide (P4)** Following the general conditions, the crude mixture was purified by flash chromatography over silica with hexane:ethyl acetate 2:1 and the product was concentrated to dryness. The product was isolated as a white solid (53 mg, 41% yield). ^{1}H-NMR ($CDCl_3$, 400 MHz, 300K) δ, ppm: 7.78 (s, 2H), 7.70 (s, 2H), 3.66 (s, 2H), 2.47 (s, 2H), 2.11 (s, 3H), 1.89 (s, 2H). ^{13}C-NMR 208.1, 168.8, 134.1, 131.9, 123.3, 40.5, 37.1, 30.2, 22.6. HRMS(ESI+) *m/z* calculated for $C_{13}H_{13}NO_3$ [M+Na]+ 254.0785, found 254.0785.

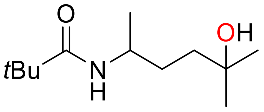

***N*-(2-(5-hydroxy-5-methylhexyl)-pivalamide (P5):** Following the general conditions, the crude mixture was purified by flash chromatography over silica with hexane:ethyl acetate 1:1 and the product was concentrated to dryness. The product was isolated as a white solid (69.3 mg, 52% yield). ^{1}H-NMR ($CDCl_3$, 400 MHz, 300K) δ, ppm: 5.55 (s, 1H), 4.04 – 3.87 (m, 1H), 2.26 (s, 1H), 1.59 - 1.42 (m, 4H), 1.19 (s, 6H), 1.17 (s, 9H), 1.11 (d, *J* = 6.6 Hz, 3H). ^{13}C-NMR 177.9, 70.4, 45.3, 39.4, 38.6, 31.6, 29.5, 29.3, 27.6, 21.1. HRMS(ESI+) *m/z* calculated for $C_{12}H_{25}NO_2$ [M+Na]+ 238.1778, found 238.1779.

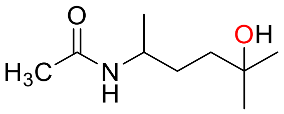

***N*-(2-(5-hydroxy-5-methylhexyl) acetamide (P6):** Following the general conditions, the crude mixture was purified by flash chromatography over silica with ethyl acetate and 8% of methanol the product was concentrated to dryness. The product was isolated as a white solid (61.4 mg, 34% yield). ^{1}H-NMR ($CDCl_3$, 400 MHz, 300K) δ, ppm: 5.55 (d, J = 8.3 Hz, 1H), 4.10 – 3.89 (m, 1H), 1.98 (s, 3H), 1.59 – 1.46 (m, 4H), 1.22 (s, 6H), 1.15 (d, J = 6.6 Hz, 3H). ^{13}C-NMR 169.6, 70.6, 45.6, 39.5, 31.6, 29.5, 29.4, 23.5, 21.2. HRMS(ESI+) *m/z* calculated for $C_9H_{19}NO_2$ [M+Na]+ 196.1308, found 196.1316.

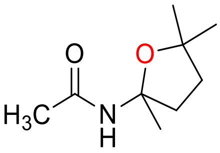

(P6_a): Following the general conditions, the crude mixture was purified by flash chromatography over silica with hexane:ethyl acetate 1:1 → ethyl acetate and the product was concentrated to dryness. The product was isolated as a white solid with 11% yield of an impurity that could not be separated (38 mg, 33% yield). ^{1}H-NMR ($CDCl_3$, 400 MHz, 300K) δ, ppm: 5.71 (d, J = 8.3 Hz, 1H), 2.73 – 2.68 (m, 1H), 2.06 – 1.99 (m, 2H), 1.93 (s, 3H), 1.82 – 1.77 (m, 1H), 1.33 (s, 3H), 1.22 (s, 1H). ^{13}C-NMR 168.5, 93.5, 82.9, 37.8, 36.8, 29.7, 28.8, 26.4, 24.2. HRMS(ESI+) *m/z* calculated for $C_9H_{17}NO_2$ [M+Na]+ 194.1151, found 194.1157.

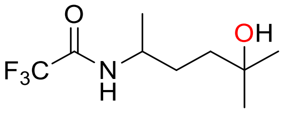

***N*-(2-(5-hydroxy-5-methylhexyl)trifluoroacetamide (P7):** Following the general conditions, the crude mixture was purified by flash chromatography over silica with hexane:ethyl acetate 1:1 and the product was concentrated to dryness. The product was isolated as a white solid (76.1 mg, 58% yield). ^{1}H-NMR ($CDCl_3$, 400 MHz, 300K) δ, ppm: 7.23 (s, 1H), 3.97 (s, 1H), 2.25 – 2.10 (m, 1H), 1.73 – 1.59 (m, 2H), 1.57 – 1.42 (m, 2H), 1.23 (s, 3H), 1.21 (s, 7H). ^{13}C-NMR 157.0, 120.2, 117.4, 114.5, 70.6, 46.8, 38.9, 30.4, 29.4, 29.3, 20.1. HRMS(ESI+) *m/z* calculated for $C_9H_{16}F_3NO_2$ [M+Na]+ 250.1025, found 250.1026.

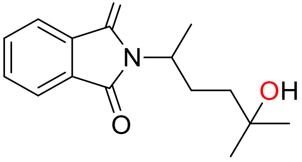

***N*-(2-(5-hydroxy-5-methylhexyl)phthalimide (P8):** Following the general conditions, the crude mixture was purified by flash chromatography over silica with hexane:ethyl acetate 1:1 and the product was concentrated to dryness. The product was isolated as a white solid (54.9 mg, 83% yield). ^{1}H-NMR ($CDCl_3$, 400 MHz, 300K) δ, ppm: 7.81 (dd, *J* = 5.4, 3.0 Hz, 2H), 7.70 (dd, *J* = 5.5, 3.1 Hz, 2H), 4.40 – 4.27 (m, 1H), 2.17 (dddd, *J* = 13.5, 12.2, 9.6, 4.7 Hz, 1H), 1.83 (dddd, *J* = 13.5, 12.3, 5.8, 4.6 Hz, 1H), 1.56 – 1.50 (m, 1H), 1.49 (d, *J* = 6.9 Hz, 3H), 1.35 (ddd, *J* = 13.4, 12.3, 4.7 Hz, 1H), 1.19 (s, 6H). ^{13}C-NMR 168.5, 133.8, 131.9, 123.1, 70.6, 47.9, 40.8, 29.4, 29.0, 28.7, 18.9. HRMS(ESI+) *m/z* calculated for $C_{15}H_{19}NO_3$ [M+Na]+ 284.1257, found 284.1257.

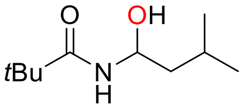

***N*-1-(1-hydroxy-3-methylbutyl)-pivalamide (P9_b):** Following the general conditions, the crude mixture was purified by flash chromatography over silica with hexane:ethyl acetate 1:1 and the product was concentrated to dryness. The product was isolated as a white solid (65.5 mg, 64% yield). ^{1}H-NMR ($CDCl_3$, 400 MHz, 300K) δ, ppm: 6.27 (d, *J* = 7.8 Hz, 1H), 5.37 (td, *J* = 7.5, 5.8 Hz, 1H), 4.55 (s, 1H), 1.73 (ddt, *J* = 13.0, 7.6, 6.5 Hz, 1H), 1.59 (ddd, *J* = 13.8, 7.4, 6.5 Hz, 1H), 1.36 (ddd, *J* = 13.5, 7.7, 5.8 Hz, 1H), 1.16 (s, 9H), 0.93 – 0.84 (m, 6H). ^{13}C-NMR 179.5, 72.9, 44.1, 38.5, 27.3, 24.5, 22.8, 22.2. HRMS(ESI+) *m/z* calculated for $C_{10}H_{21}NO_2$ [M+Na]+ 210.1465, found 210.1466.

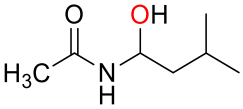

***N*-1-(1-hydroxy-3-methylbutyl)acetamide (P10_b):** Following the general conditions, the crude mixture was purified by flash chromatography over silica with hexane:ethyl acetate 1:4 and the product was concentrated to dryness. The product was isolated as a white solid (74.3 mg, 65% yield). ^{1}H-NMR ($CDCl_3$, 400 MHz, 300K) δ, ppm: 6.68 (d, *J* = 8.2 Hz, 1H), 5.38 (td, *J* = 7.7, 5.9 Hz, 1H), 4.64 (s, 1H), 1.97 (s, 3H), 1.81 – 1.66 (m, 1H), 1.57 (dt, *J* = 13.8, 7.1 Hz, 1H), 1.43 – 1.33 (m, 1H), 0.91 (dd, *J* = 6.6, 2.8 Hz, 6H). ^{13}C-NMR 171.4, 72.6, 44.1, 29.7, 24.4, 23.3, 22.2. HRMS(ESI+) *m/z* calculated for $C_7H_{15}NO_2$ [M+Na]+ 168.0995, found 168.0992.

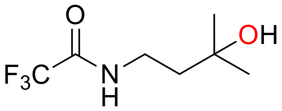

***N*-1-(3-hydroxy-3-methylbutyl)trifluoroacetamide (P11_c):** Following the general conditions, the crude mixture was purified by flash chromatography over silica with hexane:ethyl acetate 1:1 and the product was concentrated to dryness. The product was isolated as a white solid (46 mg, 48% yield). ^{1}H-NMR ($CDCl_3$, 400 MHz, 300K) δ, ppm: 7.98 (s, 1H), 3.61 – 3.42 (m, 2H), 2.28 (s, 1H), 1.84 – 1.63 (m, 2H), 1.30 (s, 6H). ^{13}C-NMR 157.2, 120.2, 117.4, 114.5, 71.8, 39.5, 36.5, 29.6. HRMS(ESI+) *m/z* calculated for $C_7H_{12}F_3NO_2$ [M+Na]+ 222.0712, found 222.0713.

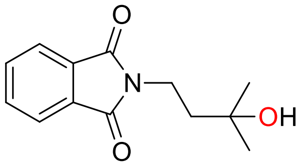

***N*-1-(3-hydroxy-3-methylbutyl)phthalimide (P12):** Following the general conditions, the crude mixture was purified by flash chromatography over silica with hexane:ethyl acetate 2:1 and the product was concentrated to dryness. The product was isolated as a white solid (57 mg, 65% yield). ^{1}H-NMR ($CDCl_3$, 400 MHz, 300K) δ, ppm: 7.86 – 7.74 (m, 2H), 7.74 – 7.60 (m, 2H), 3.91 – 3.75 (m, 2H), 2.29 (s, 1H), 1.92 – 1.80 (m, 2H), 1.30 (s, 6H). ^{13}C-NMR 168.5, 133.9, 132.2, 123.2, 69.8, 41.4, 34.0, 29.3. HRMS(ESI+) *m/z* calculated for $C_{13}H_{15}NO_3$ [M+Na]+ 256.0944, found 256.0948.

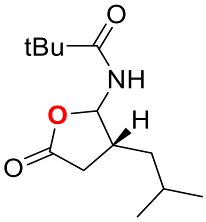

(P13_a): Following the general conditions, the crude mixture was purified by flash chromatography over silica with hexane:ethyl acetate 2:1 and the product was concentrated to dryness. The product was isolated as a white solid (24 mg, 26% yield). ^{1}H-NMR ($CDCl_3$, 400 MHz, 300K) δ, ppm: 6.53 (d, J = 9.7 Hz, 1H), 5.89 (dd, J = 9.7, 7.5 Hz, 1H), 2.78 (dd, J = 17.0, 8.1 Hz, 1H), 2.46 – 2.36 (m, 1H), 2.29 (dd, J = 17.0, 10.2 Hz, 1H), 1.59 (dt, J = 13.3, 6.7 Hz, 1H), 1.54 – 1.38 (m, 2H), 1.23 (s, 9H), 0.93 (dd, J = 11.0, 6.5 Hz, 6H).^{13}C-NMR 178.9, 174.4, 86.0, 41.4, 40.0, 40.1, 38.9, 35.8, 27.2, 26.1, 22.7, 22.3. HRMS(ESI+) *m/z* calculated for $C_{13}H_{23}NO_3$ [M+Na]+ 264.1570, found 264.1588.

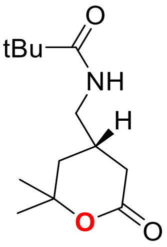

(P13_b): Following the general conditions, the crude mixture was purified by flash chromatography over silica with hexane:ethyl acetate 2:1 and the product was concentrated to dryness. The product was isolated as a white solid (7 mg, 7% yield). ^{1}H-NMR ($CDCl_3$, 400 MHz, 300K) δ, ppm: 5.81 (s, 1H), 3.37 – 3.09 (m, 2H), 2.66 (ddd, J = 17.7, 5.6, 2.1 Hz, 1H), 2.38 – 2.32 (m, 1H), 2.06 (dd, J = 17.7, 11.7 Hz, 1H), 1.85 (ddd, J = 13.7, 3.6, 2.1 Hz, 1H), 1.47 (s, 3H), 1.39 (s, 3H), 1.23 (s, 9H). ^{13}C-NMR 178.9, 170.5, 81.9, 44.2, 38.8, 38.5, 33.6, 30.7, 29.8, 27.63, 27.58. HRMS(ESI+) *m/z* calculated for $C_{13}H_{23}NO_3$ [M+Na]+ 264.1570, found 264.1555.

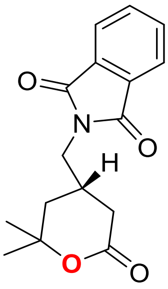

(P14) Following the general conditions, the crude mixture was purified by flash chromatography over silica with CH_2Cl_2 and 2% of MeOH and the product was concentrated to dryness. The product was isolated as a white solid (58 mg, 60% yield). ^{1}H-NMR ($CDCl_3$, 400 MHz, 300K) δ, ppm: 8.00 – 7.84 (m, 2H), 7.84 – 7.65 (m, 2H), 3.68 (d, J = 6.7 Hz, 2H), 2.68 (ddd, J = 17.4, 5.5, 2.2 Hz, 1H), 2.60 (dddd, J = 11.6, 10.4, 5.7, 3.6 Hz, 1H), 2.24 – 2.09 (m, 1H), 1.88 (ddd, J = 13.8, 3.6, 2.2 Hz, 1H), 1.47 (s, 3H), 1.38 (s, 3H), 1.28 (s, 1H). ^{13}C-NMR 169.9, 168.4, 134.3, 131.7, 123.5, 81.7, 42.4, 38.5, 33.6, 30.7, 29.2, 27.6. HRMS(ESI+) *m/z* calculated for $C_{16}H_{17}NO_4$ [M+Na]+ 310.1050, found 310.1061.

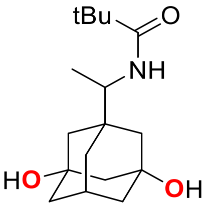

(P15_a): Following the general conditions, the crude mixture was purified by flash chromatography over silica with ethyl acetate and 10% of MeOH and the product was concentrated to dryness. The product was isolated as a white solid (47 mg, 25% yield). ^{1}H-NMR (MeOD, 400 MHz, 300K) δ, ppm: 6.87 (d, J = 9.6 Hz, 1H), 3.86 (dq, J = 9.6, 7.0 Hz, 1H), 2.32 (p, J = 3.2 Hz, 1H), 1.71 – 1.52 (m, 6H), 1.43 (s, 4H), 1.39 – 1.31 (m, 2H), 1.22 (s, 9H), 1.09 (d, J = 7.0 Hz, 3H). ^{13}C-NMR 179.2, 69.78, 69.72, 51.4, 44.8, 44.7, 42.8, 41.7, 38.4, 36.0, 30.6, 26.6, 13.4. HRMS(ESI+) *m/z* calculated for $C_{17}H_{29}NO_3$ [M+Na]+ 318.2040, found 218.2049.

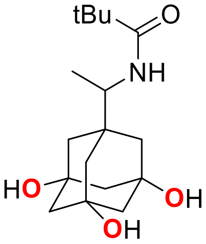

(P15_b): Following the general conditions, the crude mixture was purified by flash chromatography over silica with ethyl acetate and 10% of MeOH and the product was concentrated to dryness. The product was isolated as a white solid (109 mg, 55% yield). ^{1}H-NMR (MeOD, 400 MHz, 300K) δ, ppm: 6.94 (d, J = 9.5 Hz, 1H), 4.04 – 3.83 (m, 1H), 3.52 - 3.50 (m, 1H), 1.75 – 1.47 (m, 6H), 1.39 (s, 6H), 1.22 (s, 9H), 1.11 (d, J = 7.0 Hz, 3H). ^{13}C-NMR 179.3, 70.1, 50.9, 50.5, 43.9, 41.3, 38.4, 26.5, 13.5. HRMS(ESI+) *m/z* calculated for $C_{17}H_{29}NO_4$ [M+Na]+ 334.1989, found 334.1989.

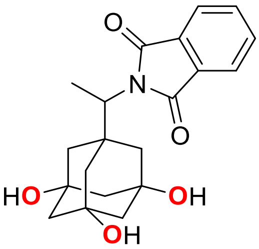

(P16): Following the general conditions, the crude mixture was purified by flash chromatography over silica with ethyl acetate and 10% of MeOH and the product was concentrated to dryness. The product was isolated as a white solid (55 mg, 41% yield). ^{1}H-NMR (MeOD, 400 MHz, 300K) δ, ppm: 7.85 – 7.69 (m, 4H), 4.22 (q, J = 7.3 Hz, 1H), 1.67 (s, 1H), 1.64 – 1.59 (m, 4H), 1.55 (d, J = 1.5 Hz, 4H), 1.53 (d, J = 3.0 Hz, 3H), 1.45 (t, J = 2.2 Hz, 2H), 1.42 (t, J = 2.3 Hz, 1H). ^{13}C-NMR 168.9, 134.6, 131.3, 122.3, 70.0, 55.2, 50.2, 44.9, 44.2, 42.4, 42.2. HRMS(ESI+) *m/z* calculated for $C_{20}H_{23}NO_5$ [M+Na]+ 380.1468, found 380.1468.

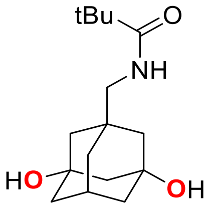

(P17_a) Following the general conditions, the crude mixture was purified by flash chromatography over silica with ethyl acetate and 10% of MeOH and the product was concentrated to dryness. The product was isolated as a white solid (82 mg, 42% yield). ^{1}H-NMR (MeOD, 400 MHz, 300K) δ, ppm: 7.44 (m, 1H), 3.05 (s, 2H), 1.68 – 1.54 (m, 7H), 1.40 (s, 4H), 1.32 (m, 2H), 1.22 (s, 9H). ^{13}C-NMR 180.1, 69.7, 51.4, 48.7, 46.3, 42.8, 39.6, 38.5, 37.8,

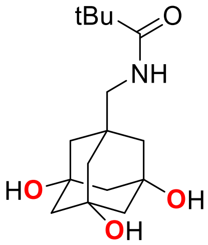

(P17_b) Following the general conditions, the crude mixture was purified by flash chromatography over silica with ethyl acetate and 10% of MeOH and the product was concentrated to dryness. The product was isolated as a white solid (37 mg, 18% yield). ^{1}H-NMR (MeOD, 400 MHz, 300K) δ, ppm: 7.49 (m, 1H), 3.10 (s, 2H), 1.67 – 1.57 (m, 6H), 1.46 (s, 6H), 1.32 (m, 2H), 1.22 (s, 9H). ^{13}C-NMR 180.2, 70.0, 50.4, 45.5, 39.1, 38.5, 26.6. HRMS(ESI+) *m/z* calculated for $C_{16}H_{27}NO_3$ [M+Na]+ 304.1883, found 304.1876. HRMS(ESI+) *m/z* calculated for $C_{16}H_{27}NO_4$ [M+Na]+ 320.1832, found 320.1819.

Experimental Section: Chapter VI.2.

Highly Enantioselective Oxidation of Nonactivated Aliphatic C–H Bonds with Hydrogen Peroxide Catalyzed by Manganese Complexes

1. Synthesis of the Complexes

Pyridine synthons **^{TIPS}PyCHO**[4] and **5-(2,6-bis(trifluoromethyl)phenyl)-2-(chloromethyl)pyridine)**[11] were synthetized following previously described procedure.

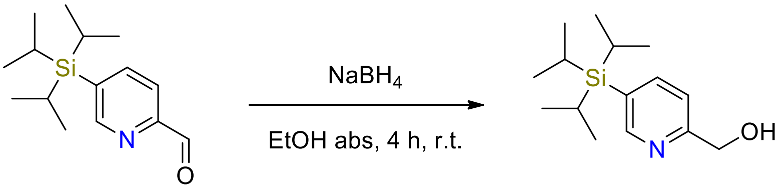

^{TIPS}PyCH$_2$OH: ^{TIPS}PyCHO (5 g, 19 mmol) was dissolved in absolute ethanol (45 ml) and NaBH$_4$ (2 eq., 38 mmol) was directly added as a solid in little portions. The reaction mixture was stirred for 4 hours at room temperature and then 10 ml of water were slowly added. After 10 minutes of stirring, the solvent was removed under reduced pressure and 10 ml of water were added. The mixture was extracted with 3 x 20 ml of CH_2Cl_2, the combined organic phases were dried with anhydrous $MgSO_4$ and the solvent was removed under reduced pressure to yield the desired product, (2.57 g, 9.68 mmol, 51% yield). ^{1}H-NMR (400 MHz, $CDCl_3$, 300 K) δ, ppm 8.62 (dd, *J* = 1.7, 1.0 Hz, 1H), 7.78 (dd, *J* = 7.7, 1.8 Hz, 1H), 7.28 (dd, *J* = 7.7, 0.9 Hz, 1H), 4.78 (s, 2H), 1.42 (hept, *J* = 7.4 Hz, 3H), 1.08 (d, *J* = 7.5 Hz, 18H).^{13}C{^{1}H}-NMR 159.3, 154.1, 143.7, 128.3, 120.1, 64.2, 18.4, 10.9, 10.6. HRMS(ESI-MS) *m/z* calculated for $C_{15}H_{27}NOSi[M+H]+$ 266.1935, found 266.1941.

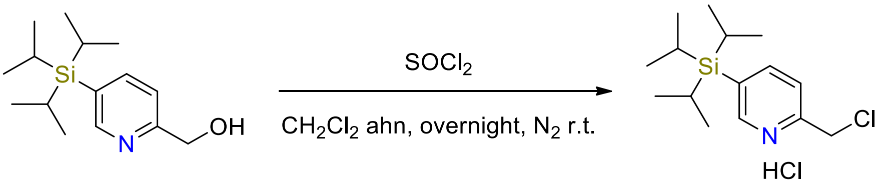

^{TIPS}PyCH$_2$Cl·HCl: ^{TIPS}PyCH$_2$OH (2.50 g, 9.42 mmol) was dissolved in 167 ml of anhydrous CH_2Cl_2 and a solution of $SOCl_2$ (5 equiv., 47.1 mmol) in anhydrous CH_2Cl_2 (20 ml) was slowly added at 0°C under inert atmosphere. The reaction mixture was stirred overnight at room temperature and then the solvent was removed at reduced pressure to yield the desired product, (2.95 g, 9.2 mmol, 98% yield). ^{1}H-NMR (400 MHz, $CDCl_3$, 300 K) δ, ppm 8.61 (s, 1H), 8.19 (d, *J* = 7.2 Hz, 1H), 7.82 (d, *J* = 7.5 Hz, 1H), 5.03 (s, 2H), 1.47 (hept, *J* = 7.4 Hz, 3H), 1.10 (d, *J* = 7.4 Hz, 18H). ^{13}C{^{1}H}-NMR 152.6, 151.3, 144.6, 136.3, 126.2, 39.5, 18.3, 18.2, 18.1, 10.7, 10.4, 10.1. HRMS(ESI-MS) *m/z* calculated for $C_{15}H_{26}NOSiCl[M+H]+$ 284.1596, found 284.1591.

1.1 Synthesis of the Ligands

***N*,*N*-1,2-cyclohexanediamine** derivatives were prepared according to the reported procedures.[12] ^{TIPS}**mcp** and ^{TIPS}**pdp** ligand was prepared according to the reported procedures.[4]

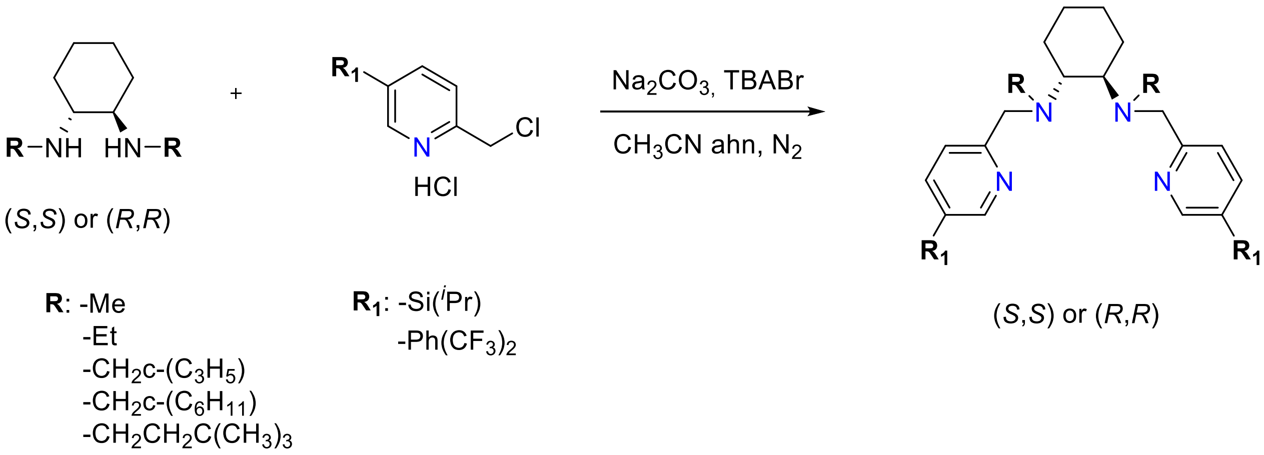

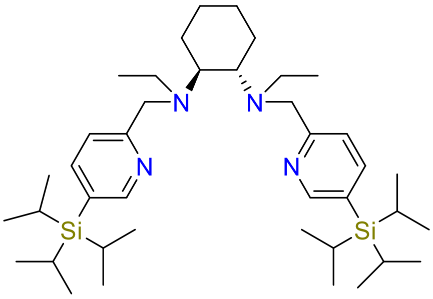

(*S*,*S*)-^{TIPS}ecp: (*S*,*S*)-*N*,*N*-Diethyl-1,2-cyclohexanediamine (0.5 g, 2.9 mmol), **^{TIPS}PyCH$_2$Cl·HCl** (2.08 g, 6.5 mmol), Na_2CO_3 (11 g, 104 mmol) and TBABr (10 mg) was dissolved in anhydrous CH_3CN (100 ml). The reaction mixture was refluxed overnight under N_2. At this point, the crude reaction was filtered and the solvent was evaporated under reduced pressure. NaOH (50 ml) was added and the organic layer was separated from the basic aqueous layer. The aqueous layer was extracted with CH_2Cl_2 (3x) and the organic layer were combined and dried over Na_2SO_4. The obtained brown oil was purified by silica column (CH_2Cl_2:MeOH:NH_3 95:4:1) and the collected fractions were removed under reduced pressure to provide 1.1 g (1.65 mmol, yield 57%) of a brown-yellow oil that turns solid after drying under vacuum. ^{1}H-NMR (400 MHz, $CDCl_3$, 300 K) δ, ppm: 8.45 (t, *J* = 1.3 Hz, 2H), 7.58 (d, *J* = 7.7 Hz, 2H), 7.52 (dd, *J* = 7.8, 1.8 Hz, 2H), 3.83 (d, *J* = 15.2 Hz, 2H), 3.55 (d, *J* = 15.2 Hz, 2H), 2.65 (d, *J* = 7.3 Hz, 2H), 2.49 (ddt, *J* = 20.1, 12.8, 6.6 Hz, 4H), 1.97 (d, *J* = 10.2 Hz, 2H), 1.67 (m, 3H), 1.59 (m, 2H), 1.37-1.24 (m, 6H), 1.00 (dd, *J* = 7.5, 1.1 Hz, 36H), 0.92 (t, *J* = 7.1 Hz, 6H).^{13}C{^{1}H}-NMR 165.5, 154.1, 142.83, 142.75, 127.2, 126.7, 122.7, 122.6, 60.8, 56.4, 53.4, 44.1, 26.1, 25.9, 18.4, 14.3, 10.9, 10.6, 10.4. HRMS(ESI-MS) *m/z* calculated for $C_{40}H_{72}N_4Si_2$[M+H]+ 665.5368, found 665.5366.

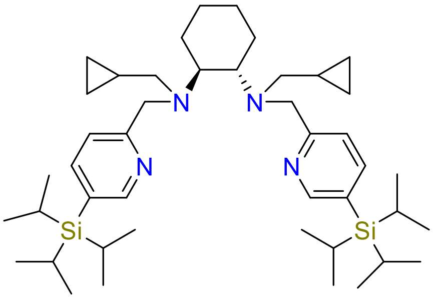

(*S*,*S*)-^{TIPS}cpcp: Following the previous conditions, the crude mixture was purified by flash chromatography over silica using CH_2Cl_2:MeOH:NH_3 96:3:1 and the product was concentrated to dryness. The product was isolated as a yellow oil (0.230 g, 61% yield). ^1H-NMR (400 MHz, $CDCl_3$, 300 K) δ, ppm: 8.49 (d, *J* = 1.6 Hz, 2H), 7.76 (d, *J* = 7.8 Hz, 2H), 7.58 (dd, *J* = 7.8, 1.8 Hz, 2H), 4.05 (d, *J* = 15.1 Hz, 2H), 3.59 (d, *J* = 15.1 Hz, 2H), 2.95 (d, *J* = 7.3 Hz, 2H), 2.63 (dd, *J* = 13.0, 5.4 Hz, 2H), 2.24 (dd, *J* = 13.0, 7.5 Hz, 2H), 2.06 (d, *J* = 10.4 Hz, 2H), 1.75 (d, *J* = 10.4 Hz, 2H), 1.36 (q, *J* = 7.4 Hz, 6H), 1.18 (d, *J* = 11.8 Hz, 4H), 1.05 (d, *J* = 7.8 Hz, 36H), 0.76 (qd, *J* = 8.0, 6.7, 3.8 Hz, 2H), 0.36 (tt, *J* = 8.8, 4.6 Hz, 2H), 0.24 (tt, *J* = 8.9, 4.6 Hz, 2H), 0.02 (dq, *J* = 9.5, 4.9 Hz, 2H), 0.09 (dq, *J* = 9.5, 4.9 Hz, 2H). $^{13}C\{^1H\}$-NMR 162.4, 154.1, 142.6, 126.6, 122.9, 61.2, 56.3, 55.6, 26.1, 25.5, 18.5, 10.6, 5.5, 2.8. HRMS(ESI-MS) *m/z* calculated for $C_{44}H_{76}N_4Si_2$[M+H]+ 717.5681, found 717.5676.

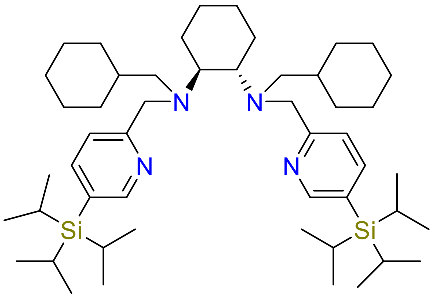

(*S*,*S*)-^{TIPS}chcp: Following the previous conditions, the crude mixture was purified by flash chromatography over silica using CH_2Cl_2:MeOH:NH_3 95:4:1 and the product was concentrated to dryness. The product was isolated as a yellow oil (0.130 g, 41% yield). ^1H-NMR (400 MHz, $CDCl_3$, 300 K) δ, ppm: 8.53 (s, 2H), 7.67 (d, *J* = 1.5 Hz, 4H), 4.03 (d, *J* = 15.2 Hz, 2H), 3.63 (d, *J* = 15.2 Hz, 2H), 2.85 – 2.72 (m, 2H), 2.42 (dd, *J* = 6.8, 3.2 Hz, 4H), 2.14 – 2.05 (m, 2H), 1.76 (m, 4H), 1.65 – 1.48 (m, 8H), 1.40 (p, *J* = 7.5 Hz, 6H), 1.34 – 1.21 (m, 6H), 1.08 (d, *J* = 7.4 Hz, 36H), 1.04 – 0.95 (m, 6H), 0.66 (dtd, *J* = 23.5, 11.8, 8.6 Hz, 4H).$^{13}C\{^1H\}$-NMR 162.4, 154.2, 142.7, 126.6, 122.6, 61.9, 58.9, 36.3, 32.14, 32.09, 26.7, 26.3, 26.2, 26.0, 18.4, 10.6. HRMS(ESI-MS) *m/z* calculated for $C_{50}H_{88}N_4Si_2$[M+H]+ 801.6620, found 801.6605.

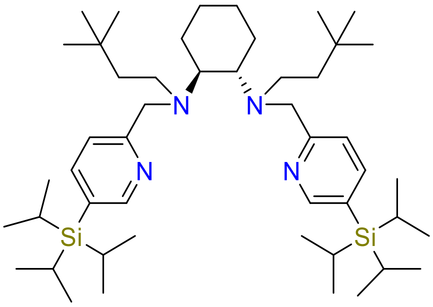

(*S*,*S*)-$^{\mathrm{TIPS}}$tBucp: Following the previous conditions, the crude mixture was purified by flash chromatography over silica using CH_2Cl_2:MeOH:NH_3 95:4:1 and the product was concentrated to dryness. The product was isolated as a brown-yellow oil (0.170 g, 23% yield). ^{1}H-NMR (400 MHz, $CDCl_3$, 300 K) δ, ppm: 8.53 (s, 2H), 7.66 (d, *J* = 7.8 Hz, 2H), 7.60 (dd, *J* = 7.8, 1.8 Hz, 2H), 3.96 (d, *J* = 15.2 Hz, 2H), 3.64 (d, *J* = 15.2 Hz, 2H), 2.76 (d, *J* = 7.7 Hz, 2H), 2.61 – 2.44 (m, 4H), 2.15 – 2.00 (m, 2H), 1.80 – 1.77 (m, 2H) 1.46 – 1.38 (m, 6H), 1.36 – 1.22 (m, 4H), 1.07 (d, *J* = 7.4 Hz, 36H), 1.02 – 0.94 (m, 4H), 0.74 (s, 18H). ^{13}C{^{1}H}-NMR 162.4, 154.1, 142.7, 126.7, 122.7, 61.3, 56.5, 46.8, 42.8, 29.8, 29.4, 26.3, 26.2, 18.4, 10.6. HRMS(ESI-MS) *m/z* calculated for $C_{48}H_{88}N_4Si_2$[M+H]+ 777.6620, found 777.6603.

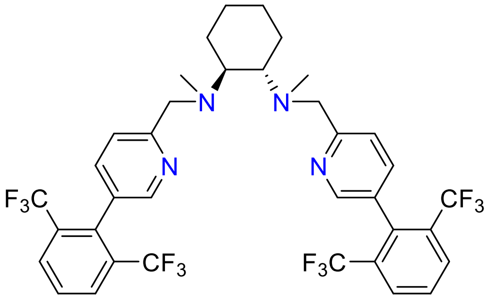

(*S*,*S*)-$^{\mathrm{CF3}}$mcp: Following the previous conditions, the crude mixture was purified by flash chromatography over silica using CH_2Cl_2:MeOH:NH_3 97:2:1 and the product was concentrated to dryness. The product was isolated as a yellow oil (0.210 g, 44% yield). ^{1}H-NMR (400 MHz, $CDCl_3$, 300 K) δ, ppm: 8.39 (s, 2H), 7.99 (dd, *J* = 8.1, 3.7 Hz, 4H), 7.68 (q, *J* = 7.9 Hz, 4H), 7.55 – 7.45 (m, 2H), 4.04 (d, *J* = 14.5 Hz, 2H), 3.87 (d, *J* = 14.5 Hz, 2H), 2.70 (d, *J* = 9.1 Hz, 2H), 2.35 (s, 6H), 2.05 (d, *J* = 12.3 Hz, 2H), 1.81 (d, *J* = 8.6 Hz, 2H), 1.41 – 1.27 (m, 2H), 1.20 (m, 2H). ^{13}C{^{1}H}-NMR 161.6, 148.5, 137.6, 137.0, 131.9, 129.3, 128.5, 127.9, 124.4, 121.3, 64.3, 60.0, 36.8, 25.8, 25.4. HRMS(ESI-MS) *m/z* calculated for $C_{36}H_{32}F_{12}N_4$ [M+H]+ 749.2508, found 749.2518.

1.2 Synthesis of the Complexes

[Fe(CF$_3$SO$_3$)$_2$(mcp)],[2] **[Fe(CF$_3$SO$_3$)$_2$(pdp)]**,[13] **[Fe(CF$_3$SO$_3$)$_2$($^{\mathrm{TIPS}}$mcp)]**,[4] **[Fe(CF$_3$SO$_3$)$_2$($^{\mathrm{TIPS}}$pdp)]**,[4] **[Mn(CF$_3$SO$_3$)$_2$(mcp)]**,[5] **[Mn(CF$_3$SO$_3$)$_2$(pdp)]**,[6] **[Mn(CF$_3$SO$_3$)$_2$($^{\mathrm{dMM}}$mcp)]**,[7] **[Mn(CF$_3$SO$_3$)$_2$($^{\mathrm{Me2N}}$pdp)]**[7] and **[Mn(CF$_3$SO$_3$)$_2$($^{\mathrm{BzIm}}$pdp)]**[14] complexes were prepared according to the reported procedures.

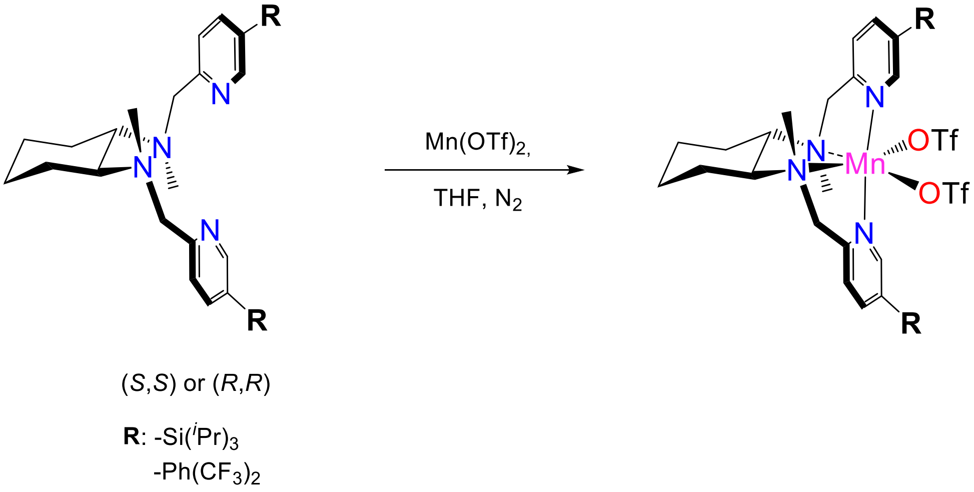

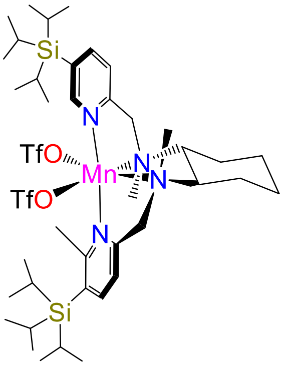

(*R*,*R*)-[Mn(CF$_3$SO$_3$)$_2$($^{\mathrm{TIPS}}$mcp)]: Under N$_2$ atmosphere, a suspension of Mn(CF$_3$SO$_3$)$_2$ (83.1 mg, 0.24 mmol) in anhydrous THF (1 mL) was added drop-wise to a vigorously stirred solution of **(*R*,*R*)- $^{\mathrm{TIPS}}$mcp** (150 mg, 0.24 mmol) in THF (1 mL). After a few second the solution became cloudy and a white precipitate appeared. After stirring for 4 hours the solution was filtered off and the resultant white solid dried under vacuum. This solid was dissolved in CH$_2$Cl$_2$ (3 mL) and the solution filtered off through Celite©. Slow diethyl ether diffusion over the resultant solution afforded, in a few days, white crystals (158 mg, 0.16 mmol, 67% yield). Anal. Calcd for $C_{40}H_{68}F_6MnN_4O_6S_2Si_2$: C, 48.52; H, 6.92; N, 5.66 Found: C, 48.65; H, 6.95; N, 5.76 %. FT-IR (ATR) ν, cm^{-1}: 2943 – 2866 (C-H)sp^3, 1592, 1459, 1311, 1233, 1211, 1164, 1026, 882, 701, 635, 567, 514. ESI-HRMS calcd. for $C_{38}H_{68}N_4Si_2MnCF_3SO_3$ [M-OTf]+: 840.3878, found: 840.3888.

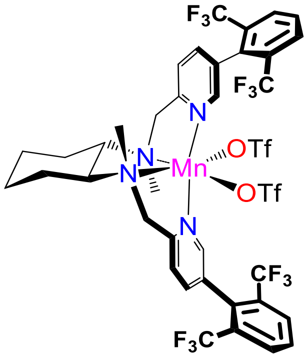

(*S*,*S*)-[Mn(CF_3SO_3)$_2$(^{CF3}mcp)]: Following the previous conditions, white crystals were obtained after slow diethyl ether diffusion in CH_2Cl_2. (286 mg, 0.26 mmol, 68% yield). Anal. Calcd for $C_{38}H_{32}F_{18}MnN_4O_6S_2$: C, 41.43 H, 2.93; N, 5.09 Found: C, 41.20; H, 2.91; N, 4.84 %. FT-IR (ATR) ν, cm^{-1}: 3458 – 2945 (C-H)sp^3, 1612, 1459, 1293, 1127, 1067, 1030, 822, 761, 677, 635, 513. ESI-HRMS calcd. for $C_{36}H_{32}N_4F_{12}MnCF_3SO_3$ [M-OTf]+: 952.1331, found: 952.1346.

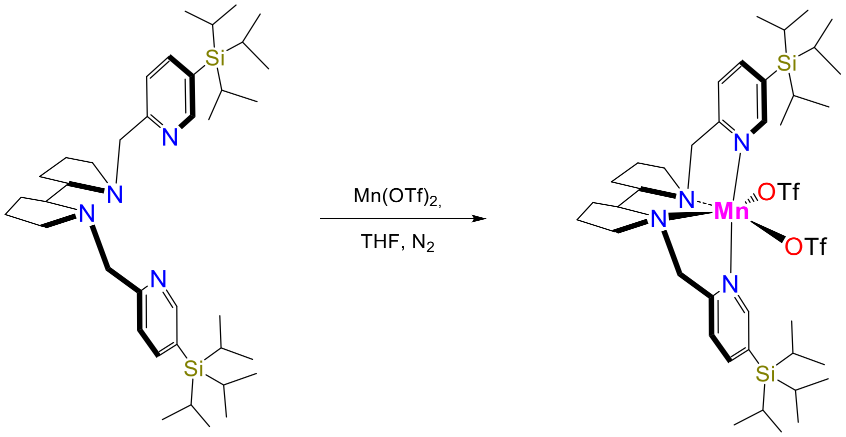

(*S*,*S*)-[Mn(CF_3SO_3)$_2$(^{TIPS}pdp)]: Under N_2 atmosphere, a suspension of Mn(CF_3SO_3)$_2$ (86.5 mg, 0.25 mmol) in anhydrous THF (1 mL) was added drop-wise to a vigorously stirred solution of **(S,*S*)- ^{TIPS}pdp** (159 mg, 0.25 mmol) in THF (1 mL). After a few second the solution became cloudy and a white precipitate appeared. After stirring for 4 hours the solution was filtered off and the resultant white solid dried under vacuum. This solid was dissolved in CH_2Cl_2 (3 mL) and the solution filtered off through Celite©. Slow diethyl ether diffusion over the resultant solution afforded, in a few days, white crystals (155 mg, 0.16 mmol, 64% yield). Anal. Calcd for $C_{40}H_{66}F_6MnN_4O_6S_2Si_2$: C, 48.62; H, 6.73; N, 5.67 Found: C, 48.83; H, 7.05; N, 5.81 %. FT-IR (ATR) ν, cm^{-1}: 2944 – 2866 (C-H)sp^3, 1593, 1463, 1307, 1229, 1030, 983, 882, 760, 682, 636, 514. ESI-HRMS calcd. for $C_{38}H_{66}N_4Si_2MnCF_3SO_3$ [M-OTf]+: 838.3721, found: 838.3723.

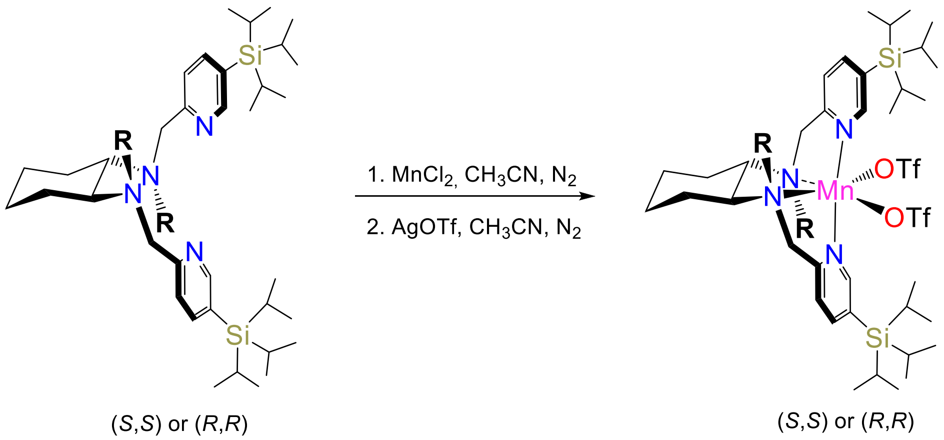

R: $-CH_2CH_3$
$-CH_2c-(C_3H_5)$
$-CH_2c-(C_6H_{11})$
$-CH_2CH_2tBu$

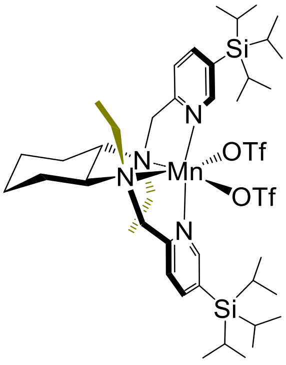

(*S,S*)-[Mn(CF_3SO_3)$_2$(^{TIPS}ecp)]: Under N_2 atmosphere, a suspension of $MnCl_2$ (30.5 mg, 0.24 mmol) in anhydrous CH_3CN (1 mL) was added drop-wise to a vigorously stirred solution of **(*S,S*)- ^{TIPS}ecp** (161 mg, 0.24 mmol) in CH_3CN (1 mL). After 4 hours 2 equiv. of $AgCF_3SO_3$ (123.3 mg, 0.48 mmol) were added to the solution. After 2 hours, the reaction mixture was filtered through Celite© and dried under vacuum. The solid was crystallized by layering CH_2Cl_2 solution of the complex with hexane to yield the desired white/brown complex (163 mg, 0.16 mmol, 68% yield). Anal. Calcd for $C_{42}H_{72}F_6MnN_4O_6S_2Si_2$: C, 49.54; H, 7.13; N, 5.5 %. Found: C, 49.71; H, 7.35; N, 5.80 %. FT-IR (ATR) ν, cm^{-1}: 2944 – 2866 (C-H)sp^3, 1592, 1462, 1309, 1211, 1163, 1111, 1028, 882, 683, 636, 568, 514. ESI-HRMS calcd. for $C_{40}H_{72}N_4Si_2MnCF_3SO_3$ [M-OTf]+: 868.4191, found: 868.4200.

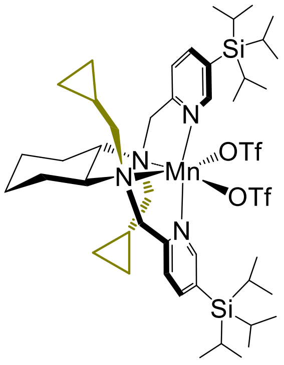

(*S,S*)-[Mn(CF_3SO_3)$_2$(^{TIPS}cpcp)]: Following the previous conditions, white crystals were obtained by layering CH_2Cl_2 solution of the complex with hexane. (153 mg, 0.14 mmol, 48% yield). Anal. Calcd for $C_{46}H_{76}F_6MnN_4O_6S_2Si_2$: C, 51.62; H, 7.16; N, 5.23 %. Found: C, 51.32; H, 7.06; N, 5.29 %. FT-IR (ATR) ν, cm^{-1}: 2944 – 2866 (C-H)sp^3, 1592, 1462, 1311, 1233, 1210, 1163, 1025, 882, 704, 682, 634, 569, 513. ESI-HRMS calcd. for $C_{44}H_{76}N_4Si_2MnCF_3SO_3$ [M-OTf]+: 920.4504, found: 920.4482.

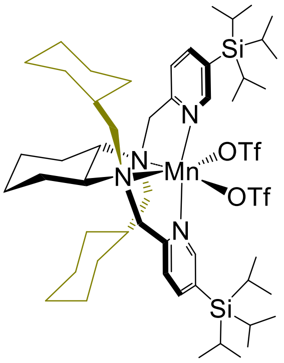

(*S,S*)-[Mn(CF_3SO_3)$_2$(^{TIPS}chcp)]: Following the previous conditions, white crystals were obtained by layering CH_2Cl_2 solution of the complex with hexane. (127 mg, 0.11 mmol, 51% yield). Anal. Calcd for $C_{52}H_{88}F_6MnN_4O_6S_2Si_2$: C, 54.10; H, 7.68; N, 4.85 %. Found: C, 49.71; H, 7.50; N, 4.98 %. FT-IR (ATR) ν, cm^{-1}: 2944 – 2866 (C-H)sp^3, 1592, 1462, 1311, 1233, 1210, 1163, 1025, 882, 704, 682, 634, 569, 513. ESI-HRMS calcd. for $C_{50}H_{88}N_4Si_2MnCF_3SO_3$ [M-OTf]+: 1004.5443, found: 1004.5470.

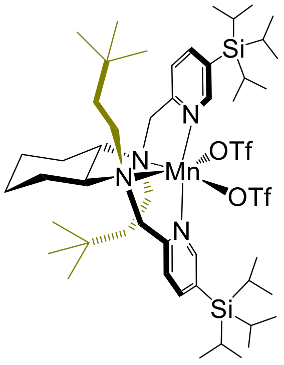

(*S,S*)-[Mn(CF_3SO_3)$_2$(^{TIPS}*t*Bucp)]: Following the previous conditions, white/ brown crystals were obtained by layering CH_2Cl_2 solution of the complex with hexane. (98 mg, 0.087 mmol, 41% yiel). Anal. Calcd for $C_{50}H_{88}F_6MnN_4O_6S_2Si_2$: C, 53.12; H, 7.85; N, 4.96 %. Found: C, 53.50; H, 8.05; N, 4.91 %. FT-IR (ATR) ν, cm^{-1}: 2944 – 2866 (C-H)sp^3, 1592, 1463, 1311, 1209, 1165, 1025, 881, 682, 635, 569, 514. ESI-HRMS calcd. for $C_{49}H_{88}N_4Si_2MnCF_3SO_3$ [M-OTf]+: 980.5448, found: 980.5451.

2. Synthesis of the Substrates

The following substrates were prepared according to the reported procedures. All the remaining ones are commercially available.

S2[15]
S3[16]
S8, **S9**, **S10**, **S11**, **S12**, **S13, S15**[17]
S18[18]
S19[19]
S20, S21, S22[20]

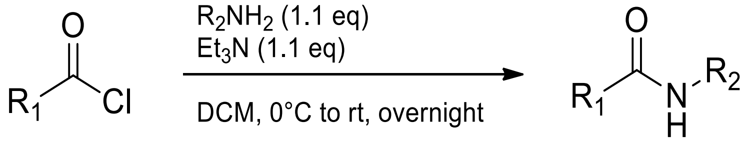

A round-bottom flask equipped with a septum and kept under nitrogen was charged with a 0.20 M solution of the amine (1.1 equiv) in dichloromethane and cooled to 0 °C. Triethylamine (1.1 equiv) was added to the reaction flask. The acyl chloride (1.0 equiv) was added dropwise and the reaction was stirred overnight at room temperature. At this point, a saturated aqueous Na_2CO_3 solution was added until pH~10-11 and then diluted with dichloromethane. The organic layer was separated from the basic aqueous layer. The aqueous layer was extracted with dichloromethane (2x) and the organic layers were combined. The organic layer was washed with 1N HCl and dried over anhydrous sodium sulfate (Na_2SO_4). The organic layer was evaporated to dryness and the crude amine was purified by flash chromatography over silica gel.

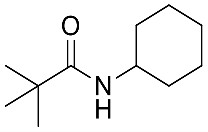

***N*-Cyclohexylpivalamide (S8):** Following the general conditions, the crude mixture was purified by flash chromatography over silica using hexane:ethyl acetate 1:1 and the product was concentrated to dryness. The product was isolated as a white solid (0.38 g, 79% yield).

^{1}H-NMR ($CDCl_3$, 400 MHz, 300K) δ, ppm: 5.46 (bs, 1H), 3.75 - 3.73 (m, 1H), 1.92 - 1.86 (m, 2H), 1.73 - 1.57 (m, 3H), 1.44 - 1.30 (m, 3H), 1.18 (s, 9H), 1.14 – 1.04 (m, 2H). ^{13}C-NMR 177.4, 47.9, 38.5, 33.1, 27.6, 25.6, 24.9 HRMS(ESI+) *m/z* calculated for $C_{11}H_{21}NO$ [M+Na]+ 206.1515, found 206.1512.

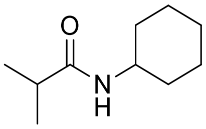

N-Cyclohexylisobutyramide (S9): Following the general conditions, the crude mixture was purified by flash chromatography over silica using hexane:ethyl acetate 1:1 and the product was concentrated to dryness. The product was isolated as a white solid (0.43 g, 83% yield).

^{1}H-NMR ($CDCl_3$, 400 MHz, 300K) δ, ppm: 5.34 (bs, 1H), 3.82 - 3.70 (m, 1H), 2.35 - 2.28 (q, 1H), 1.94 - 1.88 (m, 2H), 1.74 - 1.60 (m, 3H), 1.43 – 1.31 (m, 2H), 1.23 – 1.21 (m, 1H), 1.15 (d, 6H), 1.10 - 1.0 (m, 2H). ^{13}C-NMR 176.0, 47.8, 35.8, 33.2, 25.6, 24.9, 19.7. HRMS(ESI+) *m/z* calculated for $C_{10}H_{19}NO$ [M+Na]+ 192.1359, found 192.1358.

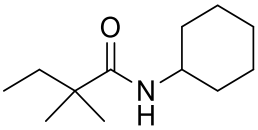

N-(cyclohexyl)-2,2-dimethylbutanamide (S10): Following the general conditions, the crude mixture was purified by flash chromatography over silica using hexane:ethyl acetate 1:1 and the product was concentrated to dryness. The product was isolated as a white solid (0.56 g, 97% yield). ^{1}H-NMR ($CDCl_3$, 400 MHz, 300K) δ, ppm: 5.45 (bs, 1H), 3.86 – 3.66 (m, 1H), 1.96 – 1.80 (m, 2H), 1.75 – 1.55 (m, 4H), 1.51 (q, *J* = 7.5 Hz, 2H), 1.44 – 1.27 (m, 2H), 1.22 – 1.14 (m, 1H), 1.12 (s, 6H), 1.10 – 1.02 (m, 1H), 0.82 (t, *J* = 7.5 Hz, 3H) .^{13}C-NMR 176.6, 47.9, 42.1, 33.9, 33.2, 25.6, 25.0, 24.9, 9.1. HRMS(ESI+) *m/z* calculated for $C_{12}H_{23}NO$ [M+Na]+ 220.1672, found 220.1673.

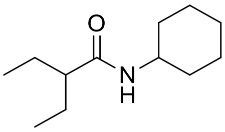

N-(cyclohexyl)-2-ethylbutanamide (S11): Following the general conditions, the crude mixture was purified by flash chromatography over silica using hexane:ethyl acetate 1:1 and the product was concentrated to dryness. The product was isolated as a white solid (0.65 g, 84% yield). ^{1}H-NMR ($CDCl_3$, 400 MHz, 300K) δ, ppm: 5.62 (bs, 1H), 3.78 (tdt, *J* = 10.7, 8.1, 3.9 Hz, 1H), 1.87 (dd, *J* = 12.5, 3.8 Hz, 2H), 1.79 (tt, *J* = 9.3, 5.1 Hz, 1H), 1.67 (dt, *J* = 13.2, 3.6 Hz, 2H), 1.62 – 1.50 (m, 3H), 1.46 – 1.26 (m, 4H), 1.18 – 1.05 (m, 3H), 0.88 – 0.80 (t, *J* = 7.4 Hz, 6H). ^{13}C-NMR 174.6, 51.4, 47.8, 33.3, 25.8, 25.5, 24.9, 12.0. HRMS(ESI+) *m/z* calculated for $C_{12}H_{23}NO$ [M+Na]+ 220.1672, found 220.1673.

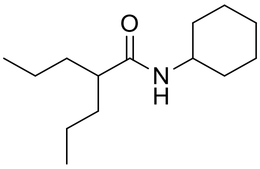

N-(cyclohexyl)-2-propylbutanamide (S12): Following the general conditions, the crude mixture was purified by flash chromatography over silica using hexane:ethyl acetate 1:1 and the product was concentrated to dryness. The product was isolated as a white solid (0.53 g, 80% yield). ^{1}H-NMR (CDCl$_3$, 400 MHz, 300K) δ, ppm: 5.39 (bs, 1H), 3.90 – 3.70, (m, 1H), 2.04 – 1.81 (m, 3H), 1.76 – 1.51 (m, 5H), 1,45 – 1.19 (m, 8H), 1.12 (ddd, *J* = 23.0, 12.1, 3.4 Hz, 3H), 0.88 (t, *J* = 7.1 Hz, 6H). ^{13}C-NMR 174.9, 47.9, 47.8, 35.4, 33.4, 25.6, 24.9, 20.8, 14.1 HRMS(ESI+) *m/z* calculated for $C_{14}H_{27}NO$ [M+Na]+ 248.1985, found 248.1981.

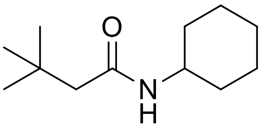

N-(cyclohexyl)-3,3-dimethylbutanamide (S13): Following the general conditions, the crude mixture was purified by flash chromatography over silica using hexane:ethyl acetate 1:1 and the product was concentrated to dryness. The product was isolated as a white solid (0.75 g, 85% yield). ^{1}H-NMR (CDCl$_3$, 400 MHz, 300K) δ, ppm: 5.26 (bs, 1H), 3.84 - 3.77 (m, 1H), 2.02 (s, 2H), 1.99 - 1.86 (m, 2H), 1.77 - 1.55 (m, 3H), 1.47 - 1.28 (m, 2H), 1.25 – 1.07 (m, 3H), 1.04 (s, 9H). ^{13}C-NMR 170.6, 50.9, 48.0, 33.3, 30.8, 29.8, 25.6, 24.9 HRMS(ESI+) *m/z* calculated for $C_{12}H_{23}NO$ [M+Na]+ 220.1672, found 220.1667.

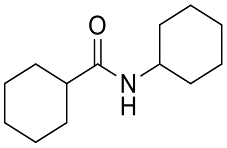

N-Cyclohexylcyclohexanecarboxamide (S15): Following the general conditions, the crude mixture was purified by flash chromatography over silica using hexane:ethyl acetate 1:1 and the product was concentrated to dryness. The product was isolated as a white solid (0.32 g, 53% yield). ^{1}H-NMR (CDCl$_3$, 400 MHz, 300K) δ, ppm: 5.34 (bs, 1H), 3.85 - 3.64 (m, 1H), 2.02 (tt, *J* = 11.7, 3.4 Hz 1H), 1.93 - 1.58 (m, 10H), 1.47 - 1.03 (m, 10H). ^{13}C-NMR 175.1, 47.7, 45.7, 33.3, 30.9, 29.7, 26.5, 25.8, 24.9 HRMS(ESI+) *m/z* calculated for $C_{13}H_{23}NO$ [M+Na]+ 232.1672, found 232.1678.

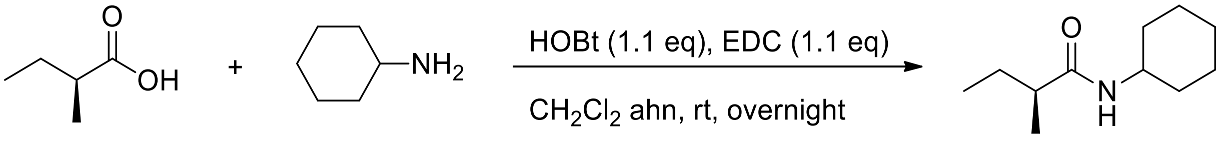

***N*-(cyclohexyl)-(S)-(+)-2-methylbutanamide (S14):** Following the traditional methodology used for peptide synthesis, the product was isolated as a white solid (0.85 g, 85% yield). ^{1}H-NMR ($CDCl_3$, 400 MHz, 300K) δ, ppm: 5.41 (bs, 1H), 3.79 (tdt, *J* = 12.2, 8.1, 3.9 Hz, 1H), 2.02 (dq, *J* = 13.5, 6.8 Hz, 1H), 1.92-1.88 (m, 2H), 1.73 - 1.56 (m, 4H), 1.49 – 1.28 (m, 4H), 1.21-1.17 (m, 2H), 1.12 (dd, *J* = 12.4, 7.9 Hz, 3H), 0.89 (t, *J* = 7.4 Hz, 3H). ^{13}C-NMR 175.4, 47.8, 43.3, 33.4, 27.4, 25.6, 24.9, 17.6, 11.9. HRMS(ESI+) *m/z* calculated for $C_{11}H_{21}NO$ [M+Na]+ 206.1515, found 206.1517.

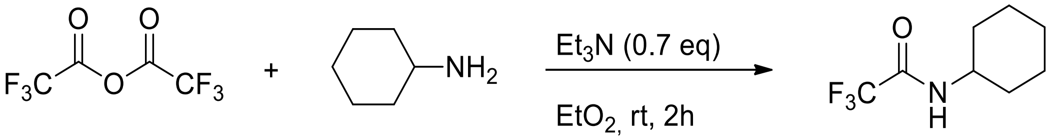

***N*-Cyclohexyltrifluoroacetamide (S17):** A round-bottom flask equipped with a septum and kept under nitrogen was charged with cyclohexylamine (1.0 equiv, 0.24 g, 2.4 mmol) and solubilized in diethylether (1.4 M). Triethylamine (0.7 equiv) was added to the reaction flask. Trifluoroacetic anhydride (1.0 equiv, 0.5 g, 2.4 mmol) in diethylether (1.4 M) was added dropwise and the reaction was stirred for 2 hours at room temperature. At this point H_2O was added and the basic aqueous layer was separated. The organic layer was extracted with $NaHCO_3$, saturated with NH_4Cl and dried over anhydrous sodium sulfate (Na_2SO_4). The organic layer was evaporated to dryness and the crude amine was purified by flash chromatography over silica gel using hexane:ethyl acetate 1:1 and the product was concentrated to dryness. The product was isolated as a white solid (0.25 g, 1.3 mmol 54% yield). ^{1}H-NMR ($CDCl_3$, 400 MHz, 300K) δ, ppm: 6.24 (bs, 1H), 3.94 - 3.69 (m, 1H), 2.08 – 1.88 (m, 2H), 1.87 - 1.59 (m, 3H), 1.52 – 1.08 (m, 5H). ^{13}C-NMR 156.5, 117.8, 113.9, 100.0, 49.2, 32.4, 25.2, 24.6 HRMS(ESI+) *m/z* calculated for $C_8H_{12}F_3NO$ [M+Na]+ 218.0763, found 218.0762.

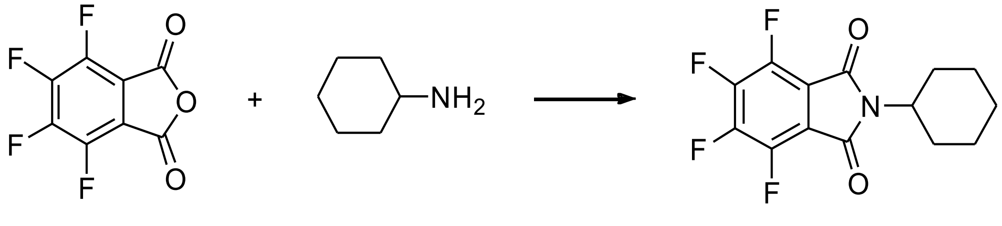

***N*-Cyclohexyltetrafluorophthalimide (S19):** Tetrafluorophthalic anhydride (0.5 g, 2.3 mmol, 1.2 eq.) was added to a solution of cyclohexylamine (0.19 g, 1.9 mmol, 1.0 eq.) in glacial acetic acid and refluxed overnight. The solvent was removed under reduced pressure and the reaction mixture was refluxed in acetic anhydride for 12 h. The solvent was evaporated and the crude amide was purified by flash chromatography over silica gel with hexane:ethyl acetate 3:1 and the product was concentrated to dryness. The product was isolated as a yellow solid (0.24 g, 82% yield). ^{1}H-NMR ($CDCl_3$, 400 MHz, 300K) δ, ppm: 4.08 (t, *J* = 12.4 Hz, 1H), 2.26 – 2.06 (m, 2H), 1.87 (d, *J* = 13.0 Hz, 2H), 1.70 (d, *J* = 12.0 Hz, 3H), 1.47 – 1.13 (m, 3H).

^{13}C-NMR 162.5, 146.2, 144.5, 143.5, 141.9, 113.8, 51.9, 29.6, 25.9, 24.9. HRMS(ESI+) *m/z* calculated for $C_{14}H_{11}F_4NO_2(CH_3OH)$ [M+Na]+ 356.0880, found 356.0885.

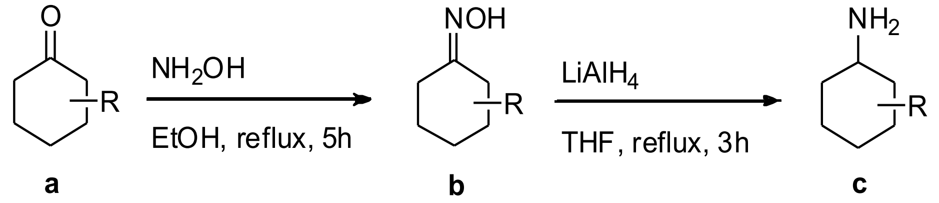

Hydroxylamine hydrochloride (1.2 equiv) followed by pyridine (3.0 equiv) was added to a solution of ketone (**a**) (1.0 equiv) in absolute ethanol and the reaction mixture was heated to reflux temperature under stirring for 5 hours. The reaction was then quenched with water and the product extracted with ethyl acetate (2 x 50 mL). The organic fractions were washed with water and dried over anhydrous $MgSO_4$. The solvent was removed under vacuum to obtain the oxime (**b**) that was used in the next step without further purification. To a stirred solution of lithium aluminium hydride (0.5 equiv) in anhydrous THF under N_2, was added a solution of intermediate **b** drop wise. The reaction was slowly heated to reflux temperature for 3 hours. After this, the reaction mixture was quenched with 1M NaOH solution at 5°C. After filtration through Celite© and extraction with ethyl acetate (2 x 50 mL) the organic fractions were dried over anhydrous $MgSO_4$, the solvent removed under vacuum and the obtained intermediate **c** was used in the next acylation step without further purification to give the corresponding amide.

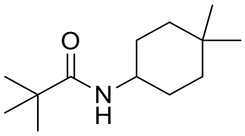

***N*-(4,4-dimethylcyclohexyl)pivalamide (S20):** Following the general conditions, the crude mixture was purified by flash chromatography over silica using hexane:ethyl acetate 1:1 and the product was concentrated to dryness. The product was isolated as a white solid (0.39 g, 94% yield). ^{1}H-NMR ($CDCl_3$, 400 MHz, 300K) δ, ppm: 5.49 (s, 1H), 3.68 (tt, *J* = 9.2, 4.8 Hz, 1H), 1.75-1.72 (m, 2H), 1.38 – 1.17 (m, 6H), 1.17 (s, 9H), 0.91 (s, 6H).^{13}C-NMR 177.6, 48.1, 38.5, 37.6, 31.5, 29.5, 28.7, 27.6, 25.1. HRMS(ESI+) *m/z* calculated for $C_{13}H_{25}NO$ [M+Na]+ 234.1828, found 234.1822.

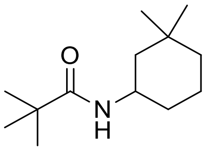

***N*-(3,3-dimethylcyclohexyl)pivalamide (S21):** Following the general conditions, the crude mixture was purified by flash chromatography over silica using hexane:ethyl acetate 1:1 and the product was concentrated to dryness. The product was isolated as a white solid (0.38 g, 70% yield). ^{1}H-NMR ($CDCl_3$, 400 MHz, 300K) δ, ppm: 5.32 (d, *J* = 7.0 Hz, 1H), 3.88 (tdt, *J* = 12.0, 8.0, 4.1 Hz, 1H), 1.95 – 1.92 (m, 1H), 1.64 – 1.46 (m, 4H), 1.35 – 1.31 (m, 1H), 1.15 (s, 9H), 1.09 – 0.99 (m, 2H), 0.94 (s, 3H), 0.91 (s, 3H), 0.88-0.84 (m, 1H).^{13}C-NMR 177.5, 46.0, 45.2, 38.53, 38.46, 33.3, 33.0, 31.7, 27.6, 24.7, 21.3. HRMS(ESI+) *m/z* calculated for $C_{13}H_{25}NO$ [M+Na]+ 234.1828, found 234.1826.

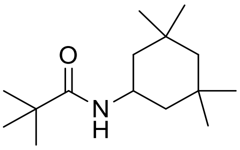

***N*-(3,3,5,5-tetramethylcyclohexyl)pivalamide (S22):** Following the general conditions, the crude mixture was purified by flash chromatography over silica using hexane:ethyl acetate 1:1 and the product was concentrated to dryness. The product was isolated as a white solid (0.41 g, 55% yield). ^{1}H-NMR ($CDCl_3$, 400 MHz, 300K) δ, ppm: ^{1}H NMR (300 MHz, Chloroform-*d*) δ 5.35 (d, *J* = 7.5 Hz, 1H), 4.07 (dtd, *J* = 12.0, 8.2, 3.9 Hz, 1H), 1.70 (dddd, *J* = 11.4, 3.7, 2.2, 1.3 Hz, 2H), 1.36 – 1.19 (m, 2H), 1.18 (s, 9H), 1.07 (s, 6H), 0.91 (s, 6H), 0.84 (d, *J* = 12.0 Hz, 2H).^{13}C-NMR 177.6, 51.7, 46.1, 43.3, 38.5, 35.1, 32.2, 27.6, 27.3. HRMS(ESI+) *m/z* calculated for $C_{15}H_{29}NO$ [M+Na]+ 262.2141, found 262.2139.

3. Reaction Protocol for Catalysis

An acetonitrile solution (400 µL) of the substrate (0.25 M) and the corresponding complex (2.5 mM) was prepared in a vial (10 mL) equipped with a stir bar cooled at -40 ºC, in a CH_3CN/N_2(liq) bath. 98 µL (neat, 17 equiv.) of acetic acid were added directly to the solution. Then, 236 µL of a 1.5 M hydrogen peroxide solution in CH_3CN (3.5 equiv.) were added by syringe pump over a period of 30 min. At this point, an internal standard (biphenyl) was added and the solution was quickly filtered through a basic alumina plug, which was subsequently rinsed with 2 x 1 mL AcOEt. GC analysis of the solution provided substrate conversions and product yields relative to the internal standard integration. Isomer ratio was determined by GC or ^{1}H-NMR. Commercially unavailable products were identified by a combination of ^{1}H, $^{13}C\{^{1}H\}$-NMR analysis, and HRMS. The oxidized products were identified by comparison to the GC retention time of racemate products.

Attempts to trap the alcohol product were performed by carrying out catalytic reactions in the presence of acetic anhydride or trifluoroacetic anhydride. Unfortunately, under these conditions oxidation did not take place. Reactions performed using substoichiometric amounts of oxidant, providing low conversion of the substrate did not result in the accumulation of the alcohol, indicating that this initial product is much more reactive against oxidation than the starting material, and cannot accumulate in solution.

Table S1. Oxidation of N-(cyclohexyl)pivalamide (S8) with (*S,S*)-[Mn(CF_3SO_3)$_2$(^{TIPS}cpcp)], (*S,S*)-[Mn(CF_3SO_3)$_2$ (^{TIPS}chcp)] and (*S,S*)-[Mn(CF_3SO_3)$_2$ (^{TIPS}tBucp)]

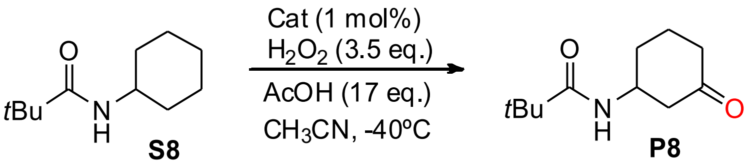

Entry	Cat.	Conv (%)[a]	Yield (%)[a]	Ee %
1	**Mn(^{TIPS}cpcp)**	85	60	80
2	**Mn(^{TIPS}chcp)**	22	10	86
3	**Mn(^{TIPS}tBucp)**	31	20	56

[a] Conversions and yields determined from crude reaction mixtures by GC. Ee's determined by GC with chiral stationary phase

Table S2. Oxidation of N-(cyclohexyl)pivalamide (S8) with (*R,R*)-[Mn(CF_3SO_3)$_2$ (^{TIPS}mcp)] using different equivalents of acetic acid

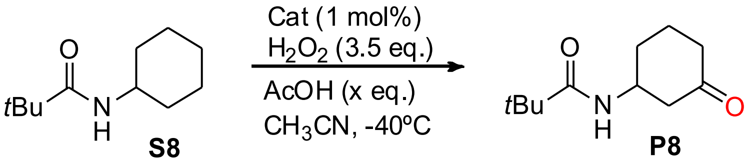

Entry	x (equiv)	Conv (%)[a]	Yield K_3 (%)[a]	Ee %
1	**50**	>99	90	72
2	**25**	>99	90	73
3	**17**	>99	90	79
4	**13**	>99	84	79
5	**10**	80	74	74
6	**8**	86	74	78
7	**5**	33	28	75

[a] Conversions and yields determined from crude reaction mixtures by GC. Ee's determined by GC with chiral stationary phase

3.1 General Procedure for Product Isolation

25 mL round bottom flask was charged with: catalyst (6 µmol, 1.0 mol%), substrate (1 equiv.), CH_3CN (3.3 mL) and a magnetic stir bar. The carboxylic acid of choice was the added (17 equiv.) and the mixture was cooled at -40 ºC in an CH_3CN/N_2(liq) bath under magnetic stirring.

Then, 1.4 mL of a 1.5 M hydrogen peroxide solution in CH_3CN (3.5 equiv.) were added by syringe pump over a period of 30 min at -40°C. At this point, 15 mL of an aqueous $NaHCO_3$ saturated solution were added to the mixture. The resultant solution was extracted with CH_2Cl_2 (3 x 10 mL). Organic fractions were combined, dried over $MgSO_4$, and the solvent was removed under reduced pressure to afford the oxidized product. This residue was filtered by silica gel column to obtain the pure product.

4. Characterization of the Isolated Products

The oxidation products obtained after oxidation of substrates **S1**, **S3**, **S4**, **S5**, **S6**, **S18** and **S19** (**P1**, **P3**, **P4**, **P5**, **P6, P18, P19**, respectively) were collected as mixtures of C3 and C4 oxidation products.

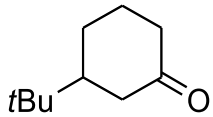

3-*tert*-butylcyclohexanone (P1 (K_3)) purification by flash chromatography (SiO_2; hexane:AcOEt 5:1) gave the product as a white solid (50% total yield (K_3+K_4), 64% ee K_3); ^{1}H-NMR ($CDCl_3$, 400 MHz, 300K) δ, ppm: 2.45-2.43 (m, 1H), 2.37-2.35 (m, 1H), 2.23 (dt, J = 6.0, 13.5 Hz, 1H), 2.12-2.08 (m, 1H), 2.04 (t, J = 12.0 Hz, 1H), 1.96-1.91 (m, 1H), 1.59-1.45 (m, 2H), 1.32 (qd, J = 3.6, 12.8 Hz, 1H), 0.89 (s, 9H). HRMS(ESI+) *m/z* calculated for $C_{10}H_{18}O$ [M+Na]+ 177.1250, found 177.1250. Chiral GC analysis with CYCLOSIL-B. Spectroscopic data are in agreement with a previous literature report.[21]

4-*tert*-butylcyclohexanone (P1 (K_4)) ^{1}H-NMR ($CDCl_3$, 400 MHz, 300K) δ, ppm: 2.41-2.39 (m, 1H), 2.33-2.31 (m, 1H), 2.23 (dt, J = 6.0, 13.5 Hz, 1H), 2.12-2.08 (m, 1H), 2.04 (t, J = 12.0 Hz, 1H), 1.96-1.91 (m, 1H), 1.59-1.45 (m, 2H), 1.32 (qd, J = 3.6, 12.8 Hz, 1H), 0.89 (s, 9H). ^{13}C-NMR 212.9, 49.4, 43.6, 41.3, 32.7, 27.2, 26.2, 25.6. Spectroscopic data are in agreement with a previous literature report.[21]

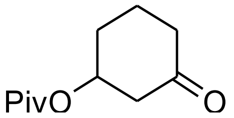

3-oxocyclohexylpivalate (P2 (K_3)) purification by flash chromatography (SiO_2; hexane:AcOEt 5:1) gave the product as a white solid (36% yield, 61% ee); ^{1}H-NMR ($CDCl_3$, 400 MHz, 300K) δ, ppm: 5.18 (tt, *J* = 5.7, 3.0 Hz, 1H), 2.57 (ddd, *J* = 15.8, 10.2, 6.1 Hz, 2H), 2.42 – 2.36 (m, 2H), 2.19 – 2.02 (m, 4H), 1.26 (s, 9H). ^{13}C-NMR 209.9, 177.8, 68.0, 39.0, 37.2, 30.4, 27.2. HRMS(ESI+) *m/z* calculated for $C_{11}H_{18}O_3$ [M+Na]+ 221.1148, found 221.1146. $[\alpha]_D^{24}$ +9.3 ($CHCl_3$, *c* 0.333). Chiral GC analysis with CYCLOSIL-B.

4-oxocyclohexylpivalate (P2 (K_4)) white solid product (9% yield); ^{1}H-NMR ($CDCl_3$, 400 MHz, 300K) δ, ppm: 5.28 (tt, *J* = 5.5, 2.8 Hz, 1H), 2.64 (dd, *J* = 14.8, 4.2 Hz, 1H), 2.56 – 2.35 (m, 4H), 2.07 (dd, *J* = 11.3, 4.6 Hz, 1H), 1.98 (d, *J* = 7.9 Hz, 1H), 1.93 – 1.85 (m, 1H), 1.20 (s, 9H). ^{13}C-NMR 208.3, 177.5, 71.2, 46.4. 41.0, 29.7, 29.1, 27.1, 20.9. HRMS(ESI+) *m/z* calculated for $C_{11}H_{18}O_3$ [M+Na]+ 221.1148, found 221.1140.

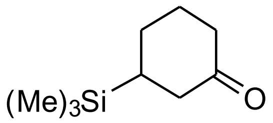

P3 (K_3)

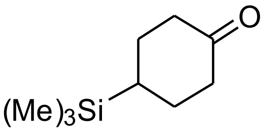

P3 (K_4)

(P3 (K_3+K_4), (*R*,*R'*)-Mn-(^{TIPS}mcp) as catalyst and cyclopropanecarboxylic acid) purification by flash chromatography (SiO_2; hexane:AcOEt 3:1) gave the product as a white solid (49% total yield, 34% ee); ^{1}H-NMR ($CDCl_3$, 400 MHz, 300K) δ, ppm: 1.81 – 1.70 (m, 8H), 1.29 – 1.21 (m, 5H), 1.10 (q, *J* = 12.7 Hz, 4H), 0.67 – 0.48 (m, 1H), -0.03 (s, *J* = 0.7 Hz, 18H). ^{13}C-NMR 28.1, 27.4, 27.0, 26.2, -3.6. HRMS(ESI+) *m/z* calculated for $C_9H_{18}OSi$ [M+Na]+ 193.1019, found 193.1019. Chiral GC analysis with CYCLOSIL-B.

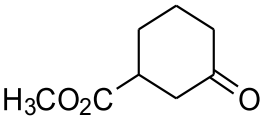

methyl-3-oxocyclohexanecarboxylate (P4 (K_3)) purification by flash chromatography (SiO_2; hexane:AcOEt 4:1) gave the product as a white solid (52% total yield (K_3+K_4), 11% ee K_3); ^{1}H-NMR ($CDCl_3$, 400 MHz, 300K) δ, ppm: 3.69 (s, 3H), 2.84-2.75 (m, 1H), 2.55 (d, J = 8.0 Hz, 2H), 2.40-2.29 (m, 2H), 2.13-2.02 (m, 2H), 1.87-1.81 (m, 1H), 1.77-1.69 (m, 1H). HRMS(ESI+) *m/z* calculated for $C_8H_{12}O_3$ [M+Na]+ 179.0679, found 179.0680. Chiral GC analysis with CYCLOSIL-B. Spectroscopic data are in agreement with a previous literature report.[22]

methyl-4-oxocyclohexanecarboxylate (P4 (K_4)) ^{1}H-NMR ($CDCl_3$, 400 MHz, 300K) δ, 3.71 (s, 3H), 2.83- 2.75 (m, 1H), 2.50-2.46 (m, 2H), 2.40-2.29 (m, 2H), 2.23-2.19 (m, 2H), 2.13-2.02 (m, 2H). Spectroscopic data are in agreement with a previous literature report.[23]

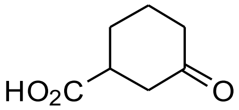

P5 (K_3)

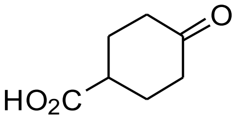

P5 (K_4)

(**P5 (K_3+K_4))** purification by flash chromatography (SiO_2; hexane:AcOEt 2:1) gave the product as a white solid (30% total yield, 9% ee K_3); ^{1}H-NMR ($CDCl_3$, 400 MHz, 300K) δ, ppm: 2.93-2.80 (m, 2H), 2.61-2.58 (m, 2H), 2.56-2.50 (m, 2H), 2.44-2.36 (m, 4H), 2.30-2.23 (m, 2H), 2.22-2.16 (m, 1H), 2.14-2.03 (m, 3H), 1.96-1.87 (m, 1H), 1.84-1.74 (m, 1H). ^{13}C-NMR 209.9, 209.0, 180.4, 179.4, 42.9, 42.7, 40.9, 40.3, 39.6, 29.7, 28.2, 27.5, 24.3. HRMS(ESI+) *m/z* calculated for $C_7H_9O_3$ [M] 141.0546, found 141.0563. Chiral GC analysis with CYCLOSIL-B. Spectroscopic data are in agreement with a previous literature report.[24] The ee was determined after esterification following a reported procedure.[24]

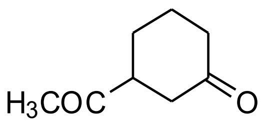

P6 (K_3)

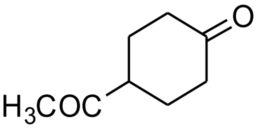

P6 (K_4)

(P6 (K_3+K_4)) purification by flash chromatography (SiO_2; hexane:AcOEt 4:1) gave the product as a white solid (66% total yield, 8% ee K_3); ^{1}H-

NMR ($CDCl_3$, 400 MHz, 300K) δ, ppm: 2.90 – 2.80 (m, 1H), 2.79 – 2.72 (m, 1H), 2.47-2.36 (m, 3H), 2.34 – 2.22 (m, 4H), 2.17 (s, 3H), 2.14 (s, 3H), 2.07-1.97 (m, 3H), 1.89-1.79 (m, 1H), 1.75-1.59 (m, 2H). ^{13}C-NMR 210.0, 209.8, 209.7, 208.5, 50.8, 48.4, 42.3, 40.8, 39.7, 28.17, 28.15, 27.8, 27.1, 24.7. HRMS(ESI+) *m/z* calculated for $C_8H_{12}O_2$ [M+Na]+ 163.0730, found 163.0738. Chiral GC analysis with CYCLOSIL-B.

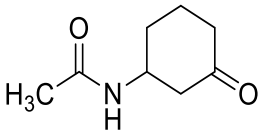

***N*-(3-oxocyclohexyl)acetamide (P7),** purification by flash chromatography (SiO_2; hexane:AcOEt 1:1) gave the product as a white solid; (61% yield, 78% ee); ^{1}H-NMR ($CDCl_3$, 400 MHz, 300K) δ, ppm: 5.79 (bs, 1H), 4.30 - 4.25 (m, 1H), 2.72-2.68 (m, 1H), 2.47-2.38 (m, 2H), 2.28 (m, 2H), 2.09 (m, 1H), 1.98 (s, 3H), 1.78 – 1.69 (m, 2H). ^{13}C-NMR 209.0, 169.4, 48.5, 47.6, 41.0, 30.8, 23.4, 22.1. HRMS(ESI+) *m/z* calculated for $C_8H_{13}NO_2$ [M+Na]+ 178.0838, found 178.0839. $[\alpha]_D^{24}$ -6.1 ($CHCl_3$, *c* 0.312). Chiral GC analysis with CYCLOSIL-B.

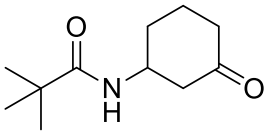

***N*-(3-oxocyclohexyl)pivalamide (P8),** purification by flash chromatography (SiO_2; hexane:AcOEt 1:1) gave the product as a white solid (84% yield, 91% ee); ^{1}H-NMR ($CDCl_3$, 400 MHz, 300K) δ, ppm: 5.60 (bs, 1H), 4.33 - 4.15 (m, 1H), 2.69 (ddt, *J* = 13.9, 4.8, 1.5 Hz, 1H), 2.49 - 2.20 (m, 3H), 2.14 – 1.97 (m, 1H), 1.99 – 1.59 (m, 3H), 1.18 (s, 6H). ^{13}C-NMR 209.0, 177.7, 48.4, 47.6, 41.0, 38.6, 30.7, 27.5, 22.2. HRMS(ESI+) *m/z* calculated for $C_{11}H_{19}NO_2$ [M+Na]+ 220.1308, found 220.1307. $[\alpha]_D^{24}$ -2.9 ($CHCl_3$, *c* 0.272). Chiral GC analysis with CYCLOSIL-B.

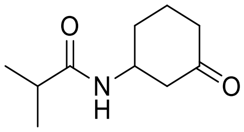

***N*-(3-oxocyclohexyl)isobutyramide (P9),** purification by flash chromatography (SiO_2; hexane:AcOEt 1:1) gave the product as a white solid (60% yield, 88% ee); ^{1}H-NMR ($CDCl_3$, 400 MHz, 300K) δ, ppm: 5.57 (bs, 1H), 4.35 - 4.17 (m, 1H), 2.69 (ddt, *J* = 13.9, 4.8, 1.4 Hz, 1H), 2.48 – 2.18 (m, 4H), 2.14 – 1.92 (m, 2H), 1.86 – 1.62 (m, 2H), 1.14 (dd, *J* = 6.9, 1.0 Hz, 6H). ^{13}C-NMR 209.0, 176.3, 48.2, 47.6, 41.0, 35.6, 30.7, 22.1, 19.6, 19.5 HRMS(ESI+) *m/z* calculated for $C_{10}H_{17}NO_2$ [M+Na]+ 206.1151, found 206.1152. $[\alpha]_D^{24}$ -6.5 ($CHCl_3$, *c* 0.232). Chiral GC analysis with CYCLOSIL-B.

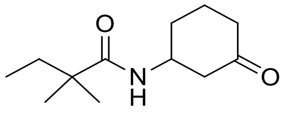

(*S*)-*N*-(3-oxocyclohexyl)-2,2-dimethylbutanamide (P10), purification by flash chromatography (SiO_2; hexane:AcOEt 1:1) gave the product as a white solid; (85%

yield, 94% ee); ^{1}H-NMR (CDCl$_3$, 400 MHz, 300K) δ, ppm: 5.81 (d, *J* = 6.3 Hz, 1H), 4.25 - 4.08 (m, 1H), 2.60 (d, *J* = 13.6 Hz, 1H), 2.38 - 2.26 (m, 1H), 2.26 – 2.13 (m, 2H), 2.00 – 1.90 (m, 1H), 1.65 (q, *J* = 12.0, 10.7 Hz, 2H), 1.46 (q, *J* = 7.3 Hz, 2H), 1.07 (s, 6H), 0.76 (t, *J* = 7.3 Hz, 3H). ^{13}C-NMR 208.9, 176.9, 48.3, 47.6, 42.2, 40.8, 33.8, 30.8, 24.84, 24.82, 22.2, 9.1. HRMS(ESI+) *m/z* calculated for $C_{12}H_{21}NO_2$ [M+H]+ 234.1465, found 234.1464. $[\alpha]_D^{24}$ -5.2 (CHCl$_3$, *c* 0.302). Chiral GC analysis with CYCLOSIL-B. Structure was confirmed by X-Ray diffraction analysis.

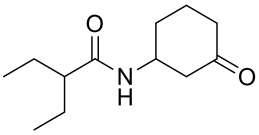

***N*-(3-oxocyclohexyl)-2-ethylbutanamide (P11),** purification by flash chromatography (SiO$_2$; hexane:AcOEt 1:1) gave the product as a white solid; (45% yield, 96% ee); ^{1}H-NMR (CDCl$_3$, 400 MHz, 300K) δ, ppm: 5.71 (d, *J* = 6.9 Hz, 1H), 4.31 (qt, *J* = 8.8, 4.4 Hz, 1H), 2.69 (dd, *J* = 14.1, 4.9 Hz, 1H), 2.45 - 2.22 (m, 2H), 2.12 – 1.93 (m, 2H), 1.83 (ddd, *J* = 14.1, 9.1, 5.1 Hz, 1H), 1.79 – 1.60 (m, 2H), 1.62 – 1.53 (m, 2H), 1.52 – 1.40 (m, 2H), 0.87 (td, *J* = 7.4, 3.4 Hz, 6H). ^{13}C-NMR 209.0, 175.0, 51.3, 48.3, 47.8, 40.9, 30.9, 25.8, 25.7, 22.1, 12.05, 12.02. HRMS(ESI+) *m/z* calculated for $C_{12}H_{21}NO_2$ [M+Na]+ 234.1465, found 234.1459. $[\alpha]_D^{24}$ -5.17 (CHCl$_3$, *c* 0.6). Chiral GC analysis with CYCLOSIL-B.

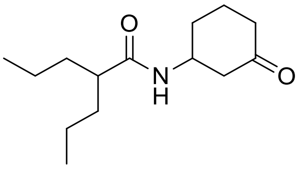

***N*-(3-oxocyclohexyl)-2-ethylbutanamide (P12),** purification by flash chromatography (SiO$_2$; hexane:AcOEt 1:1) gave the product as a white solid; (8% yield, 90% ee); ^{1}H-NMR (CDCl$_3$, 400 MHz, 300K) δ, ppm: 5.46 (d, *J* = 7.3 Hz, 1H), 4.32 (qt, *J* = 8.5, 4.3 Hz, 1H), 2.71 (dd, *J* = 14.1, 4.9 Hz, 1H), 2.46 - 2.37 (m, 1H), 2.30 (dt, *J* = 14.2, 7.9 Hz, 2H), 2.09 (dd, *J* = 12.8, 3.4, Hz, 1H), 1.98 (ddd, *J* = 12.7, 8.7, 5.1 Hz, 2H), 1.86 – 1.66 (m, 3H), 1.65 – 1.54 (m, 2H), 1.43 – 1.29 (m, 6H), 0.94 – 0.89 (m, 6H). ^{13}C-NMR 208.9, 175.3, 48.3, 47.77, 47.76, 41.0, 35.3, 35.2, 30.9, 29.7, 22.2, 20.8, 20.7, 14.1. HRMS(ESI+) *m/z* calculated for $C_{14}H_{25}NO_2$ [M+Na]+ 262.1778, found 262.1781. $[\alpha]_D^{24}$ -2.0 (CHCl$_3$, *c* 0.204). Chiral GC analysis with CYCLOSIL-B.

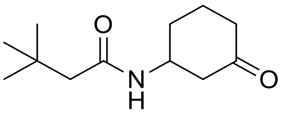

***N*-(3-oxocyclohexyl)-3,3-dimethylbutanamide (P13),** purification by flash chromatography (SiO$_2$; hexane:AcOEt 1:2) gave the product as a white solid (69% yield, 94% ee); ^{1}H-NMR (CDCl$_3$, 400 MHz, 300K) δ, ppm: 6.18 (d, *J* = 7.7 Hz, 1H), 4.21 – 4.12 (m, 1H), 2.59 (dd, *J* = 14.0, 4.8 Hz, 1H), 2.39 - 2.16 (m, 3H), 1.97 (s, 4H), 1.74 – 1.56 (m, 2H), 0.96 (s, 9H). ^{13}C-NMR 209.1, 171.0, 50.2, 48.2, 47.7, 40.8, 30.9, 30.8, 29.8, 22.1. HRMS(ESI+) *m/z* calculated for $C_{12}H_{21}NO_2$ [M+Na]+ 234.1465, found 234.1472. $[\alpha]_D^{24}$ -7.3 (CHCl$_3$, *c* 0.94). Chiral GC analysis with CYCLOSIL-B.

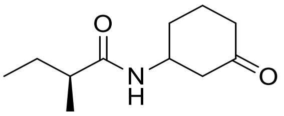

***N*-(3-oxocyclohexyl)-(S)-(+)-2-methylbutanamide (P14),** purification by flash chromatography (SiO_2; hexane:AcOEt 1:1) gave the product as a white solid; (50% yield, 91% ee); ^1H-NMR ($CDCl_3$, 400 MHz, 300K) δ, ppm: 5.97 (d, *J* = 7.2 Hz, 1H), 4.28 - 4.15 (m, 1H), 2.65 (dd, *J* = 14.1, 4.8 Hz, 1H), 2.36 (d, *J* = 14.6 Hz, 1H), 2.30 – 2.20 (m, 2H), 2.05 (dt, *J* = 16.4, 8.2 Hz, 2H), 1.97 – 1.94 (m, 1H), 1.74 – 1.67 (m, 2H), 1.65 – 1.58 (m, 1H), 1.43 – 1.36 (m, 1H), 1.08 (d, *J* = 6.9 Hz, 3H), 0.85 (t, *J* = 7.4 Hz, 3H). ^{13}C-NMR 209.0, 175.8, 48.2, 47.8, 43.0, 40.9, 30.8, 27.3, 22.1, 17.5. 11.8. HRMS(ESI+) *m/z* calculated for $C_{11}H_{19}NO_2$ [M+Na]+ 220.1308, found 220.1303. $[\alpha]_D^{24}$ +9.5 ($CHCl_3$, *c* 0.508). Chiral GC analysis with CYCLOSIL-B.

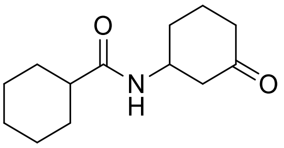

***N*-(3-oxocyclohexyl)cyclohexanecarboxamide (P15),** purification by flash chromatography (SiO_2; hexane:AcOEt 1:1) gave the product as a white solid (75% yield, 91% ee); ^1H-NMR ($CDCl_3$, 400 MHz, 300K) δ, ppm: 5.55 (d, *J* = 6.6 Hz, 1H), 4.31 – 4.23 (m, 1H), 2.69 (dd, *J* = 14.0, 4.8 Hz, 1H), 2.46 - 2.35 (m, 1H), 2.30 - 2.24 (m, 2H), 2.04 (t, *J* = 11.7 Hz, 2H), 1.79 (d, *J* = 13.8 Hz, 4H), 1.72 – 1.63 (m, 2H), 1.42 (dd, *J* = 22.9, 12.4 Hz, 2H), 1.25 (dd, *J* = 17.2, 10.9 Hz, 5H). ^{13}C-NMR 209.0, 175.4, 48.2, 47.7, 45.5, 41.0, 30.7, 29.7, 29.6, 25.68, 25.66, 22.16. HRMS(ESI+) *m/z* calculated for $C_{13}H_{21}NO_2$ [M+Na]+ 246.1465, found 246.1473. $[\alpha]_D^{24}$ -2.7 ($CHCl_3$, *c* 0.412). Chiral GC analysis with CYCLOSIL-B.

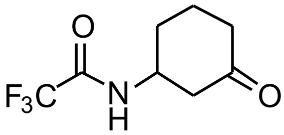

***N*-(3-oxocyclohexyl)trifluoroacetamide (P17),** purification by flash chromatography (SiO_2; hexane:AcOEt 1:1) gave the product as a white solid (65% yield, 65% ee); ^1H-NMR ($CDCl_3$, 400 MHz, 300K) δ, ppm: 7.19 (s, 1H), 4.21 (s, 1H), 2.69 (dd, *J* = 14.3, 4.9 Hz, 1H), 2.50 – 2.35 (m, 2H), 2.35 – 2.19 (m, 1H), 2.19 – 1.98 (m, 2H), 1.88 – 1.67 (m, 2H). ^{13}C-NMR 207.9, 156.8, 49.2, 46.5, 40.5, 38.8, 30.0, 21.8. HRMS(ESI+) *m/z* calculated for $C_{10}H_8F_3NO_2$ [M+H]+ 232.0580, found 232.0560. $[\alpha]_D^{24}$ -5.6 ($CHCl_3$, *c* 0.54). Chiral GC analysis with CYCLOSIL-B.

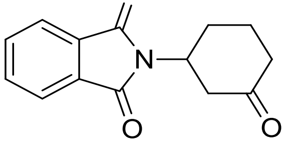

P18 (K_3)

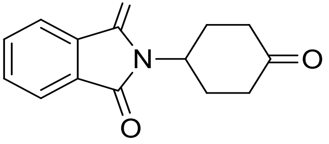

P18 (K_4)

***N*-(3-oxocyclohexyl)phthalimide (P18 (K_3+K_4)),** purification by flash chromatography (SiO_2; hexane:AcOEt 3:1) gave the product as a white solid; (37% total yield, 62% ee K_3); ^1H-NMR ($CDCl_3$, 400 MHz, 300K) δ, ppm: 7.90 – 7.80 (m, 3H), 7.78 – 7.67 (m, 3H), 4.64 (tt, *J* = 12.1, 4.1

Hz, 1H), 4.57 – 4.43 (m, 1H), 3.41 – 3.27 (m, 1H), 2.83 – 2.63 (m, 1H), 2.58 – 2.49 (m, 5H), 2.20 – 2.11 (m, 2H), 2.09 – 2.05 (m, 1H), 1.99 – 1.95 (m, 1H), 1.69 (ddddd, *J* = 17.5, 12.7, 10.4, 6.6, 3.5 Hz, 1H). ^{13}C-NMR 208.8, 207.8, 168.1, 167.9, 134.2, 134.1, 131.8, 131.7, 123.34, 123.26, 49.0, 48.3, 44.8, 40.4, 39.8, 28.6, 22.4. HRMS(ESI+) *m/z* calculated for $C_{14}H_{13}NO_3$ [M+Na]+ 266.0788, found 266.0783. HPLC analysis. Spectroscopic data are in agreement with a previous literature report.[25]

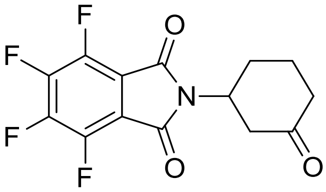

P19 (K_3)

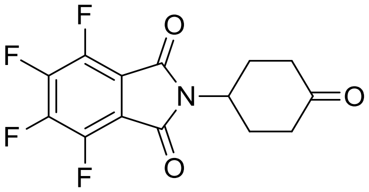

P19 (K_4)

***N*-(3-oxocyclohexyl)tetrafluorophthalimide (P19 (K_3+K_4))** purification by flash chromatography (SiO_2; hexane:AcOEt 3:1) gave the product as a white solid; (40% total yield); ^{1}H-NMR ($CDCl_3$, 400 MHz, 300K) δ, ppm: 4.62 (tt, *J* = 12.1, 4.1 Hz, 1H), 4.53 – 4.44 (m, 1H), 3.28 (ddd, *J* = 13.5, 12.4, 0.9 Hz, 1H), 2.68 (qd, *J* = 12.7, 5.5 Hz, 2H), 2.57 – 2.37 (m, 8H), 2.20 – 2.00 (m, 1H), 2.13 – 2.03 (m, 2H), 1.96 (dtt, *J* = 12.9, 3.9, 2.2 Hz, 1H), 1.78 – 1.65 (m, 1H). ^{13}C-NMR 146.4, 144.8, 143.8, 142.1, 113.5, 49.8, 49.2, 44.4, 40.3, 39.6, 28.3, 22.2. HRMS(ESI+) *m/z* calculated for $C_{14}H_9F_4NO_3$ [M+Na]+ 338.0411, found 338.0417. HPLC analysis.

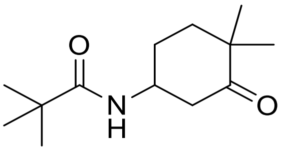

***N*-(4,4-dimethyl-3-oxocyclohexyl)pivalamide (P20),** purification by flash chromatography (SiO_2; hexane:AcOEt 1:1) gave the product as a white solid; (52% yield, 76% ee); ^{1}H-NMR ($CDCl_3$, 400 MHz, 300K) δ, ppm: 5.57 (s, 1H), 4.22 – 4.13 (m, 1H), 2.70 (ddd, *J* = 14.1, 4.9, 1.5 Hz, 1H), 2.43 (dd, *J* = 14.1, 9.6 Hz, 1H), 2.03 (ddtd, *J* = 13.4, 8.0, 4.0, 2.0 Hz, 1H), 1.87 – 1.74 (m, 1H), 1.74 – 1.61 (m, 2H), 1.20 (s, 9H), 1.15 (d, *J* = 9.9 Hz, 6H). ^{13}C-NMR 213.0, 177.7, 49.0, 44.5, 43.9, 38.7, 36.6, 27.5, 27.3, 25.0, 24.7. HRMS(ESI+) *m/z* calculated for $C_{13}H_{23}NO_2$ [M+Na]+ 248.1621, found 248.1621. $[\alpha]_D^{24}$ +19.5 ($CHCl_3$, *c* 0.574). Chiral GC analysis with CYCLOSIL-B.

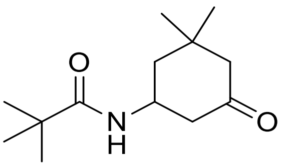

***N*-(5,5-dimethyl-3-oxocyclohexyl)pivalamide (P21),** purification by flash chromatography (SiO_2; hexane:AcOEt 1:1) gave the product as a white solid; (39% yield, 55% ee); ^{1}H-NMR ($CDCl_3$, 400 MHz, 300K) δ, ppm: 5.47 (d, *J* = 7.6 Hz, 1H), 4.28 (tddd, *J* = 12.0, 7.8, 5.0, 4.3 Hz, 1H), 2.69 (ddt, *J* = 13.7, 5.1, 1.8 Hz, 1H), 2.36 – 2.07 (m, 3H), 1.90 (ddt, *J* = 12.9, 4.0, 1.9 Hz, 1H), 1.59 – 1.42 (m, 1H), 1.19 (s, 9H), 1.09 (s, 3H), 0.95 (s, 3H). ^{13}C-NMR

208.1, 177.7, 54.1, 47.1, 45.2, 44.7, 38.6, 33.5, 31.7, 27.5, 25.9. HRMS(ESI+) *m/z* calculated for $C_{13}H_{23}NO_2$ [M+Na]+ 248.1621, found 248.1627. $[\alpha]_D^{24}$ -12.0 ($CHCl_3$, *c* 0.366). Chiral GC analysis with CYCLOSIL-B.

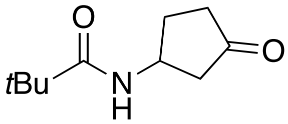

***N*-(3-oxocyclopentyl)pivalamide (P22),** purification by flash chromatography (SiO_2; hexane:AcOEt 1:1) gave the product as a white solid; (25% yield, 26% ee); ^{1}H-NMR ($CDCl_3$, 400 MHz, 300K) δ, ppm: ^{1}H NMR (400 MHz, Chloroform-d) δ 5.78 (s, 1H), 4.48 (s, 1H), 2.68 (d, J = 11.3 Hz, 1H), 2.39 (d, J = 13.4 Hz, 2H), 2.27 (d, J = 10.0 Hz, 1H), 2.17 – 2.00 (m, 1H), 1.85 (s, 1H), 1.20 (s, 9H). ^{13}C-NMR 216.1, 178.5, 47.8, 45.0, 38.6, 37.3, 29.8, 27.6. HRMS(ESI+) *m/z* calculated for $C_{10}H_{17}NO_2$ [M+Na]+ 206.1151, found 206.1147. Chiral GC analysis with CYCLOSIL-B.

Experimental Section: Chapter VI.3.

Aliphatic C–H Bond Oxidation with Hydrogen Peroxide Catalyzed by Manganese Complexes: Directing Selectivity through Torsional Effects

1. Synthesis of the Complexes

(*S,S*)-[Mn(CF_3SO_3)$_2$(pdp)],[6] **(*S,S*)**, **(*R,R*)** or the racemic mixture of **[Mn(CF_3SO_3)$_2$(^{TIPS}mcp)]**[8] and **(*S,S*)-[Mn(CF_3SO_3)$_2$(^{TIPS}ecp)]**[8] complexes were prepared according to the reported procedures.

2. Synthesis of the Substrates

The following substrates were prepared according to the reported procedures:

trans-**4**[17]
4-9[20]

Substrates *cis*/*trans*-**1-3** were synthetized according to the following procedure:

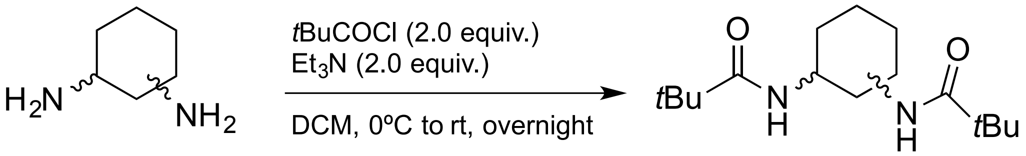

A round-bottom flask equipped with a septum and kept under nitrogen was charged with a 0.20 M solution of the diamine (1.0 equiv) in dichloromethane and cooled to 0 °C. Triethylamine (2.0 equiv) was added to the reaction flask. The pivaloyl chloride (2.0 equiv) was added dropwise and the reaction was stirred overnight at room temperature. At this point, a saturated aqueous Na_2CO_3 solution was added until pH~10-11 and then diluted with dichloromethane. The organic layer was separated from the basic aqueous layer. The aqueous layer was extracted with dichloromethane (2x) and the organic layers were combined. The organic layer was washed with 1N HCl and dried over anhydrous sodium sulfate (Na_2SO_4). The organic layer was evaporated to dryness and the crude amine was purified by flash chromatography over silica gel.

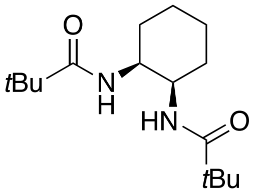

(*cis*-1): A round-bottom flask equipped with a septum and kept under nitrogen was charged with a 0.20 M solution of *cis*-1,2-diaminocyclohexane (3.7 mmol, 0.43 g, 1.0 equiv) in dichloromethane and cooled to 0 °C. Triethylamine (7.4 mmol, 1.0 mL, 2.0 equiv) was added to the reaction flask. The pivaloyl chloride (7.4 mmol, 1.0 mL, 2.0 equiv) was added dropwise and the reaction was stirred overnight at room temperature. At this point, a saturated aqueous Na_2CO_3 solution was added until pH~10-11 and then diluted with dichloromethane. The organic layer was separated from the basic aqueous layer. The aqueous layer was extracted with dichloromethane (2x) and the organic layers were combined. The organic layer was washed with 1N HCl and dried over anhydrous sodium sulfate (Na_2SO_4). The organic layer was evaporated to dryness and the crude amine was purified by flash chromatography over silica gel using CH_2Cl_2/MeOH 3% and the product was concentrated to dryness. The product was isolated as a white solid (0.81 g, 77% yield). ^{1}H-NMR ($CDCl_3$, 400 MHz, 300K) δ, ppm: 6.51 (s, 2H), 4.08 – 3.88 (m, 2H), 1.91 (q, J = 6.9, 3.7 Hz, 2H), 1.6 - 1.41 (m, 6H), 1.20 (s, 9H). ^{13}C-NMR 179.3, 50.6, 38.8, 28.3, 27.5, 22.3. HRMS(ESI+) *m/z* calculated for $C_{16}H_{30}N_2O_2$ [M+Na]+ 305.2199 , found 305.2206.

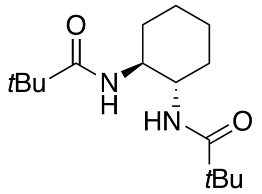

(*trans*-**1**)**:** Following the general conditions, the crude mixture was purified by flash chromatography over silica using CH_2Cl_2/MeOH 2% and the product was concentrated to dryness. The product was isolated as a white solid (0.93 g, 81% yield).

^{1}H-NMR ($CDCl_3$, 400 MHz, 300K) δ, ppm: 6.17 (s, 2H), 3.71 – 3.54 (m, 2H), 2.07 (dt, *J* = 12.8, 2.7 Hz, 2H), 1.44 – 1.27 (m, 2H), 1.23 (s, 3H), 1.17 (s, 18H). ^{13}C-NMR 179.1, 53.7, 38.5, 32.4, 27.6, 24.7. HRMS(ESI+) *m/z* calculated for $C_{16}H_{30}N_2O_2$ [M+Na]+ 305.2199, found 305.2204.

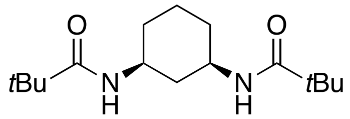

(*cis*-**2**)**:** Following the general conditions, the crude mixture was purified by flash chromatography over silica using hexane:ethyl acetate 3:1 and the product was concentrated to dryness. The product was isolated as a white solid (0.71 g, 73% yield).

^{1}H-NMR ($CDCl_3$, 400 MHz, 300K) δ, ppm: 5.42 (d, J = 7.7 Hz, 2H), 3.81 (tdt, J = 11.7, 7.9, 3.9 Hz, 2H), 2.28 – 2.26 (m, 1H), 2.08 – 1.92 (m, 2H), 1.81 (dp, J = 14.0, 3.4 Hz, 1H), 1.56 – 1.37 (m, 1H), 1.19 (s, 18H), 1.11 – 0.96 (m, 3H). ^{13}C-NMR 177.5, 47.4, 39.5, 38.5, 32.3, 27.6, 22.9. HRMS(ESI+) m/z calculated for $C_{16}H_{30}N_2O_2$ [M+Na]+ 305.2199, found 305.2206.

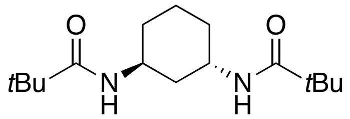

(*trans*-**2**)**:** Following the general conditions, the crude mixture was purified by flash chromatography over silica using hexane:ethyl acetate 3:1 and the product was concentrated to dryness. The product was isolated as a white solid (0.64 g, 74% yield).

^{1}H-NMR ($CDCl_3$, 400 MHz, 300K) δ, ppm: 5.67 (d, J = 5.6 Hz, 2H), 4.18 – 3.89 (m, 2H), 1.71 (dt, J = 11.6, 6.0 Hz, 4H), 1.62 – 1.52 (m, 2H), 1.52 – 1.37 (m, 2H), 1.20 (s, 18H). ^{13}C-NMR 177.8, 44.6, 38.6, 36.6, 27.6, 20.1. HRMS(ESI+) *m/z* calculated for $C_{16}H_{30}N_2O_2$ [M+Na]+ 305.2199 , found 305.2207.

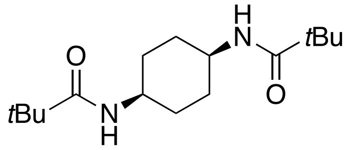

(*cis*-3): Following the general conditions, the crude mixture was purified by flash chromatography over silica using hexane:ethyl acetate 1:1 and the product was concentrated to dryness. The product was isolated as a white solid (0.46 g, 47% yield). ^{1}H-NMR ($CDCl_3$, 400 MHz, 300K) δ, ppm: 5.69 (d, J = 7.5 Hz, 2H), 3.81 (dt, J = 7.5, 3.8 Hz, 2H), 1.67 (td, J = 7.5, 6.2, 3.9 Hz, 4H), 1.47 (qd, J = 10.7, 9.7, 4.5 Hz, 4H), 1.11 (s, 18H). ^{13}C-NMR 177.6, 45.4, 38.6, 28.3, 27.5. HRMS(ESI+) *m/z* calculated for $C_{16}H_{30}N_2O_2$ [M+Na]+ 305.2199, found 305.2198.

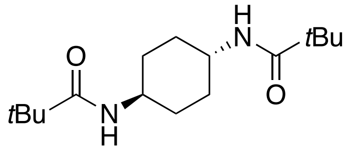

(*trans*-3): Following the general conditions, the crude mixture was purified by flash chromatography over silica using hexane:ethyl acetate 1:2 and the product was concentrated to dryness. The product was isolated as a white solid (0.51 g, 55% yield). ^{1}H-NMR ($CDCl_3$, 400 MHz, 300K) δ, ppm: 5.42 (d, *J* = 8.0 Hz, 2H), 3.76 (m, 2H), 2.08 – 1.91 (m, 4H), 1.30 – 1.22 (m, 4H), 1.20 (s, 18H). ^{13}C-NMR 177.8, 47.5, 38.6, 31.8, 27.6. HRMS(ESI+) *m/z* calculated for $C_{16}H_{30}N_2O_2$ [M+Na]+ 305.2199, found 305.2197.

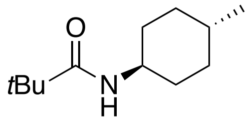

(*trans*-4): Following the general conditions, the crude mixture was purified by flash chromatography over silica using hexane:ethyl acetate 2:1 and the product was concentrated to dryness. The product was isolated as a white solid (0.58 g, 83% yield). ^{1}H-NMR ($CDCl_3$, 400 MHz, 300K) δ, ppm: 5.39 (s, 1H), 3.67 (ddq, J = 11.8, 8.1, 4.2 Hz, 1H), 1.96 (dt, J = 7.8, 3.5 Hz, 2H), 1.71 (dt, J = 7.8, 3.5 Hz, 2H), 1.37 – 1.27 (m, 1H), 1.18 (s, 9H), 1.16 – 0.98 (m, 4H), 0.90 (d, J = 6.4 Hz, 3H). ^{13}C-NMR 177.6, 48.2, 38.5, 33.9, 33.2, 32.0, 27.6, 22.2. HRMS(ESI+) *m/z* calculated for $C_{12}H_{23}NO$ [M+Na]+ 220.1672, found 220.1671.

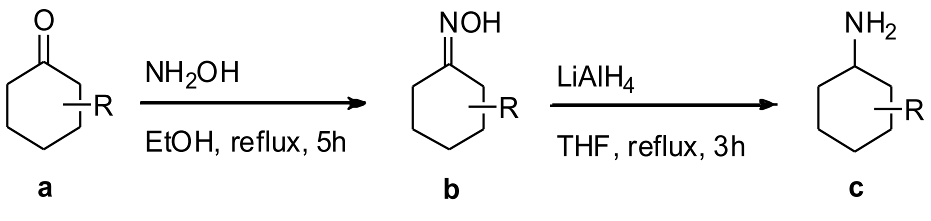

Hydroxylamine hydrochloride (1.2 equiv) followed by pyridine (3.0 equiv) was added to a solution of ketone (**a**) (1.0 equiv) in absolute ethanol and the reaction mixture was heated to reflux temperature under stirring for 5 hours. The reaction was then quenched with water and the product extracted with ethyl acetate (2 x 50 mL). The organic fractions were washed with water and dried over anhydrous $MgSO_4$. The solvent was removed under vacuum to obtain the oxime (**b**) that was used in the next step without further purification. To a stirred solution of lithium aluminium hydride (0.5 equiv) in anhydrous THF under N_2, was added a solution of intermediate **b** drop wise. The reaction was slowly heated to reflux temperature for 3 hours. After this, the reaction mixture was quenched with 1M NaOH solution at 5°C. After filtration through Celite© and extraction with ethyl acetate (2 x 50 mL) the organic fractions were dried over anhydrous $MgSO_4$, the solvent removed under vacuum and the obtained intermediate **c** was used in the next acylation step without further purification to give the corresponding amide.

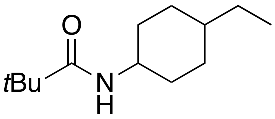

(5): Hydroxylamine hydrochloride (6.7 mmol, 0.47 g, 1.2 equiv) followed by pyridine (16.8 mmol, 1 mL, 3.0 equiv) was added to a solution of 4-ethylcyclohexanone (**a**) (5.6 mmol, 0.71 g, 1.0 equiv) in absolute ethanol and the reaction mixture was heated to reflux temperature under stirring for 5 hours. The reaction was then quenched with water and the product extracted with ethyl acetate (2 x 50 mL). The organic fractions were washed with water and dried over anhydrous $MgSO_4$. The solvent was removed under vacuum to obtain the oxime (**b**) that was used in the next step without further purification. To a stirred solution of lithium aluminium hydride (11.2 mmol, 0.43 g, 0.5 equiv) in anhydrous THF under N_2, was added a solution of intermediate **b** drop wise. The reaction was slowly heated to reflux temperature for 3 hours. After this, the reaction mixture was quenched with 1M NaOH solution at 5°C. After filtration through Celite© and extraction with ethyl acetate (2 x 50 mL) the organic fractions were dried over anhydrous $MgSO_4$, the solvent removed under vacuum and the obtained 4-ethylcyclohexylamine was used in the next acylation step without further purification to give the amide **5**. The crude mixture was purified by flash chromatography over silica using CH_2Cl_2/MeOH 1% and the product was concentrated to dryness. The product was isolated as a white solid (0.62 g, 71% yield, *cis*:*trans* = 1:1.2).

^{1}H-NMR ($CDCl_3$, 400 MHz, 300K) δ, ppm: 5.72 (s, 1H), 5.40 (s, 1H), 2.04 – 1.91 (m, 2H), 1.84 – 1.72 (m, 2H), 1.69 – 1.51 (m, 5H), 1.37 – 1.24 (m, 4H), 1.21 (s, 8H), 1.19 (s, 9H), 1.14 – 1.01 (m, 6H), 0.89 (td, J = 7.3, 6.3 Hz, 6H). ^{13}C-NMR 177.6, 177.4, 48.6, 45.2, 38.7, 38.5, 37.5, 33.2, 31.4, 29.5, 29.3, 28.2, 27.8, 27.64, 27.6, 11.59, 11.56. HRMS(ESI+) m/z calculated for $C_{13}H_{25}NO$ [M+Na]+ 234.1828, found 234.1834.

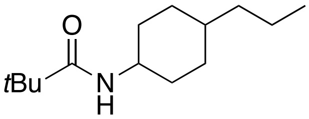

(6): Following the general conditions, the crude mixture was purified by flash chromatography over silica using CH_2Cl_2/MeOH 1% and the product was concentrated to dryness. The product was isolated as a white solid (0.32 g, 33% yield, *cis*:*trans* = 1:2).

^{1}H-NMR ($CDCl_3$, 400 MHz, 300K) δ, ppm: 5.70 (bs, 1H), 5.42 (d, J = 8.0 Hz, 1H), 4.00 – 3.93 (m, 0.5H) 3.65 (dtt, J = 11.7, 8.1, 4.0 Hz, 1H), 2.03 – 1.84 (m, 2H), 1.73 (dt, J = 11.1, 2.3 Hz, 2H), 1.67 – 1.49 (m, 3H), 1.39 – 1.20 (m, 5H), 1.16 (d, J = 6.5 Hz, 18H), 1.09 – 0.95 (m, 4H), 0.86 (td, J = 7.1, 5.9 Hz, 5H). ^{13}C-NMR 177.5, 177.3, 48.5, 45.2, 39.1, 38.6, 38.5, 37.8, 36.6, 35.3, 33.2, 31.8, 29.3, 28.1, 27.60, 27.57, 20.1, 14.31, 14.29. HRMS(ESI+) *m/z* calculated for $C_{14}H_{27}NO$ [M+Na]+ 248.1985, found 248.1987.

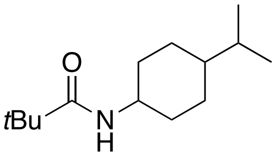

(7): Following the general conditions, the crude mixture was purified by flash chromatography over silica using hexane:ethyl acetate 4:1 and the product was concentrated to dryness. The product was isolated as a white solid (0.43 g, 85% yield, *cis*:*trans* = 1:1.4).

^{1}H-NMR ($CDCl_3$, 400 MHz, 300K) δ, ppm: 5.79 (s, 1H), 5.48 (d, *J* = 8.1 Hz, 1H), 4.00 – 3.93 (m, 1H), 3.67 – 3.54 (m, 1H), 1.94 – 1.88 (m, 2H), 1.74 – 1.61 (m, 4H), 1.57 – 1.33 (m, 6H), 1.23 – 1.21 (m, 1H), 1.14 (s, 9H), 1.11 (s, 9H), 1.07 – 0.97 (m, 6H), 0.81 (dd, *J* = 10.8, 6.8 Hz, 12H). ^{13}C-NMR 182.3, 177.7, 177.4, 48.6, 44.7, 43.2, 42.7, 38.6, 38.4, 38.3, 33.2, 32.5, 31.5, 29.6, 28.4, 27.54, 27.51, 27.1, 26.4, 24.8, 19.9, 19.8. HRMS(ESI+) *m/z* calculated for $C_{14}H_{27}NO$ [M+Na]+ 248.1985, found 248.1985.

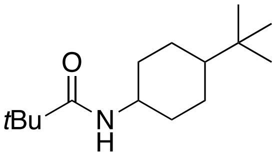

(8): Following the general conditions, the crude mixture was purified by flash chromatography over silica using CH_2Cl_2/MeOH 0.5% and the product was concentrated to dryness. The product was isolated as a white solid (2.3 g, 54% yield, *cis*:*trans* = 1:2).

^{1}H-NMR ($CDCl_3$, 400 MHz, 300K) δ, ppm: 5.77 (bs, 0.5H), 5.41 (bs, 1H), 4.07 – 4.01 (m, 0.5H), 3.69 – 3.56 (m, 1H), 1.99 - 1.96 (m, 2H), 1.85 - 1.74 (m, 3H), 1.66 – 1.62 (m, 1H), 1.52 – 1.43 (m, 1H), 126 – 1.23 (m, 2H), 1.18 (s, 4.5H), 1.15 (s, 9H), 1.08 – 1.00 (m, 5H), 0.84 (s, 4.5H), 0.82 (s, 9H). ^{13}C-NMR 177.5, 177.3, 48.5, 47.41, 47.36, 38.7, 38.5, 33.6, 32.4, 32.3, 30.3, 27.62, 27.58, 27.55, 27.4, 27.3, 26.1, 21.8. HRMS(ESI+) *m/z* calculated for $C_{15}H_{29}NO$ [M+Na]+ 262.2141, found 262.2142.

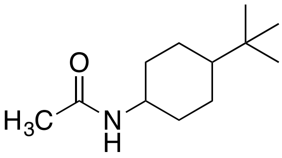

(9): Following the general conditions, the crude mixture was purified by flash chromatography over silica using hexane:ethyl acetate 1:1 and the product was concentrated to dryness. The product was isolated as a white solid (0.54 g, 64% yield, *cis*:*trans* = 1:1.4).

^{1}H-NMR ($CDCl_3$, 400 MHz, 300K) δ, ppm: 6.10 (bs, 1.5H), 4.04 – 4.02 (m, 0.7H), 3.61 – 3.54 (m, 1H), 1.94 (s, 3H), 1.89 (s, 3H), 1.82 - 1.71 (m, 3H), 1.60 – 1.55 (m, 1H), 1.48 – 1.39 (m, 1H), 1.07 – 0.98 (m, 6H), 0.81 (s, 6H), 0.78 (s, 9H). ^{13}C-NMR 169.4, 48.7, 47.7, 47.2, 44.2, 33.5, 32.4, 32.3, 30.6, 27.5, 27.4, 27.3, 26.1, 23.5, 23.4, 21.9. HRMS(ESI+) *m/z* calculated for $C_{12}H_{23}NO$ [M+Na]+ 220.1672, found 220.1671.

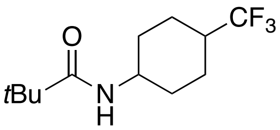

(10): Following the general conditions, the crude mixture was purified by flash chromatography over silica using hexane:ethyl acetate 2:1 and the product was concentrated to dryness. The product was isolated as a white solid (0.46 g, 34% yield, *cis*:*trans* = 1:2.4).

^{1}H-NMR ($CDCl_3$, 400 MHz, 300K) δ, ppm: 5.66 (bs, 0.5H), 5.40 (bs, 1H), 4.11 – 4.07 (m, 0.5H), 3.80 – 3.71 (m, 1H), 2.13 - 2.10 (m, 2H), 2.02 – 1.99 (m, 3H), 1.87 – 1.84 (m, 1H), 1.55 – 1.42 (m, 2.5H), 1.31 - 1.26 (m, 1H), 1.23 (s, 2H), 1.21 (s, 9H), 1.15 – 1.08 (m, 2H). ^{13}C-NMR 177.7, 128.9, 47.4, 43.8, 41.0, 38.5, 31.4, 28.2, 27.53, 27.49, 23.99, 23.97, 23.94, 23.91, 20.29, 20.26. HRMS(ESI+) *m/z* calculated for $C_{12}H_{20}F_3NO$ [M+Na]+ 274.1389, found 274.1389.

3. Estimation of the Tertiary C-H Bond BDE of *N*-Cyclohexylacetamide

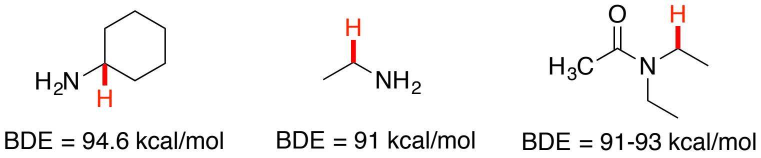

There is no value for the *N*-cyclohexylamides. The Luo book gives **94.6 kcal/mole** for the tertiary C-H bond of cyclohexylamine.[26] The α-C-H bonds of ethylamine have a BDE of **91 kcal mol**[27] while those of the C-H bonds α- to N in *N,N*-diethylacetamide are between **91** and **93 kcal/mol**[28]. If we assume that amide α-C-H bonds are about **1 kcal/mol** stronger than those of amines, and take **94.6 kcal/mole** for the tertiary C-H bond of cyclohexylamine as a reference value, we would estimate a value between **95** and **96 kcal/mol** for the tertiary C-H bond of *N*-cyclohexylacetamide.

4. Reaction Protocol for Catalysis

An acetonitrile solution (400 µL) of the substrate (0.25 M) and the corresponding complex (2.5 mM) was prepared in a vial (10 mL) equipped with a stir bar cooled at -40 ºC, in a CH_3CN/N_2(liq) bath. 98 µL (neat, 17 equiv.) of acetic acid were added directly to the solution.

Then, 236 µL of a 1.5 M hydrogen peroxide solution in CH_3CN (3.5 equiv.) were added by syringe pump over a period of 30 min. At this point, an internal standard (biphenyl) was added and the solution was quickly filtered through a basic alumina plug, which was subsequently rinsed with 2 x 1 mL AcOEt. GC analysis of the solution provided substrate conversions and product yields relative to the internal standard integration. Isomer ratio was determined by GC or ^1H-NMR. Commercially unavailable products were identified by a combination of ^1H, $^{13}C\{^1H\}$-NMR analysis, and HRMS. The oxidized products were identified by comparison to the GC retention time of racemate products obtained with the racemic mixture of **Mn(^{TIPS}mcp)**.

4.1 Optimization Experiments

The majority of the optimization experiments have been already reported in a previous work.[29]

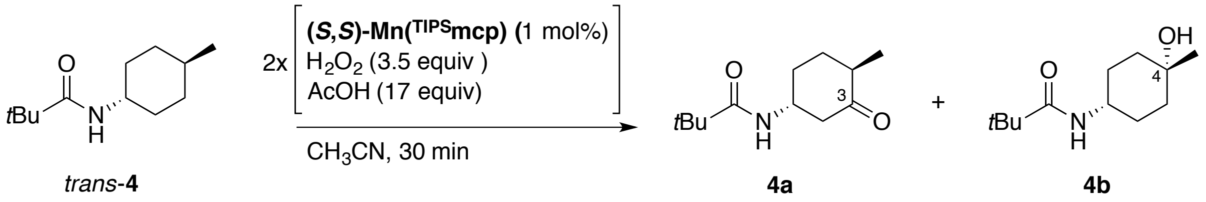
tBu
O
N
H
trans-4
2x
(S,S)-Mn(TIPSmcp) (1 mol%)
H2O2 (3.5 equiv)
AcOH (17 equiv)
CH3CN, 30 min
3
4a
+
OH
4
4b

T (ºC)	Conv (%)	Yield C3 (%)	Yield C4 (%)	ee C3 (%)
0	98	42	11	64
-40	>99	78[a]	14[a]	78

Conversions and yields determined by GC analysis. [a]Isolated yield.

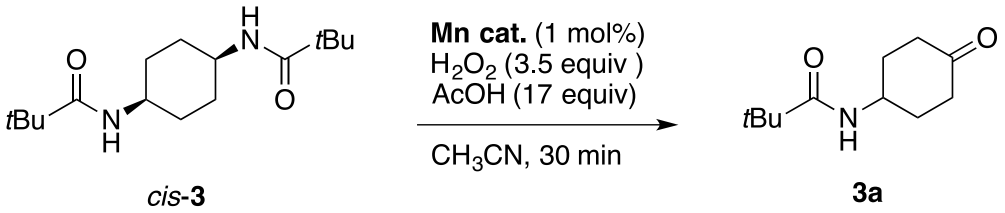
tBu
O
N
H
cis-3
Mn cat. (1 mol%)
H2O2 (3.5 equiv)
AcOH (17 equiv)
CH3CN, 30 min
3a

Cat.	T (ºC)	Conv (%)	Yield (%)
Mn(pdp)	-40	70	48
Mn(^{TIPS}ecp)	-40	49	29
Mn(^{TIPS}mcp)	-40	99	50
Mn(^{TIPS}mcp)	0	98	23

Conversions and yields determined by GC analysis.

4.2 Competition Experiments

Conversions and yields determined by GC analysis using the correspondent response factor:

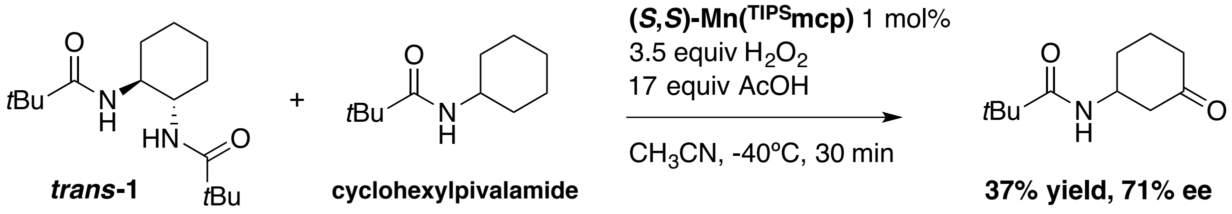
(S,S)-Mn(TIPSmcp) 1 mol%
3.5 equiv H2O2
17 equiv AcOH
CH3CN, -40°C, 30 min
tBu
O
N
H
HN
+

***trans*-1** (0.5 equiv.) **0% conv**

cyclohexylpivalamide (0.5 equiv.) **45% conv**

37% yield, 71% ee

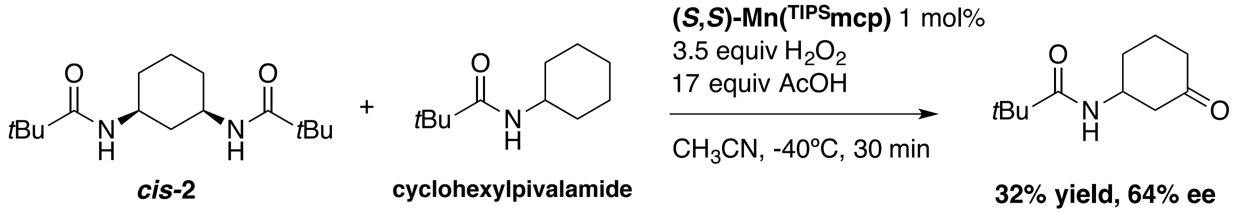
(S,S)-Mn(TIPSmcp) 1 mol%
3.5 equiv H2O2
17 equiv AcOH
CH3CN, -40°C, 30 min
tBu
O
N
H
+

***cis*-2** (0.5 equiv.) **0% conv**

cyclohexylpivalamide (0.5 equiv.) **44% conv**

32% yield, 64% ee

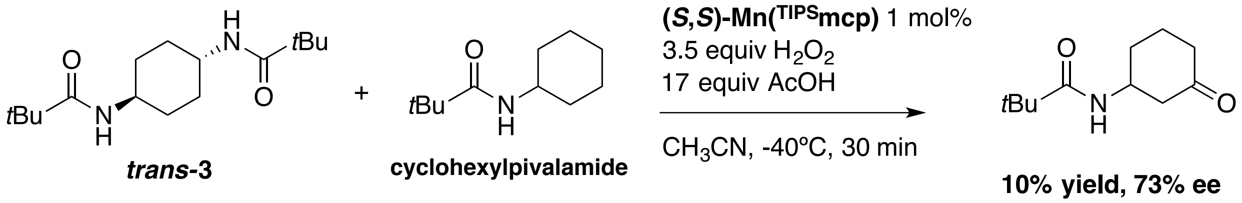
(S,S)-Mn(TIPSmcp) 1 mol%
3.5 equiv H2O2
17 equiv AcOH
CH3CN, -40°C, 30 min
tBu
O
N
H
+

***trans*-3** (0.5 equiv.) **0% conv**

cyclohexylpivalamide (0.5 equiv.) **13% conv**

10% yield, 73% ee

4.3 Reaction optimization for the isolation of the *trans* isomer

The following table reports the small-scale catalysis using substrates **5**-**10**:

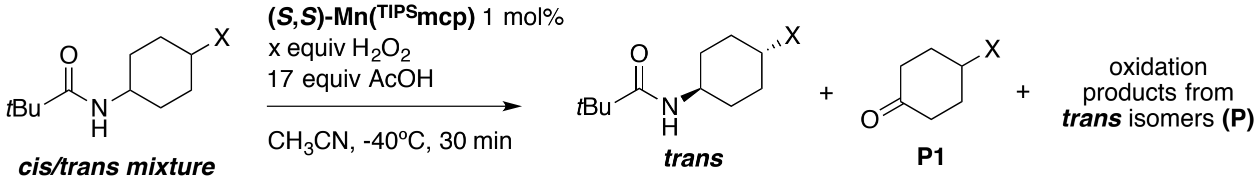

Sub	***trans:cis***	**H_2O_2 (equiv.)**	**Conv *cis* (%)[a]**	**Conv *trans* (%)[a]**	**Yield P1 (%)[a]**	**Yield P (%)[a]**
5	1.2:1	2.0	>99	32	31	31
6	2:1	2.5	>99	30	43	24
7	1.4:1	3.0	>99	26	46	10
8	2:1	3.5	>99	0	93	-
9[b]	1.4:1	3.5	>99	36	78	5
10	2.4:1	3.0	>99	10	81	5

[a] Conversions and yields determined from crude reaction mixtures by GC and ^{1}H-NMR analysis.
[b] **Mn(^{TIPS}ecp)** (1 mol%) and cyclopropane carboxylic acid.

4.4 General Procedure for Product Isolation

25 mL round bottom flask was charged with: catalyst (6 µmol, 1.0 mol%), substrate (1 equiv.), CH_3CN (3.3 mL) and a magnetic stir bar. The carboxylic acid of choice was the added (17 equiv.) and the mixture was cooled at -40 ºC in an CH_3CN/N_2(liq) bath under magnetic stirring. Then, 1.4 mL of a 1.5 M hydrogen peroxide solution in CH_3CN (3.5 equiv.) were added by syringe pump over a period of 30 min at -40°C. At this point, 15 mL of an aqueous $NaHCO_3$ saturated solution were added to the mixture. The resultant solution was extracted with CH_2Cl_2 (3 x 10 mL). Organic fractions were combined, dried over $MgSO_4$, and the solvent was removed under reduced pressure to afford the oxidized product. This residue was filtered by silica gel column to obtain the pure product.

5. Characterization of the Isolated Products

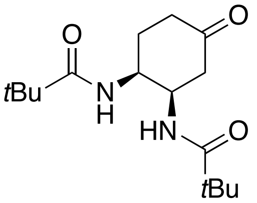

(1a), purification by flash chromatography (SiO_2; hexane:AcOEt 2:1→1:1) gave the product as a white solid (76 mg, 74% yield, 60% ee); ^{1}H-NMR ($CDCl_3$, 400 MHz, 300K) δ, ppm: 7.30 (bs, 1H), 5.93 (bs, 1H), 4.54 (s, 1H), 4.35 – 4.21 (m, 1H), 2.90 (dd, *J* = 14.5, 4.6 Hz, 1H), 2.70 – 2.52 (m, 1H), 2.50 – 2.38 (m, 2H), 1.76 – 1.65 (m, 2H), 1.22 (s, 9H), 1.20 (s, 9H). ^{13}C-NMR 208.8, 180.5, 179.4, 51.9, 51.5, 45.5, 39.0, 27.5, 27.4, 26.3. HRMS(ESI+) *m/z* calculated for $C_{16}H_{28}N_2O_3$ [M+Na]+ 319.1922, found 319.1983.

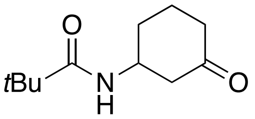

(2a), purification by flash chromatography (SiO_2; hexane:AcOEt 1:1) gave the product as a white solid (55 mg, 61% yield); ^{1}H-NMR ($CDCl_3$, 400 MHz, 300K) δ, ppm: 5.60 (bs, 1H), 4.33 - 4.15 (m, 1H), 2.69 (ddt, *J* = 13.9, 4.8, 1.5 Hz, 1H), 2.49 - 2.20 (m, 3H), 2.14 – 1.97 (m, 1H), 1.99 – 1.59 (m, 3H), 1.18 (s, 6H). ^{13}C-NMR 209.0, 177.7, 48.4, 47.6, 41.0, 38.6, 30.7, 27.5, 22.2. HRMS(ESI+) *m/z* calculated for $C_{11}H_{19}NO_2$ [M+Na]+ 220.1308, found 220.1307.

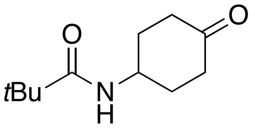

(3a), purification by flash chromatography (SiO_2; CH_2Cl_2/MeOH 3%) gave the product as a white solid (41 mg, 46% yield); ^{1}H-NMR ($CDCl_3$, 400 MHz, 300K) δ, ppm: 5.57 (s, 1H), 4.24 (tdt, J = 11.2, 7.7, 3.9 Hz, 1H), 2.55 – 2.33 (m, 4H), 2.33 – 2.17 (m, 2H), 1.76 – 1.56 (m, 2H), 1.21 (s, 9H). ^{13}C-NMR 209.7, 178.0, 46.3, 39.2, 38.7, 32.0, 27.6. HRMS(ESI+) m/z calculated for $C_{11}H_{19}NO_2$ [M+Na]+ 220.1308, found 220.1307.

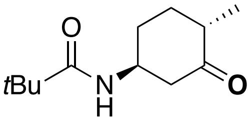

(4a), purification by flash chromatography (SiO_2; hexane:AcOEt 2:1) gave the product as a white solid (86 mg, 78% yield, 78% ee); ^{1}H-NMR ($CDCl_3$, 400 MHz, 300K) δ, ppm: 5.59 (d, J = 7.9 Hz, 1H), 4.17 – 4.02 (m, 1H), 2.72

(ddd, J = 13.1, 4.7, 2.2 Hz, 1H), 2.36 – 2.17 (m, 3H), 2.06 (ddt, J = 12.9, 5.9, 3.5 Hz, 1H), 1.61 (tdd, J = 12.7, 11.5, 3.5 Hz, 1H), 1.45 – 1.31 (m, 1H), 1.19 (s, 9H), 1.05 (d, J = 6.5 Hz, 3H). ^{13}C-NMR 209.2, 177.5, 49.0, 47.9, 44.4, 38.6, 32.1, 31.2, 27.5, 14.2. HRMS(ESI+) m/z calculated for $C_{12}H_{21}NO_2$ [M+Na]+ 234.1465, found 234.1477.

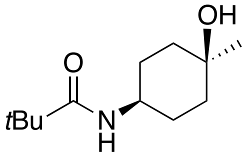

(4b), purification by flash chromatography (SiO_2; hexane:AcOEt 1:1) gave the product as a white solid (16 mg, 14% yield); ^{1}H-NMR ($CDCl_3$, 400 MHz, 300K) δ, ppm: 5.48 (d, J = 7.6 Hz, 1H), 3.74 – 3.69 (m, 1H), 1.77 (dq, J = 7.6, 4.9, 4.0 Hz, 2H), 1.66 (td, J = 10.9, 9.5, 5.5 Hz, 2H), 1.57 – 1.45 (m, 4H), 1.25 (s, 3H), 1.18 (s, 9H). ^{13}C-NMR 209.2, 177.7, 68.4, 47.5, 38.5, 37.5, 31.0, 28.3, 27.6. HRMS(ESI+) m/z calculated for $C_{12}H_{23}NO_2$ [M+Na]+ 236.1621, found 236.1628.

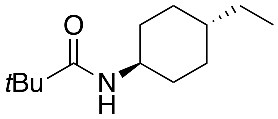

(*trans*-5), purification by flash chromatography (SiO_2; hexane:AcOEt 5:1) gave the product as a white solid (66 mg, 68% yield); ^{1}H-NMR ($CDCl_3$, 400 MHz, 300K) δ, ppm: 5.41 (s, 1H), 3.75 – 3.65 (m, 1H) 2.01 – 1.89 (m, 2H), 1.83 – 1.71 (m, 2H), 1.28 – 1.20 (m, 2H), 1.18 (s, 9H), 1.13 – 0.97 (m, 5H), 0.88 (t, J = 7.4 Hz, 3H). ^{13}C-NMR 177.5, 48.5, 38.6, 38.4, 33.1, 31.4, 29.4, 27.6, 11.6. HRMS(ESI+) *m/z* calculated for $C_{13}H_{25}NO$ [M+Na]+ 234.1828, found 234.1834.

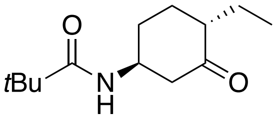

(5a), purification by flash chromatography (SiO_2; hexane:AcOEt 1:1) gave the product as a white solid (60 mg, 65% yield, 86% ee); ^{1}H-NMR ($CDCl_3$, 400 MHz, 300K) δ, ppm: 5.59 (d, *J* = 7.8 Hz, 1H), 4.19 – 4.01 (m, 1H), 2.71 (ddd, *J* = 13.0, 4.7, 2.1 Hz, 1H), 2.22 – 2.16 (m, 1H), 2.16 – 2.07 (m, 2H), 1.82 (ddd, *J* = 13.7, 7.5, 5.8 Hz, 1H), 1.60 (tdd, *J* = 12.3, 11.0, 3.4 Hz, 1H), 1.43 – 1.24 (m, 3H), 1.20 (s, 9H), 0.92 (t, *J* = 7.5 Hz, 3H). ^{13}C-NMR 209.0, 177.6, 51.3, 49.1, 48.0, 38.6, 31.7, 28.5, 27.6, 21.8, 11.6. HRMS(ESI+) *m/z* calculated for $C_{13}H_{23}NO_2$ [M+Na]+ 248.1621, found 248.1626.

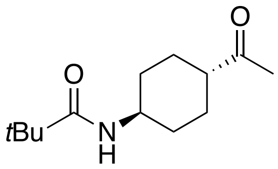

(5b), purification by flash chromatography (SiO_2; hexane:AcOEt 1:1) gave the product as a white solid (12 mg, 13% yield); ^{1}H-NMR ($CDCl_3$, 400 MHz, 300K) δ, ppm: 5.55 – 5.29 (m, 1H), 3.72 (tdt, J = 11.8, 8.0, 4.0 Hz, 1H), 2.33 – 2.21 (m, 1H), 2.15 (s, 3H), 2.11 – 2.03 (m, 2H), 2.03 – 1.91 (m, 2H), 1.53 – 1.39 (m, 2H), 1.18 (s, 9H), 1.13-1.02 (m, 1H). ^{13}C-NMR 211.2, 177.7, 50.6, 47.7, 38.5, 32.3, 27.9, 27.6, 27.2, 22.7, 14.1. HRMS(ESI+) *m/z* calculated for $C_{13}H_{23}NO_2$ [M+Na]+ 248.1621, found 248.1612.

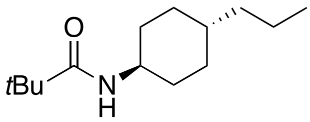

(*trans*-**6),** purification by flash chromatography (SiO_2; hexane:AcOEt 1:1) gave the product as a white solid (103 mg, 91% yield); ^{1}H-NMR ($CDCl_3$, 400 MHz, 300K) δ, ppm: 5.40 (d, J = 7.9 Hz, 1H), 3.68 (ddp, J = 11.7, 8.1, 4.0 Hz, 1H), 2.02 – 1.91 (m, 2H), 1.76 (dt, J = 12.5, 3.0 Hz, 2H), 1.36 – 1.22 (m, 4H), 1.21 (d, J = 2.7 Hz, 1H), 1.18 (s, 10H), 1.12 – 0.95 (m, 4H), 0.88 (t, J = 7.3 Hz, 3H). ^{13}C-NMR 177.5, 48.5, 39.1, 38.5, 36.6, 33.2, 31.8, 27.6, 20.1, 14.3. HRMS(ESI+) *m/z* calculated for $C_{14}H_{27}NO$ [M+Na]+ 248.1985, found 248.1994.

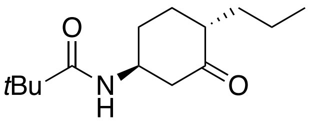

(6a), purification by flash chromatography (SiO_2; hexane:AcOEt 1:1) gave the product as a white solid (43 mg, 42% yield, 90% ee); ^{1}H-NMR ($CDCl_3$, 400 MHz, 300K) δ, ppm: 5.60 (d, *J* = 7.7 Hz, 1H), 4.19 – 4.00 (m, 1H), 2.71 (ddd, *J* = 13.0, 4.7, 2.0 Hz, 1H), 2.23 – 2.14 (m, 2H), 2.13 – 2.04 (m, 1H), 1.78 (ddt, *J* = 13.4, 8.8, 5.9 Hz, 1H), 1.60 (tdd, *J* = 12.6, 11.1, 3.6 Hz, 1H), 1.42 – 1.20 (m, 5H), 1.19 (s, 9H), 0.91 (t, *J* = 7.3 Hz, 3H). ^{13}C-NMR 209.1, 177.6, 49.5, 49.1, 47.9, 38.6, 31.6, 31.0, 28.9, 27.5, 20.2, 14.2. HRMS(ESI+) *m/z* calculated for $C_{14}H_{25}NO_2$ [M+Na]+ 262.1778, found 262.1777.

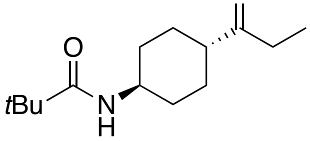

(6b), purification by flash chromatography (SiO_2; hexane:AcOEt 1:1) gave the product as a white solid (4 mg, 4% yield); ^{1}H-NMR ($CDCl_3$, 400 MHz, 300K) δ, ppm: 5.38 (d, *J* = 7.8 Hz, 1H), 3.71 (tdt, *J* = 11.8, 8.0, 4.0 Hz, 1H), 2.46 (q, *J* = 7.3 Hz, 2H), 2.28 (tt, *J* = 12.1, 3.5 Hz, 1H), 2.11 – 2.01 (m, 2H), 1.92 (dt, *J* = 13.2, 2.9 Hz, 2H), 1.48 (qd, *J* = 13.3, 3.4 Hz, 2H), 1.17 (s, 9H), 1.15 – 1.07 (m, 2H), 1.03 (t, *J* = 7.3 Hz, 3H). ^{13}C-NMR 213.7, 177.7, 49.7, 47.7, 38.5, 33.7, 32.4, 29.7, 27.6, 27.4, 7.7, 1.1. HRMS(ESI+) *m/z* calculated for $C_{14}H_{25}NO_2$ [M+Na]+ 262.1778, found 262.1777.

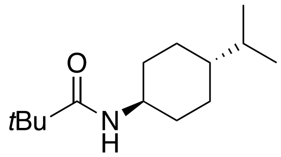

(*trans*-7), purification by flash chromatography (SiO_2; hexane:AcOEt 5:1) gave the product as a white solid (91 mg, 75% yield); ^{1}H-NMR ($CDCl_3$, 400 MHz, 300K) δ, ppm: 5.38 (d, J = 7.6 Hz, 1H), 3.61 (dtq, J = 11.7, 8.1, 4.0 Hz, 1H), 1.93 (dt, J = 11.1, 3.7 Hz, 2H), 1.69 (dt, J = 10.7, 3.0 Hz, 2H), 1.45 – 1.31 (m, 1H), 1.13 (s, 9H), 1.09 – 0.93 (m, 5H), 0.81 (d, J = 6.9 Hz, 6H). ^{13}C-NMR 177.5, 48.5, 43.3, 38.4, 33.3, 32.5, 28.4, 27.6, 19.8. HRMS(ESI+) *m/z* calculated for $C_{14}H_{27}NO$ [M+Na]+ 248.1985, found 248.1985.

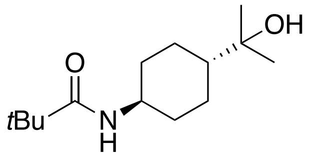

(7a), purification by flash chromatography (SiO_2; hexane:AcOEt 2:1) gave the product as a white solid (37 mg, 45% yield); ^{1}H-NMR ($CDCl_3$, 400 MHz, 300K) δ, ppm: 5.40 (s, 1H), 3.69 – 3.67 (m, 1H) , 2.00 (dd, J = 12.3, 3.6 Hz, 2H), 1.89 – 1.77 (m, 2H), 1.55 (s, 1H), 1.24 – 1.20 (m, 3H), 1.14 (s, 15H), 1.11 – 0.98 (m, 2H). ^{13}C-NMR 177.6, 72.6, 48.4, 48.3, 38.5, 33.2, 27.6, 27.1, 26.2. HRMS(ESI+) *m/z* calculated for $C_{14}H_{27}NO_2$ [M+Na]+ 264.1934, found 264.1934.

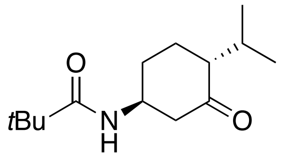

(7b), purification by flash chromatography (SiO_2; hexane:AcOEt 2:1) gave the product as a white solid (11 mg, 14% yield, 4% ee); ^{1}H-NMR ($CDCl_3$, 400 MHz, 300K) δ, ppm: 5.48 – 5.31 (m, 1H), 3.65 (dtt, J = 11.4, 7.6, 4.0 Hz, 1H), 2.00 (dd, J = 12.3, 3.6 Hz, 2H), 1.92 – 1.86 (m, 1H), 1.79 – 1.75 (m, 1H), 1.35 – 1.23 (m, 6H), 1.19 (s, 9H), 1.11 – 0.98 (m, 3H). ^{13}C-NMR 177.6, 72.5, 48.4, 48.2, 38.5, 33.2, 27.6, 27.0, 26.2. HRMS(ESI+) *m/z* calculated for $C_{14}H_{25}NO_2$ [M+Na]+ 262.1778, found 262.1760.

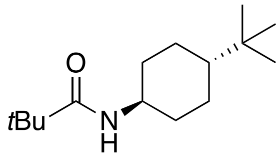

(*trans*-**8**), purification by flash chromatography (SiO_2; hexane:AcOEt 5:1) gave the product as a white solid (101 mg, 66% yield); ^{1}H-NMR ($CDCl_3$, 400 MHz, 300K) δ, ppm: 5.38 (d, J = 7.9 Hz, 1H), 3.71 – 3.61 (m, 1H), 2.09 – 1.93 (m, 2H), 1.86 – 1.70 (m, 2H), 1.19 (s, 9H), 1.17 – 1.01 (m, 4H), 0.96 (tt, J = 11.8, 3.2 Hz, 1H), 0.86 (s, 9H). ^{13}C-NMR 177.6, 48.5, 47.4, 38.5, 33.7, 32.4, 27.61, 27.58, 26.2. HRMS(ESI+) *m/z* calculated for $C_{15}H_{29}NO$ [M+Na]+ 262.2141, found 262.2142.

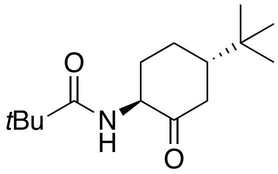

(8a), purification by flash chromatography (SiO_2; hexane:AcOEt:MeOH 99:1:0.01) gave the product as a white solid (60 mg, 34% yield, 70% ee); ^{1}H-NMR ($CDCl_3$, 400 MHz, 300K) δ, ppm: 6.68 (s, 1H), 4.40 (dtd, *J* = 12.3, 6.1, 1.3 Hz, 1H), 2.70 (ddt, *J* = 12.7, 6.3, 3.2 Hz, 1H), 2.60 (ddd, *J* = 12.5, 3.4, 2.5 Hz, 1H), 2.23 – 2.14 (m, 1H), 1.94 (dq, *J* = 9.5, 3.4 Hz, 1H), 1.61 – 1.53 (m, 3H), 1.23 (s, 9H), 0.93 (s, 9H). ^{13}C-NMR 208.8, 178.2, 57.7, 51.0, 42.7, 38.8, 33.9, 32.9, 27.5, 27.2, 25.1. HRMS(ESI+) *m/z* calculated for $C_{15}H_{27}NO_2$ [M+Na]+ 276.1934, found 276.1932.

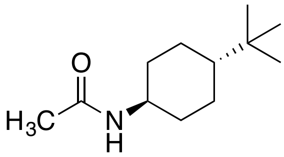

(*trans*-**9**), purification by flash chromatography (SiO_2; hexane:AcOEt 1:1) gave the product as a white solid (90 mg, 84% yield); ^{1}H-NMR ($CDCl_3$, 400 MHz, 300K) δ, ppm: 5.42 (s, 1H), 3.67 (dtd, *J* = 11.4, 7.5, 4.0 Hz, 1H), 2.07 – 2.00 (m, 2H), 1.96 (d, *J* = 0.8 Hz, 3H), 1.83 – 1.75 (m, 2H), 1.18 – 1.04 (m, 4H), 0.85 (d, *J* = 0.9 Hz, 9H). ^{13}C-NMR 169.2, 48.8, 47.3, 33.7, 32.3, 27.5, 26.1, 23.6. HRMS(ESI+) *m/z* calculated for $C_{12}H_{23}NO$ [M+Na]+ 220.1672, found 220.1670.

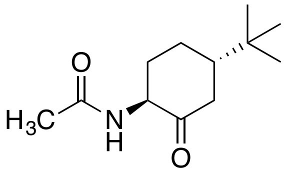

(9a), purification by flash chromatography (SiO_2; hexane:AcOEt 1:1) gave the product collected with low amount of the substrate (32 mg, 46% ee); ^{1}H-NMR ($CDCl_3$, 400 MHz, 300K) δ, ppm: 6.42 (s, 1H), 4.49 – 4.34 (m, 1H), 2.66 (d, J = 19.0 Hz, 1H), 2.56 (d, J = 12.7 Hz, 1H), 2.16 (d, J = 25.4 Hz, 1H), 2.01 (s, 3H), 1.57 (d, J = 39.8 Hz, 2H), 1.26 (d, J = 28.8 Hz, 2H), 0.89 (s, 9H). ^{13}C-NMR 208.5, 169.8, 57.8, 50.9, 42.6, 34.0, 32.9, 27.5, 27.2, 25.1. HRMS(ESI+) *m/z* calculated for $C_{12}H_{21}NO_2$ [M+Na]+ 234.1465, found 234.1468.

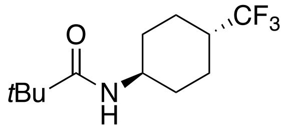

(*trans*-**10),** purification by flash chromatography (SiO_2; hexane:AcOEt 5:1) gave the product as a white solid (88 mg, 96% yield); ^{1}H-NMR ($CDCl_3$, 400 MHz, 300K) δ, ppm: 5.45 (d, J = 6.7 Hz, 1H), 3.72 (tdt, J = 11.8, 8.0, 4.0 Hz, 1H), 2.08 (dd, J = 12.8, 3.7 Hz, 2H), 2.02 – 1.88 (m, 3H), 1.55 – 1.32 (m, 2H), 1.17 (s, 9H), 1.15 – 1.02 (m, 2H). ^{13}C-NMR 177.8, 129.3, 47.5, 38.5, 31.4, 27.6, 23.98, 23.94. HRMS(ESI+) *m/z* calculated for $C_{12}H_{20}F_3NO$ [M+Na]+ 274.1389, found 274.1389.

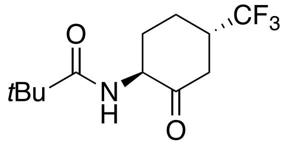

(10a), purification by flash chromatography (SiO_2; hexane:AcOEt 1:1) gave the product collected with the substrate (66 mg, 40% ee); ^{1}H-NMR ($CDCl_3$, 400 MHz, 300K) δ, ppm: 6.60 (bs, 1H), 4.48 – 4.42 (m, 1H), 2.78 – 2.72 (m, 2H), 2.52 – 2.45 (m, 2H), 2.34 – 2.22 (m, 1H), 1.84 – 1.78 (m, 2H), 1.21 (s, 9H). ^{13}C-NMR 204.0, 178.3, 131.6, 128.9, 126.1, 123.3, 57.4, 41.6, 41.3, 41.1, 40.8, 39.5, 38.8, 31.9, 27.4, 27.3. HRMS(ESI+) *m/z* calculated for $C_{12}H_{18}F_3NO_2$ [M+Na]+ 288.1182, found 288.1175.

References

1. Chen, M. S.; White, M. C., *Science* **2007,** *318*, 783-787.
2. Costas, M.; Tipton, A. K.; Chen, K.; Jo, D.-H.; Que Jr., L., *J. Am. Chem. Soc.* **2001,** *123*, 6722-6723.
3. Cussó, O.; Garcia-Bosch, I.; Ribas, X.; Lloret-Fillol, J.; Costas, M., *J. Am. Chem. Soc.* **2013,** *135*, 14871-14878.
4. Font, D.; Canta, M.; Milan, M.; Cussó, O.; Ribas, X.; Klein Gebbink, R. J. M.; Costas, M., *Angew. Chem. Int. Ed.* **2016,** *55*, 5776-5779.
5. Murphy, A.; Dubois, G.; Stack, T. D. P., *J. Am. Chem. Soc.* **2003,** *125*, 5250-5251.
6. Ottenbacher, R. V.; Bryliakov, K. P.; Talsi, E. P., *Adv. Synth. Catal.* **2011,** *353*, 885-889.
7. Cussó, O.; Garcia-Bosch, I.; Font, D.; Ribas, X.; Lloret-Fillol, J.; Costas, M., *Org. Lett.* **2013,** *15*, 6158-6161.
8. Milan, M.; Bietti, M.; Costas, M., *ACS Cent. Sci.* **2017,** *3*, 196-204.
9. Wang, X.; Miao, C. X.; Wang, S. F.; Xia, C. G.; Sun, W., *ChemCatChem* **2013,** *5*, 2489-2494.
10. Quinn, R. K.; Könst, Z. A.; Michalak, S. E.; Schmidt, Y.; Szklarski, A. R.; Flores, A. R.; Nam, S.; Horne, D. A.; Vanderwal, C. D.; Alexanian, E. J., *J. Am. Chem. Soc.* **2016,** *138*, 696-702.
11. Gormisky, P. E.; White, M. C., *J. Am. Chem. Soc.* **2013,** *135*, 14052-14055.
12. Etxebarria, J.; Degenbeck, H.; Felten, A. S.; Serres, S.; Nieto, N.; Vidal-Ferran, A., *J. Org. Chem.* **2009,** *74*, 8794-8797.
13. Chen, M. S.; White, M. C., *Science* **2007,** *318*, 783-787.
14. Wang, X.; Miao, C.; Wang, S.; Xia, C.; Sun, W., *ChemCatChem* **2013,** *5*, 2489–2494.
15. Lohr, T. L.; Li, Z.; Assary, R. S.; Curtiss, L. A.; Marks, T. J., *ACS Catal.* **2015,** *5*, 3675-3679.
16. Kitching, W.; Olszowy, H. A.; Drew, G. M.; Adcock, W., *J. Org. Chem.* **1982,** *47*, 5153-5156.
17. Bechara, W. S.; Khazhieva, I. S.; Rodriguez, E.; Charette, A. B., *Org. Lett.* **2015,** *17*, 1184-1187.
18. Schmidt, V. A.; Quinn, R. K.; Brusoe, A. T.; Alexanian, E. J., *J. Am. Chem. Soc.* **2014,** *136*, 14389-14392.
19. Makhseed, S.; Ibrahim, F.; Samuel, J., *Polymer* **2012,** *53*, 2964-2972.
20. Nirogi, R. V. S.; Konda, J. B.; Kambhampati, R.; Shinde, A.; Bandyala, T. R.; Gudla, P.; Kandukuri, K. K.; Jayarajan, P.; Kandikere, V.; Dubey, P. K., *Bioorg. Med. Chem. Lett.* **2012,** *22*, 6980-6985.
21. Chen, M. S.; White, M. C., *Science* **2010,** *327*, 566-571.
22. Sugi, M.; Sakuma, D.; Togo, H., *J. Org. Chem.* **2003,** *68*, 7629-7633.
23. Cregge, R. J.; Lentz, N. L.; Sabol, J. S., *J. Org. Chem.* **1991,** *56*, 1758-1763.
24. Gao, M.; Wang, M.; Mock, B. H.; Miller, K. D.; Sledge, G. W.; Hutchins, G. D.; Zheng, Q.-H., *Applied Radiation and Isotopes* **2008,** *66*, 523-529.
25. Li, X.; Che, X.; Chen, G.-H.; Zhang, J.; Yan, J.-L.; Zhang, Y.-F.; Zhang, L.-S.; Hsu, C.-P.; Gao, Y. Q.; Shi, Z.-J., *Org. Lett.* **2016,** *18*, 1234-1237.
26. Luo, Y.-R. C. H. o. C. B. E., CRC Press, Boca Raton, FL., **2007**.
27. Salamone, M.; DiLabio, G. A.; Bietti, M., *J. Am. Chem. Soc.* **2011,** *133*, 16625-16634.
28. Salamone, M.; Milan, M.; DiLabio, G. A.; Bietti, M., *J. Org. Chem.* **2014,** *79*, 7179-7184.
29. Milan, M.; Bietti, M.; Costas, M., *ACS Cent. Sci.* **2017,** *3*, 196-204.